

FURTHER STUDY OF (PINCER)IRIDIUM-CATALYZED AROMATIC C–H
BORYLATION AND THE DEVELOPMENT OF NEW ARYLGERMANES FOR
PALLADIUM-CATALYZED CROSS-COUPPLING REACTIONS

A Dissertation

by

MING-UEI HUNG

Submitted to the Graduate and Professional School of
Texas A&M University
in partial fulfillment of the requirements for the degree of

DOCTOR OF PHILOSOPHY

Chair of Committee,	Oleg V. Ozerov
Committee Members,	François P. Gabbaï
	David C. Powers
	Perla B. Balbuena
Head of Department,	Simon W. North

December 2021

Major Subject: Chemistry

Copyright 2021 Ming-Uei Hung

ABSTRACT

Metal-catalyzed cross-coupling reactions of aryl halides or pseudohalides with nucleophiles have been ubiquitous and powerful tools to construct new C–C bonds in synthetic organic chemistry. Among the nucleophiles, arylboronic acids and their esters (arylboronates) are the most popular reagents due to their versatile reactivity and reasonable stability. In 2016, our group reported a highly efficient aromatic C–H borylation catalyzed by (POCOP)Ir complexes. Here we continued the development of the (pincer)Ir-catalyzed system by surveying a series of iridium and rhodium complexes of pincer ligands. We have disclosed that only iridium complexes supported by pincer ligands with a central aryl donor are capable of catalyzing aromatic C–H borylation. The newly tested (PCP)Ir complex has shown improved chemoselectivity (C–H borylation vs. olefin hydroboration, and sp^2 C–H vs. sp^3 C–H borylation) compared to the previously reported (POCOP)Ir complexes. In terms of regioselectivity, C–H borylation of PhF showed certain variations when different precatalysts were examined. On the other hand, C–H borylation of PhCF₃ generally followed the state-of-the-art C–H borylation catalyzed by the iridium complexes supported by neutral bidentate ligands.

In addition to arylboron reagents, group 14 main group reagents have also shown their utility in cross-coupling chemistry. Germanium, positioned between silicon and tin on the periodic table, however, receives much less attention. There are only a few examples of cross-coupling reactions using organogermanes as nucleophiles in the existing literature. Here we have developed a robust and efficient ligandless Pd-catalyzed

germylation protocol to prepare arylgermanes with *tert*-butoxy substituents from aryl bromides. The germylation reagent, sodium tri-*tert*-butoxygermanate, is readily prepared from commercially available $\text{GeCl}_2 \cdot \text{C}_4\text{H}_8\text{O}_2$. This highly efficient catalytic system has a wide substrate scope with excellent isolated yields and only produces NaBr as a byproduct.

The newly prepared arylgermanes have been studied in the subsequent Pd-catalyzed cross-coupling reaction. We undertook a detailed screening of reaction conditions to identify the optimal condition. Using fluoride as a base is required for successful catalysis and adding water significantly increases the yield of the desired cross-coupling product. The possible roles of fluoride and water have been discussed. The reaction scope and preliminary chemoselective cross-coupling experiments have shown that the newly prepared arylgermanes indeed have useful and unique reactivity compared to the existing reagents.

DEDICATION

To my Family, and Che-Hsuan.

ACKNOWLEDGEMENTS

I would like to give my sincerest gratitude to my research advisor, Dr. Oleg Ozerov, for his guidance, patience, support, and belief in me. Appreciations also go to my committee members Dr. François Gabbai, Dr. David Powers, and Dr. Perla Balbuena.

I would like to give special thanks to the supporting staff, my teaching advisors, and my mentor in the Department of Chemistry. My Ph.D. studies couldn't have been completed without the support from Sandy Horton, Valerie McLaughlin, Dr. Joanna Pellois, Dr. Yohannes Rezenom, Dr. Nattamai Bhuvanesh, Dr. Gregory Wylie, Dr. Doug Elliott, Dr. Edward Lee, Dr. Holly Gaede, Dr. Alicia Altemose, and Dr. Tamara Powers.

I would like to thank my best friend, Olivia Gunther, for always giving me 100% of her support and love. I will treasure our friendship forever. I also want to thank everyone in the Ozerov group: Dr. Wei-Chun Shih, Dr. Chris Pell, Dr. Alex Kosanovich, Dr. Qingheng Lai, Dr. Bryan Foley, Dr. Cheng-Han Yu, Dr. Yihan Cao, Yanwu Shao, Vinh Nguyen, Derek Leong, Sam Lee, Mario Cosio, Brandy Adolph, and Ruth Ann Gholson. These five years have been full of laughter and tears and you guys know the best.

I would also like to thank all my friends in the Department of Chemistry, especially those in my class and from Taiwan. I simply can't list all the names, but I wouldn't be able to make it through without those parties, small gatherings, and drunk nights.

Last but not the least, I would love to thank Che-Hsuan Chang and my family for their endless love, support, and encouragement. Nothing can compete with the feeling that knowing they are always there for me, no matter I succeed or fail.

CONTRIBUTORS AND FUNDING SOURCES

This work was supervised by a dissertation committee consisting of Dr. Oleg V. Ozerov, Dr. François P. Gabbaï, and Dr. David C. Powers of the Department of Chemistry and Dr. Perla B. Balbuena of the Department of Chemical Engineering, the Department of Materials Science and Engineering, and the Department of Chemistry.

The XRD structures for compounds **231-HOAc**, **301**, and **307** were solved by Dr. Nattamai Bhuvanesh. The HRMS and GC-MS experiments were performed by Dr. Yohannes Rezenom. The electrochemical experiments were performed by Derek Leong.

The early studies on compounds **208** and **228-HCl** were performed by Dr. Samuel D. Timpa. The initial studies on compounds **216** and **231-HOAc** were performed by Melissa A. Schumacher, Dr. Morgan C. MacInnis, and Dr. Loren P. Press. Compound **217** was synthesized by Dr. Bryan J. Foley. Compound **233-COE** was synthesized by Dr. Alex J. Kosanovich. Compounds **234-H₄** and **239-HCl** were synthesized by Yihan Cao. Compound **235-HCl** was synthesized by Dr. Qingheng Lai.

All other work conducted for the dissertation was completed by the student independently.

This work was made possible in part by the U.S. National Science Foundation under Grant Number CHE-1565923 and the Welch Foundation under Grant Number A-1717. Its contents are solely the responsibility of the authors and do not necessarily represent the official views of the U.S. National Science Foundation or the Welch Foundation.

NOMENCLATURE

Ac	Acetyl
APCI	Atmospheric Pressure Chemical Ionization
Ar	Aryl
BINAP	2,2'-Bis(diphenylphosphino)-1,1'-binaphthyl
Boc	<i>tert</i> -Butoxycarbonyl
cat	Catecholato
cat.	Catalyst
COD	1,5-Cyclooctadiene
COE	<i>cis</i> -Cyclooctene
conv.	Conversion
Cy	Cyclohexyl
d	Day(s)
dba	Dibenzylideneacetone
DavePhos	2-Dicyclohexylphosphino-2'-(<i>N,N</i> -dimethylamino)biphenyl
DFT	Density Functional Theory
DMAP	4-Dimethylaminopyridine
DMF	<i>N,N</i> -Dimethylformamide
DPEphos	Bis[(2-diphenylphosphino)phenyl] Ether
DPPE	1,2-Bis(diphenylphosphino)ethane
DPPF	1,1'-Bis(diphenylphosphino)ferrocene

Et	Ethyl
EI	Electron Ionization
Elem. Anal.	Elemental Analysis
ESI	Electrospray Ionization
equiv	Equivalent
Fc	Ferrocene
GC–FID	Gas Chromatography–Flame Ionization Detector
GC–MS	Gas Chromatography–Mass Spectrometry
h	Hour(s)
HRMS	High Resolution Mass Spectrometry
ⁱ Pr	Isopropyl
Me	Methyl
Me ₁₀ Fc	Decamethylferrocene
MesH	Mesitylene
min	Minute(s)
ⁿ Bu	<i>n</i> -Butyl
NMP	<i>N</i> -Methyl-2-pyrrolidone
NMR	Nuclear Magnetic Resonance
OAc	Acetate
Ph	Phenyl
pin	Pinacolato
py	Pyridine

RuPhos	2-Dicyclohexylphosphino-2',6'-diisopropoxybiphenyl
rxn	Reaction
S.M.	Starting Material
SPhos	2-Dicyclohexylphosphino-2',6'-dimethoxybiphenyl
TBABr	Tri- <i>n</i> -butylammonium Bromide
TBAF	Tri- <i>n</i> -butylammonium Fluoride
TBE	<i>tert</i> -Butylethylene
tBu	<i>tert</i> -Butyl
^t Bu-bpy	4,4'-Di- <i>tert</i> -butyl-2,2'-dipyridyl
temp.	Temperature
THF	Tetrahydrofuran
Xantphos	4,5-Bis(diphenylphosphino)-9,9-dimethylxanthene
XRD	X-Ray Diffraction

TABLE OF CONTENTS

	Page
ABSTRACT	ii
DEDICATION	iv
ACKNOWLEDGEMENTS	v
CONTRIBUTORS AND FUNDING SOURCES.....	vi
NOMENCLATURE.....	vii
TABLE OF CONTENTS	x
LIST OF FIGURES.....	xiii
LIST OF TABLES	xvi
CHAPTER I INTRODUCTION AND LITERATURE REVIEW	1
1.1 Introduction to Pd-Catalyzed Cross-Coupling Reactions	1
1.2 Introduction to Preparation of Arylboronic Acid Derivatives	4
1.2.1 Conventional Borylation	4
1.2.2 Catalytic Borylation of Aryl Halides.....	5
1.2.3 Catalytic Arene C–H Borylation	5
1.3 Introduction to Preparation of Arylgermane Derivatives.....	7
1.3.1 Conventional Germylation	8
1.3.2 Catalytic Germylation of Aryl Halides	8
1.3.3 C–H Germylation	9
1.3.4 Germylene Insertion of Aryl Halides	11
1.4 Introduction to Pincer Ligands.....	12
CHAPTER II SYNTHESIS OF PXL PINCER COMPLEXES OF IRIIDIUM AND RHODIUM AND THEIR CATALYTIC REACTIVITY TO AROMATIC C–H BORYLATION	15
2.1 Introduction	15
2.1.1 The State-of-the-Art Aromatic C–H Borylation	15
2.1.2 Pincer Complexes of Iridium in Aromatic C–H Borylation.....	16
2.2 Results and Discussion.....	17

2.2.1 Synthesis of Pincer Ligands	17
2.2.2 Synthesis and Characterization of Pincer Complexes	20
2.2.3 Catalysis of Aromatic C–H Borylation	27
2.3 Conclusion.....	33
2.4 Experimental	34
2.4.1 General Consideration	34
2.4.2 Synthesis and Characterization	35
2.4.3 Screening of Methods for Metalation of LXL-Type Pincer Ligands	46
2.4.4 Catalysis of Aromatic C–H Borylation	75
2.4.5 Details of X-Ray Structural Determination of 231-HOAc (CCDC 2041134).....	80
CHAPTER III PALLADIUM-CATALYZED GERMYLATION OF ARYL BROMIDES USING SODIUM TRI- <i>TERT</i> -BUTOXYGERMANATE	83
3.1 Introduction	83
3.1.1 Germylation of Aryl Halides Using Germanium Anion Reagents.....	84
3.1.2 Preparation of Germanium Anion Reagents	85
3.2 Results and Discussion.....	86
3.2.1 Synthesis of Germanate Derivatives	86
3.2.2 Germylation of Aryl Halides Using Germanate Derivatives	89
3.2.3 Reaction Scope of Germylation of Aryl Bromides	92
3.2.4 In situ Generated Germanates in Germylation	95
3.2.5 Mechanistic Discussion.....	97
3.3 Conclusion.....	99
3.4 Experimental	99
3.4.1 General Consideration	99
3.4.2 Details of X-Ray Structural Determination of 301 (CCDC 2057607).....	102
3.4.3 Details of X-Ray Structural Determination of 307 (CCDC 2095668).....	103
3.4.4 Electrochemical experiments of 301	105
3.4.5 Synthesis of Alkali Germanate Derivatives	105
3.4.6 Development of Catalytic Germylation of Aryl Bromides Using 301	113
3.4.7 Mercury Test of the Catalytic Germylation of Aryl Bromides	113
3.4.8 Catalytic Aromatic C–Br Germylation using Other Germanium(II) Reagent.....	114
3.4.9 Preliminary Tests of Catalytic Germylation of Aryl Chlorides	117
3.4.10 Synthesis and Characterization of New Germane Products.....	117
3.4.11 Attempted Germylation of 323af , 323ag , 323ah , and 323ai and the Related Experiments.....	130
3.4.12 Germylation with in situ Generated Germanate.....	134
3.4.13 Attempted Syntheses of Pd–Ge Species.....	135
CHAPTER IV PALLADIUM-CATALYZED CROSS-COUPPLING REACTION USING ARYLTRI- <i>TERT</i> -BUTOXYGERMANES.....	136

4.1 Introduction	136
4.1.1 Early Developments Using Germatranes (1996–Early 2000s)	136
4.1.2 Discovery of Various Arylgermanes (2002–2012)	137
4.1.3 Recent Advancements (2018–present)	140
4.2 Results and Discussion	142
4.2.1 Development of the Pd-Catalyzed Cross-Coupling Reaction Using Aryltri- tert-butoxygermanes	142
4.2.2 Reaction Scope	148
4.2.3 Selective Reaction of –Bpin vs. –Ge(O ^t Bu) ₃	149
4.2.4 Mechanistic Discussion: Role of Fluoride and Water	150
4.3 Conclusion	152
4.4 Experimental	152
4.4.1 General Consideration	152
4.4.2 Determination of the Density of 4-FC ₆ H ₄ Ge(O ^t Bu) ₃ (324b)	155
4.4.3 Optimization of Reaction Conditions	156
4.4.4 Synthesis and Characterization of Biaryl Products	159
4.4.5 Selective Reaction of –Bpin vs. –Ge(O ^t Bu) ₃	164
4.4.6 Effect of Fluoride Experiments	165
CHAPTER V CONCLUSIONS	167
REFERENCES	169
APPENDIX A LIST OF PUBLICATIONS RESULTING FROM THE PH.D. WORK	191
APPENDIX B MISCELLANEOUS REACTIONS	192
B-1. Miscellaneous Synthesis	192
B-2. Miscellaneous Reactions	198

LIST OF FIGURES

	Page
Figure I-1. Pd-catalyzed cross-coupling reactions of aryl halides with various coupling partners.	2
Figure I-2. General mechanisms of Pd-catalyzed cross-coupling reactions. Left: Mizoroki–Heck reaction. Right: Other cross-coupling reactions.	3
Figure I-3. Preparation of arylboronic acid derivatives. a) Conventional synthesis through aryllithium or Grignard reagents. b) Pd-catalyzed C–X borylation. c) Ir-catalyzed C–H borylation.	5
Figure I-4. General mechanism of aromatic C–H borylation catalyzed by neutral bidentate-ligand-supported iridium complexes.	7
Figure I-5. Conventional synthesis of arylgermanes.	8
Figure I-6. Pd- or Rh-catalyzed germylation of aryl halides.	9
Figure I-7. Pd- or Rh-catalyzed C–H germylation.	10
Figure I-8. Schoenebeck’s recent reported “formal” C – H germylation.	11
Figure I-9. Germylene insertion into an aryl carbon–halide bond to form aryltrihalogermane.	12
Figure I-10. Generic pincer complexes. M = metal center; X = central donor; L = side donors; R = substituents on side donors; Y = specific arm linkers; Z = other substituents.	13
Figure I-11. Selective examples of LXL-type pincer ligands.	14
Figure II-1. Top: (POCOP)Ir-catalyzed arene C–H borylation. Bottom: Proposed reaction mechanism of (POCOP)Ir-catalyzed arene C–H borylation.	17
Figure II-2. LXL-type pincer ligands in this study.	18
Figure II-3. Synthesis of 205, 208, and 216.	19
Figure II-4. Pincer complexes of iridium and rhodium in this study.	20
Figure II-5. Different Methods for Metalation of PCP Ligands.	21
Figure II-6. Preparative synthesis of iridium and rhodium complexes.	24

Figure II-7. Two configurational isomers in 230-HClpy and 240-HClpy.	24
Figure II-8. Attempted transformations of 240-HClpy.	25
Figure II-9. The ORTEP ¹⁵¹ drawings (50% probability ellipsoids) of 231-HOAc (CCDC 2041134). Hydrogen atoms and methyl groups of <i>tert</i> -butyl arms are omitted for clarity. Selected distances (Å) and angles (deg): Ir1–C1, 1.998(3); Ir1–O2, 2.211(2); Ir1–O3, 2.296(2); P1–Ir1–S1, 164.61(3); O2–Ir1–S1, 91.38(7); O2–Ir1–P1, 103.78(7); C1–Ir1–S1, 83.98(10); C1–Ir1–P1, 81.36(10).....	26
Figure II-10. Chemoselectivity for sp ² C–H, sp ³ C–H, and C–Cl bonds.	32
Figure II-11. Structures of 242-H ₃ Bpin and 243-H ₃ Bpin.	64
Figure III-1. Examples of arylboron and arylsilicon reagents with electronegative substituents (highlighted in red) in Pd-catalyzed cross-coupling reactions.....	84
Figure III-2. Germylation of aryl halides by anionic germanium species.....	85
Figure III-3. Preparation of alkyl-/silylgermyllithium reagents.....	85
Figure III-4. The synthesis and the ORTEP ¹⁵¹ drawing (50% probability ellipsoids) of [NaGe(O ^t Bu) ₃] ₂ (301) (CCDC 2057607). Hydrogen atoms are omitted for clarity. Selected distance (Å) and angles (°): Ge1–O1, 1.911(3); Ge1–O2, 1.887(3); Ge1–O3, 1.901(3); O1–Ge1–O2, 86.97(13); O2–Ge1–O3, 95.44(13); O1–Ge1–O3, 86.99(13).	87
Figure III-5. Cyclic voltammogram (left) of 301 (1.0 mM in CH ₂ Cl ₂) (vs. Fc/Fc ⁺) and its first derivative plot (right).....	87
Figure III-6. Synthesis of germanate derivatives.	88
Figure III-7. The ORTEP ¹⁵¹ drawing (50% probability ellipsoids) of NaGe(OEt) ₃ (307) (CCDC 2095668). Hydrogen atoms are omitted for clarity. Top: Extracted dimeric structure (side view). Bottom: Polymeric structure (top view). Selected distance (Å) and angles (°): Ge1–O1, 1.862(3); Ge1–O2, 1.916(3); Ge1–O3, 1.890(3); O2–Na2, 2.373(3); O5–Na1, 2.394(3); O1–Ge1–O2, 95.20(13); O2–Ge1–O3, 89.32(13); O1–Ge1–O3, 88.54(13).....	89
Figure III-8. Reaction scope of germylation of aryl halides. Reaction condition: aryl/alkenyl bromide 323 (50 μmol, 1.0 equiv), 301 (0.5–0.6 equiv or 1.0–1.2 equiv Ge to C–Br bond), and Pd(OAc) ₂ (0.1 mol% to C–Br bond) in C ₆ D ₆ , 100 °C, 3 h. Yields were isolated yields. ^a 130 °C. ^b 1 mol% (to C–Br bond) of Pd(OAc) ₂ was used.	93

Figure III-9. Gram-scale synthesis of aryl germanes.	94
Figure III-10. Reductive coupling of nitroarene by 301.	95
Figure III-11. Proposed mechanism of Pd-catalyzed germylation of aryl bromides using [NaGe(O ^t Bu) ₃] ₂	98
Figure III-12. Germanate vs. germylene in the gemylation reaction.	99
Figure IV-1. Germatranes in Pd-catalyzed cross-coupling reaction.	137
Figure IV-2. Aryltri(2-furyl)germanes in Pd-catalyzed cross-coupling reaction.	138
Figure IV-3. Aryltrichlorogermanes and arylgermanium sesquioxides in Pd-catalyzed cross-coupling reaction.	138
Figure IV-4. Robust bis(2-naphthylmethyl)-substituted arylgermanes in Pd-catalyzed cross-coupling reaction.	139
Figure IV-5. Transfer of multiple phenyl groups in Pd-catalyzed cross-coupling reaction.	140
Figure IV-6. Intramolecularly activated alkenylgermanes in Pd-catalyzed cross- coupling reaction.	140
Figure IV-7. Structural-modified germatranes in Pd-catalyzed cross-coupling reaction.	141
Figure IV-8. Nanoparticle Pd-catalyzed cross-coupling of aryltriethylgermanes.	141
Figure IV-9. Reaction scope of Pd-catalyzed cross-coupling reaction using aryltri- <i>tert</i> -butoxygermanes.	149
Figure IV-10. The selective reaction of –Bpin vs. –Ge(O ^t Bu) ₃	150
Figure IV-11. Mass (mg) vs. volume (μL) plot of 324b.	156

LIST OF TABLES

	Page
Table II-1. Screening of methods for metalation of PCP pincer ligands. ^a	22
Table II-2. ¹ H NMR (Ir–H) and ³¹ P NMR chemical shifts of iridium complexes.	25
Table II-3. Aromatic C–H borylation experiments using iridium or rhodium precatalysts. ^a	28
Table II-4. Comparison of the steric hindrance and the chemoselectivity of iridium complexes.	29
Table II-5. Aromatic C–H borylation using different olefins. ^a	30
Table II-6. Effect of reagent ratio on product ratio using 229-HCl as a precatalyst. ^a	30
Table II-7. Regioselectivity test for aromatic C–H borylation using iridium precatalysts. ^a	32
Table II-8. Aromatic C–H borylation experiments using iridium or rhodium precatalysts without 1-hexene. ^a	77
Table III-1. Optimization of aromatic C–Br germylation reaction conditions. ^a	91
Table III-2. Preliminary ligand screening of aromatic C–Cl germylation reaction. ^a	92
Table III-3. Germylation with in situ generated tri- <i>tert</i> -butoxygermanate. ^a	96
Table III-4. Germylation with other in situ generated germanates. ^a	97
Table III-5. Detailed conditions of attempted germylation using 307.	115
Table III-6. Reductive coupling of nitroarene by 301.	132
Table IV-1. Screening of palladium precursors and phosphine ligands.	143
Table IV-2. Screening of bases and additives.	144
Table IV-3. Effect of water as an additive and solvent.	146
Table IV-4. Effect of the catalyst loading.	147
Table IV-5. Effect of the base loading and reagent ratio.	148

Table IV-6. Effect of the reaction temperature.	148
Table IV-7. Volumes and masses measurement of 324b.	155

CHAPTER I
INTRODUCTION AND LITERATURE REVIEW

1.1 Introduction to Pd-Catalyzed Cross-Coupling Reactions

Transition-metal-catalyzed reactions have become one of the most important synthetic methods in organic chemistry. One of the most important catalyzed reactions is the cross-coupling reaction of aryl halides or pseudohalides with nucleophiles to construct new C–C or carbon–heteroatom (C–N, C–B, C–O, C–S, etc.) bonds.^{1–6} In the initial stage of the development of coupling reactions in the early 1970s, palladium, nickel, and copper proved to be most useful in cross-coupling reactions, but palladium later dominated the field because the scope of Pd-catalyzed reactions quickly grew, and palladium often provided enhanced selectivity over the other two metals.⁵ Many organometallic/main group nucleophiles have been explored in the Pd-catalyzed reactions (Figure I-1).⁵ These cross-coupling reactions became extremely popular and useful in both academia and industry, especially after discovering the enhanced activity of catalysts supported by bulky, strongly σ -donating ligands in the 1990s.⁵ These great successes and their broad impact on the chemical community led to Heck, Negishi, and Suzuki being awarded the Nobel Prize in Chemistry in 2010 “for palladium-catalyzed cross coupling in organic synthesis.”^{7,8} Besides C–C bond formation, the strategies have been extended to carbon–heteroatom bond cross-coupling reactions, including Miyaura borylation (C–B),⁹ Buchwald–Hartwig amination (C–N).¹⁰

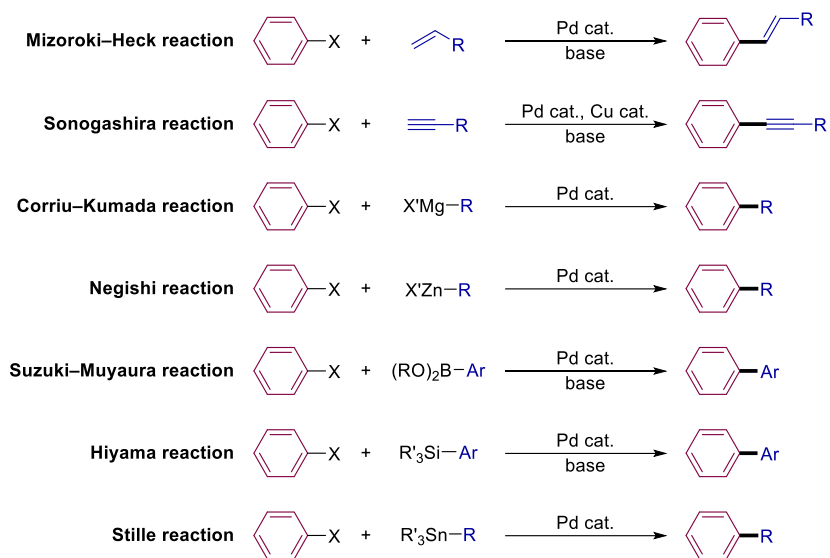


Figure I-1. Pd-catalyzed cross-coupling reactions of aryl halides with various coupling partners.

Almost all these Pd-catalyzed cross-coupling reaction follows the same general mechanism depicted in Figure I-2.⁵ The ligated palladium(0) species **A** activates aryl halide via oxidation addition to form the palladium(II) aryl/halido complex **B**. In the Mizoroki-Heck reaction, coordination and migratory insertion of the olefin into the Pd-C(aryl) bond gives the intermediate **C**. This is followed by β -hydride elimination to form the cross-coupling product. Palladium(0) species **A** is regenerated subsequently by a base-assisted elimination of hydrogen halide from intermediate **D**. However, in other reactions, such as Suzuki-Miyaura and Negishi reactions, palladium(II) aryl/halido complex **B** undergoes transmetalation with the organometallic/main group nucleophile (or heteroatom nucleophile in carbon-heteroatom cross-coupling reactions) to generate the intermediate **E**, followed by reductive elimination to give the coupled organic product and regenerate palladium(0) complex **A**.

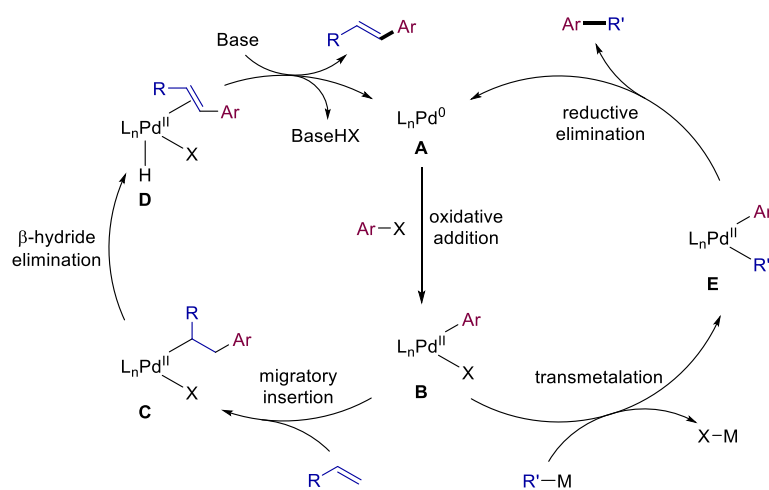


Figure I-2. General mechanisms of Pd-catalyzed cross-coupling reactions. Left: Mizoroki–Heck reaction. Right: Other cross-coupling reactions.

Among main group nucleophiles, arylboronic acids and esters, arylsilanes, and arylstannanes are commonly utilized due to their versatile reactivity and good functional group tolerance, compared to organozinc and organomagnesium reagents.^{2,5} Arylboronic acids and esters are by far the most popular coupling partners due to their operational simplicity and environmentally benign nature.^{11,12} However, some aryl boronic acids, such as 2-heteroarylboronic acids and polyfluorophenylboronic acids, suffer from difficult isolation and base and/or temperature sensitivity, which limits their application in coupling reactions.^{13–16} Arylsilanes, on the other hand, benefit from their high stability to air, moisture, and temperature. Furthermore, the low toxicity of arylsilanes and rich earth abundance of silicon provide additional advantages. However, the strong C–Si bonds are rather inert and need to be activated by high temperature and strong bases for successful transmetalation.^{17,18} Arylstannanes are advantageous from their stability to air and moisture and good reactivity, but organotin reagents are highly toxic, so special care is

needed while handling.¹⁹ The diversity of main group nucleophiles in cross-coupling reactions not only provides complementary methodologies for synthesis but also allows potential chemoselective cross-coupling reactions to construct more complex organic molecules.^{20–26}

1.2 Introduction to Preparation of Arylboronic Acid Derivatives

Arylboronic acid derivatives are useful in organic synthesis. In addition to serving as coupling partners in Suzuki–Miyaura reactions, they can be easily transformed into various carbon–heteroatom bonds (C–N, C–O, C–S, C–Cl, C–Br, etc.) with appropriate reagents.^{27–29} Therefore, the synthesis of arylboronic acid derivatives is of great interest to synthetic chemists.

1.2.1 Conventional Borylation

Traditional synthesis of arylboronic acids and esters involves organolithium or Grignard reagents (Figure I-3a).³⁰ Aryl halides are converted to strongly basic organolithium or Grignard intermediates. Treating the intermediates with boron electrophiles, such as trialkyl boronate, followed by hydrolysis or transesterification under acidic conditions, affords the desired boronic acids or esters.

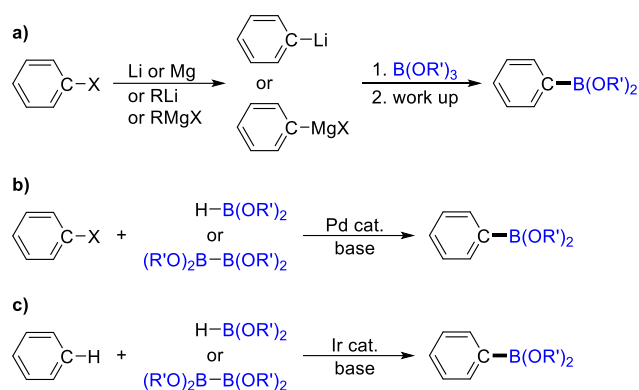


Figure I-3. Preparation of arylboronic acid derivatives. a) Conventional synthesis through aryllithium or Grignard reagents. b) Pd-catalyzed C–X borylation. c) Ir-catalyzed C–H borylation.

1.2.2 Catalytic Borylation of Aryl Halides

Compared to the traditional synthesis, catalytic synthesis of arylboronic acid derivatives via aryl halide or C–H borylation is more attractive. The catalytic approaches minimize the waste generated and have better tolerance for base-sensitive functionalities.

Catalytic borylation of aryl halides involves the coupling reaction with the B–B and B–H reagents (Figure I-3b). Since the first example of Pd-catalyzed borylation of aryl halides reported by Miyaura and co-workers in 1995,³¹ advances in borylation catalyzed by palladium⁹ as well as other transition metals, including nickel,³² copper,^{33,34} iron,^{35,36} and zinc,³⁷ have been well reported.^{38,39} Other strategies, including transition metal-free^{40,41} and photoinduced^{42–44} borylation reactions, have been reported as well.

1.2.3 Catalytic Arene C–H Borylation

Direct aromatic C–H borylation is even more appealing because it avoids the need for a pre-functionalized precursor with carbon–halogen bonds (Figure I-3c). In the past 20

years, C–H borylation has progressed tremendously from a side reaction of organometallic synthesis⁴⁵ to a prominent synthetic method.^{46–48} Although a variety of transition metal^{37,49–57} and main group⁵⁸ complexes has shown catalytic reactivity to aromatic C–H borylation, iridium complexes supported by bipyridine-based and bidentate phosphine ligands have shown remarkably high efficiency to the aromatic C–H borylation with high turnover numbers.^{59–61}

The Ir-catalyzed borylation features high efficiency with low catalyst loading and sterically controlled regioselectivity on a benzene ring.⁶² Monosubstituted benzenes usually lead to the formation of a mixture of *meta*- and *para*-borylation products. Exceptions are those arenes with small and strongly electronegative substituents, such as fluorobenzene.⁶³ Symmetrically substituted 1,2- and 1,4-disubstituted benzenes usually give a single product and 1,3-disubstituted benzenes also form a single product because only one C–H bond (*meta* to both substituents) is more sterically accessible than the others.⁶²

The generally accepted mechanism of Ir-catalyzed borylation is depicted in Figure I-4.^{60,64} The neutral-bidentate-ligand-supported iridium complex reacts with excess H–B or B–B reagent to generate the 16-electron trisboryl iridium(III) complex **F** which is responsible for C–H activation to form the intermediate **G**. Reductive elimination to form C–B bond gives the intermediate **H**. It is followed by the reaction with H–B or B–B reagent to regenerate complex **F**.

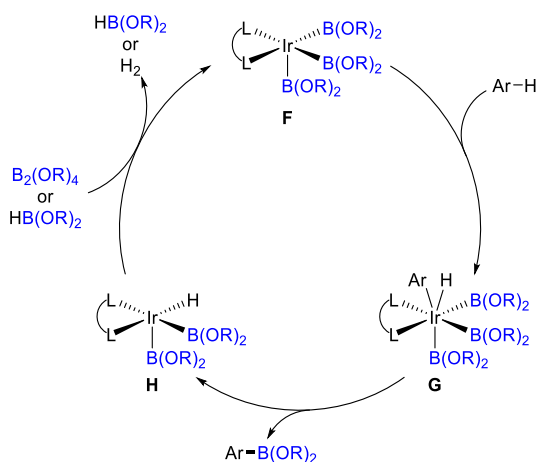


Figure I-4. General mechanism of aromatic C–H borylation catalyzed by neutral bidentate-ligand-supported iridium complexes.

1.3 Introduction to Preparation of Arylgermane Derivatives

Arylgermanes, unlike other main group aryl reagents, have been almost neglected in synthetic organic chemistry until very recently.^{24,65–69} Nonetheless, the research has shown that arylgermanes are useful transmetalation reagents in homogeneous Pd-catalyzed cross-coupling reactions.^{24,70–82} Moreover, Schoenebeck and co-workers have recently demonstrated that arylgermanes have unique, versatile, and orthogonal reactivity in cross-coupling chemistry and other transformations (vs. arylboron, arylsilicon, and aryltin reagents).^{66,67,83} Other applications include serving as traceless linkers in solid-phase synthesis,⁸⁴ Friedel–Crafts acyldegermylation,⁸⁵ synthesis of iodine(III) reagents,⁸⁶ and bulky groups to impart enhanced enantioselectivity in catalysis.⁸⁷ Over the century, synthetic chemists have developed various syntheses to prepare the desired arylgermanes.

1.3.1 Conventional Germylation

Similar to conventional borylation, traditional syntheses of arylgermanes often include nucleophilic substitution by using preformed aryllithium or Grignard reagents from aryl halides (Figure I-5, top).^{71,88-91} However, strongly basic intermediates limit the functional group tolerance on the substances. In addition, selective monoarylation of germanium tetrahalides or tetraalkoxygermanes in a controlled manner is more challenging.^{90,92} When Grignard reactions are employed, a total absence of free magnesium or strict control on the stoichiometric equivalence of reagents is required to avoid the formation of digermanes or polygermanes.^{89,93} The direct reactions by mixing halogermanes, aryl halides, and metal reductants, such as sodium,⁸⁸ magnesium,^{94,95} copper,⁹² and zinc,⁹⁶ have also been reported with limited scope (Figure I-5, bottom).

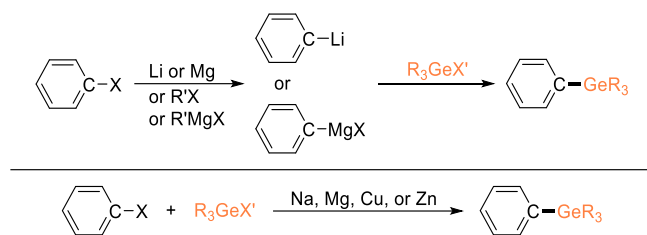


Figure I-5. Conventional synthesis of arylgermanes.

1.3.2 Catalytic Germylation of Aryl Halides

Transition metal-catalyzed germylation of aryl halides with Ge-H/Ge-Ge reagents allows smooth conversion of aryl halides to arylgermanes with better compatibility to sensitive functional groups (Figure I-6). In 1991, Tanaka and co-workers first reported the Pd-catalyzed germylation of aryl halides using Me₂ClGe-GeClMe₂.⁹⁷ In 2002, Oshima

and co-workers reported Pd-catalyzed germylation of Ar-I with tri(2-furyl)germane.⁷⁵ The resulting aryltri(2-furyl)germane is active in Pd-catalyzed cross-coupling reaction upon activation by TBAF. Pd-catalyzed germylation of aryl halides using Ge-H reagents have also been applied to the synthesis of multifunctionalized arylgermanes, arylgermatranes, and π -conjugated materials.^{24,98,99} Rh-catalyzed synthesis of arylgermatrane via germylation of aryl halides has been reported as well.¹⁰⁰

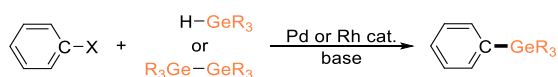


Figure I-6. Pd- or Rh-catalyzed germylation of aryl halides.

1.3.3 C-H Germylation

An alternative pathway to synthesize arylgermanes is through transition metal-catalyzed C-H germylation with Ge-H/Ge-Ge reagents (Figure I-7). The first example of dehydrogenative C-H germylation was reported by Seki, Murai, and co-workers in 1996, in which ruthenium and rhodium complexes were found to be active for the synthesis of vinylgermanes from olefins and ⁿBuGeH.¹⁰¹ Later research of dehydrogenative germylation focused more on using rhodium complexes because of their exceptional ability to activate C-H bonds. Murai, Takai, and co-workers demonstrated that rhodium complexes were promising for intramolecular dehydrogenative sp² and sp³ C-H germylation to synthesize germaheterocyclic compounds.¹⁰²⁻¹⁰⁴ The Rh-catalyzed dehydrogenative C-H germylation has been utilized to synthesize π -conjugated molecules with intriguing photophysical and electronic properties.^{99,105}

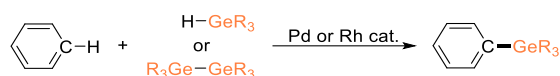


Figure I-7. Pd- or Rh-catalyzed C–H germylation.

Pd-catalyzed C–H germylation using $\text{Me}_3\text{Ge-GeMe}_3$ has also been reported. These reactions either needed directing groups to achieve regioselective C–H activation^{106–108} or were based on the known template to form palladacycle intermediates,^{109–111} followed by functionalization with Ge_2Me_6 to give germylation products. Similar sp^3 C–H germylation reactions have been reported as well.^{112,113} Notably, most of these reactions were merely “additional” examples to the silylation reaction.

Very recently, Schoenebeck and co-workers reported “formal” C–H germylation through aryl sulfonium salts (Figure I-8).^{114,115} Arylsulfonium salt intermediates were synthesized through regioselective C–H functionalization without a directing group and utilized with no further purification in the Pd-catalyzed or metal-free germylation. The corresponding 2,3,7,8-tetrafluorothianthrene and dibenzothiophene moieties can be readily recovered and reused.

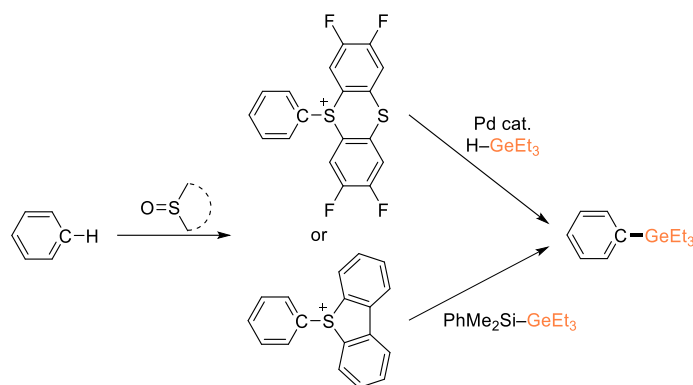


Figure I-8. Schoenebeck's recent reported "formal" C – H germylation.

It is worth mentioning that none of the abovementioned C–H germylation methods were capable of preparing arylgermanes with germanium–halogen or germanium–oxygen bonds. One reason is that many tetravalent Ge–H or Ge–Ge reagents with halogen or oxygen substituents are too unstable to isolate or simply unknown.

1.3.4 Germylene Insertion of Aryl Halides

Germylenes, germanium analogues of carbenes, are divalent germanium compounds that have a singlet ground state with an empty p-orbital and a lone pair on germanium.^{116,117} Similar to carbenes, divalent germylenes can undergo σ -bond insertion reactions to form tetravalent germanium species.^{116–118} Therefore, insertion of germanium(II) dihalides into aryl carbon–halogen bonds provides an attractive approach to synthesize aryltrihalogermanes. Free germanium dihalides are extremely reactive so early examples used germanium dihalides which were generated in situ at high temperature (over 150 °C) to react with aryl halides to give desired aryltrihalogermanes.^{92,118} In 1999, Schmidbaur and co-workers used an AlCl_3 -catalyzed

reaction of Ar–Br with germanium dichloride–dioxane complex ($\text{GeCl}_2 \cdot \text{C}_4\text{H}_8\text{O}_2$) at 80 °C to prepare arylgermanes as mixtures of ArGeBr_3 and ArGeCl_3 in excellent overall yields (Figure I-9, top).⁹⁰ Suzuki and co-workers, in 2001, reported the direct synthesis of PhGeCl_3 from elemental germanium, GeCl_4 , and PhCl .¹¹⁹ In this reaction, GeCl_2 was formed as an intermediate, and 98% of germanium was converted to PhGeCl_3 selectively (Figure I-9, bottom). Although this reaction featured remarkable atom-efficiency, the need of using an autoclave at over 300 °C made this reaction impractical to use in regular laboratory synthesis.

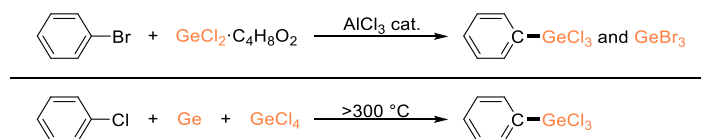


Figure I-9. Germylene insertion into an aryl carbon–halide bond to form aryltrihalogermane.

1.4 Introduction to Pincer Ligands

Pincer ligands are a broad class of tridentate chelating ligands capable of meridional coordination to a metal center. Organometallic complexes supported by meridionally chelating tridentate ligands were first reported in 1976 by Shaw and co-workers,¹²⁰ but the term “pincer” was not introduced until 1989 by van Koten.¹²¹ Since then, pincer ligands have been widely utilized and studied in organometallic chemistry and homogeneous catalysis. Pincer ligands are attractive because of their ability to impart remarkable thermal stability to the metal complexes and generate a well-defined coordination sphere.^{122,123}

The electronic and steric properties of pincer ligands can be fine-tuned by precise control on the central donor (X), side donors (LR_n), arm linkers (Y), and other substituents (Z), without significantly affecting the coordination environment at the metal center (Figure I-10).¹²² The electron-donating ability of the binding donors (X and L) affects the electronic properties of the pincer complexes. The central donor (X) particularly can impart effect at the metal center through the *trans* influence. The overall electron-donating ability of pincer ligands can be studied through combined experimental results from the DFT studies on Ir–CO¹²⁴ and Pt–Cl¹²⁵ complexes and X-ray crystallographic data of various Pd–Cl and Pd–I complexes.^{126–129} The electron-donating ability of the anionic central donor follows the order of boryl > silyl > alkyl ~ phosphido > aryl > amido. The steric properties are mainly controlled by the substituents on side donors (R). Tertiary phosphines as side donors are popular due to their well-understood properties as supporting ligands in organometallic chemistry and the steric properties have been reported by Tolman.¹³⁰

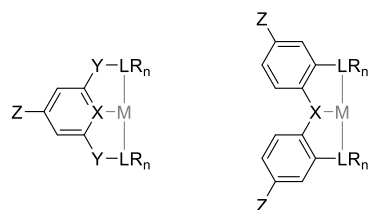


Figure I-10. Generic pincer complexes. M = metal center; X = central donor; L = side donors; R = substituents on side donors; Y = specific arm linkers; Z = other substituents.

The nomenclature of pincer ligands usually identifies three donor atoms in order, LXL. Common pincer complexes incorporate two fused five-membered metallacycles. The arm linkers (Y) can determine the ring size and consequently affect the bite angle. When it is necessary to specify the arm linkers and/or the ring sizes, the more comprehensive “[m,n]-LYXYL” nomenclature can be used, where m and n denote the ring size and Y denotes the arm linker atoms.¹³¹ Pincer ligands can be categorized according to the neutral or ionic nature of their binding donors. For example, monoanionic LXL-type pincer ligands consist of an anionic central donor and two neutral side donors (L = neutral donor; X = anionic donor). Representative examples of LXL-type pincer ligands are shown in Figure I-11.

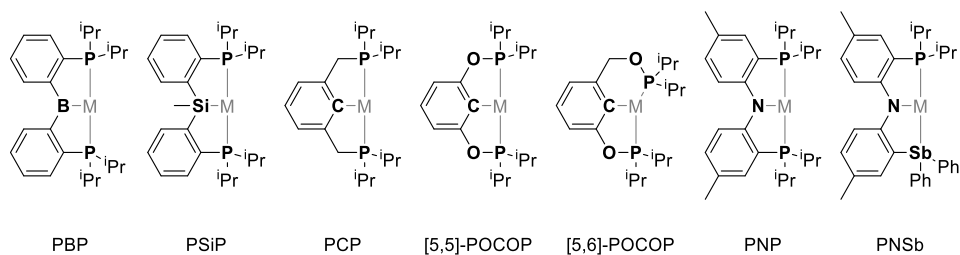


Figure I-11. Selective examples of LXL-type pincer ligands.

CHAPTER II

SYNTHESIS OF PXL PINCER COMPLEXES OF IRIDIUM AND RHODIUM AND THEIR CATALYTIC REACTIVITY TO AROMATIC C–H BORYLATION*

2.1 Introduction

2.1.1 *The State-of-the-Art Aromatic C–H Borylation*

The state-of-the-art catalytic aromatic C–H borylation uses iridium complexes supported by bipyridine-based or bidentate phosphine ligands as catalysts, which were first contemporaneously developed by Ishiyama, Miyaura, Hartwig and co-workers,⁵⁹ and Maleczka, Smith, and co-workers.⁶⁰ In the first system developed by Ishiyama, Miyaura, Hartwig, and co-workers, [Ir(COD)Cl]₂ and bipyridine were selected to catalyze the borylation under mild conditions. In this system, there was a long induction period for the formation of the active iridium species, and a large excess of arene (60 equiv) was needed.⁵⁹ Similar stoichiometric excess of one of the reagents was also required in Maleczka's and Smith's system.⁶⁰ The problems were later overcome by using the combination of [Ir(COD)(OMe)]₂ and ^tBu-bpy. This system, which catalyzes the borylation at ambient temperature and allows the use of arenes and the boryl source in a 1:1 ratio, is commonly called the “ITHM arene borylation system” (refer to the initials of the four authors).¹³²

* Part of this chapter is reprinted with permission from “Examination of a Series of Ir and Rh PXL Pincer Complexes as (Pre)catalysts for Aromatic C–H Borylation” by Hung, M.-U.; Press, L. P.; Bhuvanesh, N.; Ozerov, O. V. *Organometallics* **2021**, *40*, 1004–1013. Copyright 2021 American Chemical Society.

2.1.2 Pincer Complexes of Iridium in Aromatic C–H Borylation

Pincer-supported iridium complexes have been used in C–H borylation chemistry. In 2011, Shimada and co-workers reported (PSiP)Ir-catalyzed C–H borylation of benzene with B₂pin₂.¹³³ A year later, Driess, Hartwig, and co-workers demonstrated that the iridium complexes supported by the sterically bulky SiCSi (silylene–aryl–silylene), GeCGe (germylene–aryl–germylene), and POCOP^{tBu} pincer ligands were capable of catalyzing C–H borylation of benzene with HBpin.¹³⁴ In 2016, our group reported catalysis of aromatic C–H borylation with HBpin by iridium complexes supported by POCOP-type pincer ligands (Figure II-1 top).⁶³ These catalysts were capable of >10⁴ turnovers, rivaling the activity of the best iridium catalysts supported by bidentate ligands. Interestingly, the (POCOP)Ir catalysis proceeded by a different mechanism, in which the C–H activation happens at a 14-electron boryl-free iridium(I) center (Figure II-1 bottom). In addition, the catalysis requires the use of a sacrificial olefin for kinetic reasons. This is in contrast to the catalysis by the bidentate-ligand-supported iridium, which does not require and is indeed poisoned by simple olefins (Figure I-4).¹³⁴ On the whole, there exists a remarkable mechanistic diversity of possible C–H borylation pathways with iridium, depending on the supporting ligands and the substrate.

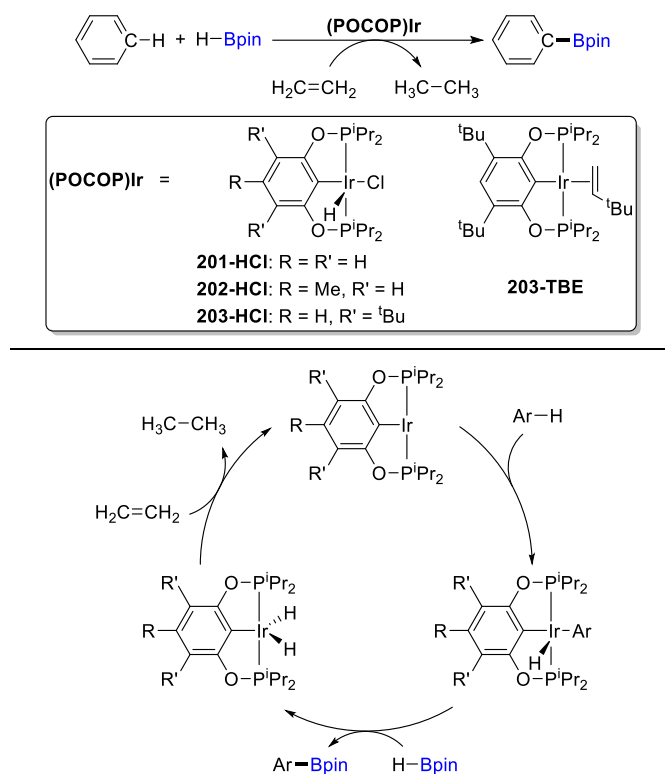


Figure II-1. Top: (POCOP)Ir-catalyzed arene C–H borylation. Bottom: Proposed reaction mechanism of (POCOP)Ir-catalyzed arene C–H borylation.

2.2 Results and Discussion

On the basis of our 2016 work, a series of iridium complexes supported by PXP- and PXL-type ligands were examined as arene C–H borylation catalysts, potentially targeting improved selectivity and activity. Some analogous pincer complexes of rhodium were tested in this work as well.

2.2.1 Synthesis of Pincer Ligands

We set out to examine a variety of ligands with a central aryl group, as well as ligands that possess other central anionic donors based on amido, boryl, or silyl (Figure

II-2). Ligands **204–215** have phosphines as L-type side donors and an aryl site as an X-type central donor (PCP ligands). The series of ligands were selected to explore steric and electronic variations in the PCP pincer structure. Ligand **216** was chosen to compare a sulfur donor to a phosphorus donor and also to examine the steric effect of three *tert*-butyl groups about the metal as opposed to four isopropyl or four *tert*-butyl groups. Ligands **217–220** were chosen to test the viability of different X-type central donors: amido, boryl, and silyl.

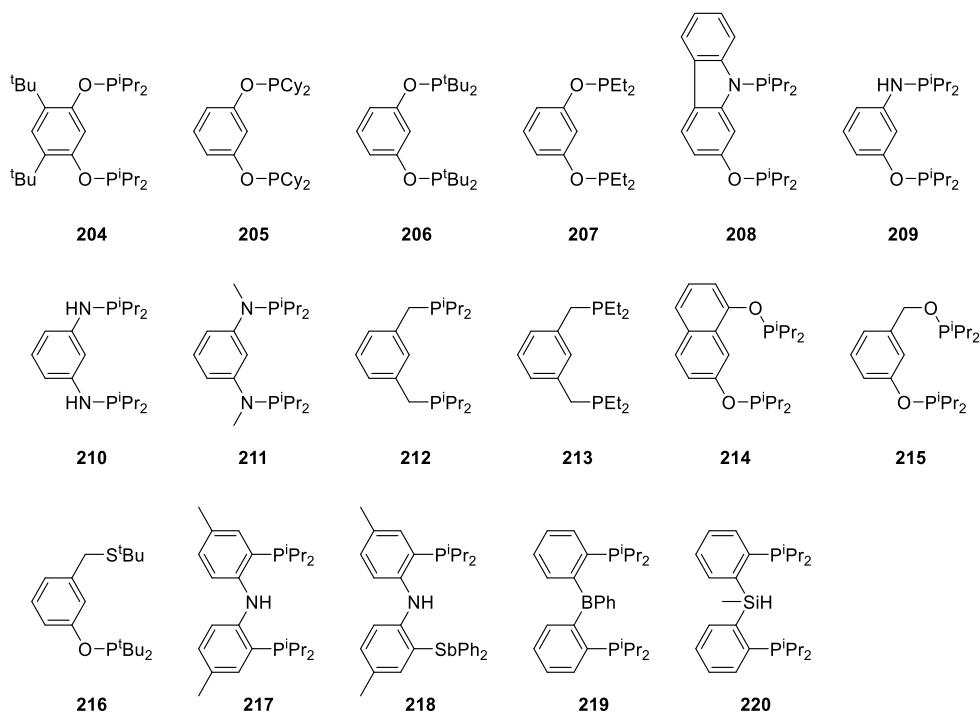


Figure II-2. LXL-type pincer ligands in this study.

204,⁶³ **206,**¹³⁵ **207,**¹³⁶ **209,**¹³⁷ **210,**¹³⁷ **211,**¹³⁸ **212,**¹³⁹ **213,**¹³⁹ **214,**¹⁴⁰ **215,**¹⁴⁰ **217,**¹²⁶ **218,**¹⁴¹ **219,**¹⁴² and **220**¹³³ have been previously reported and were synthesized as

described in the literature. **205** was prepared from 1,3-resorcinol **221**, Cy_2PCl , and Et_3N as a base. **208** was prepared analogously from 2-hydroxycarbazole **222**, ${}^i\text{Pr}_2\text{PCl}$, and ${}^n\text{BuLi}$ as a base. **208** contained two isomers in a ca. 1:1 ratio. In the ${}^{31}\text{P}\{{}^1\text{H}\}$ NMR spectrum in C_6D_6 at ambient temperature, four ${}^{31}\text{P}$ NMR resonances were observed. ${}^{31}\text{P}$ NMR resonances at δ 148.7 and 147.9 were assigned to P–O of two isomers, respectively, and ${}^{31}\text{P}$ NMR resonances at δ 61.2 and 60.6 were assigned to P–N of two isomers, respectively. The ${}^1\text{H}$ NMR spectrum also showed two sets of resonances that correspond to two isomers. The nature of the two isomers was not determined, but we tentatively assume that these are rotamers arising from restricted rotation associated with the N–P and/or C–O–P bonds. **216** was synthesized from 3-hydroxybenzyl alcohol **223**. **223** was chlorinated with SOCl_2 and pyridine to provide 3-hydroxybenzyl chloride **224**. **224** was treated with NaH and ${}^t\text{Bu}_2\text{PCl}$ to provide compound **225**. **225** was then treated with NaS^tBu to provide **216**.

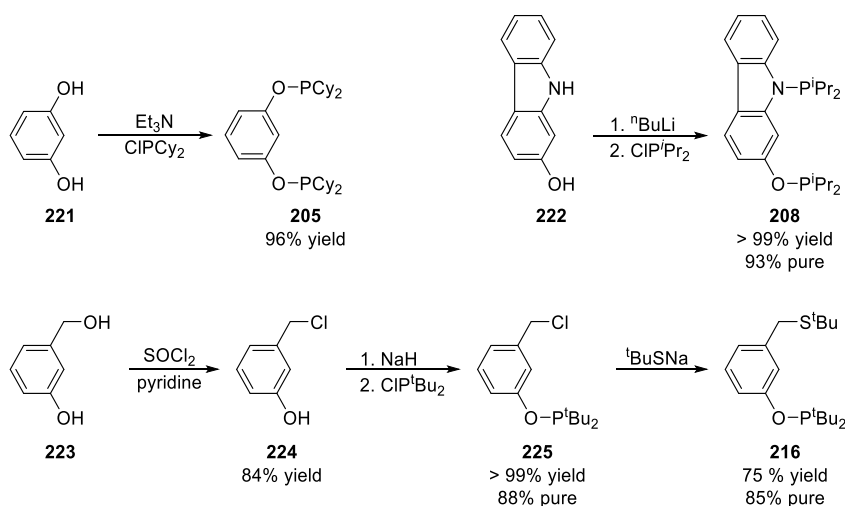


Figure II-3. Synthesis of **205**, **208**, and **216**.

2.2.2 Synthesis and Characterization of Pincer Complexes

All of the pincer complexes in this study are shown in Figure II-4. The pincer complexes of rhodium, **236-HCl**,¹⁴³ **238-H₂**,¹⁴⁴ and **239-HCl**,¹⁴² were prepared as previously described. Literature procedures were also used to obtain Ir complexes with central donors other than aryl, **232-HCl**,¹⁴⁵ **233-COE**,¹⁴¹ **234-H₄**,¹⁴⁶ and **235-HCl**.¹³³

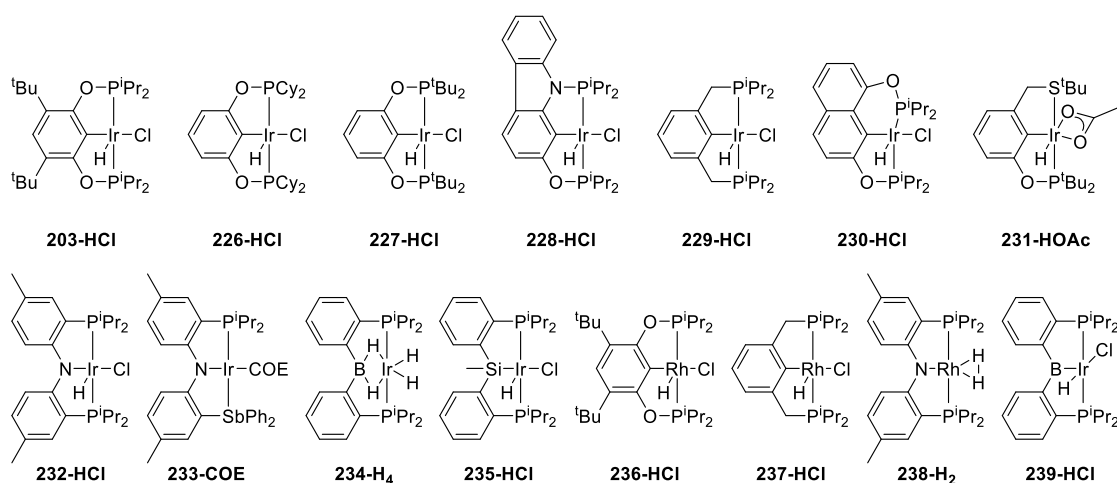


Figure II-4. Pincer complexes of iridium and rhodium in this study.

Installation of the PCP ligands into the coordination sphere of iridium is most conveniently accomplished via reaction of the ligand precursor with $[(\text{COD})\text{IrCl}]_2$ or $[(\text{COE})_2\text{IrCl}]_2$. The insertion of a metal center into the central aromatic C–H bond and the loss of the olefin placeholder ligand, COD and COE, can ideally lead to the five-coordinate iridium(III) complex (pincer)Ir(H)(Cl) (Figure II-5, method A). However, method A does not always provide for the clean formation of the desired product; therefore, different strategies were sampled to access the desired (pincer)Ir complexes.

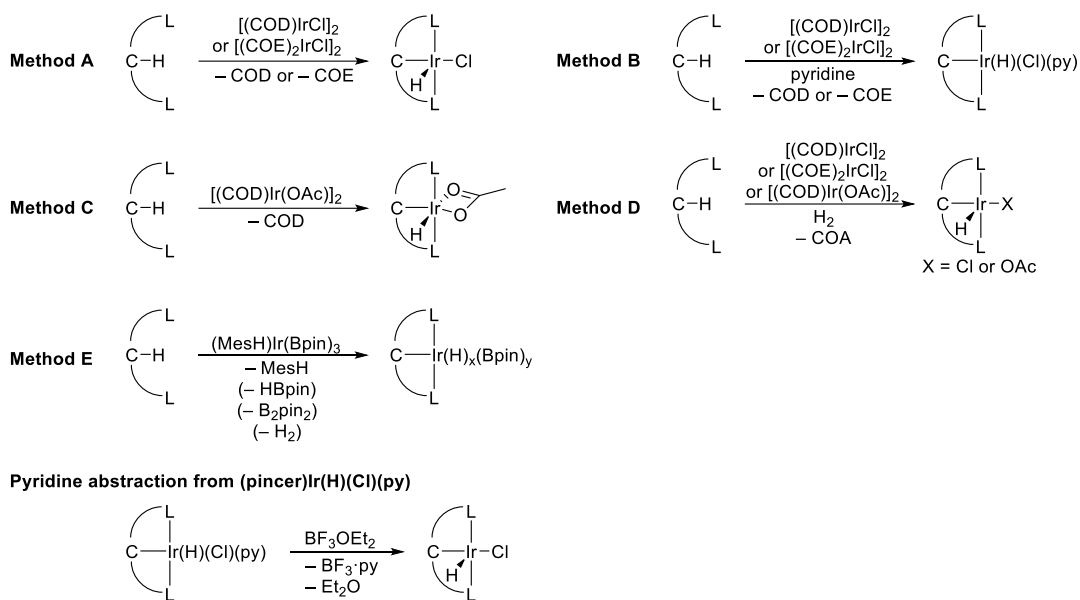


Figure II-5. Different Methods for Metalation of PCP Ligands.

Reacting $[(\text{COD})\text{IrCl}_2]$ or $[(\text{COE})_2\text{IrCl}_2]$ with pyridine prior to the addition of the ligand precursor results in the formation of a pyridine adduct, $(\text{pincer})\text{Ir(H)(Cl)(py)}$ (Figure II-5, method B). The pyridine ligand can then be abstracted with BF_3OEt_2 to give the desired five-coordinate complex $(\text{pincer})\text{Ir(H)(Cl)}$. This approach has been reported to access clean $(\text{POCOP})\text{Ir}$ and $(\text{POCOP})\text{Rh}$ complexes.^{63,140,147} Alternatively, $[(\text{COD})\text{M(OAc)}_2]$ (M = Ir, Rh) was also used in the metalation of the pincer ligands to yield the products $(\text{pincer})\text{Ir(H)(OAc)}$.^{140,148} The κ^2 -acetate ligand provides protection to the sixth coordination site of the iridium center (Figure II-5, method C). Another approach (Figure II-5, method D) was described by Waterman and co-workers, who reported that the synthesis of **201-HCl** in high yield from the ligand precursor with $[(\text{COE})_2\text{IrCl}_2]$ under an atmosphere of H_2 .¹⁴⁹ Besides iridium(I) precursor, iridium(III) trisboryl precursor,

(MesH)Ir(Bpin)₃ was tested to metalate pincer ligand, aiming to make (pincer)IrH_x(Bpin)_y complexes (Figure II-5, method E).

Methods A–E were then screened for the metalation of a PCP ligand on the 10–100 μmol scale (Table II-1). Iridium complexes **203-HCl**, **226-HCl**, **227-HCl**, and **228-HCl** were successfully formed via method A. Using method B, **230-HClpy** and **240-HClpy** were successfully formed. **231-HOAc** was formed cleanly by using method C. Method D was used to yield **226-HCl** and **229-HCl**. Unfortunately, we were not able to optimize the syntheses or isolation of the desired iridium products from the reactions using **207**, **210**, **211**, **213**, and **215**.

Table II-1. Screening of methods for metalation of PCP pincer ligands.^a

ligand	method A	method B	method C	method D	method E
204	○ ⁶³	–	–	–	–
205	○	–	–	○	–
206	○ ¹³⁵	–	–	–	–
207	–	×	×	×	×
208	△ with [(COD)IrCl] ₂ ○ with [(COE) ₂ IrCl] ₂	△	–	–	–
209	▲ with [(COD)IrCl] ₂ △ with [(COE) ₂ IrCl] ₂	○	△	△	×
210	△	△	×	×	–
211	×	×	×	×	△
212	▲ ¹⁵⁰	–	–	○	–
213	–	×	×	×	×
214	×	△ with [(COD)IrCl] ₂ ○ with [(COE) ₂ IrCl] ₂	×	×	–
215	×	×	×	×	△
216	×	–	○	×	–

^aLegend: ○, the desired product formed as the only product; △, the desired product formed as a major product (>50%); ▲, the desired product was observed as a minor product (<50%); ×, the desired product was not observed or identified; –, did not test.

Figure II-6 shows the syntheses of new iridium complexes (top) and the improved syntheses of **229-HCl** and **237-HCl** (bottom) on a preparative scale. **229-HCl** and **237-HCl** have been previously accessed via method A in low yields and with difficult workup.^{140,150} The use of method D allowed isolation of these compounds in excellent yields from a single step. **226-HCl**, **228-HCl**, **230-HClpy**, **231-HOAc**, and **240-HClpy** were then prepared in moderate to excellent yields by the best methods on the basis of the screening experiments in Table II-1. **230-HClpy** and **240-HClpy** both exist as a pair of isomers, related by the exchange of positions of pyridine and chloride about the octahedral iridium (Figure II-7). Abstraction of pyridine from **230-HClpy** and **240-HClpy** was attempted by reacting with BF_3OEt_2 . The “pyridine-free” unsaturated iridium complexes **230-HCl** and **240-HCl** were observed in the reaction mixture with excess BF_3OEt_2 , as well as the expected byproduct BF_3py . The pentane-soluble **230-HCl** was then successfully isolated in 54% yield. However, attempts at the isolation of **240-HCl** from the reaction mixture were not successful due to the similar solubilities of **240-HCl** and BF_3py . Neither recrystallization nor reprecipitation from toluene, pentane, or mixed solvents was successful. Using THF or column chromatography on silica gel to separate **240-HCl** from BF_3py resulted in the regeneration of **240-HClpy**. The preparation of (pincer)Ir(H)(Cl) through method B (+ pyridine abstraction) seemed to work only if the resulting (pincer)Ir(H)(Cl) and BF_3py have a dramatic solubility difference. Further attempts to transform **240-HClpy** to other iridium complexes did not lead to any isolable iridium complexes (Figure II-8).

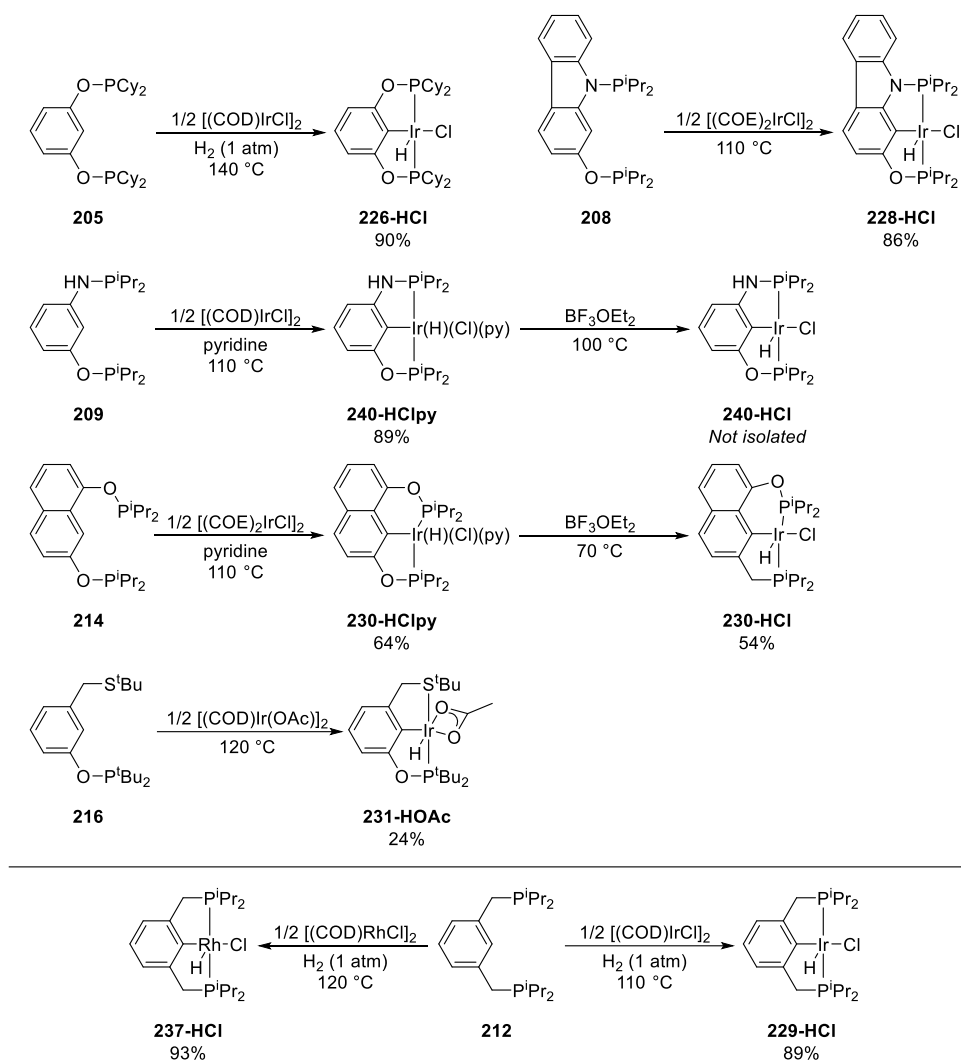


Figure II-6. Preparative synthesis of iridium and rhodium complexes.

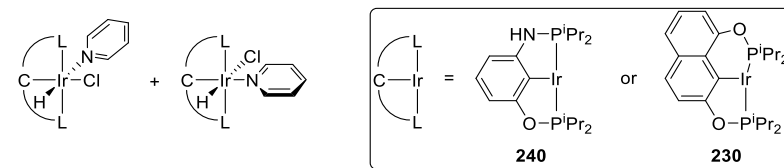


Figure II-7. Two configurational isomers in **230-HClpy** and **240-HClpy**.

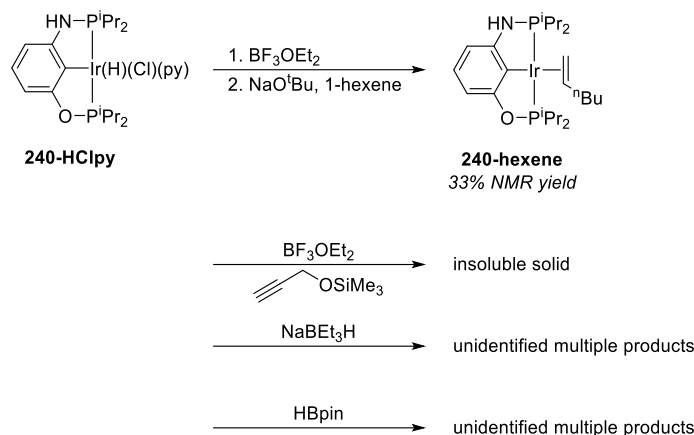


Figure II-8. Attempted transformations of **240-HClpy**.

The newly synthesized complexes **226-HCl**, **228-HCl**, **230-HCl**, and **231-HOAc** were characterized by ^1H , $^{13}\text{C}\{^1\text{H}\}$, and $^{31}\text{P}\{^1\text{H}\}$ NMR spectroscopy and elemental analysis. **230-HClpy**, **240-HClpy**, and **240-HCl** were characterized by ^1H and $^{31}\text{P}\{^1\text{H}\}$ NMR spectroscopy. The ^1H NMR chemical shifts for Ir-H and $^{31}\text{P}\{^1\text{H}\}$ NMR chemical shifts are given in Table II-2.

Table II-2. ^1H NMR (Ir-H) and ^{31}P NMR chemical shifts of iridium complexes.

	^1H NMR (Ir-H) (ppm)	^{31}P NMR (ppm)	$^2J_{\text{P-P}}$ (Hz)
203-HCl ⁶³	-36.6	173.5	-
226-HCl	-37.25	166.7	-
228-HCl	-36.77	171.1, 115.6	373
230-HClpy	-20.74 (major) -20.42 (minor)	144.6, 120.9 (major) 144.1, 112.0 (minor)	406 (major) 395 (minor)
230-HCl	-36.39	172.7, 150.1	385
231-HOAc	-28.80	156.8	-
240-HClpy	-21.20 (major) -21.33 (minor)	147.0, 80.6 (major) 145.2, 80.1 (minor)	383 (major) 373 (minor)
240-HCl	-37.42	170.9, 106.0	365

The solid-state structure of **231-HOAc** was determined by single-crystal XRD methods (Figure II-9). As expected, the pincer ligand **216** is bound meridionally (P1–Ir1–S1 = 164.61(3)°) to the iridium center. One of the oxygen atoms (O2) in the κ^2 -acetate is *trans* to the central aryl carbon (C1), and another oxygen atom (O3) is *trans* to the implied hydride ligand. The Ir1–O3 bond (2.296(2) Å) *trans* to the hydride is longer than the Ir1–O2 bond (2.211(2) Å) *trans* to C(aryl). The *tert*-butyl group on the sulfur donor is *syn* to the hydride ligand.

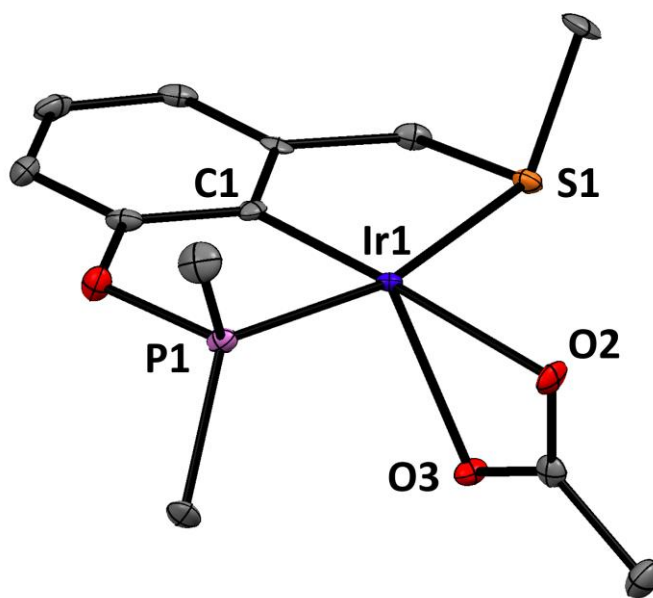


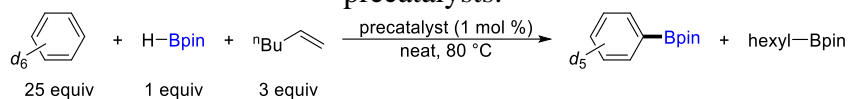
Figure II-9. The ORTEP¹⁵¹ drawings (50% probability ellipsoids) of **231-HOAc** (CCDC 2041134). Hydrogen atoms and methyl groups of *tert*-butyl arms are omitted for clarity. Selected distances (Å) and angles (deg): Ir1–C1, 1.998(3); Ir1–O2, 2.211(2); Ir1–O3, 2.296(2); P1–Ir1–S1, 164.61(3); O2–Ir1–S1, 91.38(7); O2–Ir1–P1, 103.78(7); C1–Ir1–S1, 83.98(10); C1–Ir1–P1, 81.36(10).

2.2.3 Catalysis of Aromatic C–H Borylation

We then examined the catalytic activity of the iridium and rhodium complexes in the aromatic C–H borylation. In our previous report, both 1-hexene and C₂H₄ allowed efficient catalysis with **203-HCl**.⁶³ In this study, we selected 1-hexene for its operational simplicity in the J. Young NMR tube experiments. The reaction progress was followed by ¹H NMR spectroscopy using cyclohexane as an internal standard. The model reaction used HBpin as the limiting reagent, 25 equiv of C₆D₆ as the substrate, 1 mol% precatalyst loading, and 3 equiv of 1-hexene.

The screening results are summarized in Table II-3. Iridium complexes bearing PXL-type pincer ligands with an aryl carbon as a central donor, except for **227-HCl**, catalyzed aromatic C–H borylation with moderate to good chemoselectivity over the competing hydroboration side reaction (Table II-3, entries 1–7). **227-HCl** only catalyzed hydroboration of 1-hexene (Table II-3, entry 3). Iridium complexes supported by the PBP, PNP, PNSb, and PSiP ligands did not show catalytic activity for aromatic C–H borylation; they did catalyze hydroboration (Table II-3, entries 8–11). The rhodium complexes also did not catalyze C–H borylation (Table II-3, entries 12–15). The reaction without 1-hexene was also conducted. Without 1-hexene, none of the reactions gave any detectable formation of C₆D₅Bpin.

Table II-3. Aromatic C–H borylation experiments using iridium or rhodium precatalysts.^a



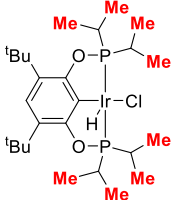
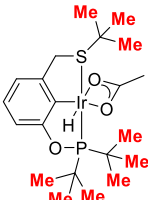
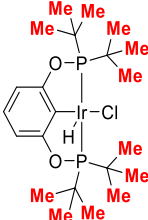
entry	precatalyst	time (h)	conversion (%) ^b	yield (%) ^b	
				C ₆ D ₅ Bpin	hexyl-Bpin
1	203-HCl	1	100	80	19
2	226-HCl	15	100	89	11
3	227-HCl	24	100	1	96
4	228-HCl	3	100	85	13
5	229-HCl	3	100	89	11
6	230-HCl	15	94	65	29
7	231-HOAc	15	95	40	45
8	232-HCl	15	100	2	98
9	233-COE	1	100	0	95
10	234-H₄	15	100	2	94
11	235-HCl	15	100	2	98
12	236-HCl	16	5	0	4
13	237-HCl	16	16	0	4
14 ^c	238-H₂	0.16	100	0	81
15	239-HCl	15	88	0	71

^aReaction conditions: HBpin (36 μ L, 0.25 mmol), 1-hexene (93 μ L, 0.75 mmol), and precatalyst (2.6 μ mol) in C₆D₆ (555 μ L, 6.27 mmol), 80 °C, under Ar. ^bConversions and yields were determined by ¹H NMR spectroscopy using cyclohexane as an internal standard. Errors were estimated to be \pm 2.5%.

^cReaction was completed at ambient temperature in 10 min.

In the previously reported (POCOP)Ir-catalyzed C–H borylation, it has been shown that the reaction is sensitive to the steric hindrance.⁶³ The steric properties at the metal center in pincer complexes are mainly controlled by substituents on side donors.¹²² Comparing the steric properties of **203-HCl**, **231-HOAc**, and **227-HCl**, and the chemoselectivity for C–H borylation over hydroboration shows that as the steric environment at the iridium center becomes more crowded, the chemoselectivity decreases (Table II-4).

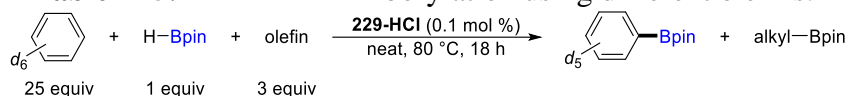
Table II-4. Comparison of the steric hindrance and the chemoselectivity of iridium complexes.

iridium complex	structure	“methyl groups” on side donors	chemoselectivity: C–H borylation/hydroboration
203-HCl		8	81/19
231-HOAc		9	47/53
227-HCl		12	1/99

After we identified the promising complexes **203-HCl**, **226-HCl**, **228-HCl**, **229-HCl**, **230-HCl**, and **231-HOAc** for aromatic C–H borylation, **229-HCl** was chosen as a precatalyst to further examine different reaction conditions because it showed the best reactivity and chemoselectivity (Table II-3, entry 5). First, we identified that 1-hexene is a promising H₂ acceptor. Table II-5 summarizes the results when various olefins were used in comparison to 1-hexene. Bulky *tert*-butylethylene and internal alkenes did not provide the desired reactivity (Table II-5, entries 2–4). Next, we investigated the effect of the reagent ratio on the reactivity and chemoselectivity, and the results are summarized in Table II-6. A large excess of arene is crucial for good chemoselectivity (Table II-6, entries 4–6 vs. entries 1–3). The chemoselectivity was not much affected by the amount of 1-

hexene added when more than 2 equiv of 1-hexene was used. However, using 3 equiv of 1-hexene allowed completion of the reaction within 19 h, while up to 38 h was required when 2 equiv of 1-hexene was used (Table II-6, entries 3 and 6 vs. entries 2 and 5). These results are consistent with the previously reported aromatic C–H borylation by (POCOP)Ir complexes.⁶³

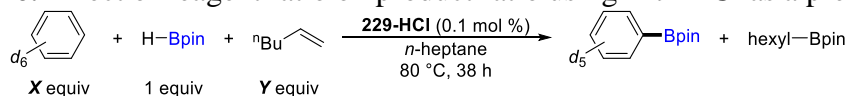
Table II-5. Aromatic C–H borylation using different olefins.^a



entry	olefin	conversion (%) ^b	yield (%) ^b	
			C ₆ D ₅ Bpin	alkyl-Bpin
1	1-hexene	100	83	17
2	<i>tert</i> -butylethylene (TBE)	100	3	1
3	<i>cis</i> -cyclooctene (COE)	100	0	0
4	norbornene	100	10	3

^aReaction conditions: HBpin (36 μ L, 0.25 mmol), **229-HCl** (0.27 μ mol), C₆D₆ (550 μ L, 6.21 mmol), olefin (0.74 mmol), 80 °C, under Ar, 18 h. ^bConversions and yields were determined by ¹H and/or ¹¹B{¹H} NMR spectroscopy using cyclohexane as a ¹H internal standard. Errors were estimated to be \pm 2.5%.

Table II-6. Effect of reagent ratio on product ratio using **229-HCl** as a precatalyst.^a



entry	C ₆ D ₆ (M) [X]	1-hexene (M) [Y]	conversion (%) ^b	yield (%) ^b	
				C ₆ D ₅ Bpin	hexyl-Bpin
1	1.7 [5]	0.33 [1]	33	23	9
2	1.7 [5]	0.66 [2]	100	72	28
3 ^c	1.7 [5]	1.0 [3]	100	64	36
4	8.4 [25]	0.33 [1]	47	40	6
5	8.4 [25]	0.66 [2]	100	86	14
6 ^c	8.4 [25]	1.0 [3]	100	83	17

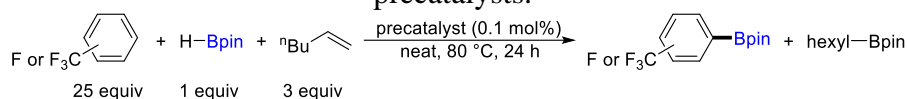
^aReaction conditions unless specified otherwise: HBpin (70 μ L, 0.48 mmol, 0.33 M), **229-HCl** (0.49 μ mol), C₆D₆, 1-hexene in *n*-heptane, 80 °C, under Ar, 38 h. ^bConversions and yields were determined by ¹¹B{¹H} NMR spectroscopy. Errors were estimated to be \pm 2.5%. ^cHBpin was consumed after 19 h.

With the optimized conditions in hand, we then tested the regioselectivity of the catalysis using complexes **203-HCl**, **226-HCl**, **228-HCl**, **229-HCl**, **230-HCl**, and **231-HOAc**. The regioselectivity of aromatic C–H borylation catalyzed by pincer catalysts in the previously reported examples, similar to those catalyzed by non-pincer iridium catalysts, is mainly sterically controlled.^{62,63} When **202-HCl** was used as a precatalyst in our 2016 study, borylation of PhF with 0.03 mol% precatalyst loading at 80 °C for 24 h under an atmosphere of C₂H₄ gave a borylated product mixture in 45% yield (*ortho/meta/para* = 40/46/14).⁶³ The same conditions for the borylation of PhCF₃ gave a mixture of borylated products in total 43% yield (*ortho/meta/para* = 0/70/30).⁶³ In this study, PhF and PhCF₃ were selected as model substrates to test the regioselectivity on sp² C–H bonds when different iridium complexes were used as precatalysts.

Table II-7 details the results of the regioselectivity tests in reactions conducted at 80 °C for 24 h with 0.1 mol% precatalyst loading using PhF and PhCF₃, respectively. **203-HCl** and **229-HCl** showed the highest reactivity, fully consuming HBpin with 0.1 mol% precatalyst loading in 24 h (Table II-7, entries 1, 4, 7, and 10). Reactions catalyzed by **229-HCl** gave the highest chemoselectivity for C–H borylation over hydroboration of up to 5.8:1. The C–H borylation of PhF, which has a small fluorine substituent, yielded mixtures of all three possible products; however, different product ratios were observed when **229-HCl**, **230-HCl**, and **231-HOAc** were used in comparison to **203-HCl** (Table II-7, entries 4–6 vs. entry 1). The borylation of PhCF₃, which has a larger substituent, gave very similar regioselectivity when different precatalysts were used (Table II-7, entries 7–12). In addition, we investigated the chemoselectivity of precatalysts **203-HCl** and **229-**

HCl with regard to the activation of sp^2 C–H, sp^3 C–H, or C–Cl bonds using 3-chlorotoluene as a test substrate (Figure II-10). In both experiments, C–Cl bonds remained untouched. **229-HCl** possessed excellent sp^2/sp^3 C–H selectivity in a ratio of 35/1, while the selectivity of **203-HCl** was 5.6/1.

Table II-7. Regioselectivity test for aromatic C–H borylation using iridium precatalysts.^a



entry	precatalyst	ArH	conversion (%) ^b	yield (%) ^b		
				Ar–Bpin	hexyl–Bpin	<i>ortho/meta/para</i> ^c
1	203-HCl	PhF	100	66	32	54/40/6
2	226-HCl	PhF	49	32	8	55/40/5
3	228-HCl	PhF	60	34	15	52/41/7
4	229-HCl	PhF	100	81	14	32/54/14
5	230-HCl	PhF	30	4	17	30/44/26
6	231-HOAc	PhF	93	19	45	22/67/11
7	203-HCl	PhCF ₃	100	66	25	0/69/31
8	226-HCl	PhCF ₃	27	12	8	0/71/29
9	228-HCl	PhCF ₃	33	15	14	0/69/31
10	229-HCl	PhCF ₃	96	72	14	0/69/31
11	230-HCl	PhCF ₃	26	3	11	0/72/28
12	231-HOAc	PhCF ₃	81	16	26	0/75/25

^aReaction conditions when PhF is used as the substrate: HBpin (62 μ L, 0.43 mmol), 1-hexene (160 μ L, 1.28 mmol), and precatalyst (0.45 μ mol) in PhF (1.00 mL, 10.7 mmol), 80 °C, under Ar, for 24 h. Reaction conditions when PhCF₃ is used as the substrate: HBpin (48 μ L, 0.33 mmol), 1-hexene (125 μ L, 1.00 mmol), and precatalyst (0.34 μ mol) in PhCF₃ (1.00 mL, 8.14 mmol), 80 °C, under Ar, for 24 h.

^bConversions and yields were determined by ¹H NMR spectroscopy using cyclohexane as an internal standard. Errors were estimated to be $\pm 2.5\%$. ^cProduct ratios were determined by ¹⁹F NMR spectroscopy.

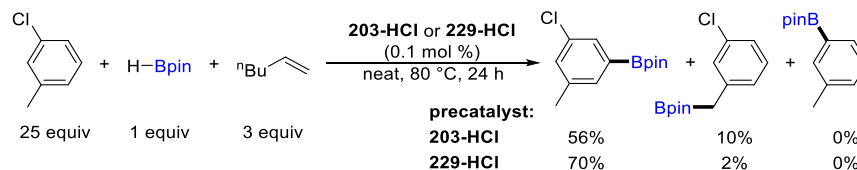


Figure II-10. Chemoselectivity for sp^2 C–H, sp^3 C–H, and C–Cl bonds.

2.3 Conclusion

This work demonstrated the synthesis of an array of PXL pincer ligands and their iridium and rhodium complexes, including several new compounds. These complexes were then tested as precursors in aromatic C–H borylation that used HBpin as the boron reagent and required an olefin additive. The role of the olefin was studied in a previous publication for the prototypical catalysts based on the POCOP ligands, where it was determined that the olefin is not merely a stoichiometric scavenger of the H₂ byproduct but is necessary to access the key unsaturated (pincer)Ir intermediate that is responsible for the C–H activation of the aromatic substrate.

In the present study, it was discovered that rhodium pincer complexes were incapable of C–H borylation, and only the iridium complexes of pincer ligands with a central aryl site displayed meaningful activity in C–H borylation. A comparison of the activity and the chemoselectivity (vs. the competing olefin hydroboration) identified iridium complexes of the originally studied **203-HCl** (POCOP type) and the newly tested **229-HCl** (PCP type) pincers as the most promising, with **229-HCl** delivering a moderate improvement over **203-HCl**. The regioselectivity of the C–H borylation in mono- and bis-substituted benzenes closely follows that observed in the “classical” iridium C–H borylation complexes supported by neutral bidentate phosphines or bipyridines. Since the mechanism of C–H borylation by Ir catalysts supported by pincer ligands is quite different, we conclude that the regioselectivity is substrate-controlled and reflects primarily a steric preference for C–H bonds without a neighboring *ortho* substituent.

2.4 Experimental

2.4.1 General Consideration

Unless specified otherwise, all manipulations were performed under an argon atmosphere using standard Schlenk or glovebox techniques. Toluene, pentane, THF, Et₂O, and isooctane were deoxygenated (by purging) and dried using an Innovative Technology Pure Solv MD-5 Solvent Purification System and stored over molecular sieves in an argon-filled glove box. C₆D₆ were dried over and distilled from a NaK/benzophenone/18-crown-6 mixture and stored over molecular sieves in an argon-filled glovebox. CDCl₃, toluene-*d*₈, CH₂Cl₂, PhF, PhCF₃, Et₃N, pyridine, MeCN, 1,4-dioxane, 1-hexene, cyclohexane, and mesitylene were dried over calcium hydride, distilled or vacuum transferred, and stored over molecular sieves in an argon-filled glove box. BF₃OEt₂ was distilled under argon and stored in an argon-filled glove box. NaH was rinsed with isooctane, dried under vacuum, and stored in an argon-filled glove box. Celite and silica were dried at 180 °C under vacuum overnight and store in an argon-filled glove box. [(COD)IrCl]₂,¹⁵² [(COE)₂IrCl]₂,¹⁵² [(COD)Ir(OAc)]₂,¹⁵³ (MesH)Ir(Bpin)₃,¹⁵⁴ [(COD)RhCl]₂,¹⁵⁵ *N,N'*-dimethyl-*m*-phenylenediamine,¹⁵⁶ **203-HCl**,⁶³ **207**,¹³⁶ **209**,¹³⁷ **210**,¹³⁷ **211**,¹³⁸ **212**,¹³⁹ **213**,¹³⁹ **214**,¹⁴⁰ **215**,¹⁴⁰ **227-HCl**,¹³⁵ **232-HCl**,¹⁴⁵ **233-COE**,¹⁴¹ **234-H₄**,¹⁴⁶ **235-HCl**,¹³³ **236-HCl**,¹⁴³ **238-H₂**,¹⁴⁴ and **239-HCl**¹⁴² were synthesized according to published procedures. NaS^tBu was synthesized according to the published procedures using ^tBuSH as a starting material.¹⁵⁷ All other chemicals were used as received from commercial vendors.

All NMR spectra were recorded on a Varian Inova 500 NMR spectrometer (^1H NMR, 499.431 MHz; $^{13}\text{C}\{^1\text{H}\}$ NMR, 125.595 MHz; $^{31}\text{P}\{^1\text{H}\}$ NMR, 202.187 MHz; ^{19}F NMR, 469.897 MHz), a Varian VnmrS 500 NMR spectrometer (^1H NMR, 499.690 MHz; ^{13}C NMR, 125.660 MHz; ^{31}P NMR, 202.292 MHz; ^{19}F NMR, 470.139 MHz), a Varian Inova 400 spectrometer (^1H NMR, 399.465 MHz; ^{11}B NMR 128.159 MHz), Bruker Avance Neo 400 spectrometers (^1H NMR, 400.2 MHz; ^{13}C NMR, 100.630 MHz, and ^1H NMR, 400.09 MHz; ^{13}C NMR, 100.603 MHz, respectively), and a Varian Inova 300 NMR (^1H NMR, 299.971 MHz; $^{31}\text{P}\{^1\text{H}\}$ NMR, 121.430 MHz) spectrometer. All spectra were recorded at ambient temperature unless otherwise noted. Chemical shifts are reported in δ (ppm). For ^1H and $^{13}\text{C}\{^1\text{H}\}$ NMR spectra, the residual solvent peak was used as an internal reference (C_6D_6 at δ 7.16 for ^1H NMR and δ 128.06 for ^{13}C NMR; CDCl_3 at δ 7.26 for ^1H NMR and δ 77.16 for ^{13}C NMR). $^{11}\text{B}\{^1\text{H}\}$ NMR spectra were referenced externally using neat BF_3OEt_2 at δ 0, $^{31}\text{P}\{^1\text{H}\}$ NMR spectra were referenced externally using 85% phosphoric acid at δ 0, and ^{19}F NMR spectra were referenced externally using neat trifluoroacetic acid at δ -78.5.

Elemental analyses were performed by Complete Analysis Laboratories, Inc. (Highland Park, NJ).

2.4.2 Synthesis and Characterization

Synthesis of 207. In a 50 mL culture tube, resorcinol (**221**) (1.138 g, 10.34 mmol) was dissolved in 5 mL of THF. Cy_2PCl (4.878 g, 20.96 mmol) was added, followed by Et_3N (8.0 mL, 57 mmol) with 15 mL of THF. The reaction was stirred at 85 °C for 20 h.

The mixture was filtered through Celite over a frit. Excess Cy_2PCl and solvent were removed under vacuum at $60\text{ }^\circ\text{C}$ to provide the product as a thick, colorless oil (5.0 g, 96% yield). The product was determined to be >95% pure by ^1H and $^{31}\text{P}\{^1\text{H}\}$ NMR spectroscopy and used without further purification. ^1H NMR (499 MHz, C_6D_6) δ 7.46 (quin, $J = 2.2$ Hz, 1H), 7.11–7.06 (m, 1H), 7.03–6.98 (m, 2H), 1.97 (br d, $J = 13.1$ Hz, 4H), 1.78–1.60 (m, 16H), 1.60–1.43 (m, 8H), 1.36–1.24 (m, 4H), 1.23–1.05 (m, 12H); $^{13}\text{C}\{^1\text{H}\}$ NMR (126 MHz, C_6D_6) δ 161.3 (d, $^2J_{\text{P-C}} = 9.6$ Hz), 130.0 (s), 112.1 (d, $^3J_{\text{P-C}} = 11.7$ Hz), 109.5 (t, $^3J_{\text{P-C}} = 11.5$ Hz), 38.5 (d, $^1J_{\text{P-C}} = 18.7$ Hz), 28.4 (d, $J_{\text{P-C}} = 18.8$ Hz), 27.4 (d, $J_{\text{P-C}} = 7.5$ Hz), 27.2 (d, $J_{\text{P-C}} = 12.6$ Hz), 27.0 (d, $J_{\text{P-C}} = 7.1$ Hz), 26.7 (s); $^{31}\text{P}\{^1\text{H}\}$ NMR (202 MHz, C_6D_6) δ 142.4.

Synthesis of 208. In a 50 mL culture tube, 2-hydroxycarbazole (**222**) (788 mg, 4.30 mmol) was dissolved in 20 mL of THF. $^n\text{BuLi}$ (3.6 mL, 9.0 mmol, 2.5 M in hexane) was added dropwise at ambient temperature. The reaction was stirred at ambient temperature for 20 min. $^i\text{Pr}_2\text{PCl}$ (1.42 g, 9.30 mmol) was then added slowly. The reaction was stirred at $85\text{ }^\circ\text{C}$ for 22 h. All volatiles were removed under vacuum. 5 mL of pentane was added, the mixture was filtered through Celite over a frit. Excess $^i\text{Pr}_2\text{PCl}$ and solvent were removed under vacuum to provide the product as a thick, yellow oil (1.8 g, >98% yield). The product tends to solidify over time. The product was determined to be >93% pure by $^{31}\text{P}\{^1\text{H}\}$ NMR spectroscopy and used without further purification. Based on the ^1H NMR spectrum, the product contains two isomers in 1:1 ratio. The exact nature of the isomers was not determined. ^1H NMR (499 MHz, C_6D_6) δ 8.26 (br q, $J = 2.2$ Hz, 1H), 8.21 (dd, $J = 8.2, 2.4$ Hz, 1H), 7.94 (d, $J = 7.3$ Hz, 1H), 7.88 (d, $J = 7.7$ Hz, 1H), 7.85 (d,

$J = 8.5$ Hz, 1H), 7.82 (d, $J = 8.4$ Hz, 1H), 7.75 (br t, $J = 2.0$ Hz, 1H), 7.44 (d, $J = 8.1$ Hz, 1H), 7.41–7.35 (m, 1H), 7.34–7.26 (m, 3H), 7.23 (t, $J = 6.9$ Hz, 1H), 7.21 (t, $J = 7.0$ Hz, 1H), 2.86 (oct, $J = 7.0$ Hz, 2H), 2.59 (oct, $J = 7.0$ Hz, 2H), 1.91–1.78 (m, 4H), 1.23 (t, $J = 7.0$ Hz, 6H), 1.21 (t, $J = 7.0$ Hz, 6H), 1.04 (dd, $J = 18.0, 7.0$ Hz, 6H), 1.04 (dd, $J = 15.7, 7.2$ Hz, 12H), 0.99 (dd, $J = 18.4, 6.9$ Hz, 6H), 0.74 (dd, $J = 13.0, 7.0$ Hz, 6H), 0.65 (dd, $J = 13.0, 7.0$ Hz, 6H); $^{13}\text{C}\{^1\text{H}\}$ NMR (126 MHz, C_6D_6) δ 159.3 (dd, $J_{\text{P-C}} = 8.7, 1.2$ Hz), 158.8 (dd, $J_{\text{P-C}} = 8.6$ Hz), 148.8 (d, $J_{\text{P-C}} = 22.6$ Hz), 147.7 (d, $J_{\text{P-C}} = 22.2$ Hz), 144.0 (d, $J_{\text{P-C}} = 11.6$ Hz), 143.2 (d, $J_{\text{P-C}} = 11.6$ Hz), 127.1 (d, $J_{\text{P-C}} = 1.2$ Hz), 125.3 (d, $J_{\text{P-C}} = 1.2$ Hz), 125.2 (d, $J_{\text{P-C}} = 3.0$ Hz), 124.7, 121.5, 121.5, 120.9, 120.7 (br, 2C), 120.4, 119.8 (d, $J_{\text{P-C}} = 2.6$ Hz), 119.5, 113.3, 113.2 (d, $J_{\text{P-C}} = 22.9$ Hz), 112.9 (d, $J_{\text{P-C}} = 9.1$ Hz), 112.6 (d, $J_{\text{P-C}} = 10.1$ Hz), 103.5 (d, $J_{\text{P-C}} = 13.5$ Hz), 103.2 (dd, $J_{\text{P-C}} = 23.5, 11.8$ Hz), 26.2 (d, $J_{\text{P-C}} = 14.4$ Hz), 26.0 (d, $J_{\text{P-C}} = 13.9$ Hz), 20.3 (d, $J_{\text{P-C}} = 30.4$ Hz), 20.2 (d, $J_{\text{P-C}} = 30.3$ Hz), 19.6 (d, $J_{\text{P-C}} = 10.9$ Hz), 19.6 (d, $J_{\text{P-C}} = 11.0$ Hz), 28.8 (d, $J_{\text{P-C}} = 18.8$ Hz), 28.8 (d, $J_{\text{P-C}} = 18.5$ Hz), 18.0 (d, $J_{\text{P-C}} = 20.5$ Hz), 17.3 (d, $J_{\text{P-C}} = 8.8$ Hz); $^{31}\text{P}\{^1\text{H}\}$ NMR (202 MHz, C_6D_6) δ 148.7, 147.9, 61.2, 60.6.

Synthesis of 211. This synthesis was based on the previous method in the literature with minor modification.¹³⁸ In a 50 mL culture tube, *N,N'*-dimethyl-*m*-phenylenediamine (1.418 g, 10.41 mmol) was dissolved in THF (10 mL). $^n\text{BuLi}$ (9.00 mL, 22.5 mmol, 2.5 M in hexane), was added dropwise at ambient temperature. THF (5 mL) was added to the reaction. The reaction was stirred at ambient temperature for 1 h. $^i\text{Pr}_2\text{PCl}$ (3.58 g, 23.4 mmol) was then added slowly. The reaction was stirred at 85 °C for 18 h. The mixture was filtered through Celite over a frit and the solvent was removed under vacuum. The residue

was re-dissolved in pentane and filtered through Celite over a frit. The solvent was removed under vacuum to provide the crude product. The crude product was purified by recrystallization from pentane at $-35\text{ }^{\circ}\text{C}$ to provide the product as a yellow solid (2.28 g, 59% yield). ^1H NMR (499 MHz, C_6D_6) δ 7.63–7.56 (m, 1H), 7.21 (t, $J = 8.2$ Hz, 1H), 6.91 (dt, $J = 8.1, 2.3$ Hz, 2H), 2.78 (d, $^3J_{\text{P-H}} = 1.4$ Hz, 6H), 1.80 (hept d, $J = 5.9, 3.3$ Hz, 4H), 1.03 (dd, $J = 16.4, 6.9$ Hz, 12H), 0.97 (dd, $J = 11.8, 7.0$ Hz, 12H); $^{13}\text{C}\{^1\text{H}\}$ NMR (126 MHz, C_6D_6) δ 153.7 (dd, $J_{\text{P-C}} = 19.9, 1.2$ Hz), 129.0 (t, $J_{\text{P-C}} = 1.3$ Hz), 107.8 (d, $J_{\text{P-C}} = 15.3$ Hz), 106.2 (t, $J_{\text{P-C}} = 18.3$ Hz), 34.6 (d, $J_{\text{P-C}} = 6.5$ Hz), 27.0 (d, $J_{\text{P-C}} = 16.8$ Hz), 19.9 (d, $J_{\text{P-C}} = 11.0$ Hz), 19.7 (d, $J_{\text{P-C}} = 27.5$ Hz); $^{31}\text{P}\{^1\text{H}\}$ NMR (202 MHz, C_6D_6) δ 71.7.

Synthesis of 3-hydroxybenzyl chloride (224). In a 50 mL culture tube, 3-hydroxybenzyl alcohol (**223**) (1.475 g, 11.88 mmol) was dissolved in CH_2Cl_2 (30 mL). Pyridine (1.60 mL, 19.9 mmol) was added. The reaction was cooled down to $0\text{ }^{\circ}\text{C}$ in an ice bath. SOCl_2 (2.60 mL, 35.6 mmol) was added dropwise to the reaction. After the addition of the SOCl_2 , the ice bath was removed, and the reaction was allowed to stir at ambient temperature for 20 h. Water (5 mL) was added to the reaction dropwise with vigorous stirring. (*Caution: Gas evolution!*) The separated CH_2Cl_2 phase was washed by water (10 mL x 2) and dried over anhydrous Na_2SO_4 . The solvent was removed under vacuum to provide the product as a white solid (1.43 g, 84% yield). The ^1H NMR and $^{13}\text{C}\{^1\text{H}\}$ NMR data matched the previously reported data in the literature.¹⁵⁸ The product was used in the next step without further purification.

Synthesis of di-*tert*-butyl(3-(chloromethyl)phenoxy)phosphine (225). In a 50 mL culture tube, 3-hydroxybenzyl chloride (**224**) (1.257g, 8.816 mmol) was dissolved in

THF (10 mL). NaH was suspended in THF (2 mL) in a 7 mL vial and added slowly to the reaction. THF (1 mL x 4) was used to rinse the 7 mL vial and added to the reaction. The reaction was stirred at ambient temperature for 3 h. ^tBu₂PCl (1.615 g, 8.939 mmol) was dissolved in THF (1 mL) in a 7 mL vial and added slowly to the reaction. THF (1 mL x 3) was used to rinse the 7 mL vial and added to the reaction. The reaction was heated at 75 °C for 23 h. The mixture was filtered through Celite over a frit and the solvent was removed under vacuum to provide the product as an orange oil (2.59 g, >99% crude yield). The product was determined to be >88% pure by ¹H and ³¹P{¹H} NMR spectroscopy and used without further purification. ¹H NMR (499 MHz, C₆D₆) δ 7.29 (br q, *J* = 2.0 Hz, 1H), 7.18 (br dtd, *J* = 8.3, 2.4, 0.8 Hz, 1H), 6.98 (t, *J* = 7.9 Hz, 1H), 6.72 (br d, *J* = 7.6 Hz, 1H), 4.07 (s, 2H), 1.10 (d, *J* = 11.7 Hz, 18H); ¹³C{¹H} NMR (126 MHz, C₆D₆) δ 160.5 (d, *J*_{P-C} = 9.3 Hz), 139.5, 129.9 (d, *J*_{P-C} = 0.6 Hz), 121.8, 118.7 (d, *J*_{P-C} = 10.2 Hz), 118.4 (d, *J*_{P-C} = 11.8 Hz), 46.0, 35.7 (d, *J*_{P-C} = 26.4 Hz), 27.5 (d, *J*_{P-C} = 15.8 Hz); ³¹P{¹H} NMR (202 MHz, C₆D₆) δ 153.6.

Synthesis of 216. In a 50 mL culture tube, di-*tert*-butyl(3-(chloromethyl)phenoxy)phosphine (**225**) (1.28 g, 4.46 mmol) was dissolved in MeCN (20 mL). NaS^tBu (500 mg, 4.46 mmol) was added to the reaction. The reaction was stirred at ambient temperature for 26 h. The mixture was filtered through Celite over a frit and the solvent was removed under vacuum. The residue was re-dissolved in pentane (5 mL) and filtered through Celite over a pipette. The solvent was removed under vacuum to provide the product as an orange oil (1.14 g, 75% yield). The product was determined to be 85% pure by ¹H NMR spectroscopy and used without further purification. ¹H NMR (400 MHz,

C_6D_6) δ 7.51 (br q, $J = 2.2$ Hz, 1H), 7.19 (br dtd, $J = 8.0, 2.4, 1.0$ Hz, 1H), 7.07 (t, $J = 7.8$ Hz, 1H), 6.95 (br d, $J = 7.5$ Hz, 1H), 3.60 (s, 2H), 1.19 (s, 9H), 1.13 (d, $J = 11.7$ Hz, 1H); $^{13}C\{^1H\}$ NMR (101 MHz, C_6D_6) δ 160.5 (d, $J_{P-C} = 9.5$ Hz), 141.1, 129.7, 122.5, 119.4 (d, $J_{P-C} = 10.8$ Hz), 117.0 (d, $J_{P-C} = 11.2$ Hz), 42.5, 35.7 (d, $J_{P-C} = 26.6$ Hz), 33.8, 31.0, 27.5 (d, $J_{P-C} = 15.7$ Hz); $^{31}P\{^1H\}$ NMR (202 MHz, C_6D_6) δ 152.5.

Synthesis of 226-HCl. In a 50 mL Teflon screw-capped Schlenk flask, **205** (598 mg, 1.19 mmol) was dissolved in 6 mL of toluene. $[(COD)IrCl]_2$ (386 mg, 0.575 mmol) was added with 5 mL of toluene. The reaction mixture was degassed by a freeze-pump-thaw cycle and the flask was refilled with H_2 (1 atm). The reaction was heated at 140 °C for 43 h. The mixture was filtered through Celite over a frit, and the solvent was removed under vacuum to provide the crude product as a brick red solid (954 mg). The product was purified by recrystallization from a concentrated PhF solution layered with pentane at -35 °C. The crystal was triturated with toluene to remove PhF to give a dark red solid (755 mg in three crops, 90% yield). A part of $^{13}C\{^1H\}$ NMR spectrum (δ 29–25) was integrated to determine the number of ^{13}C NMR resonances of $-CH_2-$ in the cyclohexyl rings. 1H NMR (499 MHz, C_6D_6) δ 6.91–6.85 (m, 1H), 6.84–6.78 (m, 2H), 2.72 (tt, $J = 12.2, 3.3$ Hz, 2H), 2.42–2.24 (m, 2H), 2.06–1.83 (m, 10H), 1.75–1.35 (m, 18H), 1.21–0.90 (m, 12H), -37.25 (t, $J = 13.7$ Hz, 1H); $^{13}C\{^1H\}$ NMR (126 MHz, C_6D_6) δ 166.5 (vt, $J_{P-C} = 6.5$ Hz), 125.8 (s), 115.5 (br s), 105.6 (t, $J_{P-C} = 5.4$ Hz), 41.3 (vt, $J_{P-C} = 14.5$ Hz), 38.7 (vt, $J_{P-C} = 16.5$ Hz), 27.7, 27.3 (br t, $J_{P-C} = 2.7$ Hz), 27.0–26.7 (m, 4C), 26.6–26.3 (m, 2C), 26.0, 26.0; $^{31}P\{^1H\}$ NMR (202 MHz, C_6D_6) δ 166.7; Elem. Anal. Calcd for $C_{30}H_{48}ClIrO_2P_2$: C, 49.34; H, 6.62. Found: C, 49.51; H, 6.53.

Synthesis of 228-HCl. In a 10 mL culture tube, **208** (110 mg, 0.265 mmol) and $[(\text{COE})_2\text{IrCl}]_2$ (112 mg, 0.125 mmol) were dissolved in 4 mL of toluene. The reaction was heated at 110 °C for 44 h. The mixture was filtered through Celite over a frit, and the solvent was removed under vacuum to provide the crude product as a purple solid (160 mg). The residue was purified by flash column chromatography on silica gel using pentane/toluene/Et₂O as gradient eluent (100/0/0 to 0/100/0 to 0/0/100) to give a pure product as a purple solid (138 mg, 86% yield). ¹H NMR (499 MHz, C₆D₆) δ 7.93–7.85 (m, 1H), 7.44 (d, *J* = 8.2 Hz, 1H), 7.27–7.18 (m, 3H), 7.01 (d, *J* = 8.2 Hz, 1H), 3.26–3.14 (m, 1H), 2.89–2.75 (m, 1H), 2.75–2.63 (m, 1H), 2.38–2.23 (m, 1H), 1.30 (dd, *J* = 19.6, 6.9 Hz, 3H), 1.29 (dd, *J* = 17.5, 7.2 Hz, 3H), 1.17 (dd, *J* = 16.5, 7.2 Hz, 3H), 1.17 (dd, *J* = 15.2, 7.1 Hz, 3H), 1.12 (dd, *J* = 18.9, 7.1 Hz, 3H), 1.04 (dd, *J* = 18.8, 7.0 Hz, 3H), 1.01 (dd, *J* = 17.6, 7.0 Hz, 3H), 0.74 (dd, *J* = 16.7, 7.0 Hz, 3H), –36.77 (t, *J* = 13.9 Hz, 1H); ¹³C{¹H} NMR (126 MHz, C₆D₆) δ 164.7 (dd, *J*_{P-C} = 6.5, 5.8 Hz), 160.1 (dd, *J*_{P-C} = 19.9, 5.7 Hz), 140.7 (dd, *J*_{P-C} = 8.0, 1.7 Hz), 132.7 (d, *J*_{P-C} = 1.6 Hz), 124.4, 122.3, 121.2, 115.3, 113.7 (d, *J*_{P-C} = 8.0 Hz), 112.6, 105.9 (d, *J*_{P-C} = 11.0 Hz), 105.3 (br), 31.5 (dd, *J*_{P-C} = 26.1, 5.6 Hz), 31.4 (dd, *J*_{P-C} = 20.4, 3.3 Hz), 29.5 (dd, *J*_{P-C} = 29.6, 5.2 Hz), 27.5 (dd, *J*_{P-C} = 24.1, 3.0 Hz), 19.2 (t, *J*_{P-C} = 2.1 Hz), 18.8 (d, *J*_{P-C} = 10.4 Hz), 18.4 (d, *J*_{P-C} = 1.3 Hz), 17.5, 17.5, 17.1 (d, *J*_{P-C} = 7.7 Hz), 17.0 (d, *J*_{P-C} = 3.6 Hz), 16.9 (t, *J*_{P-C} = 2.1 Hz); ³¹P{¹H} NMR (202 MHz, C₆D₆) δ 171.1 (d, *J* = 373 Hz), 115.6 (d, *J* = 373 Hz); Elem. Anal. Calcd for C₂₄H₃₅ClIrNOP₂: C, 44.82; H, 5.49; N, 2.18. Found: C, 45.05; H, 5.64; N, 2.07.

Synthesis of 229-HCl. This synthesis was modified from the previous method in the literature, which suffered from difficult isolation and low yield.¹⁵⁰ In a 50 mL Teflon

screw-capped Schlenk flask, **212** (153 mg, 0.452 mmol) and [(COD)IrCl]₂ (195 mg, 0.218 mmol) were dissolved in 10 mL of toluene. The reaction mixture was degassed by three freeze-pump-thaw cycles and the flask was refilled with H₂ (1 atm). The reaction was heated at 110 °C for 18 h. Volatiles were removed under vacuum. The resulting solid was rinsed with pentane (2 mL x 3) to provide the product as an orange-red solid (220 mg, 89% yield). The ¹H NMR and ³¹P{¹H} NMR data match the previously reported data in the literature.¹⁵⁰

Synthesis of 230-HClpy. In a 50 mL Teflon screw-capped Schlenk flask, [(COE)₂IrCl]₂ (302 mg, 0.337 mmol) and pyridine (0.55 mL, 6.8 mmol) were dissolved in 7 mL of toluene. **214** (275 mg, 0.700 mmol) was added to the reaction mixture with 8 mL of toluene. The reaction was heated at 150 °C for 17 h. The mixture was filtered through Celite over a frit, and the solvent was removed under vacuum to provide the crude product as a tan solid (508 mg). The crude product was further purified by reprecipitation from a concentrated PhF solution layered with pentane at -35 °C. The solid was triturated with toluene and pentane to remove PhF to give a tan solid (300 mg, 64% yield). Based on the ¹H and ³¹P{¹H} NMR spectra, the product contains two isomers in 99:1 ratio. Major isomer: ¹H NMR (499 MHz, C₆D₆) δ 11.80–7.72 (br m, 2H), 7.56 (d, *J* = 7.5 Hz, 1H), 7.43 (d, *J* = 8.5 Hz, 1H), 7.35 (d, *J* = 8.5 Hz, 1H), 7.24–7.12 (m, 2H), 6.67 (t, *J* = 7.5 Hz, 1H), 6.19 (br s, 2H), 3.08–2.81 (m, 1H), 2.70–2.48 (m, 1H), 2.48–2.26 (m, 1H), 2.25–2.02 (m, 1H), 1.58 (dd, *J* = 17.2, 7.0 Hz, 3H), 1.33 (dd, *J* = 14.4, 6.9 Hz, 3H), 1.21 (dd, *J* = 16.2, 7.0 Hz, 3H), 1.11 (dd, *J* = 12.6, 7.1 Hz, 3H), 1.04–0.91 (m, 9H), 0.88 (dd, *J* = 14.4, 7.2 Hz, 1H), -20.74 (t, *J* = 17.2 Hz, 1H); ¹³C{¹H} NMR (126 MHz, C₆D₆) δ 164.5 (dd, *J*_{P-C} =

10.6, 4.7 Hz), 155.8 (d, $J_{P-C} = 3.3$ Hz), 152.6, 136.3, 132.8, 129.0 (d, $J_{P-C} = 7.3$ Hz), 126.1, 125.3, 124.5, 122.8, 114.6 (d, $J_{P-C} = 4.6$ Hz), 114.5 (d, $J_{P-C} = 11.5$ Hz), 110.1 (dd, $J_{P-C} = 8.6, 2.6$ Hz), 32.4 (dd, $J_{P-C} = 30.1, 5.4$ Hz), 31.4 (dd, $J_{P-C} = 18.4, 8.6$ Hz), 30.1 (dd, $J_{P-C} = 31.3, 4.4$ Hz), 28.4 (dd, $J_{P-C} = 26.5, 6.9$ Hz), 18.3 (d, $J_{P-C} = 5.9$ Hz), 17.9, 17.6, 17.1 (d, $J_{P-C} = 4.0$ Hz), 16.9, 16.7 (d, $J_{P-C} = 3.4$ Hz), 16.7, 16.3; $^{31}\text{P}\{^1\text{H}\}$ NMR (202 MHz, C_6D_6) δ 144.6 (d, $J = 406$ Hz), 120.9 (d, $J = 406$ Hz). Minor isomer: ^1H NMR (499 MHz, C_6D_6) (only Ir-H can be identified) δ -20.42 (t, $J = 15.4$ Hz, 1H); $^{31}\text{P}\{^1\text{H}\}$ NMR (202 MHz, C_6D_6) δ 144.1 (d, $J = 395$ Hz), 112.0 (d, $J = 395$ Hz).

Synthesis of 230-HCl. In a J. Young NMR tube, **230-HClpy** (146 mg, 0.209 mmol) were dissolved in C_6D_6 (1 mL). BF_3OEt_2 (220 μL , 1.78 mmol) was added to the reaction mixture. The reaction was heated at 100 °C and monitored by ^1H and $^{31}\text{P}\{^1\text{H}\}$ NMR spectroscopy. After 14 h, all volatiles and excess BF_3OEt_2 were removed under vacuum. Pentane (5 mL) was added, and the mixture was allowed to sit at -35 °C overnight. The solid was filtered out through Celite over a pipette and the solid was further washed with cold pentane (2 mL x 3). Pentane was removed from the combined filtrate under vacuum to provide an orange solid (76 mg). The crude product was further purified by flash column chromatography on silica gel using pentane/toluene as gradient eluent (100/0 to 0/100) to give a pure product as an orange-red solid (74 mg, 54% yield). ^1H NMR (499 MHz, C_6D_6) δ 7.44 (d, $J = 7.6$ Hz, 1H), 7.35 (d, $J = 8.6$ Hz, 1H), 7.24 (d, $J = 8.6$ Hz, 1H), 7.12 (d, $J = 7.6$ Hz, 1H), 7.07 (t, $J = 7.6$ Hz, 1H), 2.76 (sept, $J = 7.1$ Hz, 1H), 2.71 (sept, $J = 7.1$ Hz, 1H), 2.65–2.51 (m, 1H), 2.41–2.26 (m, 1H), 1.29 (dd, $J = 17.5, 7.2$ Hz, 3H), 1.24 (dd, $J = 17.1, 7.2$ Hz, 3H), 1.21–1.09 (m, 15H), 1.03 (dd, $J = 15.9, 6.9$ Hz,

3H), -36.42 (t, $J = 13.2$ Hz, 1H); $^{13}\text{C}\{^1\text{H}\}$ NMR (126 MHz, C_6D_6) δ 166.5 (dd, $J_{\text{P-C}} = 10.1$, 5.0 Hz), 155.3 (d, $J_{\text{P-C}} = 3.7$ Hz), 132.7, 129.0 (d, $J_{\text{P-C}} = 7.5$ Hz), 127.4, 125.5, 123.1, 115.2 (d, $J_{\text{P-C}} = 5.7$ Hz), 114.4 (d, $J_{\text{P-C}} = 12.1$ Hz), 105.8 (m), 30.3 (dd, $J_{\text{P-C}} = 22.8$, 6.1 Hz), 30.1–29.5 (m, 2C), 28.9 (dd, $J_{\text{P-C}} = 29.4$, 4.6 Hz), 18.4 (d, $J_{\text{P-C}} = 3.3$ Hz), 18.3, 17.7, 17.6 (d, $J_{\text{P-C}} = 3.4$ Hz), 17.1 (d, $J_{\text{P-C}} = 6.3$ Hz), 16.9 (d, $J_{\text{P-C}} = 7.9$ Hz), 16.4 (d, $J_{\text{P-C}} = 4.1$ Hz), 16.2 (br); $^{31}\text{P}\{^1\text{H}\}$ NMR (202 MHz, C_6D_6) δ 172.7 (d, $J = 385$ Hz), 150.1 (d, $J = 385$ Hz); Elem. Anal. Calcd for $\text{C}_{22}\text{H}_{34}\text{ClIrO}_2\text{P}_2$: C, 42.61; H, 5.53. Found: C, 42.58; H, 5.58.

Synthesis of 231-HOAc. In a 10 mL culture tube, **216** (327 mg, 85% pure 0.82 mmol) and $[(\text{COD})\text{Ir}(\text{OAc})]_2$ (0.30 g, 0.42 mmol) were dissolved in 6 mL of toluene. The reaction was heated at $120\text{ }^\circ\text{C}$ for 37 h. The mixture was filtered through Celite over a frit, and the solvent was removed under vacuum to provide the crude product as a brown solid (587 mg). The residue was purified by flash column chromatography on silica gel using pentane as eluent to give a purer product. The product was then further purified by recrystallization from a saturated pentane solution at $-35\text{ }^\circ\text{C}$ to give a faint orange crystal (116 mg, 24% yield). Single crystals suitable for X-ray analysis were obtained by slow evaporation of pentane at $-35\text{ }^\circ\text{C}$. ^1H NMR (499 MHz, C_6D_6) δ 6.80–6.75 (m, 2H), 6.55–6.50 (m, 1H), 3.99 (d, $J = 16.6$ Hz, 1H), 3.71 (dd, $J = 16.6$, 2.0 Hz, 1H), 1.91 (s, 3H), 1.39 (d, $J = 14.5$ Hz, 9H), 1.34 (d, $J = 14.1$ Hz, 9H), 1.13 (s, 9H), -28.80 (d, $J = 19.6$ Hz, 1H); $^{13}\text{C}\{^1\text{H}\}$ NMR (126 MHz, C_6D_6) δ 185.7, 165.9 (d, $J_{\text{P-C}} = 3.0$ Hz), 147.6 (d, $J_{\text{P-C}} = 5.0$ Hz), 126.5, 122.7, 116.3, 107.9 (d, $J_{\text{P-C}} = 11.4$ Hz), 48.6, 42.5 (d, $J_{\text{P-C}} = 1.8$ Hz), 41.8 (d, $J_{\text{P-C}} = 23.4$ Hz), 39.6 (d, $J_{\text{P-C}} = 31.0$ Hz), 28.8 (d, $J_{\text{P-C}} = 4.7$ Hz), 28.7 (d, $J_{\text{P-C}} = 1.4$ Hz),

27.4 (d, $J_{P-C} = 4.7$ Hz), 26.0; $^{31}\text{P}\{^1\text{H}\}$ NMR (202 MHz, C_6D_6) δ 156.8; Elem. Anal. Calcd for $\text{C}_{21}\text{H}_{36}\text{IrO}_3\text{PS}$: C, 42.62; H, 6.13. Found: C, 42.91; H, 6.07.

Synthesis of 237-HCl. This synthesis was modified from the previous method in the literature, which required multi-step synthesis.¹³⁶ In a 50 mL Teflon screw-capped Schlenk flask, **212** (144 mg, 0.425 mmol) and $[(\text{COD})\text{RhCl}]_2$ (101 mg, 0.205 mmol) were dissolved in 2 mL of toluene. The reaction mixture was degassed by three freeze-pump-thaw cycles and the flask was refilled with H_2 (1 atm). The reaction was heated at 120 °C for 20 h. The reaction mixture was again degassed by three freeze-pump-thaw cycles and the flask was refilled with H_2 (1 atm). The reaction was heated at 120 °C for 22 h. Volatiles were removed under vacuum. The resulting solid was rinsed with pentane (2 mL x 3) to provide the product as a yellow solid (181 mg, 93% yield). The ^1H NMR and $^{31}\text{P}\{^1\text{H}\}$ NMR match the previously reported data in the literature.¹³⁶

Synthesis of 240-HClpy. In a 10 mL culture tube, $[(\text{COD})\text{IrCl}]_2$ (275 mg, 0.409 mmol) and pyridine (0.13 mL, 1.6 mmol) were dissolved in 7 mL of toluene. **209** (293 mg, 0.858 mmol) was added to the reaction mixture. The reaction was heated at 110 °C for 1.5 h. The mixture was filtered through Celite over a frit, and the solvent was removed under vacuum to provide the crude product as a tan powder (505 mg). The crude product was rinsed with pentane (2 mL x 3) to provide the product as a tan solid (475 mg, 89% yield). Based on the ^1H and $^{31}\text{P}\{^1\text{H}\}$ NMR spectra, the product contains two isomers in 94:6 ratio. Major isomer: ^1H NMR (400 MHz, C_6D_6) δ 10.48 (br s, 1H), 7.87 (br s, 1H), 6.95 (t, $J = 7.8$ Hz, 1H), 6.73 (d, $J = 7.9$ Hz, 1H), 6.67 (t, $J = 7.5$ Hz, 1H), 6.56 (br s, 1H), 6.31 (d, $J = 7.7$ Hz, 1H), 6.01 (br s, 1H), 3.86 (br d, $J = 3.4$ Hz, 1H), 2.48–2.31 (m, 1H),

2.05–1.87 (m, 2H), 1.80–1.66 (m, 1H), 1.44 (dd, $J = 17.5, 6.9$ Hz, 6H), 1.22 (dd, $J = 15.0, 7.0$ Hz, 3H), 1.10 (dd, $J = 13.3, 7.1$ Hz, 3H), 1.05 (dd, $J = 14.8, 6.9$ Hz, 3H), 1.01 (dd, $J = 15.9, 7.3$ Hz, 3H), 0.92 (dd, $J = 15.0, 7.4$ Hz, 3H), 0.87 (dd, $J = 13.7, 7.1$ Hz, 1H), –21.20 (t, $J = 15.9$ Hz, 1H); $^{13}\text{C}\{^1\text{H}\}$ NMR (126 MHz, C_6D_6) δ 164.4 (t, $J_{\text{P-C}} = 6.5$ Hz), 154.69 (dd, $J_{\text{P-C}} = 15.4, 5.4$ Hz), 152.1 (br), 151.9 (br), 136.2, 124.4 (br), 124.4 (br), 124.3, 117.7 (t, $J_{\text{P-C}} = 3.6$ Hz), 103.6 (d, $J_{\text{P-C}} = 11.8$ Hz), 103.0 (d, $J_{\text{P-C}} = 11.2$ Hz), 31.8 (dd, $J_{\text{P-C}} = 21.6, 7.5$ Hz), 31.1 (dd, $J_{\text{P-C}} = 29.2, 5.0$ Hz), 30.5 (dd, $J_{\text{P-C}} = 24.1, 5.3$ Hz), 30.2 (dd, $J_{\text{P-C}} = 27.5, 3.6$ Hz), 18.8 (d, $J_{\text{P-C}} = 6.6$ Hz), 18.5, 18.0, 17.9 (d, $J_{\text{P-C}} = 8.2$ Hz), 17.8 (d, $J_{\text{P-C}} = 3.6$ Hz), 17.2, 16.9 (d, $J_{\text{P-C}} = 4.7$ Hz), 16.5; $^{31}\text{P}\{^1\text{H}\}$ NMR (202 MHz, C_6D_6) δ 147.0 (d, $J = 384$ Hz), 80.6 (d, $J = 384$ Hz). Minor isomer: ^1H NMR (400 MHz, C_6D_6) (only N–H and Ir–H can be clearly identified) δ 3.93 (br d, $J = 3.5$ Hz, 1H), –21.33 (t, $J = 14.9$ Hz, 1H); $^{31}\text{P}\{^1\text{H}\}$ NMR (202 MHz, C_6D_6) δ 145.2 (d, $J = 373$ Hz), 80.1 (d, $J = 373$ Hz).

2.4.3 Screening of Methods for Metalation of LXL-Type Pincer Ligands

2.4.3.1 General Procedure for J. Young NMR Tube Reactions

Method A. The ligand (1.1 equiv), Ir–Cl precursor (1.0 equiv [Ir]; $[(\text{COD})\text{IrCl}]_2$ or $[(\text{COE})_2\text{IrCl}]_2$), and the solvent were added to a J. Young NMR tube. The J. Young NMR tube was then placed into an oil bath at the indicated temperature for the time reported and monitored by ^1H and/or $^{31}\text{P}\{^1\text{H}\}$ NMR spectroscopy.

Method B. Ir–Cl precursor (1.0 equiv [Ir]; $[(\text{COD})\text{IrCl}]_2$ or $[(\text{COE})_2\text{IrCl}]_2$), pyridine (in excess), and the solvent were added to a J. Young NMR tube. The ligand (1.1 equiv) was then added to the J. Young NMR tube. The J. Young NMR tube was then

placed into an oil bath at the indicated temperature for the time reported and monitored by ^1H and/or $^{31}\text{P}\{^1\text{H}\}$ NMR spectroscopy.

Method C. The ligand (1.1 equiv), $[(\text{COD})\text{Ir}(\text{OAc})]_2$ (1.0 equiv $[\text{Ir}]$), and the solvent were added to a J. Young NMR tube. The J. Young NMR tube was then placed into an oil bath at the indicated temperature for the time reported and monitored by ^1H and/or $^{31}\text{P}\{^1\text{H}\}$ NMR spectroscopy.

Method D. The ligand (1.1 equiv), Ir precursor (1.0 equiv $[\text{Ir}]$; $[(\text{COD})\text{IrCl}]_2$, $[(\text{COE})_2\text{IrCl}]_2$, or $[(\text{COD})\text{Ir}(\text{OAc})]_2$), and the solvent were added to a J. Young NMR tube. The J. Young NMR tube was then degassed through a freeze-pump-thaw cycle, refilled with hydrogen (H_2 ; 1 atm; ca. 2 mL, 0.08 mmol), placed into an oil bath at the indicated temperature for the time reported, and monitored by ^1H and/or $^{31}\text{P}\{^1\text{H}\}$ NMR spectroscopy. The J. Young NMR tube was degassed and refilled with H_2 if indicated during the reaction.

Method E. The ligand (1.1 equiv), $[(\text{MesH})\text{Ir}(\text{Bpin})_3]$ (1.0 equiv $[\text{Ir}]$), and the solvent were added to a J. Young NMR tube. The J. Young NMR tube was then placed into an oil bath at the indicated temperature for the time reported, and monitored by ^1H , $^{11}\text{B}\{^1\text{H}\}$, and/or $^{31}\text{P}\{^1\text{H}\}$ NMR spectroscopy.

The results of screening of methods for metalation of PXP-type pincer ligands were summarized in Table II-1.

2.4.3.2 Screening of Methods for Metalation of **205**

Method A with $[(\text{COD})\text{IrCl}]_2$. **205** (125 μL , 69 μmol , 0.55 M in toluene) and $[(\text{COD})\text{IrCl}]_2$ (21.8 mg, 32.5 μmol) were added to a J. Young NMR tube. Toluene (0.7

mL) was added to form a yellow solution. The J. Young NMR tube was closed. The yellow solution was immediately analyzed by $^{31}\text{P}\{^1\text{H}\}$ NMR spectroscopy, then again after the J. Young NMR tube was placed into an oil bath at 120 °C for 23 h, at 140 °C for 28 h and over a weekend. The yellow solution turned brown-red upon heating. Prior to heating, the $^{31}\text{P}\{^1\text{H}\}$ NMR spectrum contained multiple ^{31}P NMR resonances. After 23 h at 120 °C, the $^{31}\text{P}\{^1\text{H}\}$ NMR spectrum contained **226-HCl** (46%), free ligand (18%), and other unidentified ^{31}P NMR resonances. After 28 h at 140 °C, the $^{31}\text{P}\{^1\text{H}\}$ NMR spectrum contained **226-HCl** (67%), free ligand (6%), and other unidentified ^{31}P NMR resonances. After a weekend at 140 °C, the $^{31}\text{P}\{^1\text{H}\}$ NMR spectrum contained **226-HCl** (79%), free ligand (5%), and other unidentified ^{31}P NMR resonances.

Method A with $[(\text{COE})_2\text{IrCl}]_2$. **205** (115 μL , 63 μmol , 0.55 M in toluene) and $[(\text{COE})_2\text{IrCl}]_2$ (27 mg, 30 μmol) were added to a J. Young NMR tube. Toluene (0.7 mL) was added to form an orange solution. The J. Young NMR tube was closed. The orange solution was immediately analyzed by $^{31}\text{P}\{^1\text{H}\}$ NMR spectroscopy, then again after the J. Young NMR tube was placed into an oil bath at 120 °C for 23 h, and at 140 °C for 22 h. The yellow solution turned brown-red upon heating. Prior to heating, the $^{31}\text{P}\{^1\text{H}\}$ NMR spectrum contained multiple broad ^{31}P NMR resonances. After 23 h at 120 °C, the $^{31}\text{P}\{^1\text{H}\}$ NMR spectrum contained **226-HCl** (81%), free ligand (9%), and other unidentified ^{31}P NMR resonances. After 22 h at 140 °C, the $^{31}\text{P}\{^1\text{H}\}$ NMR spectrum contained **226-HCl** (95%) and free ligand (5%).

Method D with $(\text{COD})\text{IrCl}_2$. **205** (93 μL , 51 μmol , 0.55 M in toluene) and $(\text{COD})\text{IrCl}_2$ (16.4 mg, 24.4 μmol) were added to a J. Young NMR tube. Toluene (1 mL)

was added to form a yellow solution. The J. Young NMR tube was closed. The J. Young NMR tube was then degassed through a freeze-pump-thaw cycle and refilled with H₂ (1 atm; ca. 2 mL, 0.08 mmol). The solution was analyzed by ³¹P{¹H} NMR spectroscopy after the J. Young NMR tube was placed into an oil bath at 120 °C for 19 h, and at 140 °C over a weekend. The yellow solution turned orange upon heating, and slowly turned dark red. After 19 h at 120 °C, the ³¹P{¹H} NMR spectrum contained **226-HCl** (88%) and free ligand **205** (12%). After a weekend at 140 °C, the ³¹P{¹H} NMR spectrum contained **226-HCl** (94%) and free ligand **205** (6%).

Method D with [(COE)₂IrCl]₂. **205** (115 μL, 63 μmol, 0.55 M in toluene) and [(COE)₂IrCl]₂ (27 mg, 30 μmol) were added to a J. Young NMR tube. Toluene (1 mL) was added to form a yellow solution. The J. Young NMR tube was closed. The J. Young NMR tube was then degassed through a freeze-pump-thaw cycle and refilled with H₂ (1 atm; ca. 2 mL, 0.08 mmol). The solution was analyzed by ³¹P{¹H} NMR spectroscopy after the J. Young NMR tube was placed into an oil bath at 120 °C for 19 h. The yellow solution turned orange upon heating, and slowly turned to dark red. After 19 h at 120 °C, the ³¹P{¹H} NMR spectrum contained only **226-HCl**.

After the screening, method D with [(COE)₂IrCl]₂ was chosen to synthesize **226-HCl** on a preparative scale.

2.4.3.3 Screening of Methods for Metalation of **207**

Method B with [(COD)IrCl]₂. [(COD)IrCl]₂ (27.8 mg, 41.4 μmol) and pyridine (1.0 mL, 12 mmol) were added to a J. Young NMR tube to form a yellow solution. **207**

(25.5 mg, 89.1 μmol) was then added to the J. Young NMR tube to form a yellow solution. The J. Young NMR tube was closed. The yellow solution was immediately analyzed by $^{31}\text{P}\{^1\text{H}\}$ NMR spectroscopy, then again after the J. Young NMR tube was placed into an oil bath at 110 $^{\circ}\text{C}$ for 20 h and at 150 $^{\circ}\text{C}$ for 74 h. The yellow solution turned to a light-yellow solution after heating at 110 $^{\circ}\text{C}$ for 20 h. Prior to heating and after heating at 110 $^{\circ}\text{C}$ for 20 h, both $^{31}\text{P}\{^1\text{H}\}$ NMR spectra contained multiple unidentified ^{31}P NMR resonances. After heating at 150 $^{\circ}\text{C}$ for 74 h, the $^{31}\text{P}\{^1\text{H}\}$ NMR spectrum contained two major ^{31}P NMR resonances at δ 140.4 (13%) and 139.9 (52%), respectively, and other unidentified ^{31}P NMR resonances.

Method B with $[(\text{COE})_2\text{IrCl}]_2$. $[(\text{COE})_2\text{IrCl}]_2$ (32.9 mg, 36.7 μmol) and pyridine (0.7 mL, 9 mmol) were added to a J. Young NMR tube to form an orange-red solution. **207** (23.0 mg, 84.3 μmol) was then added to the J. Young NMR tube to form an orange solution. The J. Young NMR tube was closed. The orange solution was immediately analyzed by $^{31}\text{P}\{^1\text{H}\}$ NMR spectroscopy, then again after the J. Young NMR tube was placed into an oil bath at 110 $^{\circ}\text{C}$ for 21 h and at 150 $^{\circ}\text{C}$ for 97 h. The orange solution turned to a light-yellow solution after heating at 110 $^{\circ}\text{C}$ for 21 h. Prior to heating and after heating at 110 $^{\circ}\text{C}$ for 21 h, both $^{31}\text{P}\{^1\text{H}\}$ NMR spectra contained multiple unidentified ^{31}P NMR resonances. After heating at 150 $^{\circ}\text{C}$ for 97 h, the $^{31}\text{P}\{^1\text{H}\}$ NMR spectrum contained two major ^{31}P NMR resonances at δ 140.4 (8%) and 139.9 (37%), respectively, and other unidentified ^{31}P NMR resonances.

Method C. **207** (45 mg, 0.16 mmol) and $[(\text{COD})\text{Ir}(\text{OAc})_2]$ (53 mg, 74 μmol) were added to a J. Young NMR tube. Toluene (0.8 mL) was added to form a light-brown

solution. The J. Young NMR tube was closed. The light-brown solution was immediately analyzed by $^{31}\text{P}\{^1\text{H}\}$ NMR spectroscopy, then again after the J. Young NMR tube was placed into an oil bath at 120 °C for 18 h and at 150 °C for 73 h. The light-brown solution turned darker upon heating. Prior to heating, the $^{31}\text{P}\{^1\text{H}\}$ NMR spectrum contained multiple unidentified broad ^{31}P NMR resonances. After 18 h at 120 °C, the $^{31}\text{P}\{^1\text{H}\}$ NMR spectrum contained a sharp ^{31}P NMR resonance at δ 173.4 (6%) and other unidentified broad ^{31}P NMR resonances. After 73 h at 150 °C, the $^{31}\text{P}\{^1\text{H}\}$ NMR spectrum contained the same ^{31}P NMR resonance at δ 173.4 (13%) and other unidentified ^{31}P NMR resonances.

Method D with [(COD)Ir(OAc)]₂. 207 (22.8 mg, 79.6 μmol) and [(COD)Ir(OAc)]₂ (28.6 mg, 39.8 μmol) were added to a J. Young NMR tube. Toluene (0.4 mL) was added to form a light-brown solution. The J. Young NMR tube was closed. The J. Young NMR tube was then degassed through three freeze-pump-thaw cycles and refilled with H₂ (1 atm; ca. 2 mL, 0.08 mmol). The light-brown solution was immediately analyzed by $^{31}\text{P}\{^1\text{H}\}$ NMR spectroscopy, then again after the J. Young NMR tube was placed into an oil bath at 120 °C for 21 h and at 150 °C for 6 h. All $^{31}\text{P}\{^1\text{H}\}$ NMR spectra contained multiple unidentified ^{31}P NMR resonances.

Method E. 207 (26 mg, 91 μmol) and [(MesH)Ir(Bpin)₃] (59 mg, 85 μmol) were added to a J. Young NMR tube. C₆D₆ (0.4 mL) was added. The solution was immediately analyzed by $^{31}\text{P}\{^1\text{H}\}$ NMR spectroscopy, then again after the J. Young NMR tube was placed into an oil bath at 80 °C for 13 h and 60 h. All $^{31}\text{P}\{^1\text{H}\}$ NMR spectra contained multiple unidentified ^{31}P NMR resonances.

Since the attempted metalation reactions of **207** were not clean enough to isolate a pure complex of iridium, the synthesis on a preparative scale was not performed.

2.4.3.4 Screening of Methods for Metalation of **208**

Method A with [(COD)IrCl]₂. **208** (35 mg, 84 μmol) and [(COD)IrCl]₂ (25 mg, 37 μmol) were added to a J. Young NMR tube. Toluene (1 mL) was added to form a yellow solution. The J. Young NMR tube was closed. The yellow solution was immediately analyzed by ³¹P{¹H} NMR spectroscopy, then again after the J. Young NMR tube was placed into an oil bath at 110 °C for 42 h, and at 150 °C for 24 h. Prior to heating, the ³¹P{¹H} NMR spectrum contained multiple ³¹P NMR resonances. After 42 h at 110 °C, the ³¹P{¹H} NMR spectrum contained at least five sets of ³¹P NMR resonances for pincer complexes. After 24 h at 150 °C, the ³¹P{¹H} NMR spectrum contained three sets of ³¹P NMR resonances for pincer complexes.

Method A with [(COE)₂IrCl]₂. **208** (88 μL , 47 μmol , 0.537 M in toluene) and [(COE)₂IrCl]₂ (20.2 mg, 22.5 μmol) were added to a J. Young NMR tube. Toluene (1 mL) was added to form an orange solution. The J. Young NMR tube was closed. The orange solution was immediately analyzed by ³¹P{¹H} NMR spectroscopy, then again after the J. Young NMR tube was placed into an oil bath at 110 °C for 40 h. Prior to heating, the ³¹P{¹H} NMR spectrum contained multiple ³¹P NMR resonances. After 40 h at 110 °C, the ³¹P{¹H} NMR spectrum contained only **228-HCl**.

Method B with [(COD)IrCl]₂. [(COD)IrCl]₂ (36.5 mg, 54.3 μmol) and pyridine (10 μL , 0.12 mmol) were added to a J. Young NMR tube. Toluene (1 mL) was added to form

a yellow solution. **208** (375 μL , 108 μmol , 0.289 M in toluene) was then added to the J. Young NMR tube to form an orange solution. The J. Young NMR tube was closed. The orange solution was immediately analyzed by $^{31}\text{P}\{^1\text{H}\}$ NMR spectroscopy, then again after the J. Young NMR tube was placed into an oil bath at 110 $^{\circ}\text{C}$ for 16 h. Prior to heating, the $^{31}\text{P}\{^1\text{H}\}$ NMR spectrum contained multiple ^{31}P NMR resonances. After 16 h at 110 $^{\circ}\text{C}$, the $^{31}\text{P}\{^1\text{H}\}$ NMR spectrum contained a set of ^{31}P NMR resonances for **228-HClpy** (70%) and other unidentified ^{31}P NMR resonances.

After the screening, method A with $[(\text{COE})_2\text{IrCl}]_2$ was chosen to synthesize **228-HCl** on a preparative scale.

2.4.3.5 Screening of Methods for Metalation of **209**

Method A with $[(\text{COD})\text{IrCl}]_2$. **209** (105 μL , 61.2 μmol , 0.583 M in toluene) and $[(\text{COD})\text{IrCl}]_2$ (20.4 mg, 30.4 μmol) were added to a J. Young NMR tube. Toluene (1 mL) was added to form an orange solution. The J. Young NMR tube was closed. The orange solution was immediately analyzed by $^{31}\text{P}\{^1\text{H}\}$ NMR spectroscopy, then again after the J. Young NMR tube was placed into an oil bath at 110 $^{\circ}\text{C}$ for 43 h. The orange solution turned dark red upon heating. Prior to heating, the $^{31}\text{P}\{^1\text{H}\}$ NMR spectrum contained two major ^{31}P NMR resonances. After 43 h at 110 $^{\circ}\text{C}$, the $^{31}\text{P}\{^1\text{H}\}$ NMR spectrum contained a set of ^{31}P NMR resonances at δ 169.5 (d, $J = 367$ Hz), 104.8 (d, $J = 367$ Hz), which was assigned to **240-HCl** (46%) and other unidentified ^{31}P NMR resonances.

Method A with $[(\text{COE})_2\text{IrCl}]_2$. **209** (91 μL , 53 μmol , 0.583 M in toluene) and $[(\text{COE})_2\text{IrCl}]_2$ (23.1 mg, 25.8 μmol) were added to a J. Young NMR tube. Toluene (1 mL)

was added to form a brown suspension. The J. Young NMR tube was closed. The brown suspension was immediately analyzed by $^{31}\text{P}\{^1\text{H}\}$ NMR spectroscopy, then again after the J. Young NMR tube was placed into an oil bath at 110 °C for 23 h. The brown suspension turned purple solution upon heating. Prior to heating, the $^{31}\text{P}\{^1\text{H}\}$ NMR spectrum contained multiple broad ^{31}P NMR resonances. After 23 h at 110 °C, the $^{31}\text{P}\{^1\text{H}\}$ NMR spectrum contained **240-HCl** (71%) and other unidentified ^{31}P NMR resonances.

Method B with [(COD)IrCl]₂. [(COD)IrCl]₂ (22.7 mg, 33.8 μmol) and pyridine (6.0 μL, 74 μmol) were added to a J. Young NMR tube. Toluene (1 mL) was added to form a solution. **209** (116 μL, 67.6 μmol, 0.583 M in toluene) was then added to the J. Young NMR tube to form a yellow solution. The J. Young NMR tube was closed. The yellow solution was immediately analyzed by $^{31}\text{P}\{^1\text{H}\}$ NMR spectroscopy, then again after the J. Young NMR tube was placed into an oil bath at 110 °C for 1.5 h. The yellow solution turned faint yellow upon heating and turned yellow after 1.5 h at 110 °C. Prior to heating, the $^{31}\text{P}\{^1\text{H}\}$ NMR spectrum contained multiple ^{31}P NMR resonances. After 1.5 h at 110 °C, the $^{31}\text{P}\{^1\text{H}\}$ NMR spectrum contained a major set of ^{31}P NMR resonances at δ 146.5 (d, $J = 385$ Hz), 80.6 (d, $J = 385$ Hz), which was assigned to **240-HClpy** (93%) and other minor unidentified ^{31}P NMR resonances.

Method C. **209** (65 μL, 38 μmol, 0.583 M in toluene) and [(COD)Ir(OAc)]₂ (12.7 mg, 17.7 μmol) were added to a J. Young NMR tube. Toluene (1 mL) was added to form a brown-yellow solution. The J. Young NMR tube was closed. The brown-yellow solution was immediately analyzed by $^{31}\text{P}\{^1\text{H}\}$ NMR spectroscopy, then again after the J. Young NMR tube was placed into an oil bath at 110 °C for 42 h. The brown-yellow solution

turned light-brown upon heating. Prior to heating, the $^{31}\text{P}\{^1\text{H}\}$ NMR spectrum contained multiple broad ^{31}P NMR resonances. After 42 h at 110 °C, the $^{31}\text{P}\{^1\text{H}\}$ NMR spectrum contained two sets of ^{31}P NMR resonances for two pincer complexes (60% and 28%, respectively) and other unidentified ^{31}P NMR resonances.

Method D with $[(\text{COE})_2\text{IrCl}]_2$. **209** (91 μL , 53 μmol , 0.583 M in toluene) and $[(\text{COE})_2\text{IrCl}]_2$ (22.7 mg, 25.3 μmol) were added to a J. Young NMR tube. Toluene (1 mL) was added to form a brown suspension. The J. Young NMR tube was closed. The J. Young NMR tube was then degassed through a freeze-pump-thaw cycle and refilled with H_2 (1 atm; ca. 2 mL, 0.08 mmol). The brown suspension was analyzed by $^{31}\text{P}\{^1\text{H}\}$ NMR spectroscopy after the J. Young NMR tube was placed into an oil bath at 120 °C for 37 h. The brown suspension turned to a purple solution after 37 h at 120 °C. After 37 h at 120 °C, the $^{31}\text{P}\{^1\text{H}\}$ NMR spectrum contained **240-HCl** (84%) and other unidentified ^{31}P NMR resonances.

Method E: **209** (24 mg, 69 μmol) and $[(\text{MesH})\text{Ir}(\text{Bpin})_3]$ (44 mg, 63 μmol) were added to a J. Young NMR tube. C_6D_6 (0.5 mL) was added to form a bright orange solution. The bright orange solution was immediately analyzed by $^{31}\text{P}\{^1\text{H}\}$ NMR spectroscopy, then again after the J. Young NMR tube was placed into an oil bath at 80 °C for 66 h. Prior to heating, the $^{31}\text{P}\{^1\text{H}\}$ NMR spectrum contained only free **209**. After 66 h at 80 °C, the $^{31}\text{P}\{^1\text{H}\}$ NMR spectrum contained multiple unidentified ^{31}P NMR resonances.

Attempt at pyridine abstraction of 240-HClpy. **240-HClpy** (20 mg, 31 μmol) was dissolved in C_6D_6 (1 mL) in a J. Young NMR tube. BF_3OEt_2 (40.0 μL , 324 μmol) was added to form a dark purple solution. The reaction was heated at 100 °C for 14 h. ^1H and

$^{31}\text{P}\{^1\text{H}\}$ NMR spectroscopy showed full consumption of **240-HClpy** and clean formation of **240-HCl**. Excess BF_3OEt_2 and volatiles were removed under vacuum. The reddish-purple solid was dissolved in C_6D_6 and analyzed by ^1H and $^{31}\text{P}\{^1\text{H}\}$ NMR spectroscopy. The $^{31}\text{P}\{^1\text{H}\}$ NMR spectrum contained only **240-HCl**. The ^1H NMR spectrum contained **240-HCl**, BF_3py and trace BF_3OEt_2 . The purification was attempted by recrystallization/reprecipitation from toluene, pentane, THF, and the mixed solvents, and flash column chromatography. Recrystallization or reprecipitation were not successful methods to purify **240-HCl** because **240-HCl** and BF_3py have similar solubility in toluene and pentane. Flash column chromatography on silica gel using toluene as eluent or dissolving the mixture in THF led to partial or full regeneration of **240-HClpy**. **240-HCl** was characterized with BF_3py and trace BF_3OEt_2 by ^1H , $^{13}\text{C}\{^1\text{H}\}$, and $^{19}\text{P}\{^1\text{H}\}$ NMR spectroscopy. ^1H NMR (499 MHz, C_6D_6) δ 6.86 (t, $J = 7.8$ Hz, 1H), 6.66 (d, $J = 7.9$ Hz, 1H), 6.28–6.13 (m, 1H, overlapped with BF_3py), 3.77 (br s, 1H), 2.74–2.59 (m, 1H), 2.59–2.45 (m, 1H), 2.36–2.21 (m, 1H), 2.05–1.91 (m, 1H), 1.27 (dd, $J = 17.2, 7.2$ Hz, 3H), 1.21–1.07 (m, 12H), 1.03 (dd, $J = 15.6, 7.0$ Hz, 1H), 0.94–0.82 (m, 6H), –37.42 (br s, 1H). $^{13}\text{C}\{^1\text{H}\}$ NMR (126 MHz, C_6D_6) δ 166.6 (t, $J_{\text{P-C}} = 6.2$ Hz), 156.6 (m), 125.2, 111.1 (m), 104.1 (d, $J_{\text{P-C}} = 12.4$ Hz), 103.3 (d, $J_{\text{P-C}} = 11.5$ Hz), 31.3 (dd, $J_{\text{P-C}} = 25.2, 5.0$ Hz), 29.6–28.7 (m, 2C), 27.7 (dd, $J_{\text{P-C}} = 30.2, 3.1$ Hz), 18.0, 17.8 (d, $J_{\text{P-C}} = 7.2$ Hz), 17.7–17.4 (m, 2C), 17.2–16.9 (m, 2C), 16.9–16.6 (m, 2C). $^{31}\text{P}\{^1\text{H}\}$ NMR (202 MHz, C_6D_6) δ 170.9 (d, $J = 365$ Hz), 106.0 (d, $J = 365$ Hz).

Attempt at converting 240-HClpy to 240-hexene. **240-HClpy** (28.1 mg, 43.3 μmol) was dissolved in toluene (1 mL) in a 7 mL vial. BF_3OEt_2 (53 μL , 0.43 mmol) was

added. The reaction was stirred at ambient temperature for 24 h. The mixture was filtered through Celite over a pipette. Excess BF_3OEt_2 and volatiles were removed under vacuum. The resulting solid was suspended in pentane (10 mL) in a 50 mL culture tube. NaO^tBu (20 mg, 0.21 mmol) and 1-hexene (15 μL , 0.12 mmol) were added to the culture tube. The reaction mixture was vigorously stirred for 2 d and changed from cloudy suspension to orange solution with white precipitation. The mixture was filtered through Celite over a frit. All volatiles were removed under vacuum. The resulting solid was analyzed by $^{31}\text{P}\{^1\text{H}\}$ NMR spectroscopy. The $^{31}\text{P}\{^1\text{H}\}$ NMR spectrum contained unreacted **240-HClpy** (26%), one major set of ^{31}P NMR resonances at δ 174.4 (d, $J = 372$ Hz), 104.1 (d, $J = 372$ Hz), which was assigned to **240-hexene** (33%) and other unidentified ^{31}P NMR resonances.

Attempt at reacting 240-HCl in situ with propargyloxytrimethylsilane. **240-HClpy** (17.7 mg, 27.3 μmol) and propargyloxytrimethylsilane (20 μL , 0.13 mmol) were dissolved in C_6D_6 (1 mL) in a J. Young NMR tube. BF_3OEt_2 (17 μL , 0.13 mmol) was added. A black solid formed immediately, and the solution became colorless over time. The solution was immediately analyzed by $^{31}\text{P}\{^1\text{H}\}$ NMR spectroscopy, then again after the J. Young NMR tube was stirred at ambient temperature for 37 h. Both $^{31}\text{P}\{^1\text{H}\}$ NMR spectra showed no ^{31}P NMR resonance.

Attempt at reacting 240-HClpy with NaBEt_3H . **240-HClpy** (20.5 mg, 31.6 μmol) was dissolved in toluene (0.5 mL) in a J. Young NMR tube. NaBEt_3H (32 μL , 32 μmol , 1.0 M in toluene) was added to form a yellow solution. The solution was immediately analyzed by $^{31}\text{P}\{^1\text{H}\}$ NMR spectroscopy, then again after the J. Young NMR tube was

placed into an oil bath at 70 °C for 28 h and 80 °C for 20 h. The solution turned orange after heating at 70 °C. All $^{31}\text{P}\{^1\text{H}\}$ NMR spectra contained multiple unidentified ^{31}P NMR resonances.

Attempt at reacting 240-HClpy with HBpin. **240-HClpy** (15.7 mg, 24.2 μmol) and HBpin (18 μL , 0.12 mmol) were dissolved in toluene (0.5 mL) in a J. Young NMR tube. The light-yellow solution was immediately analyzed by $^{31}\text{P}\{^1\text{H}\}$ NMR spectroscopy, then again after the J. Young NMR tube was placed into an oil bath at 80 °C for 21 h and 100 °C for 4 h. Before heating, the ^{31}P NMR spectrum contained only **240-HClpy**. After heating at 80 °C for 21 h and 100 °C for 4 h, the ^{31}P NMR spectrum contained one major set of ^{31}P NMR resonances at δ 166.8 (d, $J = 345$ Hz), 118.4 (d, $J = 345$ Hz), and other minor unidentified resonances. All volatiles were removed under vacuum. The residue was dissolved in C_6D_6 and analyzed by ^1H and $^{31}\text{P}\{^1\text{H}\}$ NMR spectroscopy. Although the ^{31}P NMR spectrum looked approximately the same, the ^1H NMR spectrum contained multiple unidentified Ir–H peaks.

After screening, method B with $[(\text{COD})\text{IrCl}]_2$ was chosen to prepare **240-HClpy** on a preparative scale. However, the attempts to isolate **240-HCl** or other derivatives were not successful. Therefore, the preparation of **240-HCl** was not performed on a preparative scale.

2.4.3.6 Screening of Methods for Metalation of **210**

Method A with $[(\text{COD})\text{IrCl}]_2$. **210** (38.1 mg, 112 μmol) and $[(\text{COD})\text{IrCl}]_2$ (36 mg, 54 μmol) were added to a J. Young NMR tube. Toluene (1.5 mL) was added to form an

orange solution. The J. Young NMR tube was closed. The orange solution was immediately analyzed by $^{31}\text{P}\{^1\text{H}\}$ NMR spectroscopy, then again after the J. Young NMR tube was placed into an oil bath at 110 °C for 39 h. The orange solution turned to an orange-brown solution with significant precipitation upon heating, then to a dark purple solution after 39 h at 110 °C. Prior to heating, the $^{31}\text{P}\{^1\text{H}\}$ NMR spectrum contained two broad ^{31}P NMR resonances. After 39 h at 110 °C, the $^{31}\text{P}\{^1\text{H}\}$ NMR spectrum contained a major ^{31}P NMR resonance at δ 103.4 (s), which was assigned to **(210)Ir(H)(Cl)**, **241-HCl** (56%), and other unidentified ^{31}P NMR resonances.

Method A with [(COE)₂IrCl]₂. **210** (24.0 mg, 70.5 μmol) and [(COE)₂IrCl]₂ (30 mg, 33 μmol) were added to a J. Young NMR tube. Toluene (1.5 mL) was added to form a brown solution. The J. Young NMR tube was closed. The brown solution was immediately analyzed by $^{31}\text{P}\{^1\text{H}\}$ NMR spectroscopy, then again after the J. Young NMR tube was placed into an oil bath at 110 °C for 36 h and at 150 °C for 18.5 h. The brown solution formed significant precipitation upon heating, then turned to a dark purple solution after 36 h. Prior to heating, the $^{31}\text{P}\{^1\text{H}\}$ NMR spectrum contained one major ^{31}P NMR resonance. After 36 h at 110 °C, the $^{31}\text{P}\{^1\text{H}\}$ NMR spectrum contained **241-HCl** (36%) and other unidentified ^{31}P NMR resonances. After 18.5 h at 150 °C, the $^{31}\text{P}\{^1\text{H}\}$ NMR spectrum contained **241-HCl** (56%) and other unidentified ^{31}P NMR resonances.

Method B with [(COD)IrCl]₂. [(COD)IrCl]₂ (29.3 mg, 44.0 μmol) and pyridine (35 μL , 0.43 mmol) were added to a J. Young NMR tube. Toluene (1 mL) was added to form a solution. **210** (30.7 mg, 90.2 μmol) was then added to the J. Young NMR tube to form an orange solution. The J. Young NMR tube was closed. The orange solution was

immediately analyzed by $^{31}\text{P}\{^1\text{H}\}$ NMR spectroscopy, then again after the J. Young NMR tube was placed into an oil bath at 110 °C for 23 h and at 150 °C for 24 h. The orange solution turned yellow upon heating. Prior to heating, the $^{31}\text{P}\{^1\text{H}\}$ NMR spectrum contained multiple broad ^{31}P NMR resonances. After 23 h at 110 °C, the $^{31}\text{P}\{^1\text{H}\}$ NMR spectrum contained **241-HClpy** (82%) and other unidentified ^{31}P NMR resonances. After 24 h at 150 °C, the $^{31}\text{P}\{^1\text{H}\}$ NMR spectrum contained **241-HClpy** (84%) and other unidentified ^{31}P NMR resonances.

Method B with $[(\text{COE})_2\text{IrCl}]_2$. $[(\text{COE})_2\text{IrCl}]_2$ (37 mg, 41 μmol) and pyridine (33 μL , 0.41 mmol) were added to a J. Young NMR tube. Toluene (1 mL) was added to form a solution. **210** (30.4 mg, 89.3 μmol) was then added to the J. Young NMR tube to form a yellow-orange suspension. The J. Young NMR tube was closed. The yellow-orange suspension was immediately analyzed by $^{31}\text{P}\{^1\text{H}\}$ NMR spectroscopy, then again after the J. Young NMR tube was placed into an oil bath at 110 °C for 12 h. The yellow-orange suspension turned to a yellow solution upon heating and significant white precipitation formed after 12 h at 110 °C. Prior to heating, the $^{31}\text{P}\{^1\text{H}\}$ NMR spectrum contained multiple ^{31}P NMR resonances. After 12 h at 110 °C, the $^{31}\text{P}\{^1\text{H}\}$ NMR spectrum contained a major ^{31}P NMR resonance at δ 79.9 (s), which was assigned to **241-HClpy** (66%) and other unidentified ^{31}P NMR resonances.

Method C: **210** (12.1 mg, 35.5 μmol) and $[(\text{COD})\text{Ir}(\text{OAc})_2]$ (12.0 mg, 16.7 μmol) were added to a J. Young NMR tube. Toluene (1 mL) was added to form a brown-red solution. The J. Young NMR tube was closed. The brown-red solution was immediately analyzed by $^{31}\text{P}\{^1\text{H}\}$ NMR spectroscopy, then again after the J. Young NMR tube was

placed into an oil bath at 110 °C for 42 h and at 150 °C for 6 h. The brown-red solution turned light-brown upon heating. Prior to heating, the $^{31}\text{P}\{^1\text{H}\}$ NMR spectrum contained multiple broad ^{31}P NMR resonances. After 42 h at 110 °C, the $^{31}\text{P}\{^1\text{H}\}$ NMR spectrum contained three major ^{31}P NMR resonances at δ 91.6 (s) (44%), 81.2 (s) (33%), 71.9 (s) (12%), respectively, and other unidentified ^{31}P NMR resonances. After 6 h at 150 °C, the $^{31}\text{P}\{^1\text{H}\}$ NMR spectrum did not change.

Method D with [(COD)IrCl]₂: 210 (23.3 mg, 68.4 μmol) and [(COD)IrCl]₂ (21.9 mg, 32.6 μmol) were added to a J. Young NMR tube. Toluene (1 mL) was added to form a yellow solution. The J. Young NMR tube was closed. The J. Young NMR tube was then degassed through two freeze-pump-thaw cycles and refilled with H₂ (1 atm; ca. 2 mL, 0.08 mmol). The yellow solution was immediately analyzed by $^{31}\text{P}\{^1\text{H}\}$ NMR spectroscopy, then again after the J. Young NMR tube was placed into an oil bath at 110 °C for 13 h and at 150 °C for 24 h. The yellow solution turned faint yellow (almost colorless) with white precipitation after 13 h at 110 °C. Prior to heating, after 13 h at 110 °C and 24 h at 150 °C, all $^{31}\text{P}\{^1\text{H}\}$ NMR spectra contained multiple unidentified ^{31}P NMR resonances.

Method D with [(COE)₂IrCl]₂: 210 (15.7 mg, 46.1 μmol) and [(COE)₂IrCl]₂ (20.6 mg, 23.0 μmol) were added to a J. Young NMR tube. Toluene (1 mL) was added to form a brown solution. The J. Young NMR tube was closed. The J. Young NMR tube was then degassed through two freeze-pump-thaw cycles and refilled with H₂ (1 atm; ca. 2 mL, 0.08 mmol) to give a brown solid with black precipitation. The brown solution was immediately analyzed by $^{31}\text{P}\{^1\text{H}\}$ NMR spectroscopy, then again after the J. Young NMR tube was placed into an oil bath at 110 °C for 13 h and at 150 °C for 24 h. The brown solution turned

light-yellow with brown precipitation after 13 h at 110 °C. Prior to heating, the $^{31}\text{P}\{^1\text{H}\}$ NMR spectrum contained one ^{31}P NMR resonance. After 13 h at 110 °C and 24 h at 150 °C, both $^{31}\text{P}\{^1\text{H}\}$ NMR spectra contained multiple unidentified ^{31}P NMR resonances.

Since the attempted metalation reactions of **210** were not clean enough to isolate a pure complex of iridium, the synthesis on a preparative scale was not performed.

2.4.3.7 Screening of Methods for Metalation of **211**

Method A with [(COD)IrCl]₂. **211** (19.4 mg, 52.6 μmol) and [(COD)IrCl]₂ (17.0 mg, 25.3 μmol) were added to a J. Young NMR tube. Toluene (0.5 mL) was added to form an orange solution. The J. Young NMR tube was closed. The J. Young NMR tube was placed into an oil bath at 120 °C for 2 h. The orange solution turned black upon heating. After heating at 120 °C for 2 h, significant black precipitation formed and the solution became almost colorless, indicating the Ir complexes were not soluble in toluene. Further investigation was not performed.

Method B with [(COD)IrCl]₂. [(COD)IrCl]₂ (20 mg, 30 μmol) and pyridine (50 μL, 0.62 mmol) were added to a J. Young NMR tube. Toluene (0.4 mL) was added to form a solution. **211** (23.5 mg, 63.8 μmol) was then added to the J. Young NMR tube to form an orange-red solution. The J. Young NMR tube was closed. The orange-red solution was immediately analyzed by $^{31}\text{P}\{^1\text{H}\}$ NMR spectroscopy, then again after the J. Young NMR tube was placed into an oil bath at 120 °C for 12 h. The orange-red solution turned to an orange suspension upon heating. Prior to heating and after 12 h at 120 °C, both $^{31}\text{P}\{^1\text{H}\}$ NMR spectra contained multiple ^{31}P NMR resonances.

Method C. **211** (19.4 mg, 52.6 μmol) and $[(\text{COD})\text{Ir}(\text{OAc})_2]$ (19.1 mg, 26.6 μmol) were added to a J. Young NMR tube. Toluene (0.5 mL) was added to form a dark brown solution. The J. Young NMR tube was closed. The dark brown solution was immediately analyzed by $^{31}\text{P}\{^1\text{H}\}$ NMR spectroscopy, then again after the J. Young NMR tube was placed into an oil bath at 120 $^\circ\text{C}$ for 24 h and at 150 $^\circ\text{C}$ for 16 h. Prior to heating, after 24 h at 120 $^\circ\text{C}$, and after 16 h at 150 $^\circ\text{C}$, all $^{31}\text{P}\{^1\text{H}\}$ NMR spectra contained multiple broad ^{31}P NMR resonances.

Method D with $[(\text{COD})\text{IrCl}]_2$. **211** (44.1 mg, 120 μmol) and $[(\text{COD})\text{IrCl}]_2$ (36.7 mg, 54.6 μmol) were added to a J. Young NMR tube. Toluene (0.7 mL) was added to form a brown-orange solution. The J. Young NMR tube was closed. The J. Young NMR tube was then degassed through three freeze-pump-thaw cycles and refilled with H_2 (1 atm; ca. 2 mL, 0.08 mmol). The brown-orange solution was immediately analyzed by $^{31}\text{P}\{^1\text{H}\}$ NMR spectroscopy, then again after the J. Young NMR tube was placed into an oil bath at 110 $^\circ\text{C}$ for 48 h and at 150 $^\circ\text{C}$ for 16 h. The brown-orange solution turned darker with the formation of precipitation upon heating. Prior to heating, the $^{31}\text{P}\{^1\text{H}\}$ NMR spectrum contained multiple ^{31}P NMR resonances. After 48 h at 110 $^\circ\text{C}$, the $^{31}\text{P}\{^1\text{H}\}$ NMR spectrum contained three major ^{31}P NMR resonances at δ 116.2 (57%), 93.1 (21%), -2.7 (12%), respectively, and other unidentified ^{31}P NMR resonances. After 16 h at 150 $^\circ\text{C}$, the $^{31}\text{P}\{^1\text{H}\}$ NMR spectrum contained the same three major ^{31}P NMR resonances at δ 116.2 (63%), 93.1 (21%), -2.7 (10%), respectively, and other unidentified ^{31}P NMR resonances.

Method E. **211** (21.0 mg, 57.0 μmol) and $(\text{MesH})\text{Ir}(\text{Bpin})_3$ (37.8 mg, 54.5 μmol) were added to a J. Young NMR tube. Toluene (0.5 mL) was added to form a faint yellow

solution. The faint yellow solution was immediately analyzed by $^{11}\text{B}\{^1\text{H}\}$ and $^{31}\text{P}\{^1\text{H}\}$ NMR spectroscopy, then again after the J. Young NMR tube was placed into an oil bath at 80 °C for 1 h. Prior to heating, the $^{31}\text{P}\{^1\text{H}\}$ NMR spectrum contained only free **211** ligand, and the $^{11}\text{B}\{^1\text{H}\}$ NMR spectroscopy contained (MesH)Ir(Bpin)₃ precursor and trace HBpin. After 1 h at 80 °C, the $^{31}\text{P}\{^1\text{H}\}$ NMR spectrum contained a set of ^{31}P NMR resonances at δ 112.8 (d, $J = 339$ Hz), 112.1 (d, $J = 339$ Hz), which was tentatively assigned to a **242-H₃Bpin** (87%), a ^{31}P NMR resonance at δ 112.5 (s), which was tentatively assigned to **243-H₃Bpin** (10%), and other unidentified ^{31}P NMR resonances. The $^{11}\text{B}\{^1\text{H}\}$ NMR spectrum contained HBpin, tolyl-Bpin, a ^{11}B NMR resonance at δ 37.1, which was tentatively assigned to **242-H₃Bpin**, and an unknown ^{11}B NMR resonance at δ 21.4. Volatiles were removed under vacuum. The residue was dissolved in C₆D₆ and analyzed by ^1H NMR spectroscopy. The hydride region of the ^1H NMR spectrum contained two hydrides resonances at δ -8.59 (br s, 1H), -10.37 (br s, 2H), which were tentatively assigned to **242-H₃Bpin**.

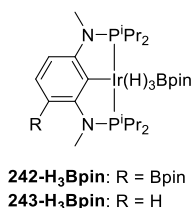


Figure II-11. Structures of **242-H₃Bpin** and **243-H₃Bpin**.

Since the attempted metalation reactions of **211** were not clean enough to isolate a pure complex of iridium, the preparation on a preparative scale was not performed.

2.4.3.8 Screening of Methods for Metalation of **213**

Method B with [(COD)IrCl]₂. [(COD)IrCl]₂ (37.9 mg, 56.4 μmol) and pyridine (1.0 mL, 12 mmol) were added to a J. Young NMR tube to form a yellow solution. **213** (37.8 mg, 134 μmol) was then added to the J. Young NMR tube to form an orange solution. The J. Young NMR tube was closed. The orange solution was immediately analyzed by ³¹P{¹H} NMR spectroscopy, then again after the J. Young NMR tube was placed into an oil bath at 110 °C for 20 h and at 150 °C for 24 h. The orange solution turned to a light-yellow solution after heating at 110 °C for 20 h. Prior to heating, ³¹P{¹H} NMR spectrum showed a broad ³¹P NMR resonance at δ -17 (br). After heating at 110 °C for 20 h and 150 °C for 24 h, both ³¹P{¹H} NMR spectra contained multiple unidentified ³¹P NMR resonances.

Method B with [(COE)₂IrCl]₂. [(COE)₂IrCl]₂ (40.3 mg, 45.0 μmol) and pyridine (0.7 mL, 9 mmol) were added to a J. Young NMR tube to form an orange-red solution. **213** (28.4 mg, 101 μmol) was then added to the J. Young NMR tube to form an orange solution. The J. Young NMR tube was closed. The orange solution was immediately analyzed by ³¹P{¹H} NMR spectroscopy, then again after the J. Young NMR tube was placed into an oil bath at 110 °C for 21 h and at 150 °C for 29 h. The orange solution turned to a light-yellow solution after heating at 110 °C for 21 h. All ³¹P{¹H} NMR spectra contained multiple unidentified ³¹P NMR resonances.

Method C. **213** (70 mg, 0.25 mmol) and [(COD)Ir(OAc)]₂ (82 mg, 0.11 mmol) were added to a J. Young NMR tube. Toluene (1.5 mL) was added to form an orange-brown solution. The J. Young NMR tube was closed. The orange-brown solution was

immediately analyzed by $^{31}\text{P}\{^1\text{H}\}$ and/or ^1H NMR spectroscopy, then again after the J. Young NMR tube was placed into an oil bath at 120 °C for 18 h and at 150 °C for 73 h. Some precipitation formed at ambient temperature in the orange-brown solution. The orange-brown solution turned to a light-orange solution upon heating. Prior to heating, the $^{31}\text{P}\{^1\text{H}\}$ NMR spectrum contained two major ^{31}P NMR resonances with other unidentified ^{31}P NMR resonances. After 18 h at 120 °C, the $^{31}\text{P}\{^1\text{H}\}$ NMR spectrum contained multiple unidentified ^{31}P NMR resonances. After 73 h at 150 °C, the $^{31}\text{P}\{^1\text{H}\}$ NMR spectrum contained a major ^{31}P NMR resonance at δ 24.6 (39%) and other unidentified ^{31}P NMR resonances. ^1H NMR spectrum contained multiple hydride ^1H NMR resonances.

Method D with [(COD)Ir(OAc)]₂. 213 (22.9 mg, 81.1 μmol) and [(COD)Ir(OAc)]₂ (27.8 mg, 38.7 μmol) were added to a J. Young NMR tube. Toluene (0.4 mL) was added to form an orange-brown solution. The J. Young NMR tube was closed. The J. Young NMR tube was then degassed through three freeze-pump-thaw cycles and refilled with H₂ (1 atm; ca. 2 mL, 0.08 mmol). The orange-brown solution was immediately analyzed by $^{31}\text{P}\{^1\text{H}\}$ NMR spectroscopy, then again after the J. Young NMR tube was placed into an oil bath at 120 °C for 21 h and at 150 °C for 6 h. Prior to heating and after heating at 120 °C for 21 h, both $^{31}\text{P}\{^1\text{H}\}$ NMR spectra contained multiple unidentified ^{31}P NMR resonances. After 6 h at 150 °C, the $^{31}\text{P}\{^1\text{H}\}$ NMR spectrum contained a major ^{31}P NMR resonance at δ 31.2 (72%) and other unidentified ^{31}P NMR resonances.

Method E. 213 (17.6 mg, 62.3 μmol) and (MesH)Ir(Bpin)₃ (42 mg, 61 μmol) were added to a J. Young NMR tube. C₆D₆ (0.4 mL) was added. The solution was immediately analyzed by $^{31}\text{P}\{^1\text{H}\}$ NMR spectroscopy, then again after the J. Young NMR tube was

placed into an oil bath at 80 °C for 13 h and 60 h. All $^{31}\text{P}\{^1\text{H}\}$ NMR spectra contained multiple unidentified ^{31}P NMR resonances.

Since the attempted metalation reactions of **213** were not clean enough to isolate a pure complex of iridium, the synthesis on a preparative scale was not performed.

2.4.3.9 Screening of Methods for Metalation of **214**

Method A with [(COD)IrCl]₂. 214 (10.0 mg, 25.4 μmol) and [(COD)IrCl]₂ (8.0 mg, 12 μmol) were added to a J. Young NMR tube. Toluene-*d*₈ (1 mL) was added to form an orange solution. The J. Young NMR tube was closed. The solution was analyzed by ^1H NMR spectroscopy after the J. Young NMR tube was placed into an oil bath at 120 °C for 21 h. The orange solution turned brown-red upon heating. Yellow precipitation was formed after 21 h. After 21 h at 120 °C, the ^1H NMR spectrum contained cyclooctadiene isomers and other unidentified ^1H NMR resonances.

Method A with [(COE)₂IrCl]₂. 214 (79 μL , 35 μmol , 0.443 M in toluene) and [(COE)₂IrCl]₂ (15.1 mg, 16.9 μmol) were added to a J. Young NMR tube. Toluene (1 mL) was added to form a yellow solution. The J. Young NMR tube was closed. The yellow solution was immediately analyzed by $^{31}\text{P}\{^1\text{H}\}$ NMR spectroscopy, then again after the J. Young NMR tube was placed into an oil bath at 110 °C for 23 h, and at 150 °C for 19 h. The yellow solution turned orange and gel-like upon heating. Significant precipitation formed after 23 h at 110 °C. The solution turned red with precipitation after 19 h at 150 °C. Prior to heating, the $^{31}\text{P}\{^1\text{H}\}$ NMR spectrum contained ^{31}P NMR resonances of free

ligand and other unidentified broad ^{31}P NMR resonances. After 23 h at 110 °C and 19 h at 150 °C, the $^{31}\text{P}\{^1\text{H}\}$ NMR spectrum showed no ^{31}P NMR resonances.

Method B with [(COD)IrCl]₂. [(COD)IrCl]₂ (19.3 mg, 28.7 μmol) and pyridine (5.2 μL, 65 μmol) were added to a J. Young NMR tube. Toluene (0.8 mL) was added to form a yellow solution. **214** (118 μL, 57.5 μmol, 0.487 M in toluene) was then added to the J. Young NMR tube to form an orange-yellow solution. The J. Young NMR tube was closed. The orange-yellow solution was immediately analyzed by $^{31}\text{P}\{^1\text{H}\}$ NMR spectroscopy, then again after the J. Young NMR tube was placed into an oil bath at 110 °C for 54 h, and at 150 °C for 20 h. The orange-yellow solution turned brown with tan precipitation after heating at 150 °C for 20 h. Prior to heating, the $^{31}\text{P}\{^1\text{H}\}$ NMR spectrum contained multiple ^{31}P NMR resonances. After 54 h at 110 °C, the $^{31}\text{P}\{^1\text{H}\}$ NMR spectrum contained multiple broad ^{31}P NMR resonances. After 20 h at 150 °C, the $^{31}\text{P}\{^1\text{H}\}$ NMR spectrum contained **230-HClpy** (66%), and other unidentified pincer complexes.

Method B with [(COE)₂IrCl]₂. [(COE)₂IrCl]₂ (29.4 mg, 32.8 μmol) and pyridine (25 μL, 0.31 mmol) were added to a J. Young NMR tube. Toluene (1 mL) was added to form an orange solution. **214** (155 μL, 68.7 μmol, 0.443 M in toluene) was then added to the J. Young NMR tube to form a light-yellow solution. The J. Young NMR tube was closed. The light-yellow solution was immediately analyzed by $^{31}\text{P}\{^1\text{H}\}$ NMR spectroscopy, then again after the J. Young NMR tube was placed into an oil bath at 150 °C for 21 h. The light-yellow solution turned darker yellow with white precipitation after 21 h. Prior to heating, the $^{31}\text{P}\{^1\text{H}\}$ NMR spectrum contained multiple ^{31}P NMR resonances. After 21 h at 150 °C, the $^{31}\text{P}\{^1\text{H}\}$ NMR spectrum contained only **230-HClpy**.

Method C. **214** (160 μL , 77.9 μmol , 0.487 M in toluene) and $[(\text{COD})\text{Ir}(\text{OAc})_2]$ (27 mg, 38 μmol) were added to a J. Young NMR tube. Toluene (1 mL) was added to form a yellow solution. The yellow solution then turned brown and gel-like immediately. The J. Young NMR tube was closed. The brown, gel-like solution was immediately analyzed by $^{31}\text{P}\{^1\text{H}\}$ NMR spectroscopy, then again after the J. Young NMR tube was placed into an oil bath at 110 $^\circ\text{C}$ for 42 h and at 150 $^\circ\text{C}$ for 8 h. The brown, gel-like solution turned brown-red, clear solution after 28 h at 110 $^\circ\text{C}$. Prior to heating, the $^{31}\text{P}\{^1\text{H}\}$ NMR spectrum contained a broad ^{31}P NMR resonance. After 42 h at 110 $^\circ\text{C}$, the $^{31}\text{P}\{^1\text{H}\}$ NMR spectrum contained multiple unidentified ^{31}P NMR resonances. After 8 h at 150 $^\circ\text{C}$, the $^{31}\text{P}\{^1\text{H}\}$ NMR spectrum contained more unidentified ^{31}P NMR resonances.

Method D with $[(\text{COD})\text{IrCl}]_2$. **214** (40 μL , 16 μmol , 0.406 M in toluene- d_8) and $[(\text{COD})\text{IrCl}]_2$ (5.5 mg, 8.2 μmol) were added to a J. Young NMR tube. Toluene- d_8 (1 mL) was added to form a light-yellow solution. The J. Young NMR tube was closed. The J. Young NMR tube was then degassed through a freeze-pump-thaw cycle and refilled with H_2 (1 atm; ca. 2 mL, 0.08 mmol). The solution was analyzed by ^1H NMR spectroscopy after the J. Young NMR tube was placed into an oil bath at 120 $^\circ\text{C}$ for 17 h. The solution turned darker and the yellow precipitation formed upon heating. The solution turned orange-red with yellow precipitation after 17 h. After 17 h at 120 $^\circ\text{C}$, the ^1H NMR spectrum contained cyclooctadiene isomers and other unidentified ^1H NMR resonances.

After screening, method B with $[(\text{COE})_2\text{IrCl}]_2$ was chosen to prepare **230-HClpy** on a preparative scale.

2.4.3.10 Screening of Methods for Metalation of **215**

Method A with [(COD)IrCl]₂. **215** (129 μL , 26.8 μmol , 0.208 M in toluene-*d*₈) and [(COD)IrCl]₂ (9.0 mg, 13 μmol) were added to a J. Young NMR tube. Toluene-*d*₈ (1 mL) was added to form an orange solution. The J. Young NMR tube was closed. The solution was analyzed by ¹H NMR spectroscopy after the J. Young NMR tube was placed into an oil bath at 120 °C for 21 h. The orange solution turned yellow-orange upon heating. After 21 h at 120 °C, the ¹H NMR spectrum contained cyclooctadiene isomers and other unidentified ¹H NMR resonances.

Method B with [(COD)IrCl]₂. [(COD)IrCl]₂ (19.5 mg, 29.0 μmol) and pyridine (5.5 μL , 68 μmol) were added to a J. Young NMR tube. Toluene (0.8 mL) was added to form a yellow solution. **215** (90 μL , 59 μmol , 0.655 M in toluene) was then added to the J. Young NMR tube to form an orange-yellow solution. The J. Young NMR tube was closed. The orange-yellow solution was immediately analyzed by ³¹P{¹H} NMR spectroscopy, then again after the J. Young NMR tube was placed into an oil bath at 110 °C for 70 h, and at 150 °C for 67 h. The orange-yellow solution turned yellow after heating at 150 °C for 20 h. Prior to heating, the ³¹P{¹H} NMR spectrum contained multiple ³¹P NMR resonances. After 70 h at 110 °C, the ³¹P{¹H} NMR spectrum contained a set of ³¹P NMR resonances for a pincer complex and other unidentified ³¹P NMR resonances. After 67 h at 150 °C, the ³¹P{¹H} NMR spectrum contained multiple unidentified ³¹P NMR resonances for numerous pincer complexes.

Method B with [(COE)₂IrCl]₂. [(COE)₂IrCl]₂ (35.5 mg, 39.6 μmol) and pyridine (8.0 μL , 99 μmol) were added to a J. Young NMR tube. Toluene (1 mL) was added to

form a solution. **215** (121 μL , 79.3 μmol , 0.655 M in toluene) was then added to the J. Young NMR tube to form an orange-yellow solution. The J. Young NMR tube was closed. The orange-yellow solution was immediately analyzed by $^{31}\text{P}\{^1\text{H}\}$ NMR spectroscopy, then again after the J. Young NMR tube was placed into an oil bath at 110 $^{\circ}\text{C}$ for 24 h, and at 150 $^{\circ}\text{C}$ for 21 h. The orange-yellow solution turned faint yellow upon heating and turned yellow after 21 h at 150 $^{\circ}\text{C}$. Prior to heating, the $^{31}\text{P}\{^1\text{H}\}$ NMR spectrum contained multiple broad ^{31}P NMR resonances. After 24 h at 110 $^{\circ}\text{C}$, the $^{31}\text{P}\{^1\text{H}\}$ NMR spectrum contained a set of ^{31}P NMR resonances for a pincer complex (39%) and other unidentified ^{31}P NMR resonances. After 21 h at 150 $^{\circ}\text{C}$, the $^{31}\text{P}\{^1\text{H}\}$ NMR spectrum contained the same set of ^{31}P NMR resonances (37%) and other unidentified ^{31}P NMR resonances.

Method C. **215** (102 μL , 66.8 μmol , 0.655 M in toluene) and $[(\text{COD})\text{Ir}(\text{OAc})_2]$ (24.0 mg, 33.3 μmol) were added to a J. Young NMR tube. Toluene (1 mL) was added to form a yellow solution. The J. Young NMR tube was closed. The yellow solution was immediately analyzed by $^{31}\text{P}\{^1\text{H}\}$ NMR spectroscopy, then again after the J. Young NMR tube was placed into an oil bath at 110 $^{\circ}\text{C}$ for 25 h and at 150 $^{\circ}\text{C}$ for 8 d. The yellow solution turned orange after 25 h at 110 $^{\circ}\text{C}$ and turned brown-red after 62 h at 150 $^{\circ}\text{C}$. Prior to heating, the $^{31}\text{P}\{^1\text{H}\}$ NMR spectrum contained multiple broad ^{31}P NMR resonances. After 25 h at 110 $^{\circ}\text{C}$, the $^{31}\text{P}\{^1\text{H}\}$ NMR spectrum contained a set of ^{31}P NMR resonances for a pincer complex (18%) and other unidentified ^{31}P NMR resonances. After 8 d at 150 $^{\circ}\text{C}$, the $^{31}\text{P}\{^1\text{H}\}$ NMR spectrum contained the same set of ^{31}P NMR resonances (58%) and other unidentified ^{31}P NMR resonances.

Method D with [(COD)IrCl]₂. 215 (68 μ L, 14 μ mol, 0.208 M in toluene-*d*₈) and [(COD)IrCl]₂ (4.7 mg, 7.0 μ mol) were added to a J. Young NMR tube. Toluene-*d*₈ (1 mL) was added to form a light-yellow solution. The J. Young NMR tube was closed. The J. Young NMR tube was then degassed through a freeze-pump-thaw cycle and refilled with H₂ (1 atm; ca. 2 mL, 0.08 mmol). The solution was analyzed by ¹H NMR spectroscopy after the J. Young NMR tube was placed into an oil bath at 120 °C for 17 h. The solution slowly turned orange-red upon heating. After 17 h at 120 °C, the ¹H NMR spectrum contained cyclooctadiene isomers and other unidentified ¹H NMR resonances.

Method D with [(COE)₂IrCl]₂. 215 (112 μ L, 73.4 μ mol, 0.655 M in toluene) and [(COE)₂IrCl]₂ (32.8 mg, 36.6 μ mol) were added to a J. Young NMR tube. Toluene (1 mL) was added to form a light-yellow solution. The J. Young NMR tube was closed. The J. Young NMR tube was then degassed through a freeze-pump-thaw cycle and refilled with H₂ (1 atm; ca. 2 mL, 0.08 mmol). The solution turned to a yellow suspension. The mixture was analyzed by ³¹P{¹H} NMR spectroscopy after the J. Young NMR tube was placed into an oil bath at 110 °C for 24 h, and at 150 °C for 21 h. The yellow suspension turned orange solution with some yellow precipitation upon heating and turned red solution after 21 h at 150 °C. After 24 h at 110 °C, the ³¹P{¹H} NMR spectrum contained multiple unidentified ³¹P NMR resonances. After 21 h at 150 °C, the ³¹P{¹H} NMR spectrum contained multiple unidentified ³¹P NMR resonances.

Method E. 215 (22 mg, 62 μ mol) and (MesH)Ir(Bpin)₃ (41 mg, 59 μ mol) were added to a J. Young NMR tube. C₆D₆ (0.5 mL) was added to form an orange-yellow solution. The orange-yellow solution was immediately analyzed by ¹H, ¹¹B{¹H}, and/or

$^{31}\text{P}\{^1\text{H}\}$ NMR spectroscopy, then again after the J. Young NMR tube was placed into an oil bath at 80 °C for 19 h. Prior to heating, the ^1H and $^{31}\text{P}\{^1\text{H}\}$ NMR spectra contained only free **215** ligand and the (MesH)Ir(Bpin) $_3$ precursor. After 19 h at 80 °C, the ^1H NMR spectrum contained free mesitylene, HBpin, C $_6$ D $_5$ Bpin, two hydrides resonances at δ – 7.72 (br, s, 1H) and –10.91 (br s, 2H), which were tentatively assigned to (**215**)IrH $_3$ Bpin, **244-H $_3$ Bpin**, and other unidentified ^1H NMR resonances. The $^{31}\text{P}\{^1\text{H}\}$ NMR spectrum contained two pincer complexes (86% and 14%, respectively). The $^{11}\text{B}\{^1\text{H}\}$ NMR spectrum contained HBpin (20%), C $_6$ D $_5$ Bpin (37%), a resonance at δ 36.5 (s), which was tentatively assigned to **244-H $_3$ Bpin** (30%), and an unidentified ^{11}B NMR resonance at δ 21.6 (s) (13%).

Since the attempted metalation reactions of **215** were not clean enough to isolate a pure complex of iridium, the synthesis on a preparative scale was not performed.

2.4.3.11 Screening of Methods for Metalation of **216**

Method A with [(COD)IrCl] $_2$. **216** (110 mg, 85% pure, 0.27 mmol) and [(COD)IrCl] $_2$ (107 mg, 0.159 mmol) were added to a J. Young NMR tube. Toluene (1 mL) was added to form a solution. The J. Young NMR tube was closed. The solution was analyzed by $^{31}\text{P}\{^1\text{H}\}$ NMR spectroscopy after the J. Young NMR tube was placed into an oil bath at 120 °C for 36 h. After 36 h at 120 °C, the $^{31}\text{P}\{^1\text{H}\}$ NMR spectrum contained multiple unidentified ^{31}P NMR resonances.

Method C. **216** (155 μL , 78.3 μmol , 0.505 M in toluene) and [(COD)Ir(OAc) $_2$] (28.3 mg, 39.4 μmol) were added to a J. Young NMR tube. Toluene (1 mL) was added to

form an orange-red solution. The J. Young NMR tube was closed. The orange-red solution was immediately analyzed by $^{31}\text{P}\{^1\text{H}\}$ NMR spectroscopy, then again after the J. Young NMR tube was placed into an oil bath at 120 °C for 37 h. Prior to heating, the $^{31}\text{P}\{^1\text{H}\}$ NMR spectrum contained two ^{31}P NMR resonances (at δ 149.1 and 148.1) and one ^{31}P NMR resonance (at δ 60.3) from the impurity in the ligand. After 37 h at 120 °C, the $^{31}\text{P}\{^1\text{H}\}$ NMR spectrum contained **231-HOAc** and the same ^{31}P NMR resonance from the impurity.

Method D with [(COD)IrCl]₂. 216 (190 μL , 96.0 μmol , 0.505 M in toluene) and [(COD)IrCl]₂ (33.0 mg, 49.0 μmol) were added to a J. Young NMR tube. Toluene (1 mL) was added to form a solution. The J. Young NMR tube was closed. The J. Young NMR tube was then degassed through two freeze-pump-thaw cycles and refilled with H₂ (1 atm; ca. 2 mL, 0.08 mmol). The resulting orange solution was immediately analyzed by $^{31}\text{P}\{^1\text{H}\}$ NMR spectroscopy, then again after the J. Young NMR tube was placed into an oil bath at 110 °C for 13 h and 150 °C for 24 h. The orange solution turned black upon heating, slowly turned orange again at 110 °C, and turned black again at 150 °C. Prior to heating, the $^{31}\text{P}\{^1\text{H}\}$ NMR spectrum contained two ^{31}P NMR resonances (at δ 156.0 and 154.0) and one ^{31}P NMR resonance (at δ 60.3) from the impurity in the ligand. After 13 h at 110 °C, the $^{31}\text{P}\{^1\text{H}\}$ NMR spectrum contained multiple unidentified ^{31}P NMR resonances and the same ^{31}P NMR resonance from the impurity. After 24 h at 150 °C, the $^{31}\text{P}\{^1\text{H}\}$ NMR spectrum did not change much.

Method D with [(COE)₂IrCl]₂. 216 (95 μL , 48 μmol , 0.505 M in toluene) and [(COE)₂IrCl]₂ (21.7 mg, 24.0 μmol) were added to a J. Young NMR tube. Toluene (1 mL)

was added to form a solution. The J. Young NMR tube was closed. The J. Young NMR tube was then degassed through two freeze-pump-thaw cycles and refilled with H₂ (1 atm; ca. 2 mL, 0.08 mmol). The resulting orange solution was immediately analyzed by ³¹P{¹H} NMR spectroscopy, then again after the J. Young NMR tube was placed into an oil bath at 110 °C for 13 h and 150 °C for 24 h. The orange solution turned darker upon heating and turned black at 150 °C. Prior to heating, the ³¹P{¹H} NMR spectrum contained multiple ³¹P NMR resonances (around δ 160–150) and one ³¹P NMR resonance (at δ 60.3) from the impurity in the ligand. After 13 h at 110 °C, the ³¹P{¹H} NMR spectrum contained multiple unidentified ³¹P NMR resonances. After 24 h at 150 °C, the ³¹P{¹H} NMR spectrum contained multiple unidentified ³¹P NMR resonances.

After the screening, method C was chosen to synthesize **231-HOAc** on a preparative scale.

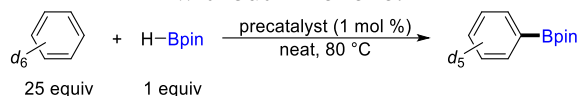
2.4.4 Catalysis of Aromatic C–H Borylation

2.4.4.1 Aromatic C–H Borylation Experiments Using Iridium or Rhodium Precatalysts

Stock solutions of iridium and rhodium precatalysts were prepared by weighing the respective compound into a 1 mL glass volumetric tube and dissolving in C₆D₆ or PhF to the line on the volumetric tube. The stock solution was stored at –35 °C in an argon-filled glove box. A stock solution of iridium and rhodium precatalyst (2.6 μmol) was added to a J. Young NMR tube. The solvent was removed under vacuum. HBpin (36 μL, 0.25 mmol), 1-hexene (93 μL, 0.75 mmol) if indicated, cyclohexane (22 μL, 0.20 mmol) as a

^1H NMR internal standard and C_6D_6 (555 μL , 6.27 mmol) were then added. The NMR tube was closed, brought out of the glovebox, and placed into an oil bath at 80 $^\circ\text{C}$ for the time reported. The reaction was monitored by ^1H and/or ^{11}B NMR spectroscopy. The conversion and yields were determined by comparing the integration of the ^1H NMR resonances of methyl groups on Bpin of HBpin (δ 1.01 in C_6D_6), $\text{C}_6\text{D}_5\text{Bpin}$ (δ 1.12 in C_6D_6), hexylBpin (δ 1.07 in C_6D_6), and hexenylBpin (δ 1.10 in C_6D_6) to the cyclohexane internal standard (δ 1.40 in C_6D_6). The errors of the quantitative NMR spectroscopy are well studied and reported within 1% under optimal conditions.¹⁵⁹ We tentatively estimated the errors in our results to be within 5% (\pm 2.5%) since the ^1H NMR resonances integrated were all well separated. The results with 1-hexene were summarized in Table II-3 and the results without 1-hexene were summarized in Table II-8.

Table II-8. Aromatic C–H borylation experiments using iridium or rhodium precatalysts without 1-hexene.^a



entry	precatalyst	time (h)	conversion (%) ^b	yield (%) ^b
1	203-HCl	15	11	0
2	226-HCl	15	0	0
3	227-HCl	24	0	0
4	228-HCl	15	0	0
5	229-HCl	15	2	0
6	230-HCl	15	0	0
7	231-HOAc	15	0	0
8	232-HCl	14	0	0
9	233-COE	14	<2	0
10	234-H₄	14	6	0
11	235-HCl	14	2	0
12	236-HCl	15	0	0
13	237-HCl	16	0	0
14	238-H₂	14	0	0
15	239-HCl	15	4	0

^aReaction conditions: HBpin (36 μL , 0.25 mmol) and precatalyst (2.6 μmol) in C_6D_6 (555 μL , 6.27 mmol), 80 $^\circ\text{C}$, under Ar. ^bConversions and yields were determined by ^1H NMR spectroscopy using cyclohexane as an internal standard. Errors were estimated to be $\pm 2.5\%$.

A representative example using **231-HOAc** as a precatalyst with 1-hexene (Table II-3, entry 7) was shown below: **231-HOAc** (13.4 mg, 22.6 μmol) was dissolved in C_6D_6 in a 1 mL glass volumetric tube to provide a stock solution (22.6 mM of **231-HOAc** in C_6D_6). The stock solution (115 μL , 2.60 μmol) was added to a J. Young NMR tube. The solvent was removed under vacuum. HBpin (36 μL , 0.25 mmol), 1-hexene (93 μL , 0.75 mmol), cyclohexane (22 μL , 0.20 mmol) and C_6D_6 (555 μL , 6.27 mmol) were then added. The J. Young NMR tube was closed. The colorless solution was immediately analyzed by ^1H NMR spectroscopy, then again after the J. Young NMR tube was placed into an oil

bath at 80 °C for 1 h and 15 h. Prior to heating, the ¹H NMR spectrum contained: HBpin (95%), C₆D₅Bpin (4%), and hexylBpin (<1%). After 1 h at 80 °C, the ¹H NMR spectrum contained: HBpin (51%), C₆D₅Bpin (35%), hexylBpin (13%), and hexenylBpin (<1%). After 15 h at 80 °C, the ¹H NMR spectrum contained: HBpin (5%), C₆D₅Bpin (40%), hexylBpin (45%), hexenylBpin (7%), and other unidentified resonances of methyl groups on Bpin (<3%).

2.4.4.2 Aromatic C–H Borylation Reactions Using Different Olefins

A stock solution of **229-HCl** in C₆D₆ (25 μL, 10.8 mM, 0.27 μmol), HBpin (36 μL, 0.25 mmol), C₆D₆ (525 μL, 550 μL in total, 6.21 mmol), cyclohexane (22 μL, 0.20 mmol) as a ¹H NMR internal standard, and olefin (0.74 mmol) were added to a J. Young NMR tube. The J. Young NMR tubes were immediately analyzed by ¹H and ¹¹B{¹H} NMR spectroscopy, then again after the J. Young NMR tubes were placed into an oil bath at 80 °C for 18 h. The results were summarized in Table II-5.

2.4.4.3 Effect of Reagent Ratio on Product Ratio Using **229-HCl** as a Precatalyst

A series of J. Young NMR tubes were each loaded with a stock solution of **229-HCl** in C₆D₆ (45 μL, 10.8 mM, 0.49 μmol) and HBpin (70 μL, 0.48 mmol). Benzene was added in the quantities indicated: entries 1–3 (170 μL, 215 μL in total, 2.4 mmol), entries 4–6 (1025 μL, 1070 μL in total, 12.1 mmol). 1-hexene was added in the quantities indicated: entries 1 and 4 (60 μL, 0.48 μmol), entries 2 and 5 (120 μL, 0.960 μmol), entries 3 and 6 (180 μL, 1.44 μmol). A known amount of heptane was added to normalize the

total solvent volume of each experiment to 1.445 mL. The J. Young NMR tubes were immediately analyzed by $^{11}\text{B}\{^1\text{H}\}$ NMR spectroscopy, then again after the J. Young NMR tubes were placed into an oil bath at 80 °C for 19 h and 38 h. In all entries, trace (<1%) quantities of unknown HBpin decomposition products were observed by $^{11}\text{B}\{^1\text{H}\}$ NMR spectroscopy. The results were summarized in Table II-6.

2.4.4.4 Regioselectivity Test for Aromatic C–H Borylation Reactions

A stock solution of precatalyst (0.001 equiv) was added to a 50 mL Teflon screw-capped Schlenk flask. The solvent was removed under vacuum. HBpin (1 equiv), 1-hexene (3 equiv), and PhF or PhCF₃ (25 equiv) were then added. The flask was closed, brought out of the glovebox, and placed into an oil bath at 80 °C for 24 h. After the reaction, 40 μL of cyclohexane was added as a ^1H NMR internal standard. The conversions were analyzed by ^1H NMR spectroscopy using C₆D₆ as a solvent. After the ^1H NMR spectroscopy analysis, volatiles were removed under vacuum. 40 μL of cyclohexane was added as a ^1H NMR internal standard. The yields and product ratios were analyzed by ^1H and ^{19}F NMR spectroscopy using CDCl₃ as a solvent, respectively. The conversions were determined by comparing the integration of the ^1H NMR resonances of methyl groups on Bpin of HBpin (δ 1.01 in C₆D₆) to the cyclohexane internal standard (δ 1.40 in C₆D₆). The yields were determined by comparing the integration of the ^1H NMR resonances of methyl groups on Bpin of 2-FC₆H₄Bpin (δ 1.37 in CDCl₃), 3-FC₆H₄Bpin (δ 1.35 in CDCl₃), 4-FC₆H₄Bpin (δ 1.34 in CDCl₃), 3-F₃CC₆H₄Bpin (δ 1.36 in CDCl₃), 4-F₃CC₆H₄Bpin (δ 1.36 in CDCl₃), and hexylBpin (δ 1.25 in CDCl₃) to the cyclohexane internal standard (δ 1.43

in CDCl₃). The product ratios were determined by comparing the integration of the ¹⁹F NMR resonances of 2-FC₆H₄Bpin (δ -103.3 in CDCl₃), 3-FC₆H₄Bpin (δ -115.0 in CDCl₃), 4-FC₆H₄Bpin (δ -109.2 in CDCl₃), 3-F₃CC₆H₄Bpin (δ -63.4 in CDCl₃), and 4-F₃CC₆H₄Bpin (δ -63.8 in CDCl₃). The errors of the quantitative NMR spectroscopy are well studied and reported within 1% under optimal conditions.¹⁵⁹ We tentatively estimated the errors in our results to be within 5% (\pm 2.5%). The results were summarized in Table II-7.

2.4.5 Details of X-Ray Structural Determination of 231-HOAc (CCDC 2041134)

2.4.5.1 Data Collection

A Leica MZ 7.5 microscope was used to identify a colorless block with very well-defined faces with dimensions (0.42 x 0.408 x 0.372 mm³) from a representative sample of crystals of the same habit. The crystal mounted on a nylon loop was then placed in a cold nitrogen stream (Oxford) maintained at 110 K.

A BRUKER APEX 2 Duo X-ray (three-circle) diffractometer was employed for crystal screening, unit cell determination, and data collection. The goniometer was controlled using the APEX3 software suite, v2017.3-0.¹⁶⁰ The sample was optically centered with the aid of a video camera such that no translations were observed as the crystal was rotated through all positions. The detector (Bruker - PHOTON) was set at 6.0 cm from the crystal sample. The X-ray radiation employed was generated from a Mo sealed X-ray tube (K_{α} = 0.71073Å with a potential of 40 kV and a current of 40 mA).

45 data frames were taken at widths of 1.0° . These reflections were used in the auto-indexing procedure to determine the unit cell. A suitable cell was found and refined by nonlinear least squares and Bravais lattice procedures. The unit cell was verified by examination of the $h k l$ overlays on several frames of data. No super-cell or erroneous reflections were observed.

After careful examination of the unit cell, an extended data collection procedure (8 sets) was initiated using omega scans.

2.4.5.2 Data Reduction, Structure Solution, and Refinement

Integrated intensity information for each reflection was obtained by reduction of the data frames with the program APEX3.¹⁶⁰ The integration method employed a three-dimensional profiling algorithm and all data were corrected for Lorentz and polarization factors, as well as for crystal decay effects. Finally, the data were merged and scaled to produce a suitable data set. The absorption correction program SADABS¹⁶¹ was employed to correct the data for absorption effects.

Systematic reflection conditions and statistical tests of the data suggested the space group $P-1$. A solution was obtained readily ($Z=4$; $Z'=2$) using XT/XS in APEX2.^{160,162–165} Hydrogen atoms were placed in idealized positions and were set riding on the respective parent atoms. All non-hydrogen atoms were refined with anisotropic thermal parameters. The absence of additional symmetry and voids were confirmed using PLATON (ADDSYM).¹⁶⁶ The structure was refined (weighted least squares refinement on F^2) to

convergence.^{162-165,167} ORTEP-3 and POV-ray were employed for the final data presentation and structure plots.^{151,168}

CHAPTER III
PALLADIUM-CATALYZED GERMYLATION OF ARYL BROMIDES USING
SODIUM TRI-*TERT*-BUTOXYGERMANATE

3.1 Introduction

We are interested in using arylgermanes in Pd-catalyzed cross-coupling reactions because of their potential orthogonal reactivity and chemoselectivity.^{24,68} However, in contrast to the arylstannane analogue, the readily prepared trialkylarylgermanes are not effective partners in homogeneous Pd-catalyzed cross-coupling.^{66,83} It appears that $\text{ArGe}(\text{alkyl})_3$ can in some cases be activated for coupling reactions by the presence of an intramolecular extra donor, but this is a synthetically limited strategy.^{73,169} Typical arylboron and arylsilicon reagents used as coupling reagents carry electronegative substituents, most commonly an alk-/aryl-/siloxide (Figure III-1). The existing evidence with germanium suggests that electronegative substituents on germanium are advantageous for Pd-catalyzed coupling reactions.^{24,74,76-78} However, to the best of our knowledge, the only report of direct construction of aryl C–Ge bonds with electronegative substituents on germanium resulted in a mixture of ArGeCl_3 and ArGeBr_3 .⁹⁰ The direct synthesis of arylgermane with oxygenated substituents has not yet been discovered or studied. Therefore, a new synthetic method to prepare such arylgermanes is of interest.

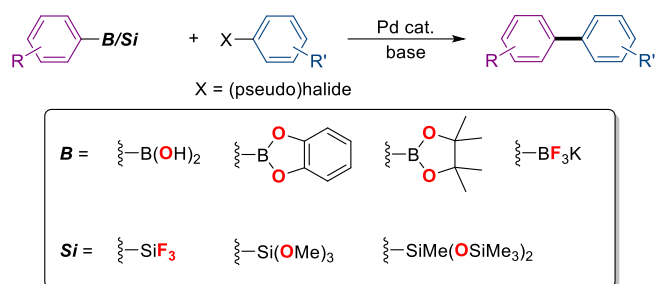


Figure III-1. Examples of arylboron and arylsilicon reagents with electronegative substituents (highlighted in red) in Pd-catalyzed cross-coupling reactions.

3.1.1 Germylation of Aryl Halides Using Germanium Anion Reagents

Although the yields are typically low (20–60%), germylation through the reactions between aryl halides and germyllithium reagents has been studied (Figure III-2, top), in addition to the aforementioned germylation methods (see Chapter 1, Section 1.3).^{170–173} The substitution of aryl halides by Et_3Ge germyl anion proceeds via two different pathways and the rates depend on the substrates. Generally, the reactions between Et_3Ge germyl anion and Ar-F , Ar-Br , and Ar-I are dominated by a free radical reaction, while in the case of Ar-Cl , both free radical and aryne processes are involved.¹⁷¹ To the best of our understanding, the reaction between aryl halides and trialkoxygermanium anion, Ge(OR)_3 , (germanate) has not been studied (Figure III-2, bottom). This transformation is attractive because it provides a direct synthesis of arylgermanes with oxygenated substituents.

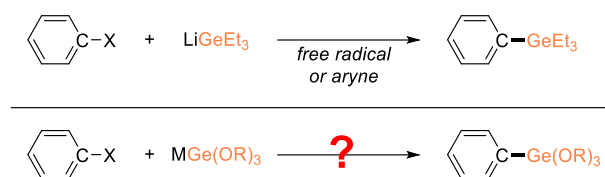


Figure III-2. Gernylation of aryl halides by anionic germanium species.

3.1.2 Preparation of Germanium Anion Reagents

Several different approaches have been reported to prepare the trialkylgermyl, trisilylgermyl, and digermanyl anions from tetravalent germanium compounds, including the reductive cleavage of Ge–Cl and Ge–Ge bonds by lithium metal,¹⁷⁴ deprotonation of Ge–H by ^tBuLi,¹⁷³ and treating Ge(SiMe₃)₄ with MeLi (Figure III-3).¹⁷² Similar germylsodium and germylpotassium compounds have been reported as well.¹⁷⁴

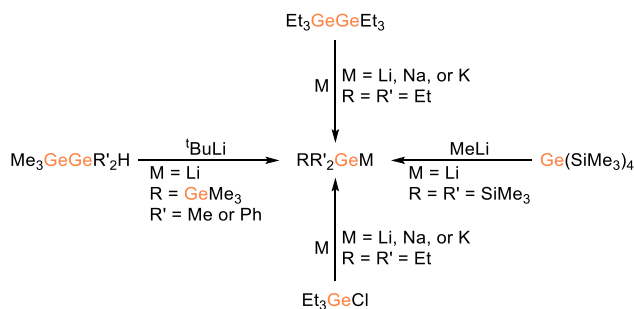


Figure III-3. Preparation of alkyl-/silylgermyllithium reagents.

The preparation of alkali germanates with oxygenated substituents has been reported as well. In 1991, Veith and co-workers reported the preparation of sodium *tert*-butoxygermanate, “NaGe(O^tBu)₃” (**301**) but only studied its application in the inorganic synthesis and main group structural research.¹⁷⁵

3.2 Results and Discussion

We were interested in using germanates with oxygenated substituents in germylation of aryl halides because they appeared stoichiometrically matched for the replacement of halide in aryl halides to form the corresponding arylgermanes. In addition, the resulting arylgermanes seem potent for the following Pd-catalyzed cross-coupling reactions.

3.2.1 Synthesis of Germanate Derivatives

First, we were able to synthesize the **301** from $\text{GeCl}_2 \cdot \text{C}_4\text{H}_8\text{O}_2$ (**302**) and NaO^tBu (**303**) (Figure III-4). “ $\text{NaGe}(\text{O}^t\text{Bu})_3$ ” can be viewed as an adduct of NaO^tBu with the di-*tert*-butoxygermylene “ $\text{Ge}(\text{O}^t\text{Bu})_2$ ” or as the conjugate base of the unknown tri-*tert*-butoxygermane, $\text{HGe}(\text{O}^t\text{Bu})_3$. **301** is soluble in nonpolar organic solvents, such as pentane, benzene, and toluene. The solid-state structure of **301** was determined by single-crystal XRD (Figure III-4). The structure is that of a dimer $[\text{NaGe}(\text{O}^t\text{Bu})_3]_2$, with the sodium cations each coordinating to four oxygens in the core of the dimer, without any close Na–Ge contacts. The structure of **301** is similar to that of its stannanate analog.¹⁷⁶ The electrochemical properties of **301** were studied via cyclic voltammetry in CH_2Cl_2 (Figure III-5). **301** showed a chemically irreversible oxidation event at a peak potential of +0.19 V (vs. the Fc/Fc^+ couple). It has been suggested that the inflection-point potentials can better represent standard electrochemical potentials of chemically irreversible waves.¹⁷⁷ Therefore, the inflection-point potentials were determined to be +0.01 V (vs. the Fc/Fc^+ couple) by using the first derivative plot.

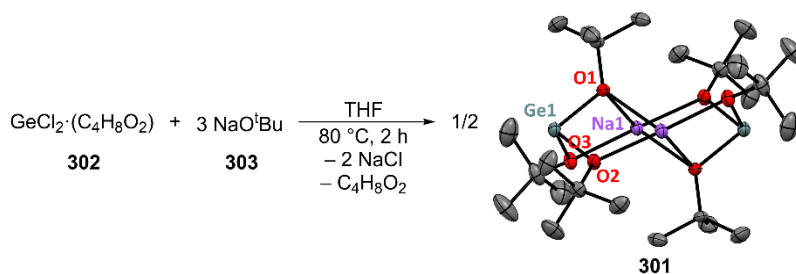


Figure III-4. The synthesis and the ORTEP¹⁵¹ drawing (50% probability ellipsoids) of [NaGe(OⁱBu)₃]₂ (**301**) (CCDC 2057607). Hydrogen atoms are omitted for clarity. Selected distance (Å) and angles (°): Ge1–O1, 1.911(3); Ge1–O2, 1.887(3); Ge1–O3, 1.901(3); O1–Ge1–O2, 86.97(13); O2–Ge1–O3, 95.44(13); O1–Ge1–O3, 86.99(13).

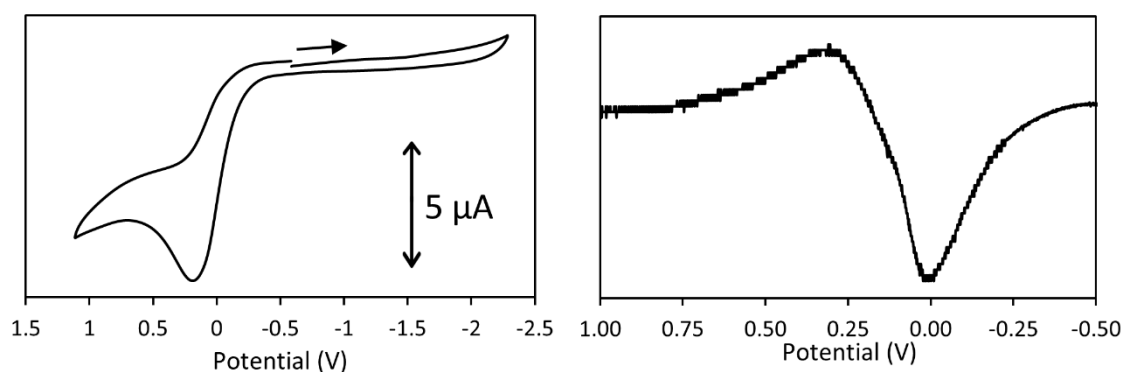


Figure III-5. Cyclic voltammogram (left) of **301** (1.0 mM in CH₂Cl₂) (vs. Fc/Fc⁺) and its first derivative plot (right).

The synthesis of a series of other alkali germanate derivatives was screened (Figure III-6). NaGe(OⁱPr)₃ (**305**) and NaGe(OEt)₃ (**307**) were synthesized analogously by reacting **302** with NaOⁱPr (**304**) and NaOEt (**306**), respectively. The reactions of **302** with NaOMe (**308**), N(CH₂CO₂Na)₃ (**310**), and sodium and lithium pyrrolides led to intractable solids. No reaction occurred when adding **303** to “NHGe” germylene (**312**). Several attempts at making LiGe(R)(OR’O) (R = Me or ⁿBu; OR’O = pinacolato or catecholato)

resulted in unidentified mixtures or intractable solids. Cation metatheses of **301** with $n\text{Bu}_4\text{NBr}$ and Ph_4PBr led to complex mixtures. Reacting **301** with $\text{N}(\text{CH}_2\text{CO}_2\text{H})_3$ (**321**) led to the partial conversion of tri-*tert*-butoxygermanate to di-*tert*-butoxygermylene, $[\text{Ge}(\text{O}^i\text{Bu})_2]_2$ (**322**), which suggests that the *tert*-butoxy group on germanium can serve as a base to deprotonate the acidic proton.

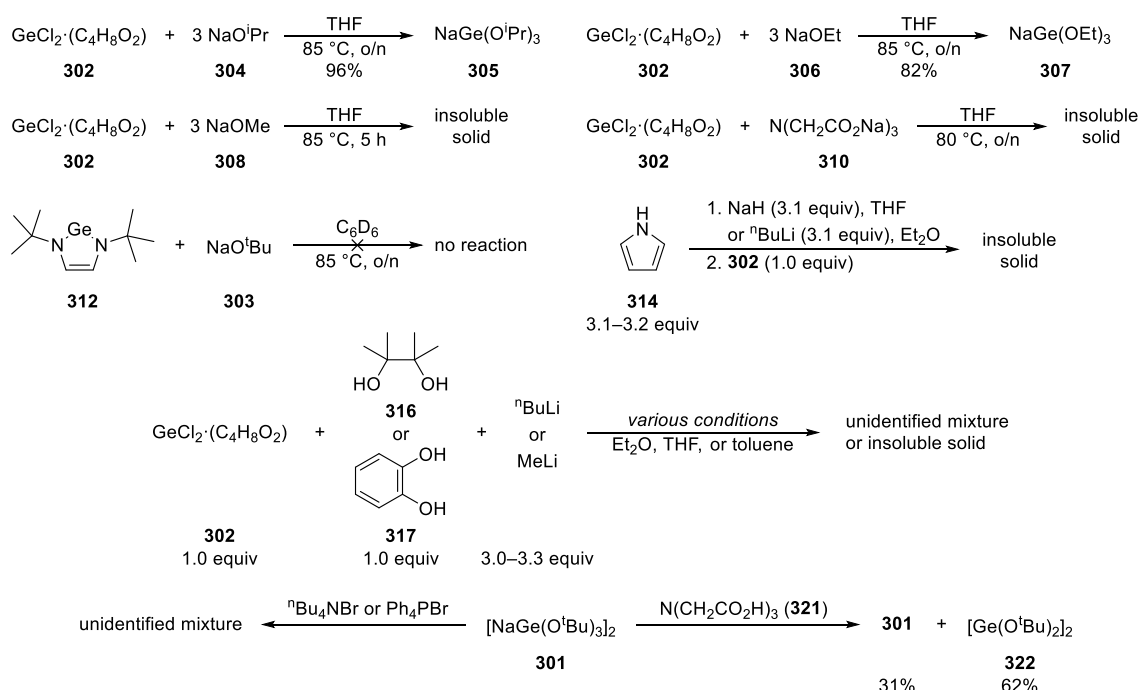


Figure III-6. Synthesis of germanate derivatives.

The solid-state structure of **307**, characterized by XRD, shared a very similar core dimer structure with **301** (Figure III-7). However, the dimeric structure forms a one-dimensional polymer by the additional Na–O coordination. In the polymeric crystal structure, each sodium cation coordinates to five oxygens, four in the dimer core and one

of the neighboring dimer. In this dissertation, **307** will be represented by the empirical formula $\text{NaGe}(\text{OEt})_3$.

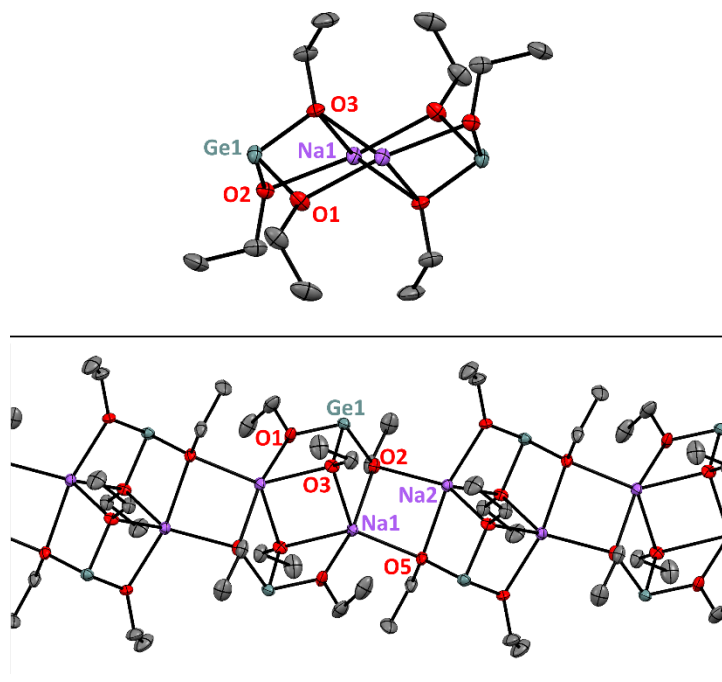
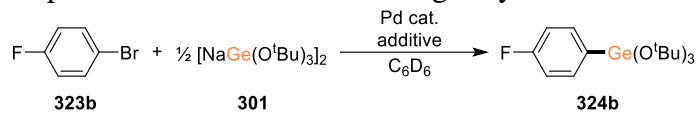


Figure III-7. The ORTEP¹⁵¹ drawing (50% probability ellipsoids) of $\text{NaGe}(\text{OEt})_3$ (**307**) (CCDC 2095668). Hydrogen atoms are omitted for clarity. Top: Extracted dimeric structure (side view). Bottom: Polymeric structure (top view). Selected distance (Å) and angles (°): Ge1–O1, 1.862(3); Ge1–O2, 1.916(3); Ge1–O3, 1.890(3); O2–Na2, 2.373(3); O5–Na1, 2.394(3); O1–Ge1–O2, 95.20(13); O2–Ge1–O3, 89.32(13); O1–Ge1–O3, 88.54(13).

3.2.2 Germylation of Aryl Halides Using Germanate Derivatives

We then investigated the application of germanates in aryl halide germylation. We first chose 4- $\text{FC}_6\text{H}_4\text{Br}$ (**323b**) and $[\text{NaGe}(\text{O}^t\text{Bu})_3]_2$ (**301**) as model substrates and screened the reaction in C_6D_6 as solvent catalyzed by palladium catalysts (Table III-1). We were able to determine that the addition of the DPPF or ^tBu -bpy ligands was not advantageous,

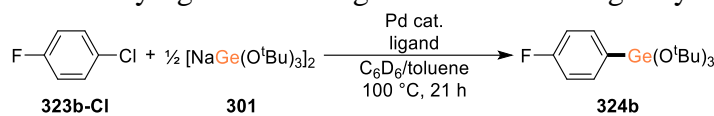
and that catalysis proceeded just as well with the “ligand-free” precursors Pd₂dba₃ and Pd(OAc)₂ (Table III-1, entries 1–4). The optimal practical conditions appear to consist of using 0.1 mol% Pd(OAc)₂ at 100 °C (oil bath temperature), allowing for the near-quantitative formation of 4-FC₆H₄Ge(O^tBu)₃, **324b** in a few hours (Table III-1, entry 5). Experiments with 0.01 mol% palladium proceeded to completion as well but took significantly longer (ca. 2 weeks) (Table III-1, entry 6). Under temperatures below 80 °C the progress of the reaction was very slow (Table III-1, entries 7–9). No germylation was observed in the absence of added palladium catalyst (Table III-1, entry 10). The fact that no traditional ligands are needed to support the catalysis is suggestive of the generation of heterogeneous palladium.^{66,178–181} In order to gain more insight, a pair of comparative experiments with and without the addition of elemental mercury to the reaction mixture was conducted. In the experiment with mercury added, the conversion was only partially depressed, rendering this result inconclusive (Table III-1, entry 10 vs. entry 11). Although we cannot exclude the possible heterogeneous catalysis, we speculate the Ge(O^tBu)₃ germanate anion itself may be envisaged to serve as a supporting ligand^{182–186} for molecular palladium species as well as the substrate nucleophile.

Table III-1. Optimization of aromatic C–Br germylation reaction conditions.^a

entry	catalyst (mol%)	additive (mol%)	temperature (°C)	time (h)	yield (%) ^b
1	Pd ₂ dba ₃ (2.5)	DPPF (6)	100	22	>95
2	Pd ₂ dba ₃ (2.5)	^t Bu-bpy (6)	100	22	>95
3	Pd ₂ dba ₃ (2.5)	–	100	2	>95
4	Pd ₂ dba ₃ (0.05)	–	100	1.5	>95
5	Pd(OAc) ₂ (0.1)	–	100	3	>95
6 ^c	Pd(OAc) ₂ (0.01)	–	100	20	32
7 ^d	Pd(OAc) ₂ (0.1)	–	80	20	>95
8	Pd(OAc) ₂ (0.1)	–	60	20	3
9	Pd(OAc) ₂ (0.1)	–	40	20	<1
10	–	–	100	22	<1
11	Pd(OAc) ₂ (0.1)	–	100	2	75
12	Pd(OAc) ₂ (0.1)	Hg (240)	100	2	45

^a**323b** (50 μmol), **301** (26 μmol, 52 μmol Ge), and palladium catalyst in C₆D₆ (0.6 mL). ^bYields were determined by ¹⁹F NMR spectroscopy using PhCF₃ as an internal standard. ^cReaction went to completion after 2 weeks. ^dOnly 23% yield after 3 h.

With the successful germylation of **323b** using **301**, we expanded the scope to other germanium(II) reagents: GeCl₂·C₄H₈O₂ (**302**), NaGe(OEt)₃ (**307**), [Ge(O^tBu)₂]₂ (**322**), CsGeCl₃ (**325**). To our surprise, none of these germanium(II) reagents provided any conversion of **323b** to the germylation products with 1 mol% Pd loading. We further tested the germylation protocol with an aryl chloride, 4-FC₆H₄Cl (**323b-Cl**), as a substrate and found it to be much less reactive (Table III-2). **324b** was formed in low yield even with 5 mol% Pd loading. Preliminary screening of supporting ligands had only modest improvement. It is likely that efficient germylation of aryl chlorides would require a carefully selected, highly donating supporting ligand that is resistant to the replacement by the excess germanate.⁵

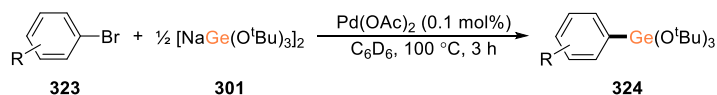
Table III-2. Preliminary ligand screening of aromatic C–Cl germylation reaction.^a

entry	Pd cat. (mol%)	ligand (mol%)	yield (%) ^b
1	Pd ₂ dba ₃ (2.5)	–	44
2	Pd(OAc) ₂ (5)	–	47
3	Pd(OAc) ₂ (5)	DPPF (5)	60
4	Pd(OAc) ₂ (5)	^t Bu-bpy (5)	39
5	Pd(OAc) ₂ (5)	<i>rac</i> -BINAP (5)	11
6	Pd(OAc) ₂ (5)	Ph ₃ PO (5)	51

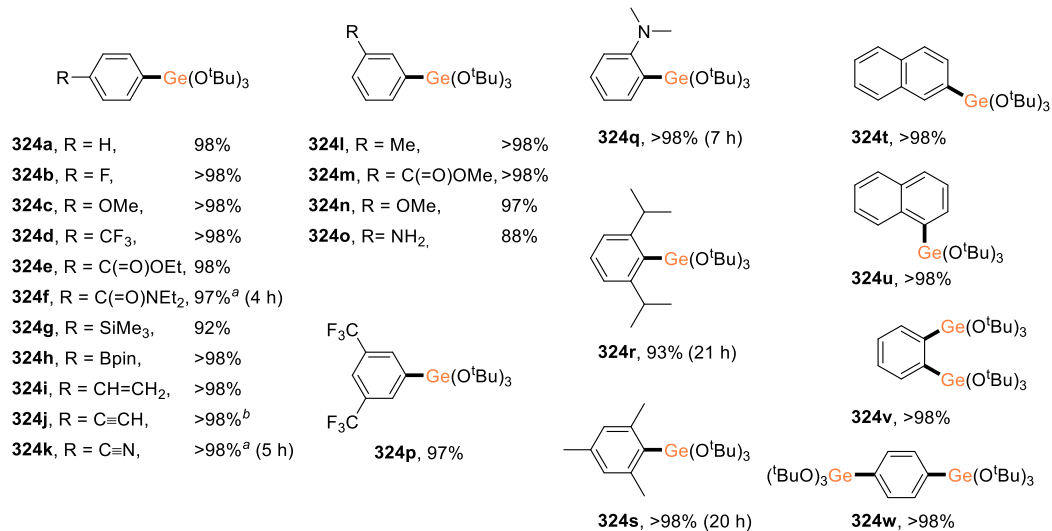
^a323b-Cl (49 μmol), 301 (26 μmol, 52 μmol Ge), Pd source, and ligand if indicated, in C₆D₆/toluene (600 μL), heated at 100 °C for 21 h. ^bYields were determined by ¹⁹F NMR spectroscopy using PhCF₃ as an internal standard.

3.2.3 Reaction Scope of Germylation of Aryl Bromides

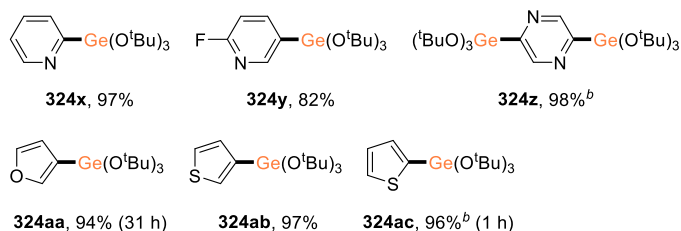
With the details of the procedure optimized for **323b**, we expanded the reaction scope with various aryl/alkenyl bromides (Figure III-8). A wide variety of functionalities were tolerated under the reaction conditions, including aryl fluoride, aryl ether and ester, carboxamide, arylsilane, boronic ester, terminal alkene, terminal alkyne, cyano group, and an unprotected amino group (Figure III-8A). Both electron-rich (**323c**, **323n**, **323o**, and **323q**) and -poor (**323d–323f**, **323k**, **323m**, and **323p**) aryl bromides were converted to the desired products in excellent yields. Reactions of aryl bromides with one or two *ortho* substituents (**323q–323s**) were significantly slower but still went to completion. Heteroaryl (Figure III-8B) and alkenyl (Figure III-8C) bromides were successfully transformed to the corresponding arylgermanes in excellent yields; however, a higher catalyst loading (1 mol%) was required for the alkenyl bromides. Representative aryl germanes **324b** and **324h** were prepared on a gram scale in >97% isolated yields (Figure III-9).



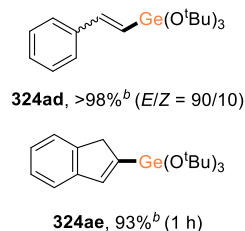
A. Substituted phenyl/naphthyl bromides



B. Heteroaryl bromides



C. Alkenyl bromides



D. Challenging bromides

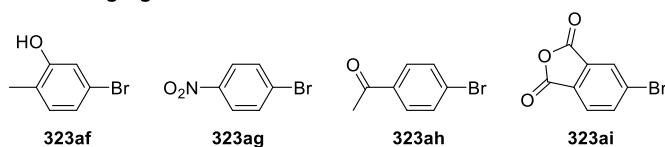


Figure III-8. Reaction scope of germylation of aryl halides. Reaction condition: aryl/alkenyl bromide **323** (50 μmol , 1.0 equiv), **301** (0.5–0.6 equiv or 1.0–1.2 equiv Ge to C–Br bond), and Pd(OAc)₂ (0.1 mol% to C–Br bond) in C₆D₆, 100 °C, 3 h. Yields were isolated yields. ^a130 °C. ^b1 mol% (to C–Br bond) of Pd(OAc)₂ was used.

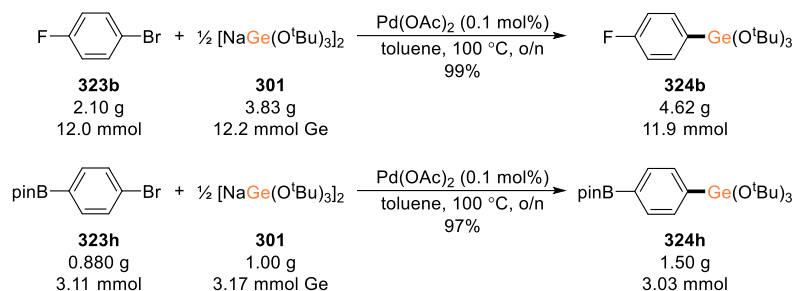


Figure III-9. Gram-scale synthesis of aryl germanes.

Unprotected hydroxy, nitro, acetyl, and carboxylic anhydride groups proved incompatible with the methodology (Figure III-8D). **301** appears to react rapidly with acidic Ar-OH and Ar-COCH₃ in **323af** and **323ah** via protolysis, with the release of free ^tBuOH. To test the sensitivity of **301** to the hydroxy group, **301** was reacted with 2,6-dimethylphenol (**326**) in an absence of palladium catalyst and free ^tBuOH was observed. The nitro group in **323ag** was reduced by **301** to the azoxy derivative¹⁸⁷ much faster than the Pd-catalyzed germylation. This reductive coupling of the nitro group was further optimized. Reaction of 4-nitrotoluene (**327**) (2 equiv) and **301** (1.5 equiv, 3 equiv Ge) at ambient temperature overnight or at 100 °C for 1 h led to a clean conversion to 4,4'-dimethylazoxybenzene (**328-MeMe**) and sodium tri-*tert*-butoxygermanolate, NaOGe(O^tBu)₃ (**329**) (Figure III-10, top). However, the attempted reductive cross-coupling of nitroarenes using **327** and **323ag** results in a mixture of all four possible products (Figure III-10, middle). The attempt to couple **327** and **323o** using **301** was not successful. **323o** was left untouched and only homocoupling of **327** was observed (Figure III-10, bottom).

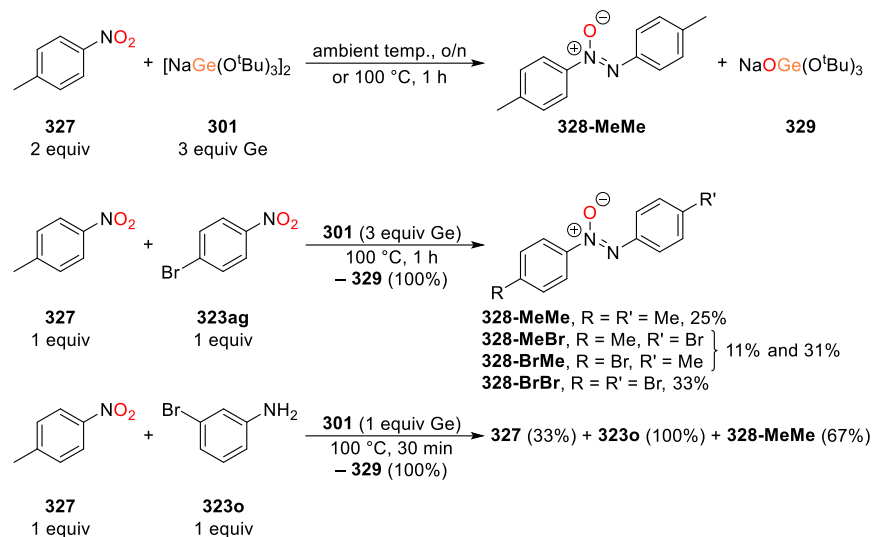


Figure III-10. Reductive coupling of nitroarene by **301**.

3.2.4 *In situ* Generated Germanates in Germylation

Seeking to further simplify the procedure, we tested whether **301** could be prepared *in situ* for germylation (Table III-3). This test reaction was successful (Table III-3, entry 2) when using a toluene/THF (50/50) mixture. The use of KO^tBu (**330**) instead of NaO^tBu (**303**) did not lead to product formation, indicating that the choice of the alkali metal cation may be critical. **324b** was prepared from **302**, **303**, and **323b** in 93% isolated yield on a 1 mmol scale.

Table III-3. Germylation with in situ generated tri-*tert*-butoxygermanate.^a

$$\text{GeCl}_2(\text{C}_4\text{H}_9\text{O}_2) + \begin{matrix} \text{NaO}^t\text{Bu, } \mathbf{303} \\ \text{or} \\ \text{KO}^t\text{Bu, } \mathbf{330} \end{matrix} + \text{F}-\text{C}_6\text{H}_4-\text{Br} \xrightarrow[100\text{ }^\circ\text{C, 20 h}]{\text{Pd(OAc)}_2 (0.1 \text{ mol}\%)} \text{F}-\text{C}_6\text{H}_4-\text{Ge(O}^t\text{Bu)}_3$$

entry	MO ^t Bu	solvent	conversion of 323b (%) ^b	yield (%) ^b
1	NaO ^t Bu (303)	toluene	26	26
2	303	toluene/THF (50/50)	>95	95
3	303	toluene/THF (80/20)	76	71
4	303	1,4-dioxane	0	0
5	KO ^t Bu (330)	toluene/THF (50/50)	16 ^c	0

^a**302** (1.0–1.1 equiv), **303** or **330** (3.0–3.3 equiv), **323b** (1.0 equiv), and Pd(OAc)₂ (0.1 mol%) in the indicated solvent were heated at 100 °C for 20 h. ^bConversions and yields were determined by ¹⁹F NMR spectroscopy using PhCF₃ as an internal standard. ^c16% of **323b** were reduced to PhF.

We then screened different sodium alkoxides and N(CH₂CO₂Na)₃ (**310**) using this approach, aiming to prepare arylgermane with different alkoxide substituents and arylgermatranone (Table III-4). With 1 mol% Pd(OAc)₂ loading, **323b** were fully consumed after heating at 100 °C for 20 h when NaOEt (**306**) and NaOⁿBu (**331**) were used. In entry 4, the resulting mixture consisted of the desired FC₆H₄Ge(OEt)₃ (**332**) (61%), presumably FC₆H₄Ge(OEt)₂(Cl/Br) (**333**) (20%), and an unknown (19%). Treating the reaction mixture with excess **306** fully converted **333** to **332** but did not affect the unknown. This result is surprising because the germylation using the isolated NaGe(OEt)₃ (**307**) did not lead to any reaction conversion. In entry 7, the resulting mixture consisted of the desired FC₆H₄Ge(OⁿBu)₃ (**334**) (69%), PhF (12%), and an unknown (16%). NaOMe (**308**), NaOⁱPr (**304**), and **310** did not lead to any conversion under this condition. In summary, using other alkoxides other than NaO^tBu (**303**) did not provide satisfactory results for preparing other arylgermane derivatives.

much less reactive than Ar–Br, which follows the traditional trend of reactivity to Pd-catalyzed cross-coupling reactions.⁵ Next, transmetalation of **301** with complex **J** leads to the elimination of NaBr and generates palladium(II) phenyl/germyl complex **K**. NaBr can be observed in all germylation experiments as a fine white powder forms as the reactions proceed. Complex **K** undergoes reductive elimination to form the desired germylation product and regenerate palladium(0) species **I** (Figure III-11). Germylene insertion is unlikely to be involved in the reaction mechanism with the evidence that germylation of **323b** using **322** did not result in observable consumption of **323b** or **322**, nor the formation of germylation product. However, when **303** (1 equiv with respect to Ge) was added to the reaction, **322** was rapidly converted to **301**. Heating the reaction gave a clean formation of **324b** quantitatively, demonstrating that germanate is a promising and important germylation reagent in the reaction (Figure III-12).

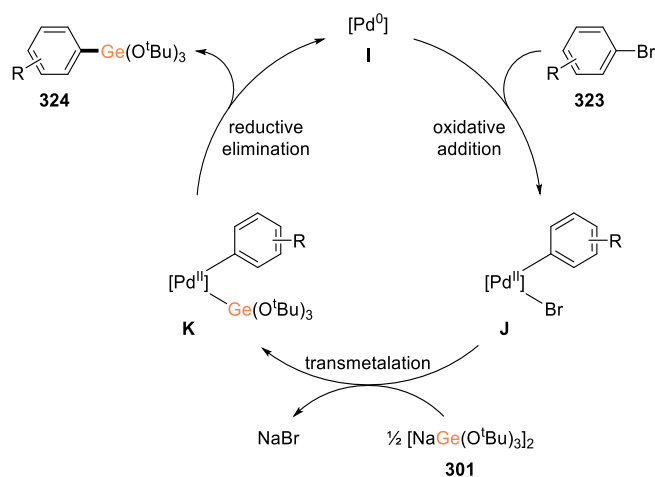


Figure III-11. Proposed mechanism of Pd-catalyzed germylation of aryl bromides using $[\text{NaGe}(\text{O}^t\text{Bu})_3]_2$.

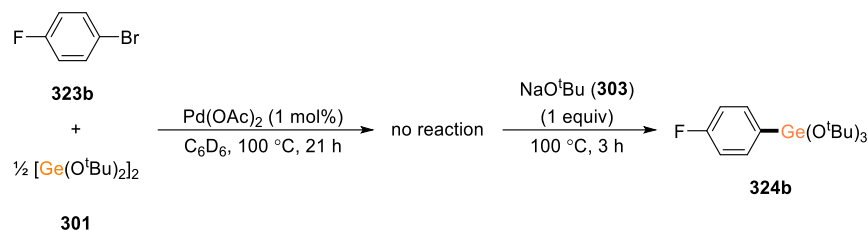


Figure III-12. Germanate vs. germylene in the gemylation reaction.

3.3 Conclusion

Sodium tri-*tert*-butoxygermanate (**301**) and sodium triethoxygermanate (**307**) were synthesized and characterized by crystal XRD. Both reagents can be easily synthesized from commercially available GeCl_4 or $\text{GeCl}_2 \cdot \text{C}_4\text{H}_8\text{O}_2$ (**302**).

A robust and efficient Pd-catalyzed catalysis for the germylation of aryl bromides with **301** has been developed. The reaction converted a broad range of aryl bromides to arylgermanes in excellent isolated yields and did not require any auxiliary ligands for palladium. Furthermore, a protocol to generate **301** in situ from **302** and NaO^tBu (**303**) for germylation has been developed for an even easier reaction set-up. A plausible mechanism was proposed, in which the germanate anion plays an important role in the transmetalation step.

3.4 Experimental

3.4.1 General Consideration

Unless specified otherwise, all manipulations were performed under an argon atmosphere using standard Schlenk or glovebox techniques. Toluene, pentane, THF, Et_2O , and isooctane were deoxygenated (by purging) and dried using an Innovative Technology

Pure Solv MD-5 Solvent Purification System and stored over molecular sieves in an argon-filled glove box. C₆D₆ were dried over and distilled from a NaK/benzophenone/18-crown-6 mixture and stored over molecular sieves in an argon-filled glovebox. CDCl₃, CD₃CN, 1,4-dioxane, PhCF₃, MeCN, EtOH, ⁱPrOH, ⁿBuOH were dried over calcium hydride, distilled or vacuum transferred, and stored over molecular sieves in an argon-filled glove box. Me₃SiCl was distilled under argon and stored in an argon-filled glove box. Catechol (**317**) and 2,6-dimethylphenol (**326**) were sublimed under vacuum and stored in an argon-filled glove box. Liquid aryl/alkenyl bromide derivatives were degassed by three freeze-pump-thaw cycles or purging, dried over molecular sieves overnight, and stored over molecular sieves in an argon-filled glove box. Celite and silica were dried at 180 °C under vacuum overnight and store in an argon-filled glove box. [NaGe(O^tBu)₃]₂ (**301**),¹⁷⁵ GeCl₂·C₄H₈O₂ (**302**),¹⁸⁸ and 1,3-di-*tert*-butyl-1,3,2-diazagermol-2-ylidene “NHGe” (**312**)¹⁸⁹ were synthesized according to published procedures. NaOⁱPr (**304**) and NaOⁿBu (**331**) were synthesized by reacting sodium metal in the corresponding alcohols. N(CH₂CO₂Na)₃ (**310**) was synthesized by reacting N(CH₂CO₂H)₃ (**321**) in an aqueous NaOH solution and dried under vacuum at 110 °C overnight. NaH was rinsed with isooctane, dried under vacuum, and stored in an argon-filled glove box. All other chemicals were used as received from commercial vendors.

All NMR spectra were recorded on a Varian Inova 500 NMR spectrometer (¹H NMR, 499.431 MHz; ¹³C{¹H} NMR, 125.595 MHz; ¹⁹F NMR, 469.897 MHz), Varian VnmrS 500 NMR spectrometers (¹³C{¹H} NMR, 125.646 MHz and ¹¹B{¹H} NMR, 160.366 MHz, respectively), and Bruker Avance Neo 400 spectrometers (¹H NMR, 400.2

MHz; ^{13}C NMR, 100.630 MHz, and ^1H NMR, 400.09 MHz; ^{13}C NMR, 100.603 MHz, respectively). All spectra were recorded at ambient temperature unless otherwise noted. Chemical shifts are reported in δ (ppm). For ^1H and $^{13}\text{C}\{^1\text{H}\}$ NMR spectra, the residual solvent peak was used as an internal reference (C_6D_6 at δ 7.16 for ^1H NMR and δ 128.06 for ^{13}C NMR; CDCl_3 at δ 7.26 for ^1H NMR and δ 77.16 for ^{13}C NMR). ^{19}F NMR spectra were referenced externally using neat trifluoroacetic acid at δ -78.5. ^{19}F NMR spectra were referenced externally using neat boron trifluoride diethyl etherate at δ 0.

ESI and APCI-HRMS experiments were performed using a Thermo Scientific Q Exactive Focus. The sample was injected into a 10 μL sample loop and carried using MeOH as a mobile phase at a flow rate of 300 $\mu\text{L}/\text{min}$. When necessary, lithium acetate was added to a sample (final concentration of 100 ng/mL in the sample) prior to sample injection for the cationization of the compound in positive ESI mode. The ESI source spray voltage was set to 3.75 kV, and the sheath gas and auxiliary gas flow rates were set to 10 and 0 arbitrary units, respectively. The auxiliary gas temperature was set to 50 $^\circ\text{C}$. For the APCI source, the discharge current was set at 5 μA , and the sheath gas and auxiliary gas flow rates were set to 30 and 0 arbitrary units, respectively. The auxiliary gas temperature was set to 250 $^\circ\text{C}$. For both ESI and APCI, the transfer capillary temperature was held at 250 $^\circ\text{C}$ and the S-Lens RF level was set at 50 V. The mass resolution was tuned to 70000 FWHM at m/z 200. Exactive Series 2.11/Xcalibur 4.2.47 software was used for data acquisition and processing.

3.4.2 Details of X-Ray Structural Determination of 301 (CCDC 2057607)

3.4.2.1 Data Collection

A Leica MZ 7.5 microscope was used to identify a suitable colorless block with very well-defined faces with dimensions (max, intermediate, and min) 0.561 x 0.457 x 0.427 mm³ from a representative sample of crystals of the same habit. The crystal mounted on a nylon loop was then placed in a cold nitrogen stream (Oxford) maintained at 110 K.

A BRUKER Quest X-ray (fixed-Chi geometry) diffractometer with a PHOTON II detector was employed for crystal screening, unit cell determination, and data collection. The goniometer was controlled using the APEX3 software suite.¹⁶⁰ The sample was optically centered with the aid of a video camera such that no translations were observed as the crystal was rotated through all positions. The X-ray radiation employed was generated from a Mo-I μ s X-ray tube ($K_{\alpha} = 0.71073\text{\AA}$).

45 data frames were taken at widths of 1°. These reflections were used to determine the unit cell. The unit cell was verified by examination of the *h k l* overlays on several frames of data. No super-cell or erroneous reflections were observed.

After careful examination of the unit cell, an extended data collection procedure (9 sets) was initiated using omega and phi scans.

3.4.2.2 Data Reduction, Structure Solution, and Refinement

Integrated intensity information for each reflection was obtained by reduction of the data frames with the program APEX3.¹⁶⁰ The integration method employed a three-dimensional profiling algorithm and all data were corrected for Lorentz and polarization

factors, as well as for crystal decay effects. Finally, the data were merged and scaled to produce a suitable data set. The absorption correction program SADABS¹⁶¹ was employed to correct the data for absorption effects.

Systematic reflection conditions and statistical tests of the data suggested the space group $P-1$. A solution was obtained readily ($Z=2$; $Z' = 2 \times 0.5$) using XT/XS in APEX3.^{160,162–165} Hydrogen atoms were placed in idealized positions and were set riding on the respective parent atoms. All non-hydrogen atoms were refined with anisotropic thermal parameters. The absence of additional symmetry and voids were confirmed using PLATON (ADDSYM).¹⁶⁶ The structure was refined (weighted least squares refinement on F^2) to convergence.^{162–165,167} Larger residual electron density peaks were present, suggesting whole molecule disorder. ORTEP-3 and POV-ray were employed for the final data presentation and structure plots.^{151,168}

3.4.3 Details of X-Ray Structural Determination of 307 (CCDC 2095668)

3.4.3.1 Data Collection

A Leica MZ 7.5 microscope was used to identify a suitable colorless block with very well-defined faces with dimensions (max, intermediate, and min) 0.204 x 0.183 x 0.109 mm³ from a representative sample of crystals of the same habit. The crystal mounted on a nylon loop was then placed in a cold nitrogen stream (Oxford) maintained at 110 K.

A BRUKER Quest X-ray (fixed-Chi geometry) diffractometer with a PHOTON II detector was employed for crystal screening, unit cell determination, and data collection. The goniometer was controlled using the APEX3 software suite.¹⁶⁰ The sample was

optically centered with the aid of a video camera such that no translations were observed as the crystal was rotated through all positions. The X-ray radiation employed was generated from a Mo-I μ s X-ray tube ($K_{\alpha} = 0.71073\text{\AA}$).

45 data frames were taken at widths of 1° . These reflections were used to determine the unit cell using CELL_NOW which suggested twinning.¹⁹⁰ The unit cell was verified by examination of the hkl overlays on several frames of data. No super-cell or erroneous reflections were observed.

After careful examination of the unit cell, an extended data collection procedure (3 sets) was initiated using omega scans.

3.4.3.2 Data Reduction, Structure Solution, and Refinement

Integrated intensity information for each reflection was obtained by reduction of the data frames with the program APEX3.¹⁶⁰ The integration method employed a three-dimensional profiling algorithm and all data were corrected for Lorentz and polarization factors, as well as for crystal decay effects. Finally, the data were merged and scaled to produce a suitable data set. The absorption correction program TWINABS¹⁹¹ was employed to correct the data for absorption effects.

Systematic reflection conditions and statistical tests of the data suggested the space group $P-1$. A solution was obtained readily ($Z = 4$; $Z' = 2$) using XT/XS in APEX3.^{160,162–165} Hydrogen atoms were placed in idealized positions and were set riding on the respective parent atoms. All non-hydrogen atoms were refined with anisotropic thermal parameters. The absence of additional symmetry and voids were confirmed using

PLATON (ADDSYM).¹⁶⁶ The structure was refined (weighted least squares refinement on F^2) to convergence.^{162-165,167} ORTEP-3 and POV-ray were employed for the final data presentation and structure plots.^{151,168}

3.4.4 Electrochemical Experiments of **301**

Electrochemical experiments were performed using a CH Instruments Model 700D Series Electrochemical Analyzer and Workstation (CH Instruments Inc., Austin, TX) in conjunction with a three electrodes electrochemical cell. The working electrode was a CHI104 glassy carbon electrode with a diameter of 3 mm (CH Instruments Inc., Austin, TX); the auxiliary electrode was a platinum wire; the reference electrode was a Ag/AgNO₃ electrode. The Ag/AgNO₃ electrode was prepared as a bulk solution of 0.01 M AgNO₃ and 0.1 M ⁿBu₄NPF₆ in CH₂Cl₂, which was separated from the analyte solutions by a fine porosity frit. Cyclic voltammetry experiments were conducted in CH₂Cl₂ with 0.1 M ⁿBu₄NPF₆ as the supporting electrolyte at a scan rate of 100 mV/s under argon at ambient temperature (23±2 °C, 296±2 K). The concentration of the **301** solution was 1.0 mM. The electrochemical potentials were externally referenced to the Me₁₀Fc/Me₁₀Fc⁺ redox couple. The collected data were then converted to be referenced to the Fc/Fc⁺ redox couple.¹⁹²

3.4.5 Synthesis of Alkali Germanate Derivatives

Synthesis of 305. GeCl₂·C₄H₈O₂ (**302**) (179 mg, 0.773 mmol) and NaOⁱPr (**304**) (206 mg, 2.51 mmol) were dissolved in THF (4 mL) in a 10 mL culture tube. The reaction

was heated at 85 °C overnight. All volatiles were removed. Pentane was then added to extract **305**. The white solid was filtered off by a pad of Celite over a frit. Pentane was removed under vacuum to give a white sticky solid (203 mg, 96% yield). ^1H NMR (499 MHz, C_6D_6) δ 4.27 (hept, $J = 6.2$ Hz, 3H), 1.27 (d, $J = 6.2$ Hz, 18H).

Synthesis of 307. $\text{GeCl}_2 \cdot \text{C}_4\text{H}_8\text{O}_2$ (**302**) (606 mg, 2.62 mmol) and NaOEt (**306**) (596 mg, 8.76 mmol) were dissolved in THF (10 mL) in a 50 mL culture tube. The reaction was heated at 85 °C overnight. All volatiles were removed from the resulting orange suspension under vacuum. Pentane was then added to extract **307**. The white solid was filtered off by a pad of Celite over a frit. Pentane was removed under vacuum to give an off-white solid as a crude product (600 mg). The crude product was purified by recrystallization from a saturated pentane solution at -35 °C to give a pure product as a white crystal (496 mg, 82% yield). ^1H NMR (499 MHz, C_6D_6) δ 3.83 (q, $J = 6.9$ Hz, 12H), 1.22 (t, $J = 6.9$ Hz, 18H); $^{13}\text{C}\{^1\text{H}\}$ NMR (126 MHz, C_6D_6) δ 57.1, 21.0.

Attempted synthesis of $\text{NaGe}(\text{OMe})_3$ (309). $\text{GeCl}_2 \cdot \text{C}_4\text{H}_8\text{O}_2$ (**302**) (502 mg, 2.17 mmol) and NaOMe (**308**) (379 mg, 2.51 mmol) were suspended in THF (15 mL) in a 50 mL culture tube. The reaction was heated at 85 °C for 5 h. The mixture was filtered through a pad of Celite over a frit. All volatiles were removed under vacuum to give a benzene-insoluble solid (410 mg).

Attempted synthesis of $\text{NaGe}[(\text{O}_2\text{CCH}_2)_3\text{N}]$ (311). $\text{GeCl}_2 \cdot \text{C}_4\text{H}_8\text{O}_2$ (**302**) (130 mg, 0.561 mmol) and $\text{N}(\text{CH}_2\text{CO}_2\text{Na})_3$ (**310**) (145 mg, 0.564 mmol) were suspended in THF (15 mL) in a 50 mL culture tube. The reaction was heated at 80 °C overnight. The

mixture was filtered through a pad of Celite over a frit. All volatiles were removed under vacuum to give a benzene- and chloroform-insoluble yellow solid.

301 (23.0 mg, 36.5 μmol , 73.0 μmol Ge) and $\text{N}(\text{CH}_2\text{CO}_2\text{H})_3$ (**321**) (15 mg, 78 μmol) were mixed in toluene (1 mL). The reaction mixture was heated at 110 °C overnight. The mixture was filtered through a pad of Celite over a frit. All volatiles were removed under vacuum to give a white solid (17 mg). ^1H NMR (C_6D_6) spectrum contained **301** (31%) and $[\text{Ge}(\text{O}^t\text{Bu})_2]_2$ (**322**) (62%).

Attempted synthesis of 313. 1,3-Di-*tert*-butyl-1,3,2-diazagermol-2-ylidene (**312**) (29 mg, 0.12 mmol) and NaO^tBu (**303**) (11 mg, 0.11 mmol) were dissolved in C_6D_6 (0.6 mL) in a J. Young NMR tube to form a light-yellow solution. The reaction was heated at 85 °C overnight and analyzed by ^1H NMR spectroscopy. The ^1H NMR spectrum contained only starting materials, indicating no reaction occurred.

Attempted synthesis of $\text{NaGe}(\text{NC}_4\text{H}_4)_3$ (315-Na). NaH (29.1 mg, 1.21 mmol) was suspended in THF (3 mL) in a 20 mL vial. To the suspension was added pyrrole (**314**) (82 μL , 1.2 mmol) at ambient temperature. (*Gas evolution!*) The reaction was stirred at ambient temperature for 1 h. $\text{GeCl}_2 \cdot \text{C}_4\text{H}_8\text{O}_2$ (**302**) (90 mg, 0.39 mmol) was added to the milky white suspension and the reaction was stirred at ambient temperature overnight. The resulting brown suspension was filtered through a pad of Celite over a frit. Volatiles were removed from the faint yellow filtrate under vacuum to give a benzene-insoluble yellow solid (69 mg).

Attempted synthesis of $\text{LiGe}(\text{NC}_4\text{H}_4)_3$ (315-Li). Pyrrole (**314**) (174 mg, 2.59 mmol) was dissolved in Et_2O (5 mL) in a 20 mL vial. The vial was cooled down to -35

°C in a freezer before the slow addition of ⁿBuLi (1.0 mL, 2.5 mmol, 2.5 M in hexane). The reaction was allowed to warm up to ambient temperature. GeCl₂·C₄H₈O₂ (**302**) (185 mg, 0.799 mmol) was added to the cloudy reaction mixture with additional Et₂O (2 mL). The reaction turned clear light-yellow solution immediately. The reaction was stirred at ambient temperature for 20 h. After 20 h, significant grey precipitation was formed, and the solution turned colorless. The colorless solution was separated, and volatiles were removed under vacuum to give a benzene-insoluble white solid (127 mg).

Attempted syntheses of LiGe(pin)ⁿBu (318). GeCl₂·C₄H₈O₂ (**302**) (96.1 mg, 0.415 mmol) and pinacol (**316**) (48.5 mg, 0.410 mmol) were dissolved in Et₂O (3 mL) in a 10 mL culture tube. The tube was cooled down to –35 °C in a freezer before the slow addition of ⁿBuLi (0.50 mL, 1.2 mmol, 2.5 M in hexane). The reaction was stirred at ambient temperature for 2 d and it turned to a yellow cloudy suspension. The mixture was filtered through a pad of Celite over a frit. Volatiles were removed from the yellow filtrate under vacuum to give a white solid (57 mg). The ¹H NMR (C₆D₆) spectrum showed various unidentified ¹H NMR resonances.

Pinacol (**316**) (55.1 mg, 0.466 mmol) was dissolved in Et₂O (0.5 mL) in a 7 mL vial. The vial was cooled down to –35 °C in a freezer before the slow addition of ⁿBuLi (0.60 mL, 1.5 mmol, 2.5 M in hexane). The milky suspension was cooled down to –35 °C again in a freezer before the addition of GeCl₂·C₄H₈O₂ (**302**) (107 mg, 0.462 mmol) with additional Et₂O (0.5 mL). The reaction was stirred at ambient temperature for 23 h and it turned to a light-yellow cloudy suspension. The mixture was filtered through a pad of Celite over a frit. Volatiles were removed from the yellow filtrate under vacuum to give a

gluey oil (76 mg). The ^1H NMR (C_6D_6) spectrum showed various unidentified ^1H NMR resonances.

$\text{GeCl}_2\cdot\text{C}_4\text{H}_8\text{O}_2$ (**302**) (82 mg, 0.35 mmol) and pinacol (**316**) (43 mg, 0.36 mmol) were dissolved in toluene (2 mL) in a 10 mL culture tube. $^n\text{BuLi}$ (0.45 mL, 1.1 mmol, 2.5 M in hexane) was added dropwise to the reaction at ambient temperature. The yellow cloudy suspension was heated at 110 °C for 44 h and it turned to a brown-orange cloudy suspension. The mixture was filtered through a pad of Celite over a frit. Volatiles were removed from the filtrate under vacuum to give a benzene-insoluble tan solid.

Pinacol (**316**) (56.5 mg, 0.478 mmol) was dissolved in toluene (0.5 mL) in a 10 mL culture tube. The tube was cooled down to -35 °C in a freezer before the slow addition of $^n\text{BuLi}$ (0.60 mL, 1.5 mmol, 2.5 M in hexane). The cloudy suspension was cooled down to -35 °C again in a freezer before the addition of $\text{GeCl}_2\cdot\text{C}_4\text{H}_8\text{O}_2$ (**302**) (108 mg, 0.466 mmol) with additional toluene (0.5 mL). The reaction was heated at 110 °C for 18 h and it turned to a brown cloudy suspension upon heating. The mixture was filtered through a pad of Celite over a frit. Volatiles were removed from the orange filtrate under vacuum to give an orange solid (72 mg). The ^1H NMR (C_6D_6) spectrum showed various unidentified ^1H NMR resonances.

Attempted syntheses of LiGe(pin)Me (319). Pinacol (**316**) (55.8 mg, 0.472 mmol) was dissolved in THF (5 mL) in a 20 mL vial. The vial was cooled down to -35 °C in a freezer before the slow addition of MeLi (1.0 mL, 1.6 mmol, 1.6 M in Et_2O). The colorless solution was cooled down to -35 °C again in a freezer before the addition of $\text{GeCl}_2\cdot\text{C}_4\text{H}_8\text{O}_2$ (**302**) (107.5 mg, 0.4641 mmol). The reaction turned yellow immediately

and was stirred at ambient temperature for 24 h. Volatiles were removed under vacuum to give a benzene- and chloroform-insoluble yellow powder.

Pinacol (**316**) (53.8 mg, 0.455 mmol) was dissolved in THF (4 mL) in a 20 mL vial. The vial was cooled down to $-35\text{ }^{\circ}\text{C}$ in a freezer before the slow addition of MeLi (0.60 mL, 0.96 mmol, 1.6 M in Et₂O). The reaction was stirred for 5 min before the addition of GeCl₂·C₄H₈O₂ (**302**) (101 mg, 0.436 mmol) and another portion of MeLi (0.30 mL, 0.48 mmol, 1.6 M in Et₂O). The yellow solution was stirred at ambient temperature for 16 h. Volatiles were removed under vacuum to give a chloroform-insoluble yellow powder.

Pinacol (**316**) (52.8 mg, 0.447 mmol) was dissolved in toluene (3 mL) in a 10 mL culture tube. MeLi (0.90 mL, 1.4 mmol, 1.6 M in Et₂O). The cloudy suspension was stirred for 5 min before the addition of GeCl₂·C₄H₈O₂ (**302**) (99.8 mg, 0.431 mmol) with additional toluene (1.5 mL). The reaction turned yellow immediately and was heated at $120\text{ }^{\circ}\text{C}$ for 14 h. The resulting orange suspension was filtered through a pad of Celite over a frit. Volatiles were removed under vacuum to give a tan solid (85 mg). The ¹H NMR (CDCl₃) spectrum showed various unidentified ¹H NMR resonances.

Attempted synthesis of LiGe(cat)Me (320). Catechol (**317**) (56.5 mg, 0.513 mmol) was dissolved in THF (4 mL) in a 20 mL vial. The vial was cooled down to $-35\text{ }^{\circ}\text{C}$ in a freezer before the dropwise addition of MeLi (1.0 mL, 1.6 mmol, 1.6 M in Et₂O). The solution turned cloudy upon addition but turned clear after full addition. The colorless solution was stirred for 10 min before the addition of GeCl₂·C₄H₈O₂ (**302**) (114 mg, 0.492 mmol). The solution turned yellow immediately and cloudy after a few minutes. The

reaction was stirred at ambient temperature for 19 h. The mixture was filtered through a pad of Celite over a frit. Volatiles were removed from the light-yellow filtrate under vacuum to give a white solid (194 mg). The ^1H NMR (CDCl_3) spectrum showed various unidentified ^1H NMR resonances.

Catechol (**317**) (50.0 mg, 0.454 mmol) was dissolved in THF (4 mL) in a 20 mL vial. The vial was cooled down to $-35\text{ }^\circ\text{C}$ in a freezer before the dropwise addition of MeLi (0.60 mL, 0.96 mmol, 1.6 M in Et_2O). The reaction was stirred for 10 min before the addition of $\text{GeCl}_2\cdot\text{C}_4\text{H}_8\text{O}_2$ (**302**) (100 mg, 0.432 mmol) and another portion of MeLi (0.30 mL, 0.48 mmol, 1.6 M in Et_2O). The solution turned yellow immediately and to a white cloudy suspension gradually. The reaction was stirred at ambient temperature for 20 h. The mixture was filtered through a pad of Celite over a frit. Volatiles were removed from the light-yellow filtrate under vacuum to give a white solid (176 mg). The ^1H NMR (CDCl_3) spectrum showed various unidentified ^1H NMR resonances.

Catechol (**317**) (60.3 mg, 0.548 mmol) was suspended in toluene (4 mL) in a 10 mL culture tube. The vial was cooled down to $-35\text{ }^\circ\text{C}$ in a freezer before the dropwise addition of MeLi (1.1 mL, 1.8 mmol, 1.6 M in Et_2O). The suspension turned clear immediately. The clear solution was stirred for 10 min before the addition of $\text{GeCl}_2\cdot\text{C}_4\text{H}_8\text{O}_2$ (**302**) (99.8 mg, 0.431 mmol). The reaction turned to a yellow suspension immediately and was heated at $120\text{ }^\circ\text{C}$ for 20 h. The supernatant was separated and volatiles were removed under vacuum to give a yellow solid. The ^1H NMR (CDCl_3) spectrum showed various unidentified ^1H NMR resonances.

Cation metathesis of 301. $[\text{NaGe}(\text{O}^t\text{Bu})_3]_2$ (**301**) (58.4 mg, 185 μmol Ge) and TBABr (60.4 mg, 187 μmol) were mixed in toluene/ Et_2O (4/4 mL) in a 20 mL vial. The reaction was stirred over a weekend at ambient temperature. The resulting white/grey solid was filtered off by a pad of Celite over a frit. Volatiles were removed from the brown filtrate under vacuum to give white crystal and orange solid (53 mg in total). ^1H NMR (C_6D_6) spectrum showed a major unknown ^1H NMR resonance for *tert*-butyl and some other unidentified minor resonances.

$[\text{NaGe}(\text{O}^t\text{Bu})_3]_2$ (**301**) (82.5 mg, 265 μmol Ge) and TBABr (86.8 mg, 269 μmol) were mixed in THF (30 mL) in a 50 mL culture tube. The reaction was heated at 80 $^\circ\text{C}$ for 90 h. The volatiles were removed under vacuum. Toluene was added and the solid was filtered off by a pad of Celite over a frit. Removal of volatiles gave a white solid (145 mg). ^1H NMR (C_6D_6) spectrum showed multiple unidentified ^1H NMR resonances.

$[\text{NaGe}(\text{O}^t\text{Bu})_3]_2$ (**301**) (20.0 mg, 63.5 μmol Ge) and Ph_4PBr (25.6 mg, 61.1 μmol) were mixed in C_6D_6 (0.6 mL) in a J. Young NMR tube to form a suspension. The reaction was stirred at ambient temperature and followed by ^1H NMR spectroscopy. After 12 d, the ^1H NMR spectrum contains only one set of ^1H NMR resonances for phenyl but three different ^1H NMR resonances for *tert*-butyl. The mixture was passed through a pad of Celite and the residue was re-dissolved in CD_3CN . The ^1H NMR (CD_3CN) spectrum contained multiple unidentified ^1H NMR resonances for phenyl and *tert*-butyl.

3.4.6 Development of Catalytic Germylation of Aryl Bromides Using **301**

Stock solutions of Pd₂dba₃ or Pd(OAc)₂, and DPPF or ^tBu-bpy, if indicated, in C₆D₆ were added to a J. Young NMR tube. [NaGe(O^tBu₃)₂] (**301**) (16 mg, 51 μmol Ge) was added as a solid. Stock solutions of 4-FC₆H₄Br (**323b**) (50 μmol) and PhCF₃ (15 μmol) in C₆D₆ were then added. A known amount of C₆D₆ was added to normalize the total solvent volume of each experiment to 0.6 mL. The J. Young NMR tube was closed, brought out of the glovebox, and placed into an oil bath at the indicated temperature for the time reported. The reaction was monitored by ¹H and/or ¹⁹F NMR spectroscopy. The conversions and yields were determined by comparing the integration of the ¹⁹F NMR resonances of 4-FC₆H₄Br (**323b**) (δ -116.4 in C₆D₆) and 4-FC₆H₄Ge(O^tBu)₃ (**324b**) (δ -110.4 in C₆D₆) to the PhCF₃ internal standard (δ -63.48 in C₆D₆). The results were summarized in Table III-1 (entries 1–10).

3.4.7 Mercury Test of the Catalytic Germylation of Aryl Bromides

[NaGe(O^tBu₃)₂] (**301**) (32.0 mg, 102 μmol Ge) and stock solutions of 4-FC₆H₄Br (**323b**) (140 μL, 99.3 μmol, 0.709 M in C₆D₆), Pd(OAc)₂ (165 μL, 0.100 μmol, 0.00607 M in C₆D₆), and PhCF₃ (60.0 μL, 28.7 μmol, 0.479 M in C₆D₆) were well mixed and diluted to 2 mL with C₆D₆ using a volumetric flask. 1 mL of the reaction mixture was transferred to a 10 mL culture tube and Hg (24.0 mg, 0.120 mmol, ca. 2.4 equiv.) was added to the culture tube. Another 1 mL of the reaction mixture was transferred to another 10 mL culture tube. Both culture tubes were closed and placed into an oil bath at 100 °C for 2 h with a vigorous stir. The reaction mixture was transferred to a J. Young NMR tube

and analyzed by ^1H and ^{19}F NMR spectroscopy. The conversions and yields were determined by comparing the integration of the ^{19}F NMR resonances of 4- $\text{FC}_6\text{H}_4\text{Br}$ (**323b**) ($\delta -116.4$ in C_6D_6) and 4- $\text{FC}_6\text{H}_4\text{Ge}(\text{O}^t\text{Bu})_3$ (**324b**) ($\delta -110.4$ in C_6D_6) to the PhCF_3 internal standard ($\delta -63.48$ in C_6D_6). The results were summarized in Table III-1 (entries 11 and 12).

3.4.8 Catalytic Aromatic C–Br Germylation using Other Germanium(II) Reagent

3.4.8.1 Germylation with $\text{GeCl}_2 \cdot \text{C}_4\text{H}_8\text{O}_2$ (**302**)

302 (12.0 mg, 51.8 μmol), stock solutions of **323b** (57 μL , 50 μmol , 0.883 M in C_6D_6), $\text{Pd}(\text{OAc})_2$ (15 μL , 0.52 μmol , 0.0345 M in C_6D_6), and PhCF_3 (40.0 μL , 15.3 μmol , 0.383 M in C_6D_6), and C_6D_6 (390 μL) were mixed in a J. Young NMR tube to form a yellow solution with some insoluble **302**. The J. Young NMR tube was closed and analyzed by ^1H and ^{19}F NMR spectroscopy, and again after placing into an oil bath at 100 $^\circ\text{C}$ for 20 h. The insoluble **302** dissolved into solution upon heating. Both ^1H and ^{19}F NMR spectra suggested there was no reaction.

3.4.8.2 Germylation with $[\text{NaGe}(\text{OEt})_3]_2$ (**307**)

Entries 1–6. **323b** (50 μmol , 1 equiv), **307**, $\text{Pd}(\text{OAc})_2$, and PhCF_3 were added to a J. Young NMR tube. A known amount of C_6D_6 was added to normalize the total solvent volume of each experiment to 0.6 mL. The J. Young NMR tube was closed and placed into an oil bath at the temperature for the time indicated. The reaction was analyzed by ^1H and ^{19}F NMR spectroscopy.

Entries 7–10. **323b** (100 μ mol, 1 equiv), **307**, Pd(OAc)₂, PhCF₃, and NaOEt (**306**) if indicated, were added a 10 mL culture tube. A known amount of toluene was added to normalize the total solvent volume of each experiment to 1 mL. The culture tube was closed and placed into an oil bath at 100 °C for 20 h. The reaction mixture was then passed through a pad of Celite over a pipette into an NMR tube and analyzed by ¹⁹F NMR spectroscopy.

The detailed conditions were summarized in Table III-5. All entries showed neither consumption of **323b** and **307**, nor the formation of FC₆H₄Ge(OEt)₃ (**332**).

Table III-5. Detailed conditions of attempted germylation using **307**.

entry	307 (equiv Ge)	Pd(OAc) ₂ (mol%)	306 (equiv)	temperature (°C)	time (h)
1	1	0.1	–	100	22
2	1	0.1	–	130	24
3	1	1	–	100	20
4	1	1	–	130	22
5	1	5	–	100	20
6	2	1	–	100	20
7	1	1	–	100	20
8	1.5	1	–	100	20
9	1	1	1	100	20
10	1	1	2	100	20

3.4.8.3 Germylation with [Ge(O^tBu)₂]₂ (**322**)

Synthesis of 322. In a 50 mL culture tube, **302** (1.55 g, 6.69 mmol) and **303** (1.31 g, 13.6 mmol) were dissolved in THF (20 mL). *Caution: Exothermic!* The reaction was heated at 100 °C for 2 h. The solid was filtered off by a pad of Celite over a frit. Volatiles were removed under vacuum. The resulting residue was purified from a saturated pentane solution at –35 °C to give a pure product as a white solid (926 mg, 63% yield). The solid-

state structure has been reported as a dimer, similar to that of its stannylene analog.^{193,194}
¹H NMR (400 MHz, C₆D₆) δ 1.48 (s, 36).

322 (12.9 mg, 58.9 μmol Ge), stock solutions of **323b** (64.0 μL, 55.7 μmol, 0.871 M in C₆D₆), Pd(OAc)₂ (24.0 μL, 0.566 μmol, 0.0236 M in C₆D₆), and PhCF₃ (40.0 μL, 15.8 μmol, 0.396 M in C₆D₆), and C₆D₆ (470 μL) were mixed in a J. Young NMR tube to form a colorless solution. The J. Young NMR tube was closed and analyzed by ¹H and ¹⁹F NMR spectroscopy, and again after placing into an oil bath at 100 °C for 3 h and 21 h. All ¹H and ¹⁹F NMR spectra suggested there was no reaction. NaO^tBu (**303**) (430 μL, 59.3 μmol, 0.138 M in C₆D₆) was added to the reaction mixture, and the ¹H NMR spectrum showed full and clean conversion of **322** to [NaGe(O^tBu)₃]₂ (**301**) at ambient temperature. The reaction was then placed into an oil bath at 100 °C for 3 h and analyzed by ¹H and ¹⁹F spectroscopy. Both ¹H and ¹⁹F spectra showed **323b** and **301** were fully consumed, and 4-FC₆H₄Ge(O^tBu)₃ (**324b**) was formed quantitatively.

3.4.8.4 Germylation with CsGeCl₃ (**325**)

325 (19.5 mg, 62.5 μmol), stock solutions of **323b** (68 μL, 59 μmol, 0.871 M in C₆D₆) and Pd(OAc)₂ (17.5 μL, 0.604 μmol, 0.0345 M in C₆D₆), toluene (0.6 mL), and THF (0.6 mL) were mixed in a 10 mL culture tube to form a colorless solution with insoluble **325**. The culture tube was closed and placed into an oil bath at 100 °C for 20 h. The resulting orange suspension was analyzed by ¹⁹F NMR spectroscopy, which suggested there was no reaction.

3.4.9 Preliminary Tests of Catalytic Germylation of Aryl Chlorides

Stock solutions of Pd₂dba₃ or Pd(OAc)₂ and ligands, if indicated, in C₆D₆ were added to a J. Young NMR tube. **301** (16 mg, 51 μmol Ge) was added as a solid. Stock solutions of 4-FC₆H₄Cl (**323b-Cl**) (50 μmol) and PhCF₃ (15 μmol) in C₆D₆ were then added. A known amount of toluene was added to normalize the total solvent volume of each experiment to 0.6 mL. The J. Young NMR tube was closed and placed into an oil bath at 100 °C for 21 h. The reaction was monitored by ¹⁹F NMR spectroscopy. The conversions and yields were determined by comparing the integration of the ¹⁹F NMR resonances of 4-FC₆H₄Cl (**323b-Cl**) (δ -116.9 in toluene) and 4-FC₆H₄Ge(O^tBu)₃ (**324b**) (δ -110.2 in toluene) to the PhCF₃ internal standard (δ -63.48 in toluene). The results were summarized in Table III-2.

3.4.10 Synthesis and Characterization of New Germane Products

3.4.10.1 General Procedures

General Procedure A. **301** (ca. 16 mg, 25 μmol, 51 μmol Ge) was added as a solid to a J. Young NMR tube. Pd(OAc)₂ (0.005 μmol) and bromobenzene derivatives **323** (ca. 50 μmol) were then added as a solid or stock solution in C₆D₆. A known amount of C₆D₆ was added to normalize the total solvent volume of each experiment to 0.6 mL. The NMR tube was closed and placed into an oil bath at 100 °C for 3 h. The mixture was filtered through a pad of Celite over a pipette, and volatiles were removed under vacuum. The residue was purified by flash column chromatography on silica gel using Et₂O as eluent.

General Procedure B. **301** (0.5 equiv, 1 equiv Ge) and bromobenzene derivatives **323** (1 equiv) was added as a solid or liquid to a 50 mL culture tube. Pd(OAc)₂ (0.001 equiv) was added. Toluene was added as a solvent. The culture tube was closed and placed into an oil bath at 100 °C overnight. The mixture was filtered through a pad of Celite over a frit, and volatiles were removed under vacuum. The residue was purified by flash column chromatography on silica gel using Et₂O as eluent.

General Procedure C. **302** (1 equiv) and **303** (3.3 equiv) were mixed in THF (5 mL) in a 50 mL culture tube. Bromobenzene derivatives **323** (1 equiv), Pd(OAc)₂ (0.001 equiv), and toluene (5 mL) were then added. The culture tube was closed and placed into an oil bath at 100 °C overnight. The mixture was filtered through a pad of Celite over a frit, and volatiles were removed under vacuum. The residue was purified by flash column chromatography on silica gel using Et₂O as eluent.

3.4.10.2 Synthesis and Characterization of Arylgermanes

Tri-tert-butoxyphenylgermane (324a). General Procedure A was used: **301** (17.0 mg, 54.0 μmol Ge) and bromobenzene (**323a**) (5.3 μL, 50 μmol) reacted to provide a colorless oil (18 mg, 98% yield). ¹H NMR (499 MHz, CDCl₃) δ 7.81–7.64 (m, 2H), 7.52–7.30 (m, 3H), 1.36 (s, 27H); ¹³C{¹H} NMR (126 MHz, CDCl₃) δ 137.6, 134.0, 130.3, 128.4, 74.3, 32.6; HRMS (ESI) *m/z* [M + Li]⁺ calculated for C₁₈H₃₂⁷⁴Ge⁷LiO₃: 377.1718, measured: 377.1716. **324a** was also independently synthesized from heating PhGeCl₃ (319 mg, 1.25 mmol) and NaO^tBu (368 mg, 3.83 mmol) in toluene (5 mL) at 140 °C for

86 h. After filtration of solid and evaporation of volatiles, **324a** can be isolated as an oil (385 mg, 83% yield)

Tri-tert-butoxy(4-fluorophenyl)germane (324b). General Procedure A was used: **301** (15.4 mg, 48.9 μmol Ge) and **323b** (54.0 μL , 47.0 μmol , 0.871 M in C_6D_6) reacted to provide a colorless oil (18 mg, >98% yield). General Procedure B was used: **301** (3.83 g, 12.2 mmol Ge) and **323b** (2.10 g, 12.0 mmol) reacted to provide a colorless oil (4.62 g, >98% yield). General Procedure C was used: **302** (240 mg, 1.04 mmol) and **303** (322 mg, 3.35 mmol) and **323b** (110 μL , 1.00 mmol) reacted to provide a colorless oil (360 mg, 93% yield). ^1H NMR (499 MHz, C_6D_6) δ 7.81–7.65 (m, 2H), 6.92–6.71 (m, 2H), 1.43 (s, 27H); ^{19}F NMR (470 MHz, C_6D_6) δ -110.4 (tt, $J_{\text{F-H}} = 9.0, 5.8$ Hz); $^{13}\text{C}\{^1\text{H}\}$ NMR (126 MHz, C_6D_6) δ 164.7 (d, $J_{\text{F-C}} = 250.0$ Hz), 136.3 (d, $J_{\text{F-C}} = 7.7$ Hz), 133.4 (d, $J_{\text{F-C}} = 3.8$ Hz), 115.8 (d, $J_{\text{F-C}} = 20.6$ Hz), 74.5, 32.7; HRMS (ESI) m/z $[\text{M} + \text{Na}]^+$ calculated for $\text{C}_{18}\text{H}_{31}\text{F}^{74}\text{GeNaO}_3$: 411.1361, measured: 411.1352.

Tri-tert-butoxy(4-methoxyphenyl)germane (324c). General Procedure A was used: **301** (16.9 mg, 53.7 μmol Ge) and 4-bromoanisole (**323c**) (85.0 μL , 52.7 μmol , 0.620 M in C_6D_6) reacted to provide a colorless oil (21 mg, >98% yield). ^1H NMR (400 MHz, C_6D_6) δ 7.85 (d, $J = 8.8$ Hz, 2H), 6.78 (d, $J = 8.8$ Hz, 2H), 3.23 (s, 3H), 1.50 (s, 27H); $^{13}\text{C}\{^1\text{H}\}$ NMR (101 MHz, C_6D_6) δ 161.8, 135.7, 128.7, 114.4, 74.3, 54.6, 32.8; HRMS (ESI) m/z $[\text{M} + \text{Li}]^+$ calculated for $\text{C}_{19}\text{H}_{34}^{74}\text{Ge}^7\text{LiO}_4$: 407.1823, measured: 407.1813.

Tri-tert-butoxy(4-trifluoromethylphenyl)germane (324d). General Procedure A was used: **301** (16.7 mg, 53.0 μmol Ge) and 1-bromo-4-(trifluoromethyl)benzene (**323d**) (50.0 μL , 200 μmol , 0.250 M in C_6D_6) reacted to provide a white solid (22 mg, >98%

yield). General Procedure B was used: **301** (319 mg, 1.01 mmol Ge) and **323d** (140 μ L, 1.00 mmol) reacted to provide a white solid (0.43 g, 98% yield). ^1H NMR (400 MHz, C_6D_6) δ 7.86–7.73 (m, 2H), 7.37–7.26 (m, 2H), 1.42 (s, 27H); ^{19}F NMR (470 MHz, C_6D_6) δ –63.9; $^{13}\text{C}\{^1\text{H}\}$ NMR (101 MHz, C_6D_6) δ 142.4, 134.5, 132.3 (q, $J_{\text{F-C}} = 32.3$ Hz), 125.2 (q, $J_{\text{F-C}} = 3.7$ Hz), 124.7 (q, $J_{\text{F-C}} = 272.4$ Hz), 74.8, 32.6; HRMS (ESI) m/z $[\text{M} + \text{Li}]^+$ calculated for $\text{C}_{19}\text{H}_{31}\text{F}_3^{74}\text{Ge}^7\text{LiO}_3$: 445.1592, measured: 445.1579.

Ethyl 4-(tri-tert-butoxygermyl)benzoate (324e). General Procedure A was used: **301** (16.6 mg, 52.7 μ mol Ge) and ethyl 4-bromobenzoate (**323e**) (90.0 μ L, 50.7 μ mol, 0.563 M in C_6D_6) reacted to provide a colorless oil (22 mg, 98% yield). ^1H NMR (400 MHz, C_6D_6) δ 8.13 (d, $J = 8.3$ Hz, 2H), 7.93 (d, $J = 8.3$ Hz, 2H), 4.09 (q, $J = 7.1$ Hz, 2H), 1.44 (s, 27H), 1.01 (t, $J = 7.1$ Hz, 3H); $^{13}\text{C}\{^1\text{H}\}$ NMR (101 MHz, C_6D_6) δ 165.9, 143.2, 134.2, 132.8, 129.5, 74.7, 61.0, 32.7, 14.2; HRMS (ESI) m/z $[\text{M} + \text{Li}]^+$ calculated for $\text{C}_{21}\text{H}_{36}^{74}\text{Ge}^7\text{LiO}_5$: 449.1929, measured: 449.1921.

N,N-Diethyl-4-(tri-tert-butoxygermyl)benzamide (324f). General Procedure A was used with modifications: The reaction was heated at 130 $^\circ\text{C}$ for 4 h. **301** (16.7 mg, 53.0 μ mol Ge) and *N,N*-diethyl-4-bromobenzamide (**323f**) (13.6 mg, 53.1 μ mol) reacted to provide a colorless oil (24 mg, 97% yield). ^1H NMR (400 MHz, C_6D_6) δ 7.92 (d, $J = 8.1$ Hz, 2H), 7.37 (d, $J = 8.1$ Hz, 2H), 3.30 (br s, 2H), 2.77 (br s, 2H), 1.46 (s, 27H), 1.04 (br s, 3H), 0.63 (br s, 3H); $^{13}\text{C}\{^1\text{H}\}$ NMR (101 MHz, C_6D_6) δ 170.0, 140.2, 138.7, 134.1, 126.9, 74.6, 43.0 (br), 39.5 (br), 32.7, 14.0 (br), 13.3 (br); HRMS (ESI) m/z $[\text{M} + \text{H}]^+$ calculated for $\text{C}_{23}\text{H}_{42}^{74}\text{GeNO}_4$: 470.2320, measured: 470.2311.

Trimethyl(4-(tri-tert-butoxygermyl)phenyl)silane (324g). General Procedure A was used: **301** (16.5 mg, 52.4 μmol Ge) and (4-bromophenyl)trimethylsilane (**323g**) (200 μL , 49.4 μmol , 0.247 M in C_6D_6) reacted to provide a colorless oil (20 mg, 92% yield). ^1H NMR (499 MHz, C_6D_6) δ 7.95 (d, $J = 7.6$ Hz, 2H), 7.47 (d, $J = 7.6$ Hz, 2H), 1.50 (s, 27H), 0.17 (s, 9H); $^{13}\text{C}\{^1\text{H}\}$ NMR (101 MHz, C_6D_6) δ 143.0, 138.4, 133.5, 133.5, 74.4, 32.8, – 1.3; HRMS (ESI) m/z $[\text{M} + \text{Li}]^+$ calculated for $\text{C}_{21}\text{H}_{40}^{74}\text{Ge}^7\text{LiO}_3^{28}\text{Si}$: 449.2113, measured: 449.2104.

Tri-tert-butoxy(4-(4,4,5,5-tetramethyl-1,3,2-dioxaborolan-2-yl)phenyl)germane (324h). General Procedure A was used: **301** (18.0 mg, 57.1 μmol Ge) and 2-(4-bromophenyl)-4,4,5,5-tetramethyl-1,3,2-dioxaborolane (**323h**) (15.0 mg, 53.0 μmol) reacted to provide a white solid (26 mg, >98% yield). General Procedure B was used: **301** (1.00 g, 3.17 mmol Ge) and **323h** (880 mg, 3.11 mmol) reacted to provide a white solid (1.50 g, 97% yield). ^1H NMR (499 MHz, C_6D_6) δ 8.19 (d, $J = 7.4$ Hz, 2H), 8.04 (d, $J = 7.4$ Hz, 2H), 1.45 (s, 27H), 1.10 (s, 12H); $^{11}\text{B}\{^1\text{H}\}$ (160 MHz, C_6D_6) δ 31.6; $^{13}\text{C}\{^1\text{H}\}$ NMR (126 MHz, C_6D_6) δ 141.4, 135.2, 133.6, 131.8 (br), 83.9, 74.4, 32.7, 24.9; HRMS (ESI) m/z $[\text{M} + \text{Li}]^+$ calculated for $\text{C}_{24}\text{H}_{43}^{11}\text{B}^{74}\text{Ge}^7\text{LiO}_5$: 503.2570, measured: 503.2559.

Tri-tert-butoxy(4-vinylphenyl)germane (324i). General Procedure A was used: **301** (16.6 mg, 52.7 μmol Ge) and 4-bromostyrene (**323i**) (180 μL , 50.0 μmol , 0.278 M in C_6D_6) reacted to provide a colorless oil (20 mg, >98% yield). ^1H NMR (400 MHz, C_6D_6) δ 7.87 (d, $J = 8.1$ Hz, 2H), 7.23 (d, $J = 8.1$ Hz, 2H), 6.49 (dd, $J = 17.6, 10.9$ Hz, 1H), 5.60 (dd, $J = 17.6, 0.9$ Hz, 1H), 5.07 (dd, $J = 10.9, 0.9$ Hz, 1H), 1.48 (s, 27H); $^{13}\text{C}\{^1\text{H}\}$ NMR (101

MHz, C₆D₆) δ 139.8, 137.3, 136.9, 134.5, 126.5, 115.0, 74.4, 32.8; HRMS (ESI) m/z [M + Li]⁺ calculated for C₂₁H₃₄⁷⁴Ge⁷LiO₃: 403.1874, measured: 403.1868.

Tri-tert-butoxy(4-ethynylphenyl)germane (324j). General Procedure A was used with modifications: **301** (16.5 mg, 52.4 μ mol Ge) and 1-bromo-4-ethynylbenzene (**323j**) (115 μ L, 49.4 μ mol, 0.430 M in C₆D₆) were heated with Pd(OAc)₂ (0.52 μ mol) at 100 °C for 1 h to provide a white solid (20 mg, >98% yield). ¹H NMR (400 MHz, C₆D₆) δ 7.78 (d, J = 8.1 Hz, 2H), 7.42 (d, J = 8.1 Hz, 2H), 2.73 (s, 1H), 1.42 (s, 27H); ¹³C{¹H} NMR (101 MHz, C₆D₆) δ 138.7, 134.1, 132.2, 124.8, 83.5, 79.2, 74.5, 32.7; HRMS (ESI) m/z [M + Li]⁺ calculated for C₂₀H₃₂⁷⁴Ge⁷LiO₃: 401.1718, measured: 401.1713.

4-(Tri-tert-butoxygermyl)benzotrile (324k). General Procedure A was used with modifications: **301** (17.0 mg, 54.0 μ mol Ge) and 4-bromobenzotrile (**323k**) (300 μ L, 50.7 μ mol, 0.169 M in C₆D₆) were heated with Pd(OAc)₂ (100 μ L, 0.051 μ mol, 0.51 mM in C₆D₆) at 130 °C for 5 h to provide a white solid (20 mg, >98% yield). ¹H NMR (400 MHz, C₆D₆) δ 7.66–7.57 (m, 2H), 7.05–6.96 (m, 2H), 1.38 (s, 27H); ¹³C{¹H} NMR (101 MHz, C₆D₆) δ 143.1, 134.3, 131.6, 118.4, 114.7, 74.8, 32.6; HRMS (APCI) m/z [M + H]⁺ calculated for C₁₉H₃₂⁷⁴GeNO₃: 396.1588, measured: 396.1580.

Tri-tert-butoxy(m-tolyl)germane (324l). General Procedure A was used: **301** (16.2 mg, 51.4 μ mol Ge) and 3-bromotoluene (**323l**) (95.0 μ L, 50.0 μ mol, 0.526 M in C₆D₆) reacted to provide a colorless oil (19 mg, >98% yield). ¹H NMR (400 MHz, CDCl₃) δ 7.61–7.48 (m, 2H), 7.29 (t, J = 7.6 Hz, 1H), 7.23 (d, J = 7.6 Hz, 1H), 2.38 (s, 3H), 1.36 (s, 27H); ¹³C{¹H} NMR (126 MHz, CDCl₃) δ 137.8, 137.3, 134.5, 131.1, 131.0, 128.2, 74.2,

32.6, 21.7; HRMS (ESI) m/z $[M + Li]^+$ calculated for $C_{19}H_{34}^{74}Ge^7LiO_3$: 391.1874, measured: 391.1869.

Methyl 3-(tri-tert-butoxygermyl)benzoate (324m). General Procedure A was used: **301** (16.6 mg, 52.7 μ mol Ge) and methyl 3-bromobenzoate (**323m**) (10.8 mg, 50.2 μ mol) reacted to provide a colorless oil (21 mg, 98% yield). 1H NMR (400 MHz, C_6D_6) δ 8.88 (s, 1H), 8.11 (d, $J = 7.8$ Hz, 1H), 8.02 (d, $J = 7.4$ Hz, 1H), 7.10 (t, $J = 7.7$ Hz, 1H), 3.44 (s, 3H), 1.46 (s, 27H); $^{13}C\{^1H\}$ NMR (101 MHz, C_6D_6) δ 166.4, 138.6, 138.3, 135.3, 131.7, 130.9, 128.6, 74.7, 51.8, 32.7; HRMS (ESI) m/z $[M + Li]^+$ calculated for $C_{20}H_{34}^{74}Ge^7LiO_5$: 435.1773, measured: 435.1769.

Tri-tert-butoxy(3-methoxyphenyl)germane (324n). General Procedure A was used: **301** (16.9 mg, 53.7 μ mol Ge) and 3-bromoanisole (**323n**) (110 μ L, 51.5 μ mol, 0.468 M in C_6D_6) reacted to provide a colorless oil (20 mg, 97% yield). 1H NMR (400 MHz, C_6D_6) δ 7.68–7.59 (m, 1H), 7.55 (dt, $J = 7.3, 1.0$ Hz, 1H), 7.15–7.10 (m, 1H), 6.78 (ddd, $J = 8.3, 2.7, 1.0$ Hz, 1H), 3.32 (s, 3H), 1.48 (s, 27H); $^{13}C\{^1H\}$ NMR (101 MHz, C_6D_6) δ 159.9, 139.1, 129.7, 126.3, 119.8, 116.1, 74.4, 54.6, 32.7; HRMS (ESI) m/z $[M + Li]^+$ calculated for $C_{19}H_{34}^{74}Ge^7LiO_4$: 407.1823, measured: 407.1818.

3-(Tri-tert-butoxygermyl)aniline (324o). General Procedure A was used with modifications: **301** (16.7 mg, 53.0 μ mol Ge) and 3-bromoaniline (**323o**) (160 μ L, 50.2 μ mol, 0.314 M in C_6D_6) reacted to provide a cloudy oil. The residue was purified by flash column chromatography on silica gel using Et_2O as eluent to give a crude product (19 mg). The crude product was extracted by cold pentane (2 mL) and the solid was filtered off by a pad of Celite. The solvent was evaporated under vacuum to give the product as a white

solid (17 mg, 88% yield). ^1H NMR (400 MHz, C_6D_6) δ 7.33 (dt, $J = 7.7, 1.0$ Hz, 1H), 7.18–7.16 (m, 1H), 7.06 (t, $J = 7.7$ Hz, 1H), 6.30 (ddd, $J = 7.7, 2.5, 1.0$ Hz, 1H), 2.79 (br s, 2H), 1.50 (s, 27H); $^{13}\text{C}\{^1\text{H}\}$ NMR (101 MHz, C_6D_6) δ 147.1, 138.4, 129.4, 123.6, 120.1, 116.9, 74.3, 32.8; HRMS (ESI) m/z $[\text{M} + \text{Li}]^+$ calculated for $\text{C}_{18}\text{H}_{33}^{74}\text{Ge}^7\text{LiNO}_3$: 392.1827, measured: 392.1819.

(3,5-Bis(trifluoromethyl)phenyl)tri-tert-butoxygermane (**324p**). General Procedure A was used: **310** (16.0 mg, 50.8 μmol Ge) and 1-bromo-3,5-bis(trifluoromethyl)benzene (**323p**) (180 μL , 49.1 μmol , 0.273 M in C_6D_6) reacted to provide a white solid (24 mg, 97% yield). ^1H NMR (499 MHz, C_6D_6) δ 8.42 (s, 2H), 7.76 (s, 1H), 1.36 (s, 27H); ^{19}F NMR (470 MHz, C_6D_6) δ -64.1 (s); $^{13}\text{C}\{^1\text{H}\}$ NMR (126 MHz, C_6D_6) δ 141.6, 134.1 (m), 131.76 (q, $J_{\text{F-C}} = 33.2$ Hz), 124.2 (m), 123.9 (q, $J = 272.9$ Hz), 75.3, 32.5; HRMS (ESI) m/z $[\text{M} + \text{Na}]^+$ calculated for $\text{C}_{20}\text{H}_{30}\text{F}_6^{74}\text{GeNaO}_3$: 529.1203, measured: 529.1206.

N,N-Dimethyl-2-(tri-tert-butoxygermyl)aniline (**324q**). General Procedure A was used with modifications: The reaction was heated at 100 $^\circ\text{C}$ for 7 h. **301** (17.2 mg, 54.6 μmol Ge) and *N,N*-dimethyl-2-bromoaniline (**323q**) (160 μL , 49.9 μmol , 0.312 M in C_6D_6) reacted to provide a white solid (21 mg, >98% yield). ^1H NMR (400 MHz, CDCl_3) δ 7.87 (dd, $J = 7.4, 1.7$ Hz, 1H), 7.40 (ddd, $J = 8.0, 7.4, 1.7$ Hz, 1H), 7.23 (dd, $J = 8.0, 1.2$ Hz, 1H), 7.14 (td, $J = 7.4, 1.2$ Hz, 1H), 2.70 (s, 6H), 1.38 (s, 27H); $^{13}\text{C}\{^1\text{H}\}$ NMR (101 MHz, C_6D_6) δ 160.1, 136.5, 136.0, 132.0, 124.9, 121.9, 74.6, 47.0, 32.6; HRMS (ESI) m/z $[\text{M} + \text{H}]^+$ calculated for $\text{C}_{20}\text{H}_{38}^{74}\text{GeNO}_3$: 414.2058, measured: 414.2049.

Tri-tert-butoxy(2,6-diisopropylphenyl)germane (324r). General Procedure A was used with modifications: The reaction was heated at 100 °C for 21 h. **301** (16.4 mg, 52.0 μmol Ge) and 2-bromo-1,3-diisopropylbenzene (**323r**) (11.4 mg, 47.3 μmol) reacted to provide a colorless oil (20 mg, 93% yield). ¹H NMR (499 MHz, CDCl₃) δ 7.35 (t, *J* = 7.7 Hz, 1H), 7.20 (d, *J* = 7.7 Hz, 2H), 4.08 (hept, *J* = 6.7 Hz, 2H), 1.42 (s, 27H), 1.24 (d, *J* = 6.7 Hz, 12H); ¹³C{¹H} NMR (126 MHz, CDCl₃) δ 155.0, 134.4, 130.6, 124.6, 75.4, 32.7, 31.8, 25.7; HRMS (ESI) *m/z* [M + Li]⁺ calculated for C₂₄H₄₄⁷⁴Ge⁷LiO₃: 461.2657, measured: 461.2649.

Tri-tert-butoxy(mesityl)germane (324s). General Procedure A was used with modifications: The reaction was heated at 100 °C for 20 h. **301** (16.4 mg, 52.0 μmol Ge) and 2-bromo-1,3,5-trimethylbenzene (**323s**) (185 μL, 49.8 μmol, 0.269 M in C₆D₆) reacted to provide a white solid (21 mg, >98% yield). ¹H NMR (400 MHz, C₆D₆) δ 6.75 (s, 2H), 2.79 (s, 6H), 2.05 (s, 3H), 1.44 (s, 27H); ¹³C{¹H} NMR (126 MHz, C₆D₆) δ 143.6, 140.1, 133.8, 130.0, 74.7, 32.7, 25.3, 21.0; HRMS (ESI) *m/z* [M + Li]⁺ calculated for C₂₁H₃₈⁷⁴Ge⁷LiO₃: 419.2187, measured: 419.2179.

Tri-tert-butoxy(naphthalen-2-yl)germane (324t). General Procedure A was used: **301** (16.5 mg, 52.4 μmol Ge) and 2-bromonaphthalene (**323t**) (10.0 mg, 48.3 μmol) reacted to provide a colorless oil (20 mg, >98% yield). ¹H NMR (400 MHz, CDCl₃) δ 8.29 (s, 1H), 8.00–7.75 (m, 4H), 7.62–7.45 (m, 2H), 1.41 (s, 27H); ¹³C{¹H} NMR (101 MHz, CDCl₃) δ 135.2, 135.0, 134.3, 133.1, 129.7, 128.6, 127.9, 127.8, 127.1, 126.3, 74.4, 32.6; HRMS (ESI) *m/z* [M + Li]⁺ calculated for C₂₂H₃₄⁷⁴Ge⁷LiO₃: 427.1874, measured: 427.1867.

Tri-tert-butoxy(naphthalen-1-yl)germane (324u). General Procedure A was used: **301** (16.2 mg, 51.4 μmol Ge) and 1-bromonaphthalene (**323u**) (145 μL , 50.0 μmol , 0.345 M in C_6D_6) reacted to provide a white solid (20 mg, 95% yield). ^1H NMR (499 MHz, C_6D_6) δ 9.03 (d, $J = 8.5$ Hz, 1H), 8.32 (d, $J = 6.9$ Hz, 1H), 7.63 (d, $J = 8.2$ Hz, 1H), 7.59 (d, $J = 8.2$ Hz, 1H), 7.48–7.40 (m, 1H), 7.30–7.23 (m, 2H), 1.49 (s, 27H); $^{13}\text{C}\{^1\text{H}\}$ NMR (101 MHz, C_6D_6) δ 136.7, 136.0, 134.6, 134.4, 131.4, 130.0, 129.1, 126.3, 126.3, 125.4, 74.9, 32.7; HRMS (ESI) m/z $[\text{M} + \text{Li}]^+$ calculated for $\text{C}_{22}\text{H}_{34}^{74}\text{Ge}^7\text{LiO}_3$: 427.1874, measured: 427.1868.

1,2-Bis(tri-tert-butoxygermyl)benzene (324v). General Procedure A was used with modifications: **301** (34.0 mg, 108 μmol Ge) and 1,2-dibromobenzene (**323v**) (240 μL , 50.2 μmol , 0.209 M in C_6D_6) reacted with $\text{Pd}(\text{OAc})_2$ (0.100 μmol) at 100 $^\circ\text{C}$ for 3 h to provide a white solid (33 mg, >98% yield). ^1H NMR (499 MHz, CDCl_3) δ 8.33–8.24 (m, 2H), 7.49–7.39 (m, 2H), 1.41 (s, 54H); $^{13}\text{C}\{^1\text{H}\}$ NMR (126 MHz, CDCl_3) δ 143.8, 137.2, 129.2, 75.3, 32.9; HRMS (ESI) m/z $[\text{M} + \text{Li}]^+$ calculated for $\text{C}_{30}\text{H}_{58}^{72}\text{Ge}^7\text{LiO}_6$: 667.2820, measured: 667.2818.

1,4-Bis(tri-tert-butoxygermyl)benzene (324w). General Procedure A was used with modifications: **301** (33.0 mg, 105 μmol Ge) and 1,4-dibromobenzene (**323w**) (11.9 mg, 50.4 μmol) reacted with $\text{Pd}(\text{OAc})_2$ (0.100 μmol) at 100 $^\circ\text{C}$ for 3 h to provide a white solid (33 mg, >98% yield). ^1H NMR (499 MHz, C_6D_6) δ 8.01 (s, 4H), 1.45 (s, 54H); $^{13}\text{C}\{^1\text{H}\}$ NMR (126 MHz, C_6D_6) δ 140.5, 134.0, 74.6, 32.7; HRMS (ESI) m/z $[\text{M} + \text{Li}]^+$ calculated for $\text{C}_{30}\text{H}_{58}^{72}\text{Ge}^7\text{LiO}_6$: 667.2820, measured: 667.2817.

2-(Tri-tert-butoxygermyl)pyridine (324x). General Procedure A was used. **301** (17.0 mg, 54.0 μmol Ge) and 2-bromopyridine (**323x**) (115 μL , 50.1 μmol , 0.436 M in C_6D_6) reacted to provide a colorless oil (18 mg, 97% yield). ^1H NMR (400 MHz, C_6D_6) δ 8.52 (dt, $J = 4.8, 1.5$ Hz, 1H), 7.88 (dt, $J = 7.6, 1.5$ Hz, 1H), 6.97 (td, $J = 7.6, 1.5$ Hz, 1H), 6.56 (ddd, $J = 7.6, 4.8, 1.5$ Hz, 1H), 1.55 (s, 27H); $^{13}\text{C}\{^1\text{H}\}$ NMR (101 MHz, C_6D_6) δ 164.3, 150.5, 134.7, 130.6, 124.2, 74.5, 32.7; HRMS (ESI) m/z $[\text{M} + \text{H}]^+$ calculated for $\text{C}_{17}\text{H}_{32}^{74}\text{GeNO}_3$: 372.1588, measured: 372.1584.

2-Fluoro-5-(tri-tert-butoxygermyl)pyridine (324y). General Procedure A was used: **301** (16.2 mg, 51.4 μmol Ge) and 2-fluoro-5-bromopyridine (**323y**) (80.0 μL , 50.0 μmol , 0.625 M in C_6D_6) reacted to provide a colorless oil (16 mg, 82% yield). ^1H NMR (400 MHz, C_6D_6) δ 8.77 (s, 1H), 7.85 (td, $J = 8.3, 1.7$ Hz, 1H), 6.36 (dd, $J = 8.3, 2.4$ Hz, 1H), 1.36 (s, 27H); ^{19}F NMR (470 MHz, C_6D_6) δ -65.2 (d, $J = 7.3$ Hz); $^{13}\text{C}\{^1\text{H}\}$ NMR (101 MHz, C_6D_6) δ 165.5 (d, $J_{\text{F-C}} = 241.6$ Hz), 153.5 (d, $J_{\text{F-C}} = 14.5$ Hz), 146.3 (d, $J_{\text{F-C}} = 7.6$ Hz), 130.7 (d, $J_{\text{F-C}} = 4.7$ Hz), 109.9 (d, $J_{\text{F-C}} = 36.1$ Hz), 75.0, 32.6; HRMS (ESI) m/z $[\text{M} + \text{H}]^+$ calculated for $\text{C}_{17}\text{H}_{31}\text{F}^{74}\text{GeNO}_3$: 390.1494, measured: 390.1486.

2,5-Bis(tri-tert-butoxygermyl)pyrazine (324z). General Procedure A was used with modifications: **301** (32.2 mg, 102 μmol Ge) and 2,5-dibromopyrazine (**323z**) (11.7 mg, 49.2 μmol) reacted with $\text{Pd}(\text{OAc})_2$ (0.99 μmol) at 100 $^\circ\text{C}$ for 1 h to provide a white solid (32 mg, 98% yield). ^1H NMR (400 MHz, C_6D_6) δ 9.43 (s, 2H), 1.45 (s, 54H); $^{13}\text{C}\{^1\text{H}\}$ NMR (101 MHz, C_6D_6) δ 160.7, 150.9, 75.1, 32.6; HRMS (ESI) m/z $[\text{M} + \text{H}]^+$ calculated for $\text{C}_{28}\text{H}_{57}^{72}\text{Ge}^{74}\text{GeN}_2\text{O}_6$: 663.2644, measured: 663.2641.

Tri-tert-butoxy(furan-3-yl)germane (324aa). General Procedure A was used with modifications: The reaction was heated at 100 °C for 31 h. **301** (17.2 mg, 54.6 μmol Ge) and 3-bromofuran (**323aa**) (125 μL, 50.5 μmol, 0.404 M in C₆D₆) reacted to provide a colorless oil (17 mg, 94% yield). ¹H NMR (400 MHz, C₆D₆) δ 7.61 (dd, *J* = 1.6, 0.8 Hz, 1H), 7.14 (t, *J* = 1.6 Hz, 1H), 6.44 (dd, *J* = 1.6, 0.8 Hz, 1H), 1.43 (s, 27H); ¹³C{¹H} NMR (101 MHz, C₆D₆) δ 149.3, 143.4, 116.9, 113.0, 74.4, 32.6; HRMS (ESI) *m/z* [M + Li]⁺ calculated for C₁₆H₃₀⁷⁴Ge⁷LiO₄: 367.1510, measured: 367.1511.

Tri-tert-butoxy(thiophen-3-yl)germane (324ab). General Procedure A was used with modifications: The reaction was heated at 100 °C for 16 h. **301** (17.3 mg, 54.9 μmol Ge) and 3-bromothiophene (**323ab**) (135 μL, 50.5 μmol, 0.374 M in C₆D₆) reacted to provide a colorless oil (19 mg, >98% yield). ¹H NMR (400 MHz, C₆D₆) δ 7.68 (dd, *J* = 2.7, 1.0 Hz, 1H), 7.33 (dd, *J* = 4.9, 1.0 Hz, 1H), 6.96 (dd, *J* = 4.9, 2.7 Hz, 1H), 1.44 (s, 27H); ¹³C{¹H} NMR (101 MHz, C₆D₆) δ 136.1, 133.3, 131.1, 126.2, 74.4, 32.7; HRMS (ESI) *m/z* [M + Li]⁺ calculated for C₁₆H₃₀⁷⁴Ge⁷LiO₃³²S: 383.1285, measured: 382.1281.

Tri-tert-butoxy(thiophen-2-yl)germane (324ac). General Procedure A was used with modifications: **301** (16.9 mg, 53.7 μmol Ge) and 2-bromothiophene (**323ac**) (130 μL, 50.0 μmol, 0.385 M in C₆D₆) reacted with Pd(OAc)₂ (0.52 μmol) at 100 °C for 1 h to provide a colorless oil (18 mg, 96% yield). ¹H NMR (400 MHz, CDCl₃) δ 7.65 (dd, *J* = 4.7, 0.9 Hz, 1H), 7.50 (dd, *J* = 3.4, 0.9 Hz, 1H), 7.21 (dd, *J* = 4.7, 3.4 Hz, 1H), 1.37 (s, 27H); ¹³C{¹H} NMR (101 MHz, CDCl₃) δ 135.9, 134.9, 131.6, 127.7, 74.7, 32.3; HRMS (ESI) *m/z* [M + Li]⁺ calculated for C₁₆H₃₀⁷⁴Ge⁷LiO₃³²S: 383.1282, measured: 382.1281.

Tri-tert-butoxy(styryl)germane (324ad). General Procedure A was used with modifications: **301** (16.7 mg, 53.0 μmol Ge) and β -bromostyrene (**323ad**) (240 μL , 50.4 μmol , 0.211 M in C_6D_6 , $E/Z = 90/10$) reacted with $\text{Pd}(\text{OAc})_2$ (0.52 μmol) at 100 $^\circ\text{C}$ for 3 h to provide a yellow oil (20 mg, >98% yield). The product contains Based on the ^1H NMR spectrum, the product contains E/Z isomers in 90:10 ratio. (*E*)-tri-tert-butoxy(styryl)germane (**E-324ad**): ^1H NMR (499 MHz, CDCl_3) δ 7.48 (d, $J = 7.4$ Hz, 2H), 7.37 (t, $J = 7.4$ Hz, 2H), 7.34–7.28 (m, 1H, overlaps with the *Z*-isomer), 7.25 (d, $J = 18.4$ Hz, 1H), 6.37 (d, $J = 18.4$ Hz, 1H), 1.38 (s, 27H); $^{13}\text{C}\{^1\text{H}\}$ NMR (101 MHz, CDCl_3) δ 146.8, 137.1, 128.9, 128.6, 126.9, 124.0, 73.9, 32.4; (*Z*)-tri-tert-butoxy(styryl)germane (**Z-324ad**): ^1H NMR (499 MHz, CDCl_3) δ 7.73 (d, $J = 6.9$ Hz, 2H), 7.43–7.34 (m, 1H, overlaps with the *E*-isomer), 7.34–7.28 (m, 3H, overlaps with the *E*-isomer), 5.85 (d, $J = 14.1$ Hz, 1H), 1.31 (s, 27H); $^{13}\text{C}\{^1\text{H}\}$ NMR (101 MHz, CDCl_3) δ 147.9, 129.2, 128.5, 127.8, 125.2, 74.1, 32.3 (one $^{13}\text{C}_{\text{sp}^2}$ resonance is missing; presumably overlaps with the *E*-isomer at δ 137.1); HRMS (ESI) m/z $[\text{M} + \text{Li}]^+$ calculated for $\text{C}_{20}\text{H}_{34}^{74}\text{Ge}^7\text{LiO}_3$: 403.1874, measured: 403.1867.

Tri-tert-butoxy(1H-inden-2-yl)germane (324ae). General Procedure A was used with modifications: **301** (17.0 mg, 54.0 μmol Ge) and 2-bromo-1*H*-indene (**323ae**) (190 μL , 50.4 μmol , 0.265 M in C_6D_6) reacted with $\text{Pd}(\text{OAc})_2$ (21 μL , 0.50 μmol , 23.6 mM in C_6D_6) at 100 $^\circ\text{C}$ for 1 h to provide a yellow oil (19 mg, 93% yield). ^1H NMR (400 MHz, CDCl_3) δ 7.58–7.50 (m, 1H), 7.50–7.45 (m, 1H), 7.42 (td, $J = 2.0, 0.7$ Hz, 1H), 7.35–7.28 (m, 1H), 7.25 (td, $J = 7.4, 1.3$ Hz, 1H), 3.65 (d, $J = 2.0$ Hz, 2H), 1.39 (s, 27H); $^{13}\text{C}\{^1\text{H}\}$ NMR (101 MHz, CDCl_3) δ 146.2, 144.3, 143.9, 143.7, 126.6, 125.8, 123.8, 121.8, 74.2,

42.6, 32.6; HRMS (ESI) m/z $[M + Li]^+$ calculated for $C_{21}H_{34}^{74}Ge^7LiO_3$: 415.1874, measured: 415.1862.

3.4.11 Attempted Germylation of 323af, 323ag, 323ah, and 323ai and the Related Experiments

3.4.11.1 Attempted Germylation of 323af

301 (17.0 mg, 54.0 μ mol Ge), 5-bromo-2-methylphenol (**323af**) (9.6 mg, 51 μ mol), $Pd(OAc)_2$ (100 μ L, 0.0518 μ mol, 0.518 mM in C_6D_6), and C_6D_6 (500 μ L) were mixed in a J. Young NMR tube to form a light-brown solution. The J. Young NMR tube was closed and analyzed by 1H NMR spectroscopy. Further heating at 100 $^\circ C$ for 3 h and 130 $^\circ C$ for 13 h did not lead to any change. The 1H NMR spectrum indicated the formation of tBuOH from the deprotonation of **323af**. Other products were not identified. The formation of tBuOH was observed by reacting 2,6-dimethylphenol with **301** in 3:1 or 1:1 (OH:Ge) ratio as well.

3.4.11.2 Attempted Germylation of 323ag

301 (17.8 mg, 56.5 μ mol Ge), 1-bromo-4-nitrobenzene (**323ag**) (11.1 mg, 54.9 μ mol), $Pd(OAc)_2$ (90 μ L, 0.055 μ mol, 0.607 mM in C_6D_6), and C_6D_6 (510 μ L) were mixed in a J. Young NMR tube to form an orange solution. The color turned darker over time at ambient temperature. The NMR tube was closed and placed into an oil bath at 100 $^\circ C$ for 3 h. The resulting mixture was analyzed by 1H NMR spectroscopy. The 1H NMR spectrum, in the aromatic region, contained 4,4'-dibromoazoxybenzene (**328-BrBr**)

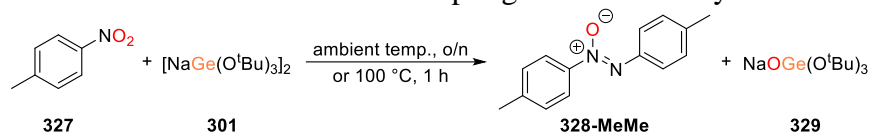
(69%) at δ 7.96 (d, $J = 8.9$ Hz, 2H), 7.80 (d, $J = 9.0$ Hz, 2H), 7.26 (d, $J = 8.9$ Hz, 2H), 7.05 (d, $J = 9.0$ Hz, 2H) and unreacted **323ag** (31%). **301** was fully converted to NaOGe(O^tBu)₃ (**329**) at δ 1.53 (s, 27H). **329** was detected by HRMS (ESI) m/z [M – Na][–] calculated for C₁₂H₂₇⁷⁴GeO₄: 309.1127, measured: 309.1126. The addition of Me₃SiCl to the reaction mixture led to the formation of Me₃SiOGe(O^tBu)₃ (**335**). The ¹H and ¹³C{¹H} NMR data of **335** observed in this experiment match the data for the independently synthesized **335**.

Synthesis of Me₃SiOGe(O^tBu)₃ (335). GeCl₄ (110 μ L, 0.964 mmol) and KO^tBu (**330**) (283 mg, 2.94 mmol), and THF (2 mL) were mixed in a 10 mL culture tube. The culture tube was closed and placed into an oil bath at 100 °C for 1 h. KOSiMe₃ (490 μ L, 1 μ mol, 2 M in THF) was added to the reaction mixture. The culture tube was closed and placed into an oil bath at 100 °C for 2 h. The solid was filtered off by a pad of Celite, and volatiles were removed under vacuum to give the product as a colorless oil (347 mg, 94% yield). ¹H NMR (499 MHz, C₆D₆) δ 1.41 (s, 27H), 0.29 (s, 9H); ¹³C{¹H} NMR (126 MHz, C₆D₆) δ 74.9, 32.3, 2.5; HRMS (ESI) m/z [M + Na]⁺ calculated for C₁₅H₃₆⁷⁴GeNaO₄²⁸Si: 405.1487, measured: 405.1489.

Reductive coupling of 327 to 328-MeMe by 301. **301**, 4-nitrotoluene (**327**), and C₆D₆ were mixed in a J. Young NMR tube. The NMR tube was closed and shaken at ambient temperature overnight or placed into an oil bath at 100 °C for 1 h. The resulting mixtures were analyzed by ¹H NMR spectroscopy. The results were summarized in Table III-6. 4,4'-dimethylazoxybenzene (**328-MeMe**) has ¹H NMR resonances (400 MHz, C₆D₆) at δ 8.32 (d, $J = 8.0$ Hz, 1H), 8.21 (d, $J = 8.1$ Hz, 1H), 7.04 (d, $J = 8.0$ Hz, 1H), 6.87

(d, $J = 8.1$ Hz, 1H), 2.08 (s, 3H), 1.99 (s, 3H). The ^1H NMR spectroscopy data in CDCl_3 match the previously reported data in the literature.¹⁹⁵

Table III-6. Reductive coupling of nitroarene by **301**.



entry	327 (equiv)	301 (equiv Ge)	unreacted S.M. (%)		yield (%)	
			327	301	328-MeMe	329
1	1.0	1.0	30	0	70	100
2	1.0	1.5	0	0	100	100
3	1.0	2.0	0	23	100	77

Attempted reductive cross-coupling of nitroarene. 327 (12.8 mg, 93.3 μmol), **323ag** (19.4 mg, 96.0 μmol), **301** (89.6 mg, 284 μmol Ge) were dissolved in C_6D_6 (1 mL) in a J. Young NMR tube. The J. Young NMR tube was placed into an oil bath at 100 $^\circ\text{C}$ for 1 h. The resulting mixture was analyzed by ^1H NMR spectroscopy. The ^1H NMR spectrum showed all four possible azoxyarenes: **328-MeMe** (25%), **328-BrBr** (33%), **328-MeBr**, and **328-BrMe**. For the last two species, the yields were 11% and 31%; however, due to the spectral similarity, it is difficult to determine which value corresponds to which species.

Attempted coupling of nitroarene and aniline. 327 (350 μL , 73.8 μmol , 0.211 M in C_6D_6), **323o** (235 μL , 73.8 μmol , 0.314 M in C_6D_6), **301** (23.2 mg, 73.7 μmol Ge) were mixed in a J. Young NMR tube. The J. Young NMR tube was placed into an oil bath at 100 $^\circ\text{C}$ for 30 min. The resulting mixture was analyzed by ^1H NMR spectroscopy. The ^1H

NMR spectrum showed a full conversion of **301** to **329**, untouched **323o**, **328-MeMe**, and leftover **327**.

3.4.11.3 Attempted Germylation of **323ah**

301 (17.1 mg, 54.2 μmol Ge), 4'-bromoacetophenone (**323ah**) (10.0 mg, 50.2 μmol), Pd(OAc)₂ (85 μL , 0.052 μmol , 0.607 mM in C₆D₆), and C₆D₆ (520 μL) were mixed in a J. Young NMR tube to form a colorless solution. The NMR tube was closed and placed into an oil bath at 100 °C for 3 h. The resulting mixture was analyzed by ¹H NMR spectroscopy. The ¹H NMR spectrum contained multiple unidentified ¹H NMR resonances in the aromatic region and leftover **301** and free ^tBuOH in the aliphatic region. A reaction of **301** and **323ah** without Pd(OAc)₂ added gave similar results.

3.4.11.4 Attempted Germylation of **323ai**

301 (17.1 mg, 54.3 μmol Ge), 4-bromophthalic anhydride (**323ai**) (11 mg, 48 μmol), Pd(OAc)₂ (100 μL , 0.0518 μmol , 0.518 mM in C₆D₆), C₆D₆ (200 μL), and THF (300 μL) were mixed in a J. Young NMR tube to form a light-yellow solution. The NMR tube was closed and placed into an oil bath at 100 °C for 3 h. The solution turned a bit cloudy after heating for 1 h. The resulting mixture was analyzed by ¹H NMR spectroscopy. The ¹H NMR spectrum contained two major sets of aromatic resonances at δ 7.99 (s, 1H), 8.28 (d, J = 8.3 Hz, 1H), 8.18 (d, J = 8.3 Hz, 1H), and 7.69 (d, J = 8.3 Hz, 1H), 7.54 (s, 1H), 7.33 (d, J = 8.3 Hz, 1H), respectively, and other unidentified minor resonances.

3.4.12 Germylation with *in situ* Generated Germanate

3.4.12.1 Tri-*tert*-butoxygermanate

302 (entries 1–3, 48 μmol ; entries 4 and 5, 65 μmol) and **303** or **330** (entries 1–3, 150 μmol ; entries 4 and 5, 200 μmol) were mixed with solvent (entries 1–3, 1.0 mL; entries 4 and 5, 1.2 mL) in a 10 mL culture tube. **323b** (entries 1–3, 46 μmol ; entries 4 and 5, 60 μmol), $\text{Pd}(\text{OAc})_2$ (entries 1–3, 0.045 μmol ; entries 4 and 5, 0.061 μmol), and PhCF_3 were then added. The culture tube was closed and placed into an oil bath at 100 °C for 20 h. The reaction mixture was transferred to a J. Young NMR tube and analyzed by ^1H and ^{19}F NMR spectroscopy. The conversions and yields were determined by comparing the integration of the ^{19}F NMR resonances of **323b** ($\delta -116.4$ in C_6D_6) and **324b** ($\delta -110.4$ in C_6D_6) to the PhCF_3 internal standard ($\delta -63.48$ in C_6D_6). The results were summarized in Table III-3.

3.4.12.2 Other Germanates

302 (ca. 15 mg, 65 μmol), sodium alkoxide (200 μmol) or **310** (18 mg, 70 μmol) were mixed in THF (0.6 mL) in a 10 mL culture tube. **323b** (60 μmol), $\text{Pd}(\text{OAc})_2$ (entries 1 and 2, 0.060 μmol ; entries 3–8, 0.62 μmol), and toluene (0.6 mL) were added to the reaction. The culture tube was closed and placed into an oil bath at 100 °C for 20–21 h. The reaction mixture was transferred to a J. Young NMR tube and analyzed by ^{19}F NMR spectroscopy. The results were summarized in Table III-4.

In entry 4, after heating the reaction at 100 °C for 20 h, ^{19}F NMR (THF/toluene) spectrum contained two broad peaks at $\delta -109.3$ and -110.4 . The reaction mixture was

passed through a pad of silica gel over a pipette. After removing volatiles under vacuum, the resulting white solid was analyzed by ^1H and ^{19}F NMR spectroscopy in a J. Young NMR tube. The ^{19}F NMR (C_6D_6) spectrum with better resolution contained $\text{FC}_6\text{H}_4\text{Ge}(\text{OEt})_3$ (**332**) at $\delta -108.71$ (61%), presumably $\text{FC}_6\text{H}_4\text{Ge}(\text{OEt})_2(\text{Cl}/\text{Br})$ (**333**) at $\delta -108.66$ (20%), and an unknown at $\delta -109.7$ (19%). NaOEt (**306**) (10.7 mg, 157 μmol) was added to the J. Young NMR tube. The J. Young NMR tube was placed into an oil bath at 100 $^\circ\text{C}$ for 20 h and analyzed by ^1H and ^{19}F NMR spectroscopy again. The ^{19}F NMR (C_6D_6) spectrum showed a full conversion of **333** to **332**. The isolation of **332** from the unknown was attempted by flash column chromatography on silica gel using pentane, toluene, Et_2O , and THF as eluents. However, the purification of **332** was not successful.

In entry 7, after heating the reaction at 100 $^\circ\text{C}$ for 21 h, ^{19}F NMR (THF/toluene) spectrum contained $\text{FC}_6\text{H}_4\text{Ge}(\text{O}^t\text{Bu})_3$ (**334**) at $\delta -109.3$ (69%), PhF at $\delta -114.5$ (12%), a major unknown at $\delta -110.4$ (16%), and other minor unidentified ^{19}F NMR resonances.

3.4.13 Attempted Syntheses of Pd–Ge Species

$[\text{NaGe}(\text{O}^t\text{Bu})_3]_2$ (**301**) (1–3 equiv Ge) was added to a J. Young NMR tube. A stock solution of $\text{Pd}(\text{OAc})_2$ or Pd_2dba_3 (20–100 μmol , 1 equiv Pd) in C_6D_6 was added to a J. Young NMR tube. The J. Young NMR tube was closed and analyzed by ^1H NMR spectroscopy. Significant insoluble tan or black solid formed when the tube was placed in an oil bath at 50 or 80 $^\circ\text{C}$. All ^1H NMR spectra contained unidentified mixtures.

CHAPTER IV
PALLADIUM-CATALYZED CROSS-COUPPLING REACTION USING ARYLTRI-
TERT-BUTOXYGERMANES

4.1 Introduction

The use of arylgermanes in cross-coupling chemistry has been much less extensively explored and studied than their silane and stannane counterparts. Nonetheless, the handful of existing examples shows their potential in the Pd-catalyzed cross-coupling reactions to construct new C–C bonds. This section will provide an overview and chronologically introduce the developments of Pd-catalyzed cross-coupling reactions using arylgermanes and alkenylgermanes as coupling partners.

4.1.1 Early Developments Using Germatranes (1996–Early 2000s)

The first example of the Pd-catalyzed cross-coupling reaction using arylgermanes was described by Kosugi and co-workers in 1996. The report demonstrated the reactions of 4-MeC₆H₄Br with a series of germatrane reagents supported by a N(CH₂CH₂CH₂)₃ substituent (also called “carbagermatranes”) (Figure IV-1, top). Notably, this reaction does not require a base additive, presumably due to the N→Ge dative interaction to create a pentavalent germanium center. However, the practical application of these carbagermatrane reagents is limited due to the expensive and difficult synthesis using Schwartz’s reagent.⁷³

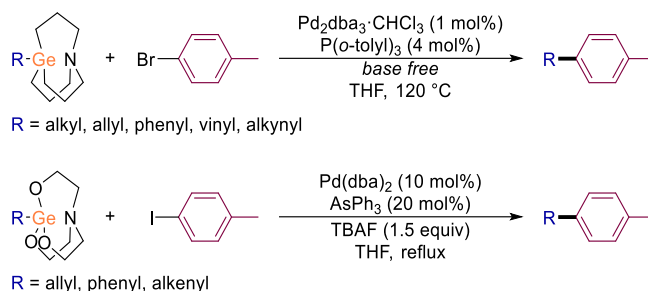


Figure IV-1. Germatranes in Pd-catalyzed cross-coupling reaction.

Compared to the trialkyl-substituted analogs, germatranes supported by $\text{N}(\text{CH}_2\text{CH}_2\text{O}^-)_3$ substituents are more easily prepared by treating aryltrihalogermanes or aryltrialkoxygermanes with triethanolamine and base. In 2002, Faller and co-workers reported the use of allyl-, phenyl-, alkenyl-, and alkynylgermatranes in the Pd-catalyzed cross-coupling reaction (Figure IV-1, bottom). In this reaction, TBAF was introduced as a base and the yields were generally lower than those reported by using Kosugi's carbagermatranes.⁷⁴

4.1.2 Discovery of Various Arylgermanes (2002–2012)

In 2002, Oshima and co-workers described the Pd-catalyzed cross-coupling reaction of aryltri(2-furyl)germanes with aryl bromides/iodides (Figure IV-2). Aryltri(2-furyl)germanes used in the reaction were readily prepared from a Pd-catalyzed germylation of aryl iodides with tri(2-furyl)germane. Upon the activation by TBAF, all furyl groups were cleaved by fluoride, and hypervalent $[\text{ArGe}(\text{OH})_3\text{F}]^-$ species was suggested to undergo transmetalation with the palladium species.⁷⁵

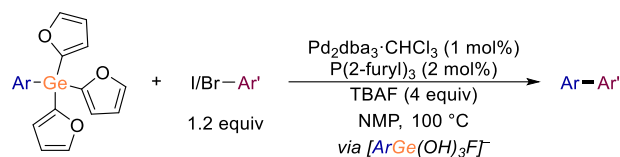


Figure IV-2. Aryltri(2-furyl)germanes in Pd-catalyzed cross-coupling reaction.

Aryltrichlorogermanes and their completely hydrolyzed products, arylgermanium sesquioxides, were reported by Kosugi, Fugami, and co-workers to be competent cross-coupling reagents upon activation by NaOH, avoiding expensive and toxic fluoride base. The active transmetalation species were assumed to be hypervalent $[\text{ArGe}(\text{OH})_{3+n}]^{n-}$ ($n = 1$ or 2) species. These methods featured simple reaction components and potential recyclability of inorganic germanium byproducts.^{76,77}

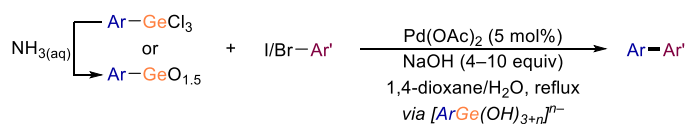


Figure IV-3. Aryltrichlorogermanes and arylgermanium sesquioxides in Pd-catalyzed cross-coupling reaction.

In 2007, Spivey and co-workers identified that arylgermanes require at least two fluoride/chloride substituents on germanium to allow efficient nucleophilic activation by fluoride base in the Pd-catalyzed cross-coupling reactions. Bis(2-naphthylmethyl)-substituted arylgermanes were demonstrated to be remarkably robust precursors and the 2-naphthylmethyl–germanium bonds can be photochemically cleaved to form Ge–F bonds with $\text{Cu}(\text{BF}_4)_2$. The generated difluoro-substituted arylgermanes can be used in the

subsequent cross-coupling reaction with aryl bromides (Figure IV-4). The synthesis of an agrochemical fungicide Boscalid was demonstrated by this method.^{78,79}

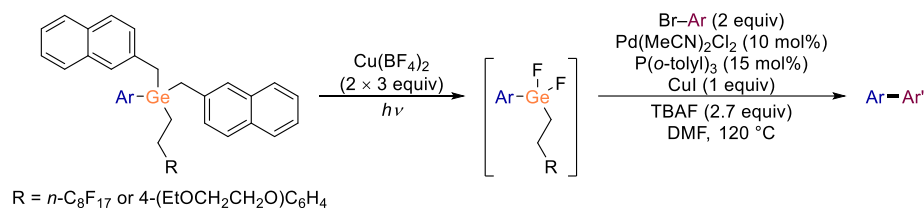


Figure IV-4. Robust bis(2-naphthylmethyl)-substituted arylgermanes in Pd-catalyzed cross-coupling reaction.

In 2004 and 2005, Wnuk and co-workers reported the preparation and catalytic application of alkenyltris(trimethylsilyl)germanes in the Pd-catalyzed cross-coupling reaction. The Ge–Si bonds were suggested to be oxidatively cleaved by peroxides under basic conditions to form Ge–OH bonds.^{196,197} In 2010, the same research group demonstrated multiple transfers of the phenyl group from Ph_{*n*}GeCl_{4-*n*} (*n* = 1–3) in the cross-coupling reaction (Figure IV-5). A head-to-head comparison between silanes, germanes, and stannanes was studied. The chlorophenylstannanes were shown to be the most reactive. Even without any chloride substituent, tetraphenylstannane can be activated by fluoride to promote the transfer of up to four phenyl groups, while in the silane and germane counterparts, one chloride on silicon or germanium center is required and sufficiently allowed the efficient transfer of up to three phenyl groups in the Pd-catalyzed cross-coupling reaction with aryl halides.^{80,81} In 2011, they further reported chemoselective transfer of phenyl or allyl group from allylphenylgermanes (Figure IV-5). Allyl groups were transferred when NaOH was used as a base in the cross-coupling

catalyzed reaction. The newly developed arylgermatranes tolerated hypervalent iodide reagents and remained inert to the Suzuki–Miyaura reaction condition when fluoride was not used, which provided opportunities for chemoselective synthesis of complex molecules.²⁴

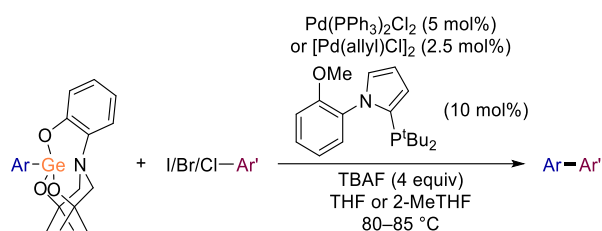


Figure IV-7. Structural-modified germatranes in Pd-catalyzed cross-coupling reaction.

In 2019, Schoenebeck and co-workers reported cross-coupling of aryltriethylgermanes with aryl iodides or iodonium reagents catalyzed by palladium nanoparticles (Figure IV-8).⁶⁶ The Ar–GeEt₃ bond was shown to be inert to homogenous Pd-catalyzed reactions, which gave it exceptional orthogonal reactivity toward many common organic reactions. Various orthogonal transformations of Ar–GeEt₃ (vs. arylboron, arylsilicon, and aryltin reagents), including halogenation and Au-catalyzed arylation, have been described as well.^{65,67–69,83}

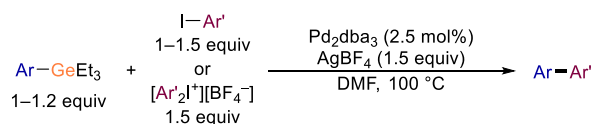


Figure IV-8. Nanoparticle Pd-catalyzed cross-coupling of aryltriethylgermanes.

4.2 Results and Discussion

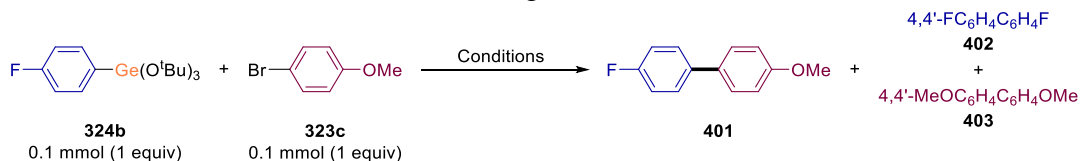
In Chapter III, we have developed an efficient catalytic synthesis of aryltri-*tert*-butoxygermanes **324** with a wide substrate scope. The *tert*-butoxy substituents seem sufficiently electronegative to allow activation at the germanium center by a base additive to form a hypervalent germanium species. Therefore, we aimed to explore the application of aryltri-*tert*-butoxygermanes in the Pd-catalyzed cross-coupling reaction.

4.2.1 Development of the Pd-Catalyzed Cross-Coupling Reaction Using Aryltri-*tert*-butoxygermanes

We first selected FC₆H₄Ge(O^tBu)₃ (**324b**) and 4-MeOC₆H₄Br (**323c**) as model substrates to screen various conditions. We initially tested the reaction using different palladium precursors and phosphine ligands. The model reaction used **324b** (0.10 mmol, 1 equiv), **323c** (0.10 mmol, 1 equiv) as coupling partners, TBAF (0.3 mmol, 3 equiv) as a base, 5 mol% Pd catalyst loading in toluene (2 mL) at 120 °C (oil bath temperature) for 20 h (Table IV-1). To our delight, when Pd(PPh₃)₂Cl₂ was used, the desired cross-coupling biaryl product **401** was observed in 68% yield, although a significant amount of homocoupling product of arylgermane **402** (15%) was detected (Table IV-1, entry 1). We then screened other phosphine ligands using Pd₂dba₃ as a palladium precursor, including monodentate phosphines (Table IV-1, entries 5–11), bidentate phosphines (Table IV-1, entries 12, 13, 18, and 19), and some Buchwald phosphine ligands (Table IV-1, entries 15–17). In all entries, the homocoupling product of aryl bromides **403** was detected in <5% yields. We determined that the combination of Pd₂dba₃ and tris(4-

most common organic solvent-soluble fluoride source, TBAF (Table IV-2). Under three different conditions, TBAF outperformed all other bases and was identified as the most advantageous base (Table IV-2, entries 1–3).

Table IV-2. Screening of bases and additives.



Condition A: Pd(PPh₃)₂Cl₂ (5 mol%), base, toluene (2 mL), 120 °C, 20 h.

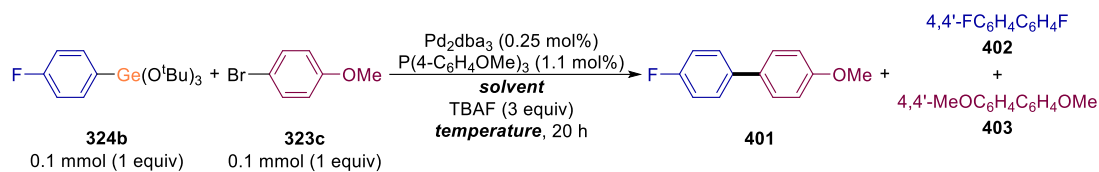
Condition B: Pd(PPh₃)₂Cl₂ (5 mol%), base, THF (2 mL), 80 °C, 20 h.

Condition C: Pd₂dba₃ (0.5 mol%), P(4-C₆H₄OMe)₃ (2.3 mol%), base/additive, toluene/THF (1/1 mL), 100 °C, 24 h.

entry	condition	base and additives (equiv)	yield ^a		
			401	402	403
1	A	ⁿ Bu ₄ NF (5)	67	14	2
2	B	ⁿ Bu ₄ NF (5)	63	15	4
3	C	ⁿ Bu ₄ NF (3)	61	7	<1
4	C	ⁿ Bu ₄ NF (3) + Et ₃ N·3HF (3)	3	<1	9
5	A	CsF (5)	2	3	1
6	B	CsF (5)	0	0	0
7	A	LiF (5)	0	0	0
8 ^b	A	AgF (5)	21	24	1
9	A	KHF ₂ (5)	0	0	0
10	C	KHF ₂ (3)	0	0	0
11	C	Et ₃ N·3HF (3)	<1	<1	<1
12	C	NaOH (3)	<1	0	<1
13	A	NaOEt (5)	<1	0	0
14	B	NaOEt (5)	1	<1	1
15	A	NaO ^t Bu (5)	<1	0	2
16	B	NaO ^t Bu (5)	1	0	3
17	C	KO ^t Bu (3)	5	<1	<1
18	C	KOSiMe ₃ (3)	1	<1	<1
19	A	Cs ₂ CO ₃ (5)	7	10	<1
20	B	Cs ₂ CO ₃ (5)	<1	3	<1
21	C	K ₃ PO ₄ (3)	<1	0	<1

^aYields were determined by GC using *n*-decane as an internal standard. ^bThe reaction was wrapped with aluminum foil to avoid light.

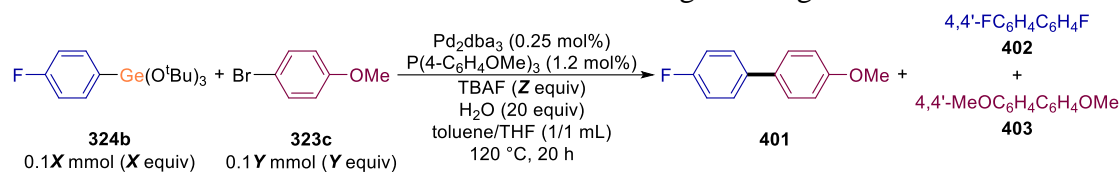
In the previous work by Wnuk and co-workers, the reactions of chlorophenylgermanes or allylphenylgermanes proceeded more favorably with the intentional addition of water (7–40 equiv with respect to Ge).^{80–82} In addition, Ge–O bonds, especially with sterically small alkoxy substituents, are prone to hydrolysis, and Kosugi, Fugami, and co-workers demonstrated that aryltrichloroorganes under hydrolysis conditions (NaOH/H₂O) and the completely hydrolyzed products, arylgermanium sesquioxides, were competent coupling partners in Pd-catalyzed cross-coupling reactions.^{76,77} Therefore, we tested the effect of water as an additive or solvent to our system (Table IV-3). First, we identified that a cosolvent of toluene and THF gave the best result because it allowed reasonable solubility to all substrates and higher reaction temperature (Table IV-3, entry 2 vs. entries 1 and 3). When a cosolvent of THF and water was used, no desired coupling products were obtained (Table IV-3, entry 4). Interestingly, when 5–20 equiv of water was added as an additive to the reaction, a noticeable increase in the yield of **401** was observed (Table IV-3, entries 5–7). However, when more than 30 equiv of water was added, the yield of **401** started to drop and the yield of **402** was increased (Table IV-3, entries 8 and 9). A similar trend in the influence of water addition has been reported in the literature.⁸⁰ These results suggested that arylgermanium sesquioxides were not important intermediates in the reaction because >20 equiv of water had a disadvantageous effect on the reaction. To further confirm this conclusion and the importance of fluoride, we performed the reaction using NaOH as a base with adding water. As expected, no desired coupling products were observed (Table IV-3, entry 10).

Table IV-3. Effect of water as an additive and solvent.

entry	solvent	temperature (°C)	H ₂ O (equiv)	yield ^a		
				401	402	403
1 ^b	toluene	120	–	54	4	<1
2 ^b	toluene/THF (50/50)	120	–	68	2	<1
3 ^b	THF	80	–	26	<1	<1
4 ^b	THF/H ₂ O	80	–	0	0	4
5	toluene/THF (50/50)	120	5	78	2	<1
6	toluene/THF (50/50)	120	10	78	1	<1
7	toluene/THF (50/50)	120	20	80	2	<1
8	toluene/THF (50/50)	120	30	74	3	1
9	toluene/THF (50/50)	120	50	55	10	3
10 ^c	toluene/THF (50/50)	120	20	1	<1	<1

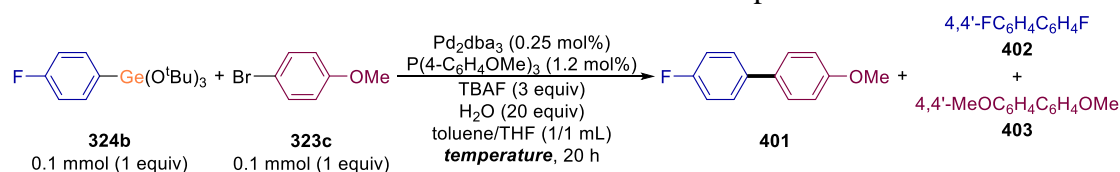
^aYields were determined by GC using *n*-decane as an internal standard. ^bPd₂dba₃ (0.5 mol%) and P(4-C₆H₄OMe)₃ (2.3 mol%) were used. ^cNaOH (3 equiv) instead of TBAF was used as a base.

We then further optimized the reaction conditions by varying the catalyst loading, base loading, reagent ratio, and reaction temperature to see how these differences would affect the reaction. The results of varying catalyst loading were summarized in Table IV-4. With 5 or 20 equiv of water, 0.25 mol% of Pd₂dba₃ and 1.1 mol% of P(4-C₆H₄OMe)₃ were sufficient to efficiently catalyze the cross-coupling reaction and gave the desired **401** in 80% yield (Table IV-4, entries 5 and 6). Further lowering the catalyst loading led to a drop in the yields but even with a catalyst loading of as low as 0.05 mol% Pd₂dba₃, **401** was still produced in 65% yield, which gave a turnover number up to 650 (Table IV-4, entry 1). The results of varying base loading and the reagent ratio were summarized in Table IV-5. Three equivalents of TBAF (with respect to Ge) were required to maintain both good reactivity and selectivity (cross-coupling vs. homocoupling) (Table IV-5, entry 3). For

Table IV-5. Effect of the base loading and reagent ratio.

entry	X	Y	Z	yield ^a		
				401	402	403
1	1.0	1.0	1.0	37	6	<1
2	1.0	1.0	2.0	74	5	1
3	1.0	1.0	3.0	80	2	<1
4	1.0	1.0	4.0	85	2	<1
5	1.0	1.0	5.0	83	2	<1
6	1.0	1.5	3.0	85	2	1
7	1.0	2.0	3.0	86	2	1
8	1.5	1.0	4.5	83	1	<1
9	2.0	1.0	6.0	83	1	<1

^aYields were determined by GC using *n*-decane as an internal standard.

Table IV-6. Effect of the reaction temperature.

entry	temperature (oil bath) (°C)	yield ^a		
		401	402	403
1	120	80	2	<1
2	100	48	<1	<1
3	80	9	<1	0
4	60	1	0	0

^aYields were determined by GC using *n*-decane as an internal standard.

4.2.2 Reaction Scope

With the optimized conditions in hand, we expanded the scope of reaction with various arylgermanes and aryl bromides. Both electron-rich and -deficient, as well as

sterically hindered and heteroaromatic arylgermanes and aryl bromides were converted to the biaryl compounds in moderate to good isolated yields (Figure IV-9).

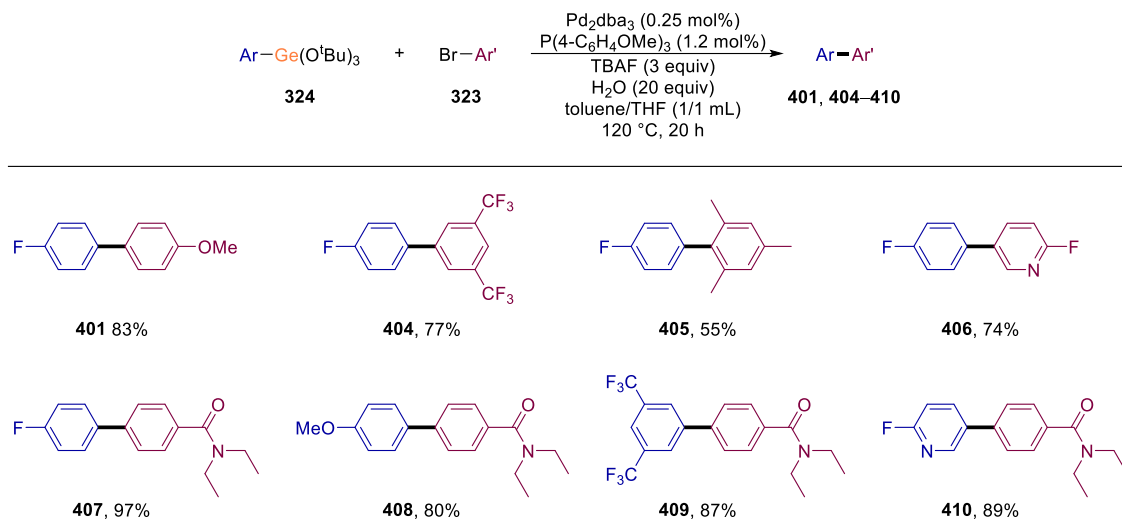


Figure IV-9. Reaction scope of Pd-catalyzed cross-coupling reaction using aryltri-*tert*-butoxygermanes.

4.2.3 Selective Reaction of *-Bpin* vs. *-Ge(O^tBu)₃*

To compare the reactivity between aryl-Ge(O^tBu)₃ and arylboronate during the transmetalation, **324h** was chosen to perform the cross-coupling reaction. Under a typical Suzuki-Miyaura reaction condition with a base of K₃PO₄, **324h** was partially converted to **411**, indicating the arylation on the boron site (Figure IV-10). **411** was characterized by ¹H NMR spectroscopy and HRMS (ESI). Further optimization will need to be done to isolate **411** in good yield but the current result has shown no formation of **412** and **413**, suggesting that cross-coupling only took place between Ar-Br and Ar-Bpin and the -Ge(O^tBu)₃ fragment still remained intact.

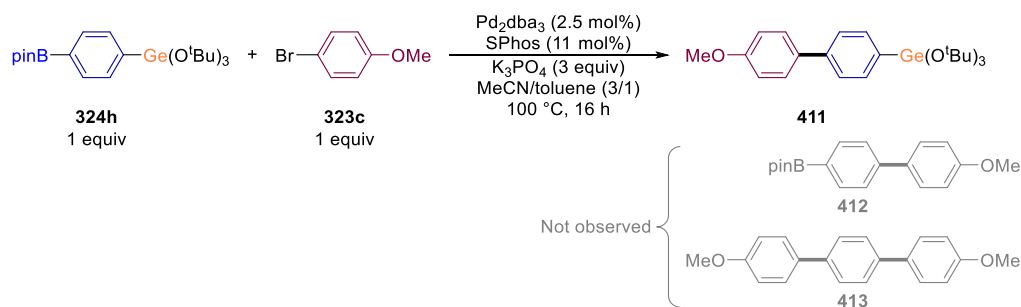


Figure IV-10. The selective reaction of –Bpin vs. –Ge(O^tBu)₃.

4.2.4 Mechanistic Discussion: Role of Fluoride and Water

We believe this reaction follows the general Pd-catalyzed cross-coupling reaction mechanism (Figure I-2, right). Fluoride activation is the key to the transmetalation process. It has been widely reported that “permanent” hypervalency at the germanium center seems to be required for the germanium species to undergo transmetalation with the palladium complex.^{24,70,73–82,169,196,197} To gain more mechanistic insight into how fluoride activates Ar–Ge(O^tBu)₃ and what the active transmetalation species is, we heated 4-FC₆H₄Ge(O^tBu)₃ (**324b**) with or without TBAF (3 equiv) at 120 °C and followed the reaction by ¹⁹F and/or ¹H NMR spectroscopy. Without TBAF, **324b** was thermally stable in a toluene solution with no indication of decomposition at 120 °C for 1 h. With TBAF, the ¹⁹F NMR spectrum showed ca. 45% of **324b** were consumed upon mixing at ambient temperature in a toluene solution to form multiple products. After heating at 120 °C for 1 h, no peaks were detected in the ¹⁹F NMR spectrum. In a C₆D₆ solution, heating **324b** with TBAF (3 equiv) at 120 °C led to a complex mixture. ¹H NMR spectrum contained minor leftover **324b**, ^tBuOH, ⁿBu₃N, 1-butene, and multiple other unidentified resonances. The formation of ⁿBu₃N and 1-butene came from the Hoffman elimination of ⁿBu₄N⁺ cation.

The formation of ^tBuOH suggested that fluoride can attack at the germanium center to form a hypervalent species but also can substitute a Ge–O^tBu bond with a Ge–F bond. The observations were in accordance with the literature⁷⁵ and we speculate the active transmetalation germanium species to be $[\text{ArGe}(\text{O}^t\text{Bu})_{3-n}\text{F}_{1+n}]^-$.

Water can play several roles in the fluoride-promoted Pd-catalyzed cross-coupling reaction.⁷⁰ It is worth mentioning the commercially available TBAF solution usually contained water in the solution. The formation of arylgermanium sesquioxide has likely been excluded from the productive catalytic cycle because performing this reaction with water/THF used as a cosolvent or in a presence of NaOH did not yield the desired cross-coupling product. In fact, the formation of arylgermanium sesquioxide might be responsible for terminating the reaction when too much water was added. Denmark and co-workers have described the importance of water in the fluoride-activated Pd-catalyzed cross-coupling reaction of alkenylsilanols with aryl nonaflates and triflates. The amount of water in the hydrated crystalline of TBAF dramatically affected the yields of the reaction. When the anhydrous tetramethylammonium fluoride was used, the yield of the desired dropped to 1%; in contrast, TBAF·6H₂O promoted the reaction effectively to give the product in 99% yield.¹⁹⁸ In addition, the Pd–OH species has been reported to highly active towards transmetalation in the Suzuki–Miyaura reaction via the coordination of Pd–OH to boronic acids.¹⁹⁹ The formation of Pd–OH species from halide/hydroxide exchange may be beneficial to the transmetalation involving the germanium species as well. Finally, water has been reported to suppress the basicity of TBAF^{200,201} and accelerate the

substitution of bulky silyl chloride to silyl fluoride.²⁰² The addition of water might also accelerate of fluorination of the Ge–O^tBu bond.

4.3 Conclusion

We have successfully developed a Pd-catalyzed cross-coupling reaction using aryltri-*tert*-butoxygermanes and aryl bromides with the activation with TBAF and water. With the currently limited scope, the catalysis tolerates electron-rich and -deficient, sterically bulky, and heteroaryl bromides and germanes. Preliminary results suggest a different reactivity between Ar–Ge(O^tBu)₃ and Ar–Bpin, which provides a potential for chemoselective functionalization.

Mechanistically, fluoride is required for efficient transmetalation. The role of fluoride is to activate the germanium center via substitution of *tert*-butoxide to form Ge–F and the formation of hypervalent germanium species. Water is not required but significantly beneficial to the reaction when 5–20 equiv were added. The role of water is unclear but it has been reported in the literature to be advantageous to fluoride-promoted cross-coupling as well as fluorination reaction.

4.4 Experimental

4.4.1 General Consideration

Unless specified otherwise, all manipulations were performed under an argon atmosphere using standard Schlenk or glovebox techniques. Toluene, pentane, THF, Et₂O, and isooctane were deoxygenated (by purging) and dried using an Innovative Technology

Pure Solv MD-5 Solvent Purification System and stored over molecular sieves in an argon-filled glove box. C_6D_6 were dried over and distilled from a NaK/benzophenone/18-crown-6 mixture and stored over molecular sieves in an argon-filled glovebox. Celite and silica were dried at 180 °C under vacuum overnight and store in an argon-filled glove box. **324b**, **324c**, **324h**, **324p**, and **324y** were synthesized according to the procedures in Chapter 3. The authentic samples of **401**²⁰³ and **402**²⁰³ for GC analysis were synthesized according to the published procedures. All other chemicals were used as received from commercial vendors.

All NMR spectra were recorded on a Varian Inova 500 NMR spectrometer (1H NMR, 499.431 MHz; $^{13}C\{^1H\}$ NMR, 125.595 MHz; ^{19}F NMR, 469.897 MHz), a Varian VnmrS 500 NMR spectrometer (1H NMR, 499.690 MHz; ^{13}C NMR, 125.660 MHz; ^{19}F NMR, 470.139 MHz), and Bruker Avance Neo 400 spectrometers (1H NMR, 400.2 MHz; ^{13}C NMR, 100.630 MHz, and 1H NMR, 400.09 MHz; ^{13}C NMR, 100.603 MHz, respectively). All spectra were recorded at ambient temperature unless otherwise noted. Chemical shifts are reported in δ (ppm). For 1H and $^{13}C\{^1H\}$ NMR spectra, the residual solvent peak was used as an internal reference (C_6D_6 at δ 7.16 for 1H NMR and δ 128.06 for ^{13}C NMR; $CDCl_3$ at δ 7.26 for 1H NMR and δ 77.16 for ^{13}C NMR). ^{19}F NMR spectra were referenced externally using neat trifluoroacetic acid at δ -78.5.

GC-FID experiments were performed on Varian 450-GC (Agilent Technologies; Santa Clara, CA). In standard split/splitless mode, 1 μ L of the sample was injected. The inlet temperature was kept at 250 °C. HP-5 was used as a gas chromatographic column with dimensions of 30 m length, 0.32 mm inner diameter, and 0.25 μ m film thickness

(Agilent Technologies; Santa Clara, CA). Helium was used as a carrier gas at a constant flow of 4.0 mL/min. The column temperature was maintained at 60 °C for 1 min, raised to 300 °C at 40 °C/min, and held for 1 min (total time: 8 min). FID detector was used at 300 °C with helium as a make-up gas at a constant flow of 25 mL/min, and H₂ and air as combustion gases at a constant flow of 30 and 300 mL/min, respectively. Galaxie Chromatography Data System software was used for data acquisition and processing.

ESI and APCI-HRMS experiments were performed using a Thermo Scientific Q Exactive Focus. The sample was injected into a 10 µL sample loop and carried using MeOH as a mobile phase at a flow rate of 300 µL/min. The ESI source spray voltage was set to 3.75 kV, and the sheath gas and auxiliary gas flow rates were set to 10 and 0 arbitrary units, respectively. The auxiliary gas temperature was set to 50 °C. For the APCI source, the discharge current was set at 5 µA, and the sheath gas and auxiliary gas flow rates were set to 30 and 0 arbitrary units, respectively. The auxiliary gas temperature was set to 250 °C. For both ESI and APCI, the transfer capillary temperature was held at 250 °C and the S-Lens RF level was set at 50 V. The mass resolution was tuned to 70000 FWHM at m/z 200. Exactive Series 2.11/Xcalibur 4.2.47 software was used for data acquisition and processing. GC-MS experiments were performed on Ultra GC/DSQ (ThermoElectron; Waltham, MA). DB-5MS was used as a gas chromatographic column with dimensions of 30 m length, 0.25 mm inner diameter, and 0.25 µm film thickness (Agilent Technologies; Santa Clara, CA). Helium was used as a carrier gas at a constant flow of 1.2 mL/min. In splitless mode, 1 µL of the sample was injected. The inlet temperature was kept at 225 °C.

The column temperature was maintained at 50 °C for 3 min and raised to 300 °C at 20 °C/min and held for 3 min. Transfer line and ion source were held at 250 °C.

4.4.2 Determination of the Density of 4-FC₆H₄Ge(O^tBu)₃ (**324b**)

An aluminum weighing dish was placed on an analytical balance in a glovebox at ambient temperature (23±2 °C, 296±2 K). **324b** was added by using a 100 µL gas-tight syringe. The mass was allowed to stabilize for at least 10 sec before each mass reading. The mass was read after each addition of **324b**. Three trials were done, and the results were summarized in Table IV-7. The density of **324b** was determined by plotting the masses against the volumes of all three trials (Figure IV-11). The linear trend line equation is $y = 1.0674x + 0.1814$. The density of **324b** was determined to be 1.07±0.01 g/mL. The errors for the density were defined as double the standard deviation of the slope provided by the LINEST function in MS Excel.

Table IV-7. Volumes and masses measurement of **324b**.

trial 1		trial 2		trial 3	
volume (µL)	mass (mg)	volume (µL)	mass (mg)	volume (µL)	mass (mg)
10.0	10.9	20.0	21.8	30.0	32.2
20.0	21.6	40.0	42.6	60.0	64.6
40.0	42.5	60.0	64.1	90.0	97.0
70.0	74.6				
100.0	106.5				

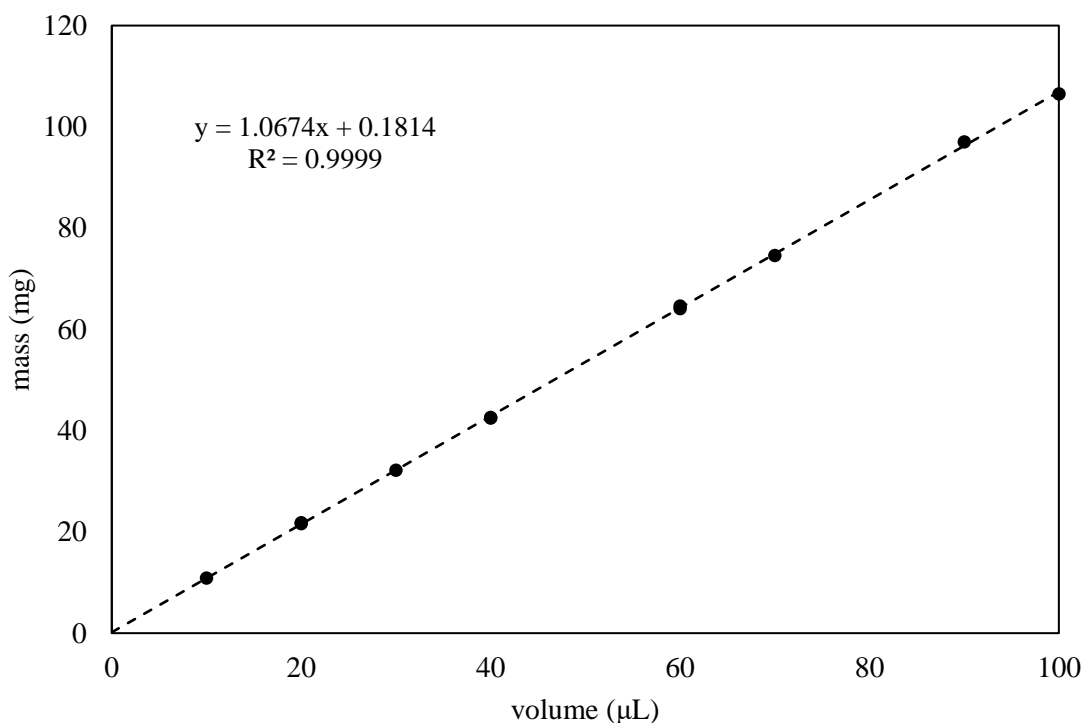


Figure IV-11. Mass (mg) vs. volume (μL) plot of **324b**.

4.4.3 Optimization of Reaction Conditions

Screening of palladium precursors and phosphine ligands. TBAF (0.30 mL, 300 μmol, 1 M in THF) was added into a 10 mL culture tube. THF was then removed under vacuum. Tri-*tert*-butoxy(4-fluorophenyl)germane (**324b**) (36.5 μL, 101 μmol), 4-bromoanisole (**323c**) (12.5 μL, 99.9 μmol), *n*-decane (20.0 μL, 103 μmol) as an internal standard, a stock solution of premixed Pd precursor and ligand were added to the culture tube. A known amount of toluene was added to normalize the total solvent volume of each experiment to 2 mL. The culture tube was closed, brought out of the glovebox, and placed into an oil bath at 120 °C for 20 h. The reaction mixture was passed through a pad of Celite over a pipette and analyzed by GC. The results were summarized in Table IV-1.

Screening of bases and additives. Condition A: **324b** (36.5 μL , 101 μmol), **323c** (12.5 μL , 99.9 μmol), $\text{Pd}(\text{PPh}_3)_2\text{Cl}_2$ (3.5 mg, 5.0 μmol), the base (0.5 mmol), and *n*-decane (20.0 μL , 103 μmol) as an internal standard, were added to a 10 mL culture tube. Toluene (2 mL) was then added. The culture tube was closed, brought out of the glovebox, and placed into an oil bath at 120 $^\circ\text{C}$ for 20 h. The reaction mixture was passed through a pad of Celite over a pipette and analyzed by GC. Condition B: **324b** (36.5 μL , 101 μmol), **323c** (12.5 μL , 99.9 μmol), $\text{Pd}(\text{PPh}_3)_2\text{Cl}_2$ (3.5 mg, 5.0 μmol), the base (0.5 mmol), and *n*-decane (20.0 μL , 103 μmol) as an internal standard, were added to a 10 mL culture tube. THF (2 mL) was then added. The culture tube was closed, brought out of the glovebox, and placed into an oil bath at 80 $^\circ\text{C}$ for 20 h. Condition C: A stock solution of **324b** (101 μmol), **323c** (102 μmol), and *n*-decane (101 μmol) as an internal standard, and a stock solution of premixed Pd_2dba_3 and tris(4-methoxyphenyl)phosphine (1.0 μmol Pd and 2.3 μmol , respectively), were added to a 10 mL culture tube. The base/additive (0.3 mmol) and toluene/THF (1/1, 2 mL) were then added. The culture tube was closed, brought out of the glovebox, and placed into an oil bath at 100 $^\circ\text{C}$ for 24 h. The reaction mixture was passed through a pad of Celite over a pipette and analyzed by GC. The results were summarized in Table IV-2.

Effect of water. **324b** (36.5 μL , 101 μmol), **323c** (12.5 μL , 99.9 μmol), *n*-decane (20.0 μL , 103 μmol) as an internal standard, a stock solution of premixed Pd_2dba_3 and tris(4-methoxyphenyl)phosphine (0.5 μmol Pd and 1.1 μmol , respectively), TBAF (0.30 mL, 300 μmol , 1 M in THF), H_2O were added to a 10 mL culture tube. A known amount of solvent was added to normalize the total solvent volume of each experiment to 2 mL.

The culture tube was closed, brought out of the glovebox, and placed into an oil bath at 120 °C for 20 h. The reaction mixture was passed through a pad of Celite over a pipette and analyzed by GC. The results were summarized in Table IV-3.

Effect of the Pd loading. **324b** (36.5 μL , 101 μmol), **323c** (12.5 μL , 99.9 μmol), *n*-decane (20.0 μL , 103 μmol) as an internal standard, a stock solution of premixed Pd_2dba_3 and tris(4-methoxyphenyl)phosphine, TBAF (0.30 mL, 300 μmol , 1 M in THF), H_2O were added to a 10 mL culture tube. A known amount of toluene/THF was added to normalize the total solvent volume of each experiment to 2 mL. The culture tube was closed, brought out of the glovebox, and placed into an oil bath at 120 °C for 20 h. The reaction mixture was passed through a pad of Celite over a pipette and analyzed by GC. The results were summarized in Table IV-4.

Effect of the base loading. **324b** (36.5 μL , 101 μmol), **323c** (12.5 μL , 99.9 μmol), *n*-decane (20.0 μL , 103 μmol) as an internal standard, a stock solution of premixed Pd_2dba_3 and tris(4-methoxyphenyl)phosphine (0.5 μmol Pd and 1.1 μmol , respectively), TBAF, H_2O (36 μL , 2.0 mmol) were added to a 10 mL culture tube. A known amount of toluene/THF was added to normalize the total solvent volume of each experiment to 2 mL. The culture tube was closed, brought out of the glovebox, and placed into an oil bath at 120 °C for 20 h. The reaction mixture was passed through a pad of Celite over a pipette and analyzed by GC. The results were summarized in Table IV-5, entries 1–5.

Effect of the reagent ratio. **324b**, **323c**, *n*-decane (20.0 μL , 103 μmol) as an internal standard, a stock solution of premixed Pd_2dba_3 and tris(4-methoxyphenyl)phosphine (0.5 μmol Pd and 1.2 μmol , respectively), TBAF (1 M in THF),

H₂O (36 μL, 2.0 mmol) were added to a 10 mL culture tube. A known amount of toluene/THF was added to normalize the total solvent volume of each experiment to 2 mL. The culture tube was closed, brought out of the glovebox, and placed into an oil bath at 120 °C for 20 h. The reaction mixture was passed through a pad of Celite over a pipette and analyzed by GC. The results were summarized in Table IV-5, entries 3, 6–9.

Effect of the reaction temperature. **324b** (36.5 μL, 101 μmol), **323c** (12.5 μL, 99.9 μmol), *n*-decane (20.0 μL, 103 μmol) as an internal standard, a stock solution of premixed Pd₂dba₃ and tris(4-methoxyphenyl)phosphine (0.5 μmol Pd and 1.1 μmol, respectively), TBAF (0.30 mL, 300 μmol, 1 M in THF), H₂O (36 μL, 2.0 mmol) were added to a 10 mL culture tube. A known amount of toluene/THF was added to normalize the total solvent volume of each experiment to 2 mL. The culture tube was closed, brought out of the glovebox, and placed into an oil bath at the indicated temperature for 20 h. The reaction mixture was passed through a pad of Celite over a pipette and analyzed by GC. The results were summarized in Table IV-6.

4.4.4 Synthesis and Characterization of Biaryl Products

General procedures. Aryltri-*tert*-butoxygermane (**324**) (0.5 mmol), aryl bromide (**323**) (0.5 mmol), a stock solution of premixed Pd₂dba₃ and tris(4-methoxyphenyl)phosphine in toluene (2.6 μmol Pd and 5.5 μmol, respectively), and toluene (5 mL in total) were added to a 50 mL culture tube. TBAF (1.5 mL, 1.5 mmol, 1 M in THF), H₂O (180 μL, 10 mmol), and THF (5 mL in total) were added to the reaction mixture. The culture tube was closed, brought out of the glovebox, and placed into an oil

bath at 120 °C for 20 h. After 20 h, the volatiles were removed under vacuum. 10 mL of CH₂Cl₂ and 10 mL of H₂O were added to the reaction. The organic phase was separated, and the aqueous phase was extracted with CH₂Cl₂ (10 mL x 2). The combined organic phase was washed with brine (20 mL) and concentrated under vacuum. The residue was purified by column chromatography on silica gel to provide the product.

Synthesis of 4-fluoro-4'-methoxybiphenyl (401). Following the general procedure, tri-*tert*-butoxy(4-fluorophenyl)germane (**324b**) (181 μL, 0.500 mmol) was reacted with 4-bromoanisole (**323c**) (64.0 μL, 0.511 mmol). The product was purified by column chromatography on silica gel using EtOAc/hexane (5/95) as eluent to provide a white solid (84 mg, 83% yield). The NMR data match the previously reported data in the literature.²⁰⁴ ¹H NMR (400 MHz, CDCl₃) δ 7.66–7.39 (m, 4H), 7.22–7.08 (m, 2H), 7.07–6.91 (m, 2H), 3.87 (s, 3H); ¹³C{¹H} NMR (101 MHz, CDCl₃) δ 162.2 (d, *J*_{F-C} = 245.5 Hz), 159.2, 137.1 (d, *J*_{F-C} = 3.2 Hz), 132.9, 128.3 (d, *J*_{F-C} = 7.9 Hz), 128.1, 115.6 (d, *J*_{F-C} = 21.4 Hz), 114.4, 55.4; ¹⁹F NMR (470 MHz, CDCl₃) δ -116.6 (tt, *J*_{F-H} = 8.6, 5.3 Hz); HRMS (APCI) *m/z* [M + H]⁺ calculated for C₁₃H₁₂FO: 203.0867, measured: 203.0865.

Synthesis of 4'-fluoro-3,5-bis(trifluoromethyl)biphenyl (404). Following the general procedure, **324b** (181 μL, 0.500 mmol) was reacted with 1-bromo-3,5-bis(trifluoromethyl)benzene (**323p**) (87.0 μL, 0.505 mmol). The product was purified by column chromatography on silica gel using hexane as eluent to provide a colorless oil which solidified over time (119 mg, 77% yield). The NMR data match the previously reported data in the literature.⁶⁸ ¹H NMR (400 MHz, CDCl₃) δ 7.98 (s, 2H), 7.87 (s, 1H), 7.65–7.53 (m, 2H), 7.25–7.16 (m, 2H); ¹³C{¹H} NMR (101 MHz, CDCl₃) δ 163.5 (d, *J*_{F-}

c = 249.3 Hz), 142.5, 134.6 (d, J_{F-C} = 3.3 Hz), 132.4 (q, J_{F-C} = 33.3 Hz), 129.2 (d, J_{F-C} = 8.4 Hz), 127.2 (q, J_{F-C} = 3.9 Hz), 123.5 (q, J_{F-C} = 272.7 Hz), 121.1 (hept, J_{F-C} = 3.9 Hz), 116.5 (d, J_{F-C} = 21.8 Hz); ^{19}F NMR (470 MHz, CDCl_3) δ -63.8 (s, 6F), -113.7 (tt, J_{F-H} = 8.4, 5.0 Hz, 1F); GC-MS (EI) m/z $[\text{M}]^+$ calculated for $\text{C}_{14}\text{H}_7\text{F}_7$: 308, measured: 308.

Synthesis of 4'-fluoro-2,4,6-trimethylbiphenyl (405). Following the general procedure, **324b** (181 μL , 0.500 mmol) was reacted with 2-bromo-1,3,5-trimethylbenzene (**323s**) (77.0 μL , 0.503 mmol). The product was purified by column chromatography on silica gel using hexane as eluent to provide a white solid (59 mg, 55% yield). ^1H NMR (400 MHz, CDCl_3) δ 7.18–7.14 (m, 2H), 7.14–7.10 (m, 2H), 6.99 (s, 2H), 2.37 (s, 3H), 2.04 (s, 6H); $^{13}\text{C}\{^1\text{H}\}$ NMR (101 MHz, CDCl_3) δ 161.8 (d, J_{F-C} = 244.8 Hz), 138.1, 137.0 (d, J_{F-C} = 3.5 Hz), 136.9, 136.3, 131.0 (d, J_{F-C} = 7.8 Hz), 128.3, 115.4 (d, J_{F-C} = 21.1 Hz), 21.1, 20.9; ^{19}F NMR (470 MHz, CDCl_3) δ -117.2 (quin, J_{F-H} = 7.1 Hz); HRMS (APCI) m/z $[\text{M} + \text{H}]^+$ calculated for $\text{C}_{15}\text{H}_{16}\text{F}$: 215.1231, measured: 215.1228.

Synthesis of 2-fluoro-5-(4-fluorophenyl)pyridine (406). Following the general procedure, **324b** (181 μL , 0.500 mmol) was reacted with 5-bromo-2-fluoropyridine (**323y**) (52.0 μL , 0.505 mmol). The product was purified by column chromatography on silica gel using EtOAc/hexane (5/95) as eluent to provide a white solid (71 mg, 74% yield). ^1H NMR (400 MHz, CDCl_3) δ 8.38 (br d, J = 2.3 Hz, 1H), 7.92 (td, J = 8.3, 2.6 Hz, 1H), 7.59–7.40 (m, 2H), 7.23–7.11 (m, 2H), 7.00 (dd, J = 8.5, 2.9 Hz, 1H); $^{13}\text{C}\{^1\text{H}\}$ NMR (101 MHz, CDCl_3) δ 163.2 (d, J_{F-C} = 239.4 Hz), 163.0 (d, J_{F-C} = 248.0 Hz), 145.8 (d, J_{F-C} = 14.8 Hz), 139.7 (d, J_{F-C} = 7.9 Hz), 134.0 (d, J_{F-C} = 4.7 Hz), 132.9 (d, J_{F-C} = 3.3 Hz), 128.9 (d, J_{F-C} = 8.2 Hz), 116.2 (d, J_{F-C} = 21.7 Hz), 109.6 (d, J_{F-C} = 37.7 Hz); ^{19}F NMR (470 MHz,

CDCl₃) δ -71.2 (br d, $J_{F-H} = 7.6$ Hz), -114.8 (tt, $J_{F-H} = 8.6, 5.3$ Hz); HRMS (APCI) m/z [M + H]⁺ calculated for C₁₁H₈F₂N: 192.0619, measured: 192.0615.

Synthesis of *N,N*-Diethyl-4'-fluoro-[1,1'-biphenyl]-4-carboxamide (407).

Following the general procedure, **324b** (181 μ L, 0.500 mmol) was reacted with *N,N*-diethyl-4-bromobenzamide (**323f**) (129 mg, 0.504 mmol). The product was purified by column chromatography on silica gel using EtOAc/hexane (30/70) as eluent to provide a white solid (131 mg, 97% yield). ¹H NMR (400 MHz, CDCl₃) δ 7.58–7.48 (m, 4H), 7.48–7.38 (m, 2H), 7.16–7.07 (m, 2H), 3.55 (br s, 2H), 3.30 (br s, 2H), 1.24 (br s, 3H), 1.14 (br s); ¹³C{¹H} NMR (101 MHz, CDCl₃) δ 171.0, 162.7 (d, $J_{F-C} = 247.0$ Hz), 141.0, 136.6 (d, $J_{F-C} = 3.2$ Hz), 136.2, 128.8 (d, $J_{F-C} = 8.1$ Hz), 127.0, 127.0, 115.8 (d, $J_{F-C} = 21.5$ Hz), 43.4 (br), 39.3 (br), 14.3 (br), 13.0 (br); ¹⁹F NMR (470 MHz, CDCl₃) δ -115.8 (tt, $J = 8.5, 5.3$ Hz); HRMS (ESI) m/z [M + H]⁺ calculated for C₁₇H₁₉FNO: 272.1445, measured: 272.1457.

Synthesis of *N,N*-Diethyl-4'-methoxy-[1,1'-biphenyl]-4-carboxamide (408).

Following the general procedure, tri-*tert*-butoxy(4-methoxyphenyl)germane (**324c**) (203 mg, 0.509 mmol) was reacted with **323f** (135 mg, 0.527 mmol). The product was purified by column chromatography on silica gel using EtOAc/CH₂Cl₂ (3/97) as eluent to provide a white solid (116 mg, 80% yield). The NMR data match the previously reported data in the literature.²⁰⁵ ¹H NMR (400 MHz, CDCl₃) δ 7.57–7.53 (m, 2H), 7.53–7.48 (m, 2H), 7.44–7.37 (m, 2H), 7.00–6.92 (m, 2H), 3.81 (s, 3H), 3.53 (br s, 2H), 3.30 (br s, 2H), 1.22 (br s, 3H), 1.14 (br s); ¹³C{¹H} NMR (101 MHz, CDCl₃) δ 171.2, 159.4, 141.6, 135.4,

132.8, 128.1, 126.9, 126.5, 114.3, 55.3, 43.3 (br), 39.3 (br), 14.2 (br), 12.9 (br); HRMS (ESI) m/z $[M + H]^+$ calculated for $C_{18}H_{22}NO_2$: 284.1645, measured: 284.1657.

Synthesis of *N,N*-Diethyl-3',5'-bis(trifluoromethyl)-[1,1'-biphenyl]-4-carboxamide (409). Following the general procedure, (3,5-Bis(trifluoromethyl)phenyl)tri-*tert*-butoxygermane (**324p**) (256 mg, 0.507 mmol) was reacted with **323f** (130 mg, 0.508 mmol). The product was purified by column chromatography on silica gel using EtOAc/CH₂Cl₂ (2/98) as eluent to provide a white solid (172 mg, 87% yield). ¹H NMR (499 MHz, CDCl₃) δ 8.01 (s, 2H), 7.86 (s, 1H), 7.69–7.59 (m, 2H), 7.57–7.45 (m, 2H), 3.57 (br s, 2H), 3.29 (br s, 2H), 1.26 (br s, 3H), 1.14 (br s); ¹³C{¹H} NMR (126 MHz, CDCl₃) δ 170.6, 142.6, 139.0, 137.9, 132.3 (q, J_{F-C} = 33.3 Hz), 127.4, 127.3 (m), 127.3 (m), 123.4 (q, J_{F-C} = 272.8 Hz), 121.4 (hept, J_{F-C} = 3.9 Hz), 43.4 (br), 39.5 (br), 14.3 (br), 13.0 (br); ¹⁹F NMR (470 MHz, CDCl₃) δ –63.7 (s); HRMS (ESI) m/z $[M + H]^+$ calculated for $C_{19}H_{18}F_6NO$: 390.1287, measured: 390.1302.

***N,N*-Diethyl-4-(6-fluoropyridin-3-yl)benzamide (410).** Following the general procedure, 2-fluoro-5-(tri-*tert*-butoxygermyl)pyridine (**324y**) (198 mg, 0.510 mmol) was reacted with **323f** (134 mg, 0.523 mmol). The product was purified by column chromatography on silica gel using EtOAc/CH₂Cl₂ (8/92) as eluent to provide a white solid (124 mg, 89% yield). ¹H NMR (400 MHz, CDCl₃) δ 8.41 (dt, J = 2.7, 0.9 Hz, 1H), 7.96 (ddd, J = 8.4, 7.6, 2.6 Hz, 1H), 7.60–7.51 (m, 2H), 7.51–7.42 (m, 2H), 7.00 (ddd, J = 8.5, 3.0, 0.5 Hz, 1H), 3.55 (br s, 2H), 3.29 (br s, 2H), 1.24 (br s, 3H), 1.14 (br s); ¹³C{¹H} NMR (100 MHz, CDCl₃) δ 170.7, 163.4 (d, J_{F-C} = 239.9 Hz), 146.0 (d, J_{F-C} = 14.9 Hz), 139.8 (d, J_{F-C} = 8.0 Hz), 137.5, 137.2, 134.2 (d, J_{F-C} = 4.7 Hz), 127.3, 127.2, 109.7 (d, J_{F-C}

$c = 37.6$ Hz), 43.4 (br), 39.4 (br), 14.4 (br), 13.0 (br); ^{19}F NMR (470 MHz, CDCl_3) δ – 70.6 (d, $J_{\text{F-H}} = 6.0$ Hz); HRMS (ESI) m/z $[\text{M} + \text{H}]^+$ calculated for $\text{C}_{16}\text{H}_{18}\text{FN}_2\text{O}$: 273.1398, measured: 273.1409.

4.4.5 Selective Reaction of *-Bpin* vs. *-Ge(O^tBu)₃*

Tri-*tert*-butoxy(4-(4,4,5,5-tetramethyl-1,3,2-dioxaborolan-2-yl)phenyl)germane (**324h**) (48.4 mg, 97.8 μmol), 4-bromoanisole (**323c**) (12.5 μL , 99.9 μmol), a stock solution of premixed Pd_2dba_3 (445 μL , 2.4 μmol , 4.9 2.4 μmol Pd, 5.5 mM in MeCN/toluene) and SPhos (445 μL , 11 μmol , 25 mM in MeCN/toluene), K_3PO_4 (62.6 mg, 293 μmol), and MeCN (555 μL) were mixed in a 10 mL culture tube. The tube was closed and placed into an oil bath at 100 °C for 16 h. The mixture was pass through a pad of Celite over a frit. Volatiles were removed under vacuum. The residue (56 mg) was analyzed by ^1H NMR spectroscopy and HRMS. The ^1H NMR (C_6D_6) spectrum contained unreacted **324h**, tri-*tert*-butoxy(4'-methoxy-[1,1'-biphenyl]-4-yl)germane (**411**), and other unidentified ^1H NMR resonances but did not contained 2-(4'-Methoxy-[1,1'-biphenyl]-4-yl)-4,4,5,5-tetramethyl-1,3,2-dioxaborolane (**412**) and 4,4''-dimethoxy-1,1':4',1'''-terphenyl (**413**). Characterization of **411**: ^1H NMR (499 MHz, C_6D_6) δ 8.00 (d, $J = 7.8$ Hz, 2H), 7.51 (d, $J = 7.8$ Hz, 2H), 7.39 (d, $J = 8.4$ Hz, 2H), 6.81 (d, $J = 8.4$ Hz, 2H), 3.33 (s, 3H), 1.52 (s, 27H); HRMS (ESI) m/z $[\text{M} + \text{Na}]^+$ calculated for $\text{C}_{25}\text{H}_{38}^{74}\text{GeO}_4\text{Na}$: 499.1874, measured: 499.1869.

4.4.6 Effect of Fluoride Experiments

Tri-*tert*-butoxy(4-fluorophenyl)germane (**324b**) (18 μL , 50 μmol) and a stock solution of PhCF_3 (25 μL , 9.9 μmol , 0.396 M in C_6D_6) were mixed in toluene (1 mL) in a J. Young NMR tube. The J. Young NMR tube was closed. The colorless solution was analyzed by ^{19}F NMR spectroscopy immediately and again after placing it into an oil bath at 120 $^\circ\text{C}$ for 1 h. Both ^{19}F NMR spectra were the same, indicating no changes were made.

TBAF (0.15 mL, 150 μmol , 1 M in THF) was added to a J. Young NMR tube. The volatiles were removed under vacuum. **324b** (18 μL , 50 μmol), a stock solution of PhCF_3 (25 μL , 9.9 μmol , 0.396 M in C_6D_6), and toluene (1 mL) were added. The J. Young NMR tube was closed. The colorless solution was analyzed by ^{19}F NMR spectroscopy immediately and again after placing it into an oil bath at 120 $^\circ\text{C}$ for 1 h. Before heating, the ^{19}F NMR spectrum contained PhCF_3 , **324b** (55%), and several other unidentified ^{19}F NMR resonances at δ -109.6, -113.1, -113.4, and -148.8. After heating at 120 $^\circ\text{C}$ for 1 h, the ^{19}F NMR spectrum contained only PhCF_3 .

To a J. Young NMR tube were added TBAF (0.10 mL, 100 μmol , 1 M in THF), **324b** (12 μL , 33 μmol), and C_6D_6 (0.4 mL). The J. Young NMR tube was closed. The colorless solution was analyzed by ^1H and ^{19}F NMR spectroscopy immediately and again after placing it into an oil bath at 120 $^\circ\text{C}$ for 30 min. Before heating, the ^1H NMR spectrum contained **324b**, THF, $^n\text{Bu}_4\text{N}^+$, minor Bu_3N , and several other unidentified ^1H NMR resonances; the ^{19}F NMR spectrum contained mostly **324b** (55%) and two other unidentified ^{19}F NMR resonances at δ -111.9, -112.6. After heating at 120 $^\circ\text{C}$ for 30 min, the ^1H NMR spectrum contained THF, $^n\text{Bu}_3\text{N}$, $^t\text{BuOH}$, 1-butene, and several other

unidentified ^1H NMR resonances; the ^{19}F NMR spectrum contained multiple unidentified ^{19}F NMR resonances.

CHAPTER V

CONCLUSIONS

Further development of the previously demonstrated aromatic C–H borylation catalyzed by (pincer)Ir complexes has been accomplished. A series of PXL type pincer ligand and their complexes of iridium and rhodium were synthesized and characterized. The catalytic reactivity of these complexes was tested in the aromatic C–H borylation reaction using HBpin as the boron source and 1-hexene as the H₂ acceptor. It has been shown that iridium complexes of PNP, PNSb, PSiP, and PBP pincer ligands, as well as rhodium complexes, were incompetent in the aromatic C–H borylation. Only iridium complexes of pincer ligands with a central aryl site showed meaningful activity in C–H borylation. **203-HCl** (POCOP type) and **229-HCl** (PCP type) demonstrated the best reactivity and chemoselectivity (vs. competing olefin hydroboration) over other pincer complexes. **229-HCl** showed a modest improvement, compared to the previously reported **203-HCl**, and was chosen to further optimize the reaction condition. The newly optimized conditions were in general accordance with the previously reported ones. The regioselectivity of the C–H borylation was tested using PhF and PhCF₃ as model substrates, and the results basically followed the state-of-the-art aromatic C–H borylation system catalyzed by iridium complexes bearing neutral bidentate ligands.

A robust and efficient Pd-catalyzed germylation of aryl/alkenyl bromides using sodium tri-*tert*-butoxygermanate [NaGe(O^tBu)₃]₂ (**301**) was reported. **301** can be used in the germylation reaction as a pure isolated form or generated in situ from GeCl₂·C₄H₈O₂

(**302**) and NaO^tBu (**303**), which allows practical utilization in a regular organic synthesis laboratory. This catalytic reaction featured a simple reaction set-up with no auxiliary ligand, readily prepared germanium reagent, and easy isolation. Aryl bromides were converted to arylgermanes in almost quantitative yield with NaBr as a sole byproduct. The resulting ArGe(O^tBu)₃ (**324**) are poised for subsequent cross-coupling reactions.

A Pd-catalyzed cross-coupling reaction to construct new C–C bonds using ArGe(O^tBu)₃ (**324**) was then developed. A thorough screening of reaction conditions allowed the identification of the optimized conditions, which consist of using TBAF as a base and water as an additive. The reaction scope demonstrated a reasonable tolerance to electron-donating and -withdrawing, and sterically bulky substituents. A preliminary study on chemoselective cross-coupling using 4-pinBC₆H₄Ge(O^tBu)₃ (**324h**) showed a reactivity difference between –Bpin and –Ge(O^tBu)₃. Further investigation is required to gain deeper insight. Fluoride has been identified to be an important reagent which cleaves the Ge–O^tBu bond to generate the hypervalent germanium species [ArGe(O^tBu)_{3–n}F_{1–n}][–] for transmetalation.

REFERENCES

- (1) *Handbook of Organopalladium Chemistry for Organic Synthesis*; Negishi, E., de Meijere, A., Eds.; John Wiley & Sons, Inc.: New York, NY, USA, 2002; Vol. 1–2.
- (2) Cross Coupling Reactions: A Practical Guide. *Top. Curr. Chem.* **2002**, *219*, 1–248.
- (3) *Metal-Catalyzed Cross-Coupling Reactions*, 2nd ed.; de Meijere, A., Diederich, F., Eds.; Wiley-VCH: Weinheim, Germany, 2004.
- (4) Tsuji, J. *Palladium Reagents and Catalysts: New Perspectives for the 21st Century*, 2nd ed.; John Wiley & Sons Ltd.: Chichester, UK, 2004.
- (5) Johansson Seechurn, C. C. C.; Kitching, M. O.; Colacot, T. J.; Snieckus, V. Palladium-Catalyzed Cross-Coupling: A Historical Contextual Perspective to the 2010 Nobel Prize. *Angew. Chem., Int. Ed.* **2012**, *51*, 5062–5085.
- (6) Campeau, L.-C.; Hazari, N. Cross-Coupling and Related Reactions: Connecting Past Success to the Development of New Reactions for the Future. *Organometallics* **2019**, *38*, 3–35.
- (7) Suzuki, A. Cross-Coupling Reactions of Organoboranes: An Easy Way to Construct C–C Bonds (Nobel Lecture). *Angew. Chem., Int. Ed.* **2011**, *50*, 6722–6737.
- (8) Negishi, E. Magical Power of Transition Metals: Past, Present, and Future (Nobel Lecture). *Angew. Chem., Int. Ed.* **2011**, *50*, 6738–6764.
- (9) Ishiyama, T.; Miyaura, N. Chemistry of Group 13 Element-Transition Metal Linkage — the Platinum- and Palladium-Catalyzed Reactions of (Alkoxo)diborons. *J. Organomet. Chem.* **2000**, *611*, 392–402.

- (10) Ruiz-Castillo, P.; Buchwald, S. L. Applications of Palladium-Catalyzed C–N Cross-Coupling Reactions. *Chem. Rev.* **2016**, *116*, 12564–12649.
- (11) Miyaura, N.; Suzuki, A. Palladium-Catalyzed Cross-Coupling Reactions of Organoboron Compounds. *Chem. Rev.* **1995**, *95*, 2457–2483.
- (12) Suzuki, A. Recent Advances in the Cross-Coupling Reactions of Organoboron Derivatives with Organic Electrophiles, 1995–1998. *J. Organomet. Chem.* **1999**, *576*, 147–168.
- (13) Frohn, H.-J.; Adonin, N. Y.; Bardin, V. V.; Starichenko, V. F. Polyfluoroorganoboron-Oxygen Compounds. 2 Base-Catalysed Hydrodeboration of Polyfluorophenyl(dihydroxy)boranes. *Z. Anorg. Allg. Chem.* **2002**, *628*, 2834–2838.
- (14) Lozada, J.; Liu, Z.; Perrin, D. M. Base-Promoted Protodeboronation of 2,6-Disubstituted Arylboronic Acids. *J. Org. Chem.* **2014**, *79*, 5365–5368.
- (15) Cox, P. A.; Leach, A. G.; Campbell, A. D.; Lloyd-Jones, G. C. Protodeboronation of Heteroaromatic, Vinyl, and Cyclopropyl Boronic Acids: pH–Rate Profiles, Autocatalysis, and Disproportionation. *J. Am. Chem. Soc.* **2016**, *138*, 9145–9157.
- (16) Cox, P. A.; Reid, M.; Leach, A. G.; Campbell, A. D.; King, E. J.; Lloyd-Jones, G. C. Base-Catalyzed Aryl-B(OH)₂ Protodeboronation Revisited: From Concerted Proton Transfer to Liberation of a Transient Aryl Anion. *J. Am. Chem. Soc.* **2017**, *139*, 13156–13165.
- (17) Denmark, S. E.; Ober, M. H. Organosilicon Reagents: Synthesis and Application to Palladium-Catalyzed Cross-Coupling Reactions. *Aldrichimica Acta* **2003**, *36*, 75–85.
- (18) Sore, H. F.; Galloway, W. R. J. D.; Spring, D. R. Palladium-Catalysed Cross-Coupling of Organosilicon Reagents. *Chem. Soc. Rev.* **2012**, *41*, 1845–1866.
- (19) Cordovilla, C.; Bartolomé, C.; Martínez-Ilarduya, J. M.; Espinet, P. The Stille Reaction, 38 Years Later. *ACS Catal.* **2015**, *5*, 3040–3053.

- (20) Yamamoto, Y.; Seko, T.; Nemoto, H. New Method for the Synthesis of Boron-10 Containing Nucleoside Derivatives for Neutron-Capture Therapy via Palladium-Catalyzed Reaction. *J. Org. Chem.* **1989**, *54*, 4734–4736.
- (21) Linshoeft, J.; Heinrich, A. C. J.; Segler, S. A. W.; Gates, P. J.; Staubitz, A. Chemoselective Cross-Coupling Reactions with Differentiation between Two Nucleophilic Sites on a Single Aromatic Substrate. *Org. Lett.* **2012**, *14*, 5644–5647.
- (22) Heinrich, A. C. J.; Thiedemann, B.; Gates, P. J.; Staubitz, A. Dual Selectivity: Electrophile and Nucleophile Selective Cross-Coupling Reactions on a Single Aromatic Substrate. *Org. Lett.* **2013**, *15*, 4666–4669.
- (23) Qiu, D.; Wang, S.; Tang, S.; Meng, H.; Jin, L.; Mo, F.; Zhang, Y.; Wang, J. Synthesis of Trimethylstannyl Arylboronate Compounds by Sandmeyer-Type Transformations and Their Applications in Chemoselective Cross-Coupling Reactions. *J. Org. Chem.* **2014**, *79*, 1979–1988.
- (24) Song, H.-J.; Jiang, W.-T.; Zhou, Q.-L.; Xu, M.-Y.; Xiao, B. Structure-Modified Germatranes for Pd-Catalyzed Biaryl Synthesis. *ACS Catal.* **2018**, *8*, 9287–9291.
- (25) Kim, J.; Lee, E.; Cho, S. H. Chemoselective Palladium-Catalyzed Suzuki-Miyaura Cross-Coupling of (Diborylmethyl)silanes with Alkenyl Bromides. *Asian J. Org. Chem.* **2019**, *8*, 1664–1667.
- (26) Ashikari, Y.; Kawaguchi, T.; Mandai, K.; Aizawa, Y.; Nagaki, A. A Synthetic Approach to Dimetalated Arenes Using Flow Microreactors and the Switchable Application to Chemoselective Cross-Coupling Reactions. *J. Am. Chem. Soc.* **2020**, *142*, 17039–17047.
- (27) Brewster, J. H.; Negishi, E.-I. Brown: Passes Through the Mountains. *Science* **1980**, *207*, 44–46.
- (28) Pelter, A.; Smith, K.; Brown, H. C. *Borane Reagents*; Academic Press: New York, NY, USA, 1988.

- (29) Qiao, J. X.; Lam, P. Y. S. Copper-Promoted Carbon–Heteroatom Bond Cross-Coupling with Boronic Acids and Derivatives. *Synthesis* **2011**, *2011*, 829–856.
- (30) *Boronic Acids: Preparation and Applications in Organic Synthesis, Medicine and Materials*, 2nd ed.; Hall, D. G., Ed.; Wiley-VCH: Weinheim, Germany, 2011.
- (31) Ishiyama, T.; Murata, M.; Miyaura, N. Palladium(0)-Catalyzed Cross-Coupling Reaction of Alkoxydiboron with Haloarenes: A Direct Procedure for Arylboronic Esters. *J. Org. Chem.* **1995**, *60*, 7508–7510.
- (32) Morgan, A. B.; Jurs, J. L.; Tour, J. M. Synthesis, Flame-Retardancy Testing, and Preliminary Mechanism Studies of Nonhalogenated Aromatic Boronic Acids: A New Class of Condensed-Phase Polymer Flame-Retardant Additives for Acrylonitrile–Butadiene–Styrene and Polycarbonate. *J. Appl. Polym. Sci.* **2000**, *76*, 1257–1268.
- (33) Zhu, W.; Ma, D. Formation of Arylboronates by a CuI-Catalyzed Coupling Reaction of Pinacolborane with Aryl Iodides at Room Temperature. *Org. Lett.* **2006**, *8*, 261–263.
- (34) Hemming, D.; Fritzeimer, R.; Westcott, S. A.; Santos, W. L.; Steel, P. G. Copper-Boryl Mediated Organic Synthesis. *Chem. Soc. Rev.* **2018**, *47*, 7477–7494.
- (35) Bedford, R. B.; Brenner, P. B.; Carter, E.; Gallagher, T.; Murphy, D. M.; Pye, D. R. Iron-Catalyzed Borylation of Alkyl, Allyl, and Aryl Halides: Isolation of an Iron(I) Boryl Complex. *Organometallics* **2014**, *33*, 5940–5943.
- (36) Yoshida, T.; Iliés, L.; Nakamura, E. Iron-Catalyzed Borylation of Aryl Chlorides in the Presence of Potassium *t*-Butoxide. *ACS Catal.* **2017**, *7*, 3199–3203.
- (37) Bose, S. K.; Deißberger, A.; Eichhorn, A.; Steel, P. G.; Lin, Z.; Marder, T. B. Zinc-Catalyzed Dual C–X and C–H Borylation of Aryl Halides. *Angew. Chem., Int. Ed.* **2015**, *54*, 11843–11847.
- (38) Chow, W. K.; Yuen, O. Y.; Choy, P. Y.; So, C. M.; Lau, C. P.; Wong, W. T.; Kwong, F. Y. A Decade Advancement of Transition Metal-Catalyzed Borylation of Aryl Halides and Sulfonates. *RSC Adv.* **2013**, *3*, 12518–12539.

- (39) Kubota, K.; Iwamoto, H.; Ito, H. Formal Nucleophilic Borylation and Borylative Cyclization of Organic Halides. *Org. Biomol. Chem.* **2017**, *15*, 285–300.
- (40) Zhang, J.; Wu, H.-H.; Zhang, J. Cesium Carbonate Mediated Borylation of Aryl Iodides with Diboron in Methanol. *Eur. J. Org. Chem.* **2013**, *2013*, 6263–6266.
- (41) Liu, Q.; Hong, J.; Sun, B.; Bai, G.; Li, F.; Liu, G.; Yang, Y.; Mo, F. Transition-Metal-Free Borylation of Alkyl Iodides via a Radical Mechanism. *Org. Lett.* **2019**, *21*, 6597–6602.
- (42) Jiang, M.; Yang, H.; Fu, H. Visible-Light Photoredox Borylation of Aryl Halides and Subsequent Aerobic Oxidative Hydroxylation. *Org. Lett.* **2016**, *18*, 5248–5251.
- (43) Mfuh, A. M.; Doyle, J. D.; Chhetri, B.; Arman, H. D.; Larionov, O. V. Scalable, Metal- and Additive-Free, Photoinduced Borylation of Haloarenes and Quaternary Arylammonium Salts. *J. Am. Chem. Soc.* **2016**, *138*, 2985–2988.
- (44) Tian, Y.-M.; Guo, X.-N.; Braunschweig, H.; Radius, U.; Marder, T. B. Photoinduced Borylation for the Synthesis of Organoboron Compounds. *Chem. Rev.* **2021**, *121*, 3561–3597.
- (45) Nguyen, P.; Blom, H. P.; Westcott, S. A.; Taylor, N. J.; Marder, T. B. Synthesis and Structures of the First Transition-Metal Tris(boryl) Complexes: Iridium Complexes (η^6 -Arene)Ir(BO₂C₆H₄)₃. *J. Am. Chem. Soc.* **1993**, *115*, 9329–9330.
- (46) Mkhaliid, I. A. I.; Barnard, J. H.; Marder, T. B.; Murphy, J. M.; Hartwig, J. F. C–H Activation for the Construction of C–B Bonds. *Chem. Rev.* **2010**, *110*, 890–931.
- (47) Hartwig, J. F. Borylation and Silylation of C–H Bonds: A Platform for Diverse C–H Bond Functionalizations. *Acc. Chem. Res.* **2012**, *45*, 864–873.
- (48) Xu, L.; Wang, G.; Zhang, S.; Wang, H.; Wang, L.; Liu, L.; Jiao, J.; Li, P. Recent Advances in Catalytic C–H Borylation Reactions. *Tetrahedron* **2017**, *73*, 7123–7157.

- (49) Chen, H.; Hartwig, J. F. Catalytic, Regiospecific End-Functionalization of Alkanes: Rhenium-Catalyzed Borylation under Photochemical Conditions. *Angew. Chem., Int. Ed.* **1999**, *38*, 3391–3393.
- (50) Murphy, J. M.; Lawrence, J. D.; Kawamura, K.; Incarvito, C.; Hartwig, J. F. Ruthenium-Catalyzed Regiospecific Borylation of Methyl C–H Bonds. *J. Am. Chem. Soc.* **2006**, *128*, 13684–13685.
- (51) Mazzacano, T. J.; Mankad, N. P. Base Metal Catalysts for Photochemical C–H Borylation That Utilize Metal–Metal Cooperativity. *J. Am. Chem. Soc.* **2013**, *135*, 17258–17261.
- (52) Obligacion, J. V.; Semproni, S. P.; Chirik, P. J. Cobalt-Catalyzed C–H Borylation. *J. Am. Chem. Soc.* **2014**, *136*, 4133–4136.
- (53) Furukawa, T.; Tobisu, M.; Chatani, N. C–H Functionalization at Sterically Congested Positions by the Platinum-Catalyzed Borylation of Arenes. *J. Am. Chem. Soc.* **2015**, *137*, 12211–12214.
- (54) Dombay, T.; Werncke, C. G.; Jiang, S.; Grellier, M.; Vendier, L.; Bontemps, S.; Sortais, J.-B.; Sabo-Etienne, S.; Darcel, C. Iron-Catalyzed C–H Borylation of Arenes. *J. Am. Chem. Soc.* **2015**, *137*, 4062–4065.
- (55) Esteruelas, M. A.; Oliván, M.; Vélez, A. POP–Rhodium-Promoted C–H and B–H Bond Activation and C–B Bond Formation. *Organometallics* **2015**, *34*, 1911–1924.
- (56) Zhang, H.; Hagihara, S.; Itami, K. Aromatic C–H Borylation by Nickel Catalysis. *Chem. Lett.* **2015**, *44*, 779–781.
- (57) Furukawa, T.; Tobisu, M.; Chatani, N. Nickel-Catalyzed Borylation of Arenes and Indoles via C–H Bond Cleavage. *Chem. Commun.* **2015**, *51*, 6508–6511.
- (58) Legare, M.-A.; Courtemanche, M.-A.; Rochette, E.; Fontaine, F.-G. Metal-Free Catalytic C–H Bond Activation and Borylation of Heteroarenes. *Science* **2015**, *349*, 513–516.

- (59) Ishiyama, T.; Takagi, J.; Miyaura, N.; Anastasi, N. R.; Hartwig, J. F. Mild Iridium-Catalyzed Borylation of Arenes. High Turnover Numbers, Room Temperature Reactions, and Isolation of a Potential Intermediate. *J. Am. Chem. Soc.* **2002**, *124*, 390–391.
- (60) Cho, J.-Y.; Tse, M. K.; Holmes, D.; Maleczka, Jr., R. E.; Smith, III, M. R. Remarkably Selective Iridium Catalysts for the Elaboration of Aromatic C–H Bonds. *Science* **2002**, *295*, 305–308.
- (61) Preshlock, S. M.; Ghaffari, B.; Maligres, P. E.; Krska, S. W.; Maleczka, Jr., R. E.; Smith, III, M. R. High-Throughput Optimization of Ir-Catalyzed C–H Borylation: A Tutorial for Practical Applications. *J. Am. Chem. Soc.* **2013**, *135*, 7572–7582.
- (62) Hartwig, J. F. Regioselectivity of the Borylation of Alkanes and Arenes. *Chem. Soc. Rev.* **2011**, *40*, 1992–2002.
- (63) Press, L. P.; Kosanovich, A. J.; McCulloch, B. J.; Ozerov, O. V. High-Turnover Aromatic C–H Borylation Catalyzed by POCOP-Type Pincer Complexes of Iridium. *J. Am. Chem. Soc.* **2016**, *138*, 9487–9497.
- (64) Boller, T. M.; Murphy, J. M.; Hapke, M.; Ishiyama, T.; Miyaura, N.; Hartwig, J. F. Mechanism of the Mild Functionalization of Arenes by Diboron Reagents Catalyzed by Iridium Complexes. Intermediacy and Chemistry of Bipyridine-Ligated Iridium Trisboryl Complexes. *J. Am. Chem. Soc.* **2005**, *127*, 14263–14278.
- (65) Fricke, C.; Dahiya, A.; Reid, W. B.; Schoenebeck, F. Gold-Catalyzed C–H Functionalization with Aryl Germanes. *ACS Catal.* **2019**, *9*, 9231–9236.
- (66) Fricke, C.; Sherborne, G. J.; Funes-Ardoiz, I.; Senol, E.; Guven, S.; Schoenebeck, F. Orthogonal Nanoparticle Catalysis with Organogermanes. *Angew. Chem., Int. Ed.* **2019**, *58*, 17788–17795.
- (67) Fricke, C.; Deckers, K.; Schoenebeck, F. Orthogonal Stability and Reactivity of Aryl Germanes Enables Rapid and Selective (Multi)Halogenations. *Angew. Chem., Int. Ed.* **2020**, *59*, 18717–18722.

- (68) Sherborne, G. J.; Gevondian, A. G.; Funes-Ardoiz, I.; Dahiya, A.; Fricke, C.; Schoenebeck, F. Modular and Selective Arylation of Aryl Germanes (C–GeEt₃) over C–Bpin, C–SiR₃ and Halogens Enabled by Light-Activated Gold Catalysis. *Angew. Chem., Int. Ed.* **2020**, *59*, 15543–15548.
- (69) Dahiya, A.; Fricke, C.; Schoenebeck, F. Gold-Catalyzed Chemoselective Couplings of Polyfluoroarenes with Aryl Germanes and Downstream Diversification. *J. Am. Chem. Soc.* **2020**, *142*, 7754–7759.
- (70) Spivey, A. C.; Gripton, C. J. G.; Hannah, J. P. Recent Advances in Group 14 Cross-Coupling: Si and Ge-Based Alternatives to the Stille Reaction. *Curr. Org. Synth.* **2004**, *1*, 211–226.
- (71) Spivey, A. C.; Diaper, C. M. Aryl- and Heteroarylgermanes. *Sci. Synth.* **2003**, *5*, 149–157.
- (72) Spivey, A. C.; Tseng, C.-C. Aryl- and Heteroarylgermanes (Update 2010). *Sci. Synth.* **2010**, *1*, 41–47.
- (73) Kosugi, M.; Tanji, T.; Tanaka, Y.; Yoshida, A.; Fugami, K.; Kameyama, M.; Migita, T. Palladium-Catalyzed Reaction of 1-Aza-5-germa-5-organobicyclo[3.3.3]undecane with Aryl Bromide. *J. Organomet. Chem.* **1996**, *508*, 255–257.
- (74) Faller, J. W.; Kultyshev, R. G. Palladium-Catalyzed Cross-Coupling Reactions of Allyl, Phenyl, Alkenyl, and Alkynyl Germa-tranes with Aryl Iodides. *Organometallics* **2002**, *21*, 5911–5918.
- (75) Nakamura, T.; Kinoshita, H.; Shinokubo, H.; Oshima, K. Biaryl Synthesis from Two Different Aryl Halides with Tri(2-furyl)germane. *Org. Lett.* **2002**, *4*, 3165–3167.
- (76) Enokido, T.; Fugami, K.; Endo, M.; Kameyama, M.; Kosugi, M. Palladium-Catalyzed Cross-Coupling Reaction by Means of Organogermanium Trichlorides. *Adv. Synth. Catal.* **2004**, *346*, 1685–1688.

- (77) Endo, M.; Fugami, K.; Enokido, T.; Sano, H.; Kosugi, M. Palladium-Catalyzed Cross-Coupling Reaction Using Arylgermanium Sesquioxide. *Adv. Synth. Catal.* **2007**, *349*, 1025–1027.
- (78) Spivey, A. C.; Tseng, C.-C.; Hannah, J. P.; Gripton, C. J. G.; de Fraine, P.; Parr, N. J.; Scicinski, J. J. Light-Fluorous Safety-Catch Arylgermanes – Exceptionally Robust, Photochemically Activated Precursors for Biaryl Synthesis by Pd(0) Catalysed Cross-Coupling. *Chem. Commun.* **2007**, 2926–2928.
- (79) Spivey, A. C.; Gripton, C. J. G.; Hannah, J. P.; Tseng, C.-C.; de Fraine, P.; Parr, N. J.; Scicinski, J. J. The Development of a ‘Safety-Catch’ Arylgermane for Biaryl Synthesis by Palladium-Catalysed Germyl-Stillé Cross-Coupling. *Appl. Organometal. Chem.* **2007**, *21*, 572–589.
- (80) Pitteloud, J.-P.; Zhang, Z.-T.; Liang, Y.; Cabrera, L.; Wnuk, S. F. Fluoride-Promoted Cross-Coupling of Chloro(mono-, di-, or triphenyl)germanes with Aryl Halides in “Moist” Toluene. Multiple Transfer of the Phenyl Group from Organogermane Substrates and Comparison of the Coupling Efficiencies of Chloro(phenyl)germanes with Their Corresponding Stannane and Silane Counterparts. *J. Org. Chem.* **2010**, *75*, 8199–8212.
- (81) Zhang, Z.-T.; Pitteloud, J.-P.; Cabrera, L.; Liang, Y.; Toribio, M.; Wnuk, S. F. Arylchlorogermanes/TBAF/“Moist” Toluene: A Promising Combination for Pd-Catalyzed Germyl-Stillé Cross-Coupling. *Org. Lett.* **2010**, *12*, 816–819.
- (82) Pitteloud, J.-P.; Liang, Y.; Wnuk, S. F. Chemoselective Transfer of Allyl or Phenyl Group from Allyl(phenyl)germanes in Pd-Catalyzed Reactions with Aryl Halides. *Chem. Lett.* **2011**, *40*, 967–969.
- (83) Fricke, C.; Schoenebeck, F. Organogermanes as Orthogonal Coupling Partners in Synthesis and Catalysis. *Acc. Chem. Res.* **2020**, *53*, 2715–2725.
- (84) Spivey, A. C.; Diaper, C. M. Silicon and Germanium Linker Units. In *Linker Strategies In Solid-Phase Organic Synthesis*; Scott, P. J. H., Ed.; John Wiley & Sons, Ltd.: Chichester, UK, 2009; pp 467–504.
- (85) Spivey, A. C.; Gripton, C. J. G.; Noban, C.; Parr, N. J. The Synthesis of Arylketones via Friedel–Crafts Acyldegermylation. *Synlett* **2005**, 2167–2170.

- (86) Komami, N.; Matsuoka, K.; Nakano, A.; Kojima, M.; Yoshino, T.; Matsunaga, S. Synthesis of Functionalized Monoaryl- λ^3 -iodanes through Chemo- and Site-Selective *ipso*-Substitution Reactions. *Chem. - Eur. J.* **2019**, *25*, 1217–1220.
- (87) Xi, Y.; Su, B.; Qi, X.; Pedram, S.; Liu, P.; Hartwig, J. F. Application of Trimethylgermyl-Substituted Bisphosphine Ligands with Enhanced Dispersion Interactions to Copper-Catalyzed Hydroboration of Disubstituted Alkenes. *J. Am. Chem. Soc.* **2020**, *142*, 18213–18222.
- (88) Eaborn, C.; Pande, K. C. Organogermanium Compounds. Part I. Preparation of Substituted Triethyl- and Tricyclohexyl-phenylgermanes. *J. Chem. Soc.* **1960**, 3200–3203.
- (89) Lesbre, M.; Mazerolles, P.; Satgé, J. *The Organic Compounds Of Germanium*; Wiley-Interscience: New York, NY, USA, 1971.
- (90) Riedmiller, F.; Wegner, G. L.; Jockisch, A.; Schmidbaur, H. Preparation, Structure, and ^{73}Ge NMR Spectroscopy of Arylgermanes ArGeH_3 , Ar_2GeH_2 , and Ar_3GeH . *Organometallics* **1999**, *18*, 4317–4324.
- (91) *The Chemistry of Organic Germanium, Tin and Lead Compounds*; Rappoport, Z., Ed.; John Wiley & Sons, Ltd.: Chichester, UK, 2002; Vol. 2.
- (92) Mironov, V. F.; Fedotov, N. S. A New Method of Preparation of Phenyltrichloro- and Phenyltribromogermane. *Zh. Obshch. Khim.* **1964**, *34*, 4122.
- (93) Roller, S.; Simon, D.; Dräger, M. Über Polygermane: XIV. Polygermane als Nebenprodukte der Grignard-Reaktion von PhMgBr mit GeCl_4 . *J. Organomet. Chem.* **1986**, *301*, 27–40.
- (94) David-Quillot, F.; Lunot, S.; Marsacq, D.; Duchêne, A. A Novel Access to Organogermanium Compounds. *Tetrahedron Lett.* **2000**, *41*, 4905–4907.
- (95) Langle, S.; David-Quillot, F.; Balland, A.; Abarbri, M.; Duchêne, A. General Access to *para*-Substituted Styrenes. *J. Organomet. Chem.* **2003**, 113–119.

- (96) Fomina, N. V.; Shverdina, N. I.; Dobrova, E. I.; Sosnina, I. V.; Kocheshkov, K. A. Alkylation of Germanium Salts by Alkyl and Aryl Iodides in the Presence of Zinc. *Dokl. Akad. Nauk SSSR* **1973**, *210*, 621–622.
- (97) Reddy, N. P.; Hayashi, T.; Tanaka, M. Palladium-Catalyzed Germylation of Organic Halides with a Digermane. Unexpected Formation of Germylene-Insertion Type Products. *Chem. Lett.* **1991**, *20*, 677–680.
- (98) Lesbani, A.; Kondo, H.; Yabusaki, Y.; Nakai, M.; Yamanoi, Y.; Nishihara, H. Integrated Palladium-Catalyzed Arylation of Heavier Group 14 Hydrides. *Chem. - Eur. J.* **2010**, *16*, 13519–13527.
- (99) Akahori, S.; Sakai, H.; Hasobe, T.; Shinokubo, H.; Miyake, Y. Synthesis and Photodynamics of Tetragermatetraphia[8]circulene. *Org. Lett.* **2018**, *20*, 304–307.
- (100) Murata, M.; Yamasaki, H.; Uogishi, K.; Watanabe, S.; Masuda, Y. Synthesis of Organosilatrane via Rhodium(I)-Catalyzed Silylation of Organic Iodides with Hydrosilatrane. *Synthesis* **2007**, 2944–2946.
- (101) Furukawa, N.; Kouroggi, N.; Seki, Y.; Kakiuchi, F.; Murai, S. Transition Metal-Catalyzed Dehydrogenative Germylation of Olefins with Tri-*n*-butylgermane. *Organometallics* **1999**, *18*, 3764–3767.
- (102) Murai, M.; Matsumoto, K.; Okada, R.; Takai, K. Rhodium-Catalyzed Dehydrogenative Germylation of C–H Bonds: New Entry to Unsymmetrically Functionalized 9-Germafluorenes. *Org. Lett.* **2014**, *16*, 6492–6495.
- (103) Murai, M.; Takeshima, H.; Morita, H.; Kuninobu, Y.; Takai, K. Acceleration Effects of Phosphine Ligands on the Rhodium-Catalyzed Dehydrogenative Silylation and Germylation of Unactivated C(sp³)–H Bonds. *J. Org. Chem.* **2015**, *80*, 5407–5414.
- (104) Murai, M.; Okada, R.; Asako, S.; Takai, K. Rhodium-Catalyzed Silylative and Germylative Cyclization with Dehydrogenation Leading to 9-Sila- and 9-Germafluorenes: A Combined Experimental and Computational Mechanistic Study. *Chem. - Eur. J.* **2017**, *23*, 10861–10870.

- (105) Zhou, D.; Gao, Y.; Tan, Q.; Xu, B. Synthesis of Silicon and Germanium-Containing Heterosumanenes via Rhodium-Catalyzed Cyclodehydrogenation of Silicon/Germanium–Hydrogen and Carbon–Hydrogen Bonds. *Org. Lett.* **2017**, *19*, 4628–4631.
- (106) Kanyiva, K. S.; Kuninobu, Y.; Kanai, M. Palladium-Catalyzed Direct C–H Silylation and Germanylation of Benzamides and Carboxamides. *Org. Lett.* **2014**, *16*, 1968–1971.
- (107) Chen, C.; Guan, M.; Zhang, J.; Wen, Z.; Zhao, Y. Palladium-Catalyzed Oxalyl Amide Directed Silylation and Germanylation of Amine Derivatives. *Org. Lett.* **2015**, *17*, 3646–3649.
- (108) Modak, A.; Patra, T.; Chowdhury, R.; Raul, S.; Maiti, D. Palladium-Catalyzed Remote *meta*-Selective C–H Bond Silylation and Germanylation. *Organometallics* **2017**, *36*, 2418–2423.
- (109) Lv, W.; Yu, J.; Ge, B.; Wen, S.; Cheng, G. Palladium-Catalyzed Catellani-Type Bis-silylation and Bis-germylation of Aryl Iodides and Norbornenes. *J. Org. Chem.* **2018**, *83*, 12683–12693.
- (110) Lv, W.; Wen, S.; Yu, J.; Cheng, G. Palladium-Catalyzed *ortho*-Silylation of Aryl Iodides with Concomitant Arylsilylation of Oxanorbornadiene: Accessing Functionalized (*Z*)- β -Substituted Vinylsilanes and Their Analogues. *Org. Lett.* **2018**, *20*, 4984–4987.
- (111) Wollenburg, M.; Bajohr, J.; Marchese, A. D.; Whyte, A.; Glorius, F.; Lautens, M. Palladium-Catalyzed Disilylation and Digermanylation of Alkene Tethered Aryl Halides: Direct Access to Versatile Silylated and Germanylated Heterocycles. *Org. Lett.* **2020**, *22*, 3679–3683.
- (112) Deb, A.; Singh, S.; Seth, K.; Pimparkar, S.; Bhaskararao, B.; Guin, S.; Sunoj, R. B.; Maiti, D. Experimental and Computational Studies on Remote γ -C(sp³)-H Silylation and Germanylation of Aliphatic Carboxamides. *ACS Catal.* **2017**, *7*, 8171–8175.

- (113) Zhou, Z.-X.; Rao, W.-H.; Zeng, M.-H.; Liu, Y.-J. Facile Synthesis of Unnatural β -Germyl- α -Amino Amides via Pd(II)-Catalyzed Primary and Secondary C(sp³)-H Bond Germylation. *Chem. Commun.* **2018**, *54*, 14136–14139.
- (114) Selmani, A.; Gevondian, A. G.; Schoenebeck, F. Germylation of Arenes via Pd(I) Dimer Enabled Sulfonium Salt Functionalization. *Org. Lett.* **2020**, *22*, 4802–4805.
- (115) Selmani, A.; Schoenebeck, F. Transition-Metal-Free, Formal C–H Germylation of Arenes and Styrenes via Dibenzothiophenium Salts. *Org. Lett.* **2021**, *23*, 4779–4784.
- (116) Neumann, W. P. Germylenes and Stannylenes. *Chem. Rev.* **1991**, *91*, 311–334.
- (117) Mizuhata, Y.; Sasamori, T.; Tokitoh, N. Stable Heavier Carbene Analogues. *Chem. Rev.* **2009**, *109*, 3479–3511.
- (118) Stag e, J.; Massol, M.; Rivier e, P. Divalent Germanium Species as Starting Materials and Intermediates in Organogermanium Chemistry. *J. Organomet. Chem.* **1973**, *56*, 1–39.
- (119) Okamoto, M.; Asano, T.; Suzuki, E. Phenyltrichlorogermane Synthesis by the Reaction of Chlorobenzene and the Dichlorogermylene Intermediate Formed from Elemental Germanium and Tetrachlorogermane. *Organometallics* **2001**, *20*, 5583–5585.
- (120) Moulton, C. J.; Shaw, B. L. Transition Metal-Carbon Bonds. Part XLII. Complexes of Nickel, Palladium, Platinum, Rhodium and Iridium with the Tridentate Ligand 2,6-Bis[(di-*t*-butylphosphino)methyl]phenyl. *J. Chem. Soc., Dalton Trans.* **1976**, 1020–1024.
- (121) van Koten, G. Tuning the Reactivity of Metals Held in a Rigid Ligand Environment. *Pure Appl. Chem.* **1989**, *61*, 1681–1694.
- (122) Peris, E.; Crabtree, R. H. Key Factors in Pincer Ligand Design. *Chem. Soc. Rev.* **2018**, *47*, 1959–1968.

- (123) *The Chemistry of Pincer Compounds*, 1st ed.; Morales-Morales, D., Jensen, C. M., Eds.; Elsevier: Boston, MA, USA, 2007.
- (124) Martin, C.; Mallet-Ladeira, S.; Miqueu, K.; Bouhadir, G.; Bourissou, D. Combined Experimental/Computational Study of Iridium and Palladium Hydride PP(O)P Pincer Complexes. *Organometallics* **2014**, *33*, 571–577.
- (125) Zhu, J.; Lin, Z.; Marder, T. B. Trans Influence of Boryl Ligands and Comparison with C, Si, and Sn Ligands. *Inorg. Chem.* **2005**, *44*, 9384–9390.
- (126) Fan, L.; Foxman, B. M.; Ozerov, O. V. N–H Cleavage as a Route to Palladium Complexes of a New PNP Pincer Ligand. *Organometallics* **2004**, *23*, 326–328.
- (127) Mazzeo, M.; Lamberti, M.; Massa, A.; Scettri, A.; Pellecchia, C.; Peters, J. C. Phosphido Pincer Complexes of Palladium as New Efficient Catalysts for Allylation of Aldehydes. *Organometallics* **2008**, *27*, 5741–5743.
- (128) Comanescu, C. C.; Vyushkova, M.; Iluc, V. M. Palladium Carbene Complexes as Persistent Radicals. *Chem. Sci.* **2015**, *6*, 4570–4579.
- (129) Schuhknecht, D.; Ritter, F.; Tauchert, M. E. Isolation and Properties of a Palladium PBP Pincer Complex Featuring an Ambiphilic Boryl Site. *Chem. Commun.* **2016**, *52*, 11823–11826.
- (130) Tolman, C. A. Steric Effects of Phosphorus Ligands in Organometallic Chemistry and Homogeneous Catalysis. *Chem. Rev.* **1977**, *77*, 313–348.
- (131) Fryzuk, M. D.; MacNeil, P. A. Hybrid Multidentate Ligands. Tridentate Amidophosphine Complexes of Nickel(II) and Palladium(II). *J. Am. Chem. Soc.* **1981**, *103*, 3592–3593.
- (132) Ishiyama, T.; Takagi, J.; Hartwig, J. F.; Miyaura, N. A Stoichiometric Aromatic C–H Borylation Catalyzed by Iridium(I)/2,2'-Bipyridine Complexes at Room Temperature. *Angew. Chem., Int. Ed.* **2002**, *41*, 3056–3058.

- (133) Fang, H.; Choe, Y.-K.; Li, Y.; Shimada, S. Synthesis, Structure, and Reactivity of Hydridoiridium Complexes Bearing a Pincer-Type PSiP Ligand. *Chem. - Asian J.* **2011**, *6*, 2512–2521.
- (134) Brück, A.; Gallego, D.; Wang, W.; Irran, E.; Driess, M.; Hartwig, J. F. Pushing the σ -Donor Strength in Iridium Pincer Complexes: Bis(silylene) and Bis(germylene) Ligands Are Stronger Donors than Bis(phosphorus(III)) Ligands. *Angew. Chem., Int. Ed.* **2012**, *51*, 11478–11482.
- (135) Göttker-Schnetmann, I.; White, P.; Brookhart, M. Iridium Bis(phosphinite) *p*-XPCP Pincer Complexes: Highly Active Catalysts for the Transfer Dehydrogenation of Alkanes. *J. Am. Chem. Soc.* **2004**, *126*, 1804–1811.
- (136) Pell, C. J.; Ozerov, O. V. Catalytic Dehydrogenative Borylation of Terminal Alkynes by POCOP-Supported Palladium Complexes. *Inorg. Chem. Front.* **2015**, *2*, 720–724.
- (137) Ozerov, O. V.; Guo, C.; Foxman, B. M. Missing Link: PCP Pincer Ligands Containing P–N Bonds and Their Pd Complexes. *J. Organomet. Chem.* **2006**, *691*, 4802–4806.
- (138) Murugesan, S.; Stöger, B.; Carvalho, M. D.; Ferreira, L. P.; Pittenauer, E.; Allmaier, G.; Veiros, L. F.; Kirchner, K. Synthesis and Reactivity of Four- and Five-Coordinate Low-Spin Cobalt(II) PCP Pincer Complexes and Some Nickel(II) Analogues. *Organometallics* **2014**, *33*, 6132–6140.
- (139) Shih, W.-C.; Ozerov, O. V. One-Pot Synthesis of 1,3-Bis(phosphinomethyl)arene PCP/PNP Pincer Ligands and Their Nickel Complexes. *Organometallics* **2015**, *34*, 4591–4597.
- (140) Pell, C. J.; Ozerov, O. V. A Series of Pincer-Ligated Rhodium Complexes as Catalysts for the Dimerization of Terminal Alkynes. *ACS Catal.* **2014**, *4*, 3470–3480.
- (141) Kosanovich, A. J.; Jordan, A. M.; Bhuvanesh, N.; Ozerov, Oleg. V. Synthesis and Characterization of Rhodium, Iridium, and Palladium Complexes of a Diarylamido-Based PNSb Pincer Ligand. *Dalton Trans.* **2018**, *47*, 11619–11624.

- (142) Shih, W.-C.; Gu, W.; MacInnis, M. C.; Timpa, S. D.; Bhuvanesh, N.; Zhou, J.; Ozerov, O. V. Facile Insertion of Rh and Ir into a Boron–Phenyl Bond, Leading to Boryl/Bis(phosphine) PBP Pincer Complexes. *J. Am. Chem. Soc.* **2016**, *138*, 2086–2089.
- (143) Timpa, S. D.; Zhou, J.; Bhuvanesh, N.; Ozerov, O. V. Potential Carbon–Fluorine Reductive Elimination from Pincer-Supported Rh(III) and Dominating Side Reactions: Theoretical and Experimental Examination. *Organometallics* **2014**, *33*, 6210–6217.
- (144) Weng, W.; Guo, C.; Çelenligil-Çetin, R.; Foxman, B. M.; Ozerov, O. V. Skeletal Change in the PNP Pincer Ligand Leads to a Highly Regioselective Alkyne Dimerization Catalyst. *Chem. Commun.* **2006**, 197–199.
- (145) Ozerov, O. V.; Guo, C.; Papkov, V. A.; Foxman, B. M. Facile Oxidative Addition of N–C and N–H Bonds to Monovalent Rhodium and Iridium. *J. Am. Chem. Soc.* **2004**, *126*, 4792–4793.
- (146) Shih, W.-C.; Ozerov, O. V. Synthesis and Characterization of PBP Pincer Iridium Complexes and Their Application in Alkane Transfer Dehydrogenation. *Organometallics* **2017**, *36*, 228–233.
- (147) Timpa, S. D.; Fafard, C. M.; Herbert, D. E.; Ozerov, O. V. Catalysis of Kumada–Tamao–Corriu Coupling by a (P^oC^oP)Rh Pincer Complex. *Dalton Trans.* **2011**, *40*, 5426–5429.
- (148) Foley, B. J.; Ozerov, O. V. Air- and Water-Tolerant (PNP)Ir Precatalyst for the Dehydrogenative Borylation of Terminal Alkynes. *Organometallics* **2020**, *39*, 2352–2355.
- (149) Mucha, N. T.; Waterman, R. Iridium Pincer Catalysts for Silane Dehydrocoupling: Ligand Effects on Selectivity and Activity. *Organometallics* **2015**, *34*, 3865–3872.
- (150) Lee, C.-I.; DeMott, J. C.; Pell, C. J.; Christopher, A.; Zhou, J.; Bhuvanesh, N.; Ozerov, O. V. Ligand Survey Results in Identification of PNP Pincer Complexes of Iridium as Long-Lived and Chemoselective Catalysts for Dehydrogenative Borylation of Terminal Alkynes. *Chem. Sci.* **2015**, *6*, 6572–6582.

- (151) Farrugia, L. J. ORTEP-3 for Windows – A Version of ORTEP-III with a Graphical User Interface (GUI). *J. Appl. Crystallogr.* **1997**, *30*, 565.
- (152) Herd , J. L.; Lambert, J. C.; Senoff, C. V. Cyclooctene and 1,5-Cyclooctadiene Complexes of Iridium(I). *Inorg. Synth.* **1974**, *15*, 18–20.
- (153) Merola, J. S.; Husebo, T. L.; Matthews, K. E. Aqueous Organometallic Chemistry of *mer*-Ir(H)₂(PMe₃)₃X Complexes. *Organometallics* **2012**, *31*, 3920–3929.
- (154) Chotana, G. A.; Vanchura, B. A.; Tse, M. K.; Staples, R. J.; Maleczka, Jr., R. E.; Smith, III, M. R. Getting the Sterics Just Right: A Five-Coordinate Iridium Trisboryl Complex That Reacts with C–H Bonds at Room Temperature. *Chem. Commun.* **2009**, 5731–5733.
- (155) Giordano, G.; Crabtree, R. H. Di- μ -Chloro-Bis(η^4 -1,5-cyclooctadiene)dirhodium(I). *Inorg. Synth.* **1990**, *28*, 88–90.
- (156) Redko, B.; Albeck, A.; Gellerman, G. Facile Synthesis and Antitumor Activity of Novel *N*(9) Methylated AHMA Analogs. *New. J. Chem.* **2012**, *36*, 2188.
- (157) Scattolin, T.; Senol, E.; Yin, G.; Guo, Q.; Schoenebeck, F. Site-Selective C–S Bond Formation at C–Br over C–OTf and C–Cl Enabled by an Air-Stable, Easily Recoverable, and Recyclable Palladium(I) Catalyst. *Angew. Chem., Int. Ed.* **2018**, *57*, 12425–12429.
- (158) Pouliot, M.-F.; Mah , O.; Hamel, J.-D.; Desroches, J.; Paquin, J.-F. Halogenation of Primary Alcohols Using a Tetraethylammonium Halide/[Et₂NSF₂]BF₄ Combination. *Org. Lett.* **2012**, *14*, 5428–5431.
- (159) Holzgrabe, U. Quantitative NMR Spectroscopy in Pharmaceutical Applications. *Prog. Nucl. Magn. Reson. Spectrosc.* **2010**, *57*, 229–240.
- (160) *APEX3: Program for Data Collection on Area Detectors*; Bruker AXS Inc.: Madison, WI, USA, 2016.

- (161) Sheldrick, G. M. *SADABS: Program for Absorption Correction for Data from Area Detector Frames*; Bruker AXS Inc.: Madison, WI, USA, 2008.
- (162) Sheldrick, G. M. A Short History of *SHELX*. *Acta Crystallogr., Sect. A: Found. Crystallogr.* **2008**, *64*, 112–122.
- (163) Sheldrick, G. M. *SHELXT* – Integrated Space-Group and Crystal-Structure Determination. *Acta Crystallogr., Sect. A: Found. Crystallogr.* **2015**, *71*, 3–8.
- (164) Sheldrick, G. M. Crystal Structure Refinement with *SHELXL*. *Acta Crystallogr., Sect. C: Struct. Chem.* **2015**, *71*, 3–8.
- (165) *XT, XS*; Bruker AXS Inc.: Madison, WI, USA.
- (166) Spek, A. L. Single-Crystal Structure Validation with the Program *PLATON*. *J. Appl. Crystallogr.* **2003**, *36*, 7–13.
- (167) Dolomanov, O. V.; Bourhis, L. J.; Gildea, R. J.; Howard, J. A. K.; Puschmann, H. *OLEX2: A Complete Structure Solution, Refinement and Analysis Program*. *J. Appl. Cryst.* **2009**, *42*, 339–341.
- (168) POV-Ray - The Persistence of Vision Raytracer. <http://www.povray.org/> (Accessed on August 9, 2020).
- (169) Matsumoto, K.; Shindo, M. Palladium-Catalyzed Fluoride-Free Cross-Coupling of Intramolecularly Activated Alkenylsilanes and Alkenylgermanes: Synthesis of Tamoxifen as a Synthetic Application. *Adv. Synth. Catal.* **2012**, *354*, 642–650.
- (170) Quintard, J. P.; Hauvette-Frey, S.; Pereyre, M.; Couret, C.; Satgé, J. Metalation of Aryl Halides by Germyllithiums. *C. R. Seances Acad. Sci., Ser. C* **1978**, *287*, 247–250.
- (171) Mochida, K.; Matsushige, N. Reactions of Aryl Halides with Triethylgermyl Anions. *J. Organomet. Chem.* **1982**, *229*, 11–20.

- (172) Brook, A. G.; Abdesaken, F.; Söllradl, H. Synthesis of Some Tris(trimethylsilyl)germyl Compounds. *J. Organomet. Chem.* **1986**, *299*, 9–13.
- (173) Mochida, K.; Ogawa, S.; Naito, N.; Gaber, A. E.-A.; Usui, Y.; Nanjo, M. Preparation, Structural Characterization, and Reactivities of (Digermanyl)lithium. Its Application to the Synthesis of Bis(1,1-diphenyl-2,2,2-trimethyldigermanyl)platinum(II). *Chem. Lett.* **2007**, *36*, 414–415.
- (174) Bulten, E. J.; Noltes, J. G. Investigations on Organogermanium Compounds: XI. Preparation and Structure of Trialkylgermyl Alkali Metal Compounds in Hexamethylphosphoric Triamide (HMPT). *J. Organomet. Chem.* **1971**, *29*, 397–407.
- (175) Veith, M.; Hans, J.; Stahl, L.; May, P.; Huch, V.; Sebald, A. Alkoxigermanate(II), -stannate(II) und -plumbate(II) Zweiwertiger Metallionen, I. *Z. Naturforsch.* **1991**, *46b*, 403–424.
- (176) Veith, M.; Rösler, R. Alkoxistannate, II Tri(*tert*-butoxi)alkalistannate(II): Darstellung und Strukturen. *Z. Naturforsch.* **1986**, *41b*, 1071–1080.
- (177) Espinoza, E. M.; Clark, J. A.; Soliman, J.; Derr, J. B.; Morales, M.; Vullev, V. I. Practical Aspects of Cyclic Voltammetry: How to Estimate Reduction Potentials When Irreversibility Prevails. *J. Electrochem. Soc.* **2019**, *166*, H3175–H3187.
- (178) Reetz, M. T.; de Vries, J. G. Ligand-Free Heck Reactions Using Low Pd-Loading. *Chem. Commun.* **2004**, 1559–1563.
- (179) Phan, N. T. S.; Van Der Sluys, M.; Jones, C. W. On the Nature of the Active Species in Palladium Catalyzed Mizoroki–Heck and Suzuki–Miyaura Couplings – Homogeneous or Heterogeneous Catalysis, A Critical Review. *Adv. Synth. Catal.* **2006**, *348*, 609–679.
- (180) Deraedt, C.; Astruc, D. “Homeopathic” Palladium Nanoparticle Catalysis of Cross Carbon–Carbon Coupling Reactions. *Acc. Chem. Res.* **2014**, *47*, 494–503.
- (181) Eremin, D. B.; Ananikov, V. P. Understanding Active Species in Catalytic Transformations: From Molecular Catalysis to Nanoparticles, Leaching,

- “Cocktails” of Catalysts and Dynamic Systems. *Coord. Chem. Rev.* **2017**, *346*, 2–19.
- (182) Crociani, B.; Boschi, T.; Nicolini, M. Novel Palladium(II)-Tin and Palladium(II) Germanium Complexes. *Inorg. Chim. Acta* **1970**, *4*, 577–580.
- (183) Antonov, P. G.; Zhamsueva, T. Ts.; Agapov, I. A.; Konovalov, L. V. Palladium(II) Complex Formation with Germanium(II) in HCl Aqueous Solutions. *Zh. Prikl. Khim. (S.-Peterburg, Russ. Fed.)* **1993**, *66*, 2695–2701.
- (184) Antonov, P. G.; Zhamsueva, T. Ts. Complex Formation of Palladium(II) with Germanium(II) in Aqueous Solutions of Hydrofluoric Acid. *Russ. J. Gen. Chem.* **1997**, *67*, 1505–1508.
- (185) Antonov, P. G.; Manasevich, D. S. Palladium(II) Complexation with Tin(II) and Germanium(II) in Aqueous Solutions of Pyridine-2-Carboxylic Acid. *Zh. Prikl. Khim. (S.-Peterburg, Russ. Fed.)* **2000**, *74*, 1774–1777.
- (186) Kireenko, M. M.; Zaitsev, K. V.; Oprunenko, Y. F.; Churakov, A. V.; Tafeenko, V. A.; Karlov, S. S.; Zaitseva, G. S. Palladium Complexes with Stabilized Germylene and Stannylene Ligands. *Dalton Trans* **2013**, *42*, 7901–7912.
- (187) Rück-Braun, K.; Priewisch, B. Azoxyarenes (Di- and Monoaryldiazene Oxides). *Sci. Synth.* **2007**, *31b*, 1401–1424.
- (188) Lemierre, V.; Chrostowska, A.; Dargelos, A.; Baylère, P.; Leigh, W. J.; Harrington, C. R. Flash Vacuum Thermolysis of 3,4-Dimethyl-1-germacyclopent-3-enes: UV Photoelectron Spectroscopic Characterization of GeH₂ and GeMe₂. *Appl. Organometal. Chem.* **2004**, *18*, 676–683.
- (189) Herrmann, W. A.; Denk, M.; Behm, J.; Scherer, W.; Klingan, F.-R.; Bock, H.; Solouki, B.; Wagner, M. Stable Cyclic Germanediyls (“Cyclogermylenes”): Synthesis, Structure, Metal Complexes, and Thermolyses. *Angew. Chem., Int. Ed. Engl.* **1992**, *31*, 1485–1488.

- (190) Sheldrick, G. M. *Cell_Now (version 2008/1): Program for Obtaining Unit Cell Constants from Single Crystal Data*; University of Göttingen: Göttingen, Germany, 2008.
- (191) Sheldrick, G. M. *TWINABS: Program for Absorption Correction for Data from Area Detector Frames*; Bruker AXS Inc.: Madison, WI, USA, 2008.
- (192) Noviandri, I.; Brown, K. N.; Fleming, D. S.; Gulyas, P. T.; Lay, P. A.; Masters, A. F.; Phillips, L. The Decamethylferrocenium/Decamethylferrocene Redox Couple: A Superior Redox Standard to the Ferrocenium/Ferrocene Redox Couple for Studying Solvent Effects on the Thermodynamics of Electron Transfer. *J. Phys. Chem. B* **1999**, *103*, 6713–6722.
- (193) Veith, M.; Töllner, F. Cyclische Diazastannylene: XVII. Zur Umsetzung Eines 1,3-Diaza-2-sila-4 λ^2 -stannetidins mit Cyclischen Dienen. *J. Organometal. Chem.* **1983**, *246*, 219–226.
- (194) Veith, M.; Hobein, P.; Rösler, R. Cyclische Diazastannylene, XXX Symmetrisch Und Asymmetrisch Substituierte German- und Stannandiyle mit Amid-, Alkoholat- Und Thiolat-Liganden, Teil I. *Z. Naturforsch.* **1989**, *44b*, 1067–1081.
- (195) Nguyen-Tran, H.-H.; Zheng, G.-W.; Qian, X.-H.; Xu, J.-H. Highly Selective and Controllable Synthesis of Arylhydroxylamines by the Reduction of Nitroarenes with an Electron-Withdrawing Group Using a New Nitroreductase BaNTR1. *Chem. Commun.* **2014**, *50*, 2861–2864.
- (196) Wnuk, S. F.; Garcia, P. I.; Wang, Z. Radical-Mediated Silyl- and Germyldesulfonylation of Vinyl and (α -Fluoro)vinyl Sulfones: Application of Tris(trimethylsilyl)silanes and Tris(trimethylsilyl)germanes in Pd-Catalyzed Couplings. *Org. Lett.* **2004**, *6*, 2047–2049.
- (197) Wang, Z.; Wnuk, S. F. Application of Vinyl Tris(trimethylsilyl)germanes in Pd-Catalyzed Couplings. *J. Org. Chem.* **2005**, *70*, 3281–3284.
- (198) Denmark, S. E.; Sweis, R. F. Cross-Coupling Reactions of Alkenylsilanols with Fluoroalkylsulfonates. *Org. Lett.* **2002**, *4*, 3771–3774.

- (199) Matos, K.; Soderquist, J. A. Alkylboranes in the Suzuki–Miyaura Coupling: Stereochemical and Mechanistic Studies. *J. Org. Chem.* **1998**, *63*, 461–470.
- (200) Landini, D.; Maia, A.; Rampoldi, A. Dramatic Effect of the Specific Solvation on the Reactivity of Quaternary Ammonium Fluorides and Poly(hydrogen fluorides), $(\text{HF})_n \cdot \text{F}^-$, in Media of Low Polarity. *J. Org. Chem.* **1989**, *54*, 328–332.
- (201) Albanese, D.; Landini, D.; Penso, M. Hydrated Tetrabutylammonium Fluoride as a Powerful Nucleophilic Fluorinating Agent. *J. Org. Chem.* **1998**, *63*, 9587–9589.
- (202) Lickiss, P. D.; Lucas, R. Rate Increases in the Fluorination of Bulky Chlorosilanes Caused by Ultrasound or by Water. *J. Organometal. Chem.* **1996**, *510*, 167–172.
- (203) Liu, C.; Znan, Y.; Liu, N.; Qiu, J. A Simple and Efficient Approach for the Palladium-Catalyzed Ligand-Free Suzuki Reaction in Water. *Green Chem.* **2012**, *14*, 2999–3003.
- (204) Döbele, M.; Vanderheiden, S.; Jung, N.; Bräse, S. Synthesis of Aryl Fluorides on a Solid Support and in Solution by Utilizing a Fluorinated Solvent. *Angew. Chem., Int. Ed.* **2010**, *49*, 5986–5988.
- (205) Liu, N.; Wang, Z.-X. Kumada Coupling of Aryl, Heteroaryl, and Vinyl Chlorides Catalyzed by Amido Pincer Nickel Complexes. *J. Org. Chem.* **2011**, *76*, 10031–10038.

APPENDIX A

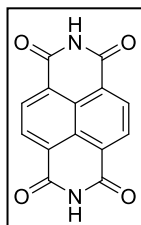
LIST OF PUBLICATIONS RESULTING FROM THE PH.D. WORK

- (1) Hung, M.-U.; Press, L. P.; Bhuvanesh, N.; Ozerov, O. V. Examination of a Series of Ir and Rh PXL Pincer Complexes as (Pre)catalysts for Aromatic C–H Borylation. *Organometallics* **2021**, *40*, 1004–1013. DOI: 10.1021/acs.organomet.1c00081
- (2) Hung, M.-U.; Rezenom, Y. H.; Bhuvanesh, N.; Ozerov, O. V. High-Turnover Pd-Catalyzed Germylation of Aryl Bromides Using [NaGe(O^tBu)₃]₂. *Manuscript in Preparation*.

APPENDIX B

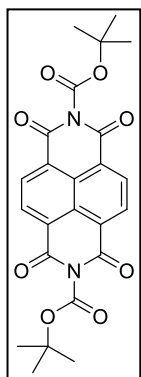
MISCELLANEOUS REACTIONS

B-1. Miscellaneous Synthesis



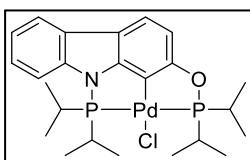
Synthesis of 1,4,5,8-naphthalenetetracarboxylic diimide (601).

1,4,5,8-Naphthalenetetracarboxylic dianhydride (5.07 g, 18.9 mmol), NH_4OAc (29 g, 0.38 mmol) were refluxed in AcOH (100 mL) in a 250 mL round-bottom flask for 5 h. The solid was collected by vacuum filtration, washed by copious AcOH, water, and Et_2O , and dried under vacuum to give a pure product as a tan solid (4.65 g, 92% yield). $^1\text{H NMR}$ (499 MHz, $\text{DMSO}-d_6$) δ 12.1 (s, 2H), 8.62 (s, 4H).



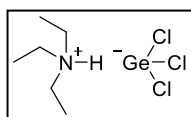
Synthesis of *N,N'*-di-*tert*-butoxycarbonyl-1,4,5,8-naphthalenetetracarboxylic diimide (602).

1,4,5,8-naphthalenetetracarboxylic diimide (53 mg, 0.20 mmol), $(\text{Boc})_2\text{O}$ (184 mg, 0.84 mmol), and DMAP (61 mg, 0.50 mmol) were dissolved in anhydrous DMF (3 mL) in a 10 mL Schlenk tube. The reaction was stirred at ambient temperature overnight. Volatiles were removed under vacuum. The residue was dissolved in CH_2Cl_2 (30 mL). The organic layer was washed with 1 M aqueous HCl (25 mL x 3), water (25 mL), and brine (25 mL) and dried over MgSO_4 . Volatiles removed under vacuum to provide a pale-yellow solid (64 mg, 69% yield). $^1\text{H NMR}$ (500 MHz, CDCl_3) δ 8.80 (s, 4H), 1.68 (s, 18 H).



Synthesis of (carbazole-PNCOP)PdCl (603). In a J. Young

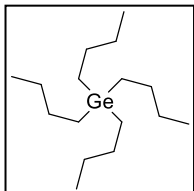
NMR tube, **208** (58.9 mg, 0.142 mmol) and (COD)PdCl₂ (38.9 mg, 0.136 mg) were dissolved in 0.5 mL of C₆D₆. To the mixture was added 2,6-lutidine (33 μL, 0.28 mmol). The reaction mixture was heated at 100 °C in an oil bath for 16 h. The ³¹P{¹H} NMR spectrum showed a full conversion to the desired product. The mixture was filtered by a pad of Celite over a pipette. Volatiles were removed under vacuum. The crude product was purified by recrystallization from toluene/pentane at -35 °C to provide a yellow solid (48 mg, 63% yield). ¹H NMR (500 MHz, C₆D₆) δ 7.83 (ddd, *J* = 7.3, 1.8, 0.8 Hz, 1H), 7.51 (dt, *J* = 8.3, 1.4 Hz, 1H), 7.24–7.16 (m, 2H), 7.14 – 7.11 (m, 1H), 6.94 (dd, *J* = 8.3, 0.6 Hz, 1H), 2.70–2.56 (m, 2H), 2.31–2.19 (m, 2H), 1.40 (dd, *J* = 19.1, 7.1 Hz, 6H), 1.40 (dd, *J* = 19.0, 7.2 Hz, 6H), 1.16 (dd, *J* = 15.3, 7.0 Hz, 6H), 0.96 (dd, *J* = 16.1, 7.0 Hz, 6H); ¹³C{¹H} NMR (126 MHz, C₆D₆) δ 165.1 (dd, *J*_{P-C} = 11.1, 2.5 Hz), 160.8 (d, *J*_{P-C} = 26.8 Hz), 140.0 (dd, *J*_{P-C} = 9.9, 2.0 Hz), 132.6 (d, *J*_{P-C} = 0.6 Hz), 124.7, 121.8, 121.4, 119.9 (dd, *J*_{P-C} = 4.5, 1.2 Hz), 118.3, 114.7 (d, *J*_{P-C} = 11.2 Hz), 112.6, 106.2 (d, *J*_{P-C} = 14.8 Hz), 29.5 (dd, *J*_{P-C} = 18.9, 5.5 Hz), 28.1 (dd, *J*_{P-C} = 13.9, 3.4 Hz), 18.9, 18.5 (d, *J*_{P-C} = 9.1 Hz), 17.4 (d, *J*_{P-C} = 6.8 Hz), 16.9 (d, *J*_{P-C} = 1.8 Hz); ³¹P NMR (202 MHz, C₆D₆) δ 192.7 (d, *J* = 410 Hz), 121.1 (d, *J* = 410 Hz); Elem. Anal. Calcd for C₂₄H₃₄ClN₂O₂Pd: C, 51.81; H, 6.16; N, 2.52. Found: C, 52.10; H, 5.89; N, 2.49.



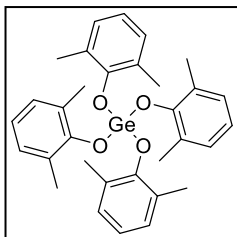
Synthesis of triethylammonium trichlorogermanate (604).

GeCl₄ (50 μL, 0.44 mmol) and HSiCl₃ (45 μL, 0.45 mmol) were dissolved in C₆D₆ (0.5 mL) in a J. Young NMR tube. The reaction was stirred at ambient temperature for 30 min. Et₃N (62 μL, 0.44 mmol) was added. The reaction was stirred over a weekend.

Two layers were formed. All the volatiles were removed under vacuum. ^1H NMR (499 MHz, CDCl_3) δ 7.62 (s, 1H), 3.20 (q, $J = 7.3$ Hz, 6H), 1.34 (t, $J = 7.3$ Hz, 9H).

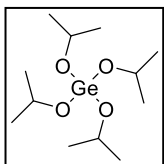


Synthesis of tetra-*n*-butylgermane (605). A THF solution (40 mL) of 1-bromobutane (9.03 g, 65.9 mmol) was slowly added via syringe to a warm (50 °C) suspension of $\text{Ge}(\text{OMe})_4$ (2.89 g, 14.7 mmol), magnesium (1.79 mg, 73.6 mmol) in THF (20 mL) under argon. (*Caution: Exothermic!*) The reaction was refluxed under argon for 17 h. The reaction mixture was passed through a pad of Celite over a frit using hexane and Et_2O . Volatiles were removed under vacuum. Water was added, and the organic products were extracted by hexane and Et_2O . The combined organic phase was washed with brine and dried over MgSO_4 . Volatiles were removed under vacuum to give a crude product as a yellow liquid (3.07 g). The liquid was purified by vacuum distillation to give a pure product as a colorless liquid (2.23 g, 50% yield). ^1H NMR (499 MHz, CDCl_3) δ 1.37–1.24 (m, 16H), 0.95–0.84 (m, 12H), 0.75–0.62 (m, 8H); ^1H NMR (499 MHz, C_6D_6) δ 1.50–1.32 (m, 16H), 0.95 (t, $J = 7.1$ Hz, 12H), 0.84–0.76 (m, 8H); $^{13}\text{C}\{^1\text{H}\}$ NMR (126 MHz, CDCl_3) δ 27.7, 26.8, 14.0, 12.6; $^{13}\text{C}\{^1\text{H}\}$ NMR (126 MHz, C_6D_6) δ 28.0, 27.2, 14.1, 12.9.

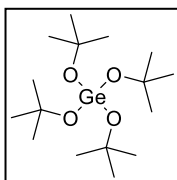


Synthesis of tetrakis(2,6-dimethylphenoxy)germane (606). GeCl_4 (89 mg, 0.42 mmol) and 2,6-dimethylphenol (0.25 g, 2.0 mmol) were dissolved in toluene (4 mL). Et_3N (300 μL , 2.15 mmol) was added dropwise. The resulting white suspension was stirred at ambient temperature overnight. The solid was filtered off by a pad of Celite over a frit. Volatiles were removed to give a crude product as a white solid (264 mg). The excess 2,6-

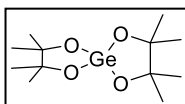
dimethylphenol was vacuum distilled off by heating the residue at 85 °C under vacuum for 3 h to give a pure product as a white solid (204 mg, 88% yield). ^1H NMR (499 MHz, C_6D_6) δ 6.80–6.71 (m, 12H), 2.20 (s, 24H); $^{13}\text{C}\{^1\text{H}\}$ NMR (126 MHz, C_6D_6) δ 153.1, 129.7, 129.1, 123.5, 17.3.



Synthesis of tetraisopropoxygermane (607). GeCl_4 (3.10 g, 14.5 mmol), $i\text{PrOH}$ (5.6 mL, 73 mmol), and Et_3N (10 mL, 72 mmol) were mixed in toluene (100 mL) in a 250 mL round-bottom flask. The reaction was stirred at ambient temperature overnight. The solid was filtered off by a pad of Celite over a frit. Volatiles were removed to give a crude product. The residue was purified by vacuum distillation to give a pure product as a colorless liquid (2.69 g, 60% yield). ^1H NMR (499 MHz, C_6D_6) δ 4.63–4.22 (m, 4H), 1.27 (d, $J = 6.1$ Hz, 24H); $^{13}\text{C}\{^1\text{H}\}$ NMR (126 MHz, C_6D_6) δ 67.7, 26.1.

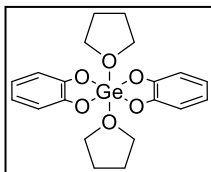


Synthesis of tetra-*tert*-butoxygermane (608). GeCl_4 (2.12 g, 9.89 mmol) and NaO^tBu (4.2 g, 44 mmol) were dissolved in THF (30 mL) in a 50 mL culture tube. (*Caution: Exothermic!*) The reaction was heated at 85 °C overnight. The solid was filtered off by a pad of Celite over a frit. Volatiles were removed to give a crude product (3.53 g). The residue was purified by vacuum distillation to give a pure product as a white solid (2.32 g, 64% yield). ^1H NMR (499 MHz, C_6D_6) δ 1.47 (s, 36H); $^{13}\text{C}\{^1\text{H}\}$ NMR (101 MHz, C_6D_6) δ 74.9, 32.4.



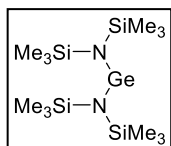
Synthesis of $\text{Ge}(\text{pin})_2$ (609). $\text{Ge}(\text{OMe})_4$ (44 mg, 0.22 mmol) and pinacol (55 mg, 0.47 mmol) were dissolved in C_6D_6 (0.5 mL) in a J. Young NMR tube. The reaction was heated at 90 °C for 20 h. Volatiles were removed under

vacuum to give a white solid (69 mg, >98% yield). ^1H NMR (499 MHz, C_6D_6) δ 1.14 (s, 24H); $^{13}\text{C}\{^1\text{H}\}$ NMR (126 MHz, C_6D_6) δ 80.5, 25.0.



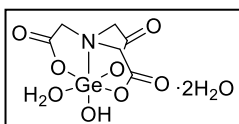
Synthesis of $\text{Ge}(\text{cat})_2(\text{THF})_2$ (610). $\text{Ge}(\text{OMe})_4$ (25 μL , 0.17 mmol) and catechol (37.3 mg, 0.339 mmol), C_6D_6 (0.4 mL), and CDCl_3 (0.5 mL) were added to a J. Young NMR tube. The reaction was

transferred to a Schlenk flask, and the NMR tube was rinsed by THF. Volatiles were removed under vacuum to yield a white solid. ^1H NMR (499 MHz, CDCl_3) δ 6.92 (br s, 4H), 6.79–6.34 (m, 4H), 4.23–3.67 (m, 8H), 1.93–1.51 (m, 8H); $^{13}\text{C}\{^1\text{H}\}$ NMR (126 MHz, CDCl_3) δ 147.5, 119.2, 112.5, 70.8, 24.8.



Synthesis of bis[bis(trimethylsilyl)amino]germylene (611).

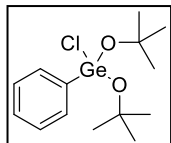
$^n\text{BuLi}$ (0.4 mL, 1 mmol, 2.5 M in hexane) was added to a cold solution of $(\text{Me}_3\text{Si})_2\text{NH}$ (183 mg, 1.13 mmol) in Et_2O (1 mL). The resulting solution $(\text{Me}_3\text{Si})_2\text{NLi}$ was added to a cold suspension of $\text{GeCl}_2 \cdot \text{C}_4\text{H}_8\text{O}_2$ (**302**) in Et_2O (2 mL). Additional Et_2O (ca. 8 mL) was used to fully transfer $(\text{Me}_3\text{Si})_2\text{NLi}$. The resulting orange suspension was stirred at ambient temperature for 19 h. Volatiles were removed under vacuum. Toluene was added. The mixture was passed through a pad of Celite over a frit. Volatiles were removed again under vacuum to give a solid (167 mg, 83% yield). ^1H NMR (499 MHz, C_6D_6) δ 0.33 (s, 24H); $^{13}\text{C}\{^1\text{H}\}$ NMR (126 MHz, C_6D_6) δ 5.4.



Synthesis of $\text{N}(\text{CH}_2\text{CO}_2)_3\text{Ge}(\text{OH})(\text{OH}_2) \cdot (\text{H}_2\text{O})_2$ (612).

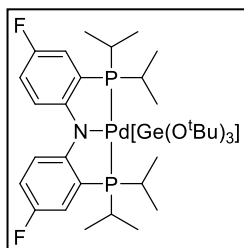
GeO_2 (72.8 mg, 0.696 mmol) and $\text{N}(\text{CH}_2\text{CO}_2\text{H})_3$ (**321**) (135 mg, 0.706) were refluxed in water (2 mL) until the suspension turned to a clear solution. The volatiles were removed under vacuum. The solid was dried at 60 $^\circ\text{C}$ under vacuum to yield

a white solid (169 mg, 69% yield). ^1H NMR (499 MHz, $\text{DMSO}-d_6$) δ 3.90 (s, 6H); $^{13}\text{C}\{^1\text{H}\}$ NMR (126 MHz, $\text{DMSO}-d_6$) δ 167.6, 62.4.



Synthesis of di-*tert*-butoxychlorophenylgermane (613).

Trichlorophenylgermane (315 μL , 1.95 mmol) and $^t\text{BuOH}$ (740 μL , 7.80 mmol) were dissolved in toluene (5 mL). Et_3N (1.2 mL, 8.6 mmol) was added. The reaction was heated at 105 $^\circ\text{C}$ for 20 h. The mixture was passed through a pad of Celite over a frit. Volatiles were removed under vacuum to give a colorless oil (0.64 g, >98% yield). ^1H NMR (400 MHz, C_6D_6) δ 7.84–7.72 (m, 2H), 7.11–6.99 (m, 3H), 1.40 (s, 18H); $^{13}\text{C}\{^1\text{H}\}$ NMR (101 MHz, C_6D_6) δ 136.3, 133.3, 131.4, 128.9, 76.4, 32.3.



Synthesis of $(^{\text{F}}\text{PNP})\text{Pd}[\text{Ge}(\text{O}^t\text{Bu})_3]$ (614). $(^{\text{F}}\text{PNP})\text{Pd}(\text{OTf})$

(203 mg, 0.293 mmol) and $[\text{NaGe}(\text{O}^t\text{Bu})_3]_2$ (**301**) (175 mg, 0.556 mol Ge) were dissolved in toluene (10 mL) in a 50 mL round-bottom flask. The reaction was stirred at ambient temperature overnight. The color of the solution changed from dark purple to orange with precipitation. Toluene was removed under vacuum. Pentane (5 mL) was added and the solid was filtered off by a pad of Celite over a frit. Volatiles were removed under vacuum to give a yellow solid (232 mg, 95% yield). ^1H NMR (499 MHz, C_6D_6) δ 7.46–7.35 (m, 2H), 7.00–6.97 (m, 2H), 6.76–6.63 (m, 2H), 3.20–2.88 (m, 4H), 1.56 (s, 27H), 1.28–1.17 (m, 12H), 1.10 (dvt, $J = 7.0$, 6.9 Hz, 12H); $^{13}\text{C}\{^1\text{H}\}$ NMR (101 MHz, C_6D_6) δ 159.7 (vt, $J_{\text{P-C}} = 9.8$ Hz), 154.1 (dvt, $J_{\text{F-C}} = 236.6$, $J_{\text{P-C}} = 4.5$ Hz), 121.5 (vtd, $J_{\text{P-C}} = 18.2$, $J_{\text{F-C}} = 4.7$ Hz), 119.2 (d, $J = 21.5$ Hz), 118.3 (d, $J = 22.6$ Hz), 115.8 (app. q, $J = 6.3$ Hz), 74.0, 34.1, 26.3 (vt, $J_{\text{P-C}} = 11.7$ Hz),

20.8 (vt, $J_{P-C} = 2.7$ Hz), 18.8; ^{19}F NMR (470 MHz, C_6D_6) $\delta -129.6$ (dd, $J = 7.2, 4.8$ Hz); $^{31}\text{P}\{^1\text{H}\}$ NMR (202 MHz, C_6D_6) $\delta 52.4$.

B-2. Miscellaneous Reactions

$[\text{NaGe}(\text{O}^t\text{Bu})_3]_2$ (**301**) (30.2 mg, 95.9 μmol Ge) and $\text{GeCl}_2 \cdot \text{C}_4\text{H}_8\text{O}_2$ (**302**) (11.0 mg, 47.5 μmol) were dissolved in THF (1.5 mL) in a 10 mL culture tube. The reaction was heated at 85 °C for 2 h. The mixture was passed through a pad of Celite, and volatiles were removed under vacuum to give a white solid. The ^1H NMR (C_6D_6) spectrum indicated the clean and quantitative formation of $[\text{Ge}(\text{O}^t\text{Bu})_2]_2$ (**322**).

$[\text{NaGe}(\text{O}^t\text{Bu})_3]_2$ (**301**) (19.1 mg, 60.6 μmol Ge, “182 μmol ” *tert*-butoxy) and $[\text{Ge}(\text{O}^t\text{Bu})_2]_2$ (**322**) (20.5 mg, 93.7 μmol Ge, “187 μmol ” *tert*-butoxy) were dissolved in C_6D_6 (0.5 mL) in a J. Young NMR tube. The reaction was analyzed by ^1H NMR spectroscopy immediately and again after placing it in an oil bath at 90 °C for 16 h. Both ^1H NMR spectra showed two well-defined ^1H NMR resonances, assigned to **301** and **322**, respectively, with no changes. The results suggested there is no fast exchange of *tert*-butoxy groups in the NMR time scale.

$[\text{Ge}(\text{O}^t\text{Bu})_2]_2$ (**322**) (17.9 mg, 81.8 μmol Ge) and $\text{Ge}(\text{O}^t\text{Bu})_4$ (**608**) (405 μL , 82.2 μmol , 0.203 M in C_6D_6) were dissolved in C_6D_6 (0.2 mL) in a J. Young NMR tube. The reaction was analyzed by ^1H NMR spectroscopy immediately and after placing it in an oil bath at 70 °C for 13 h, and at 120 °C for 11 h. All ^1H NMR spectra showed no changes.

$[\text{NaGe}(\text{O}^t\text{Bu})_3]_2$ (**301**) (23.1 mg, 73.3 μmol Ge) and $\text{Ge}(\text{O}^t\text{Bu})_4$ (**608**) (360 μL , 73.1 μmol , 0.203 M in C_6D_6) were dissolved in C_6D_6 (240 μL) in a J. Young NMR tube. The

reaction was analyzed by ^1H NMR spectroscopy immediately and after placing it in an oil bath at $70\text{ }^\circ\text{C}$ for 13 h, and at $120\text{ }^\circ\text{C}$ for 11 h. All ^1H NMR spectra showed no changes.

$[\text{NaGe}(\text{O}^t\text{Bu})_3]_2$ (**301**) (14.4 mg, $45.7\text{ }\mu\text{mol}$ Ge) and GeCl_4 ($285\text{ }\mu\text{L}$, $46.2\text{ }\mu\text{mol}$, 0.162 M in C_6D_6) were dissolved in C_6D_6 ($315\text{ }\mu\text{L}$) in a J. Young NMR tube. The reaction was analyzed by ^1H NMR spectroscopy immediately, after sitting at ambient temperature for 21 h and placing it in an oil bath at $80\text{ }^\circ\text{C}$ for 7 h. Precipitation formation was observed after sitting at ambient temperature for 21 h. Much more precipitation formation was observed upon heating. The ^1H NMR spectra before heating showed multiple unidentified resonances, presumably due to the formation of mixtures of $\text{GeCl}_x(\text{O}^t\text{Bu})_{2-x}$, $[\text{GeCl}_y(\text{O}^t\text{Bu})_{3-y}]^-$, and $\text{GeCl}_z(\text{O}^t\text{Bu})_{4-z}$. After heating at $80\text{ }^\circ\text{C}$ for 7 h, the ^1H NMR spectrum showed the formation of isobutylene, indicating the cleavage of the $\text{O}-^t\text{Bu}$ bonds.

$\text{Ge}(\text{O}^t\text{Bu})_4$ (**608**) (28.1 mg, $77.0\text{ }\mu\text{mol}$) and GeCl_4 ($160\text{ }\mu\text{L}$, $25.9\text{ }\mu\text{mol}$, 0.162 M in C_6D_6) were dissolved in C_6D_6 ($440\text{ }\mu\text{L}$) in a J. Young NMR tube. The reaction was analyzed by ^1H NMR spectroscopy immediately, after sitting at ambient temperature for 21 h and placing it in an oil bath at $80\text{ }^\circ\text{C}$ for 24 h. The ^1H NMR spectra before heating showed no changes. After heating at $80\text{ }^\circ\text{C}$ for 24 h, the ^1H NMR spectrum showed the formation of new species with a ca. 13% conversion of **608**.

$[\text{NaGe}(\text{O}^t\text{Bu})_3]_2$ (**301**) (35.0 mg, $111\text{ }\mu\text{mol}$ Ge), C_6F_6 ($12.5\text{ }\mu\text{L}$, $108\text{ }\mu\text{mol}$), and PhCF_3 ($15.0\text{ }\mu\text{L}$, $122\text{ }\mu\text{mol}$) were dissolved in C_6D_6 (0.7 mL) in a J. Young NMR tube. The reaction was analyzed by ^1H and ^{19}F NMR spectroscopy immediately and after

placing it in an oil bath at 100 °C for 2 h, and at 120 °C for 23 h. All ^1H and ^{19}F NMR spectra showed no changes.

$[\text{NaGe}(\text{O}^t\text{Bu})_3]_2$ (**301**) (17.0 mg, 54.0 μmol Ge) and $\text{C}_6\text{F}_5\text{Br}$ (200 μL , 50.2 μmol , 0.251 M in C_6D_6) were dissolved in C_6D_6 (0.7 mL) in a J. Young NMR tube. White precipitation formed upon mixing. The reaction was analyzed by ^1H and ^{19}F NMR spectroscopy immediately. Both ^1H and ^{19}F NMR spectra showed the consumption of **301** and the formation of $\text{C}_6\text{F}_5\text{Ge}(\text{O}^t\text{Bu})_3$. The reaction was sitting at ambient temperature for 2 h and followed by ^1H and ^{19}F NMR spectroscopy. After 2 h, the ^1H and ^{19}F NMR spectra showed the full consumption of **301** and $\text{C}_6\text{F}_5\text{Br}$. The mixture was passed through silica gel by using Et_2O as an eluent. Volatiles were removed under vacuum to provide a colorless oil (24 mg). Based on the ^{19}F NMR spectrum, $\text{C}_6\text{F}_5\text{Ge}(\text{O}^t\text{Bu})_3$ was determined to be 86% pure. Interestingly, the reaction does not require a palladium catalyst. The addition of $\text{Pd}(\text{OAc})_2$ (0.1 mol%) did not affect the reaction and provided almost the same purity of the final product (87% pure, based on the ^{19}F NMR spectrum). The characterization data of $\text{C}_6\text{F}_5\text{Ge}(\text{O}^t\text{Bu})_3$: ^1H NMR (499 MHz, C_6D_6) δ 1.44 (s, 27H); ^{19}F NMR (470 MHz, C_6D_6) δ -126.6 (br d, $J = 18.3$ Hz, 2F), -150.5 (br t, $J = 18.4$ Hz, 1F), -161.6 (br s, 2F); HRMS (ESI) m/z $[\text{M} + \text{Na}]^+$ calculated for $\text{C}_{18}\text{H}_{27}^{74}\text{GeNaO}_3$: 483.0984, measured: 483.0969.